OPERATIONAL ASPECTS OF DECISION FEEDBACK EQUALIZERS

Rodney Andrew Kennedy

B.E. (Hons.) UNSW

M.E. N'cle, NSW

A thesis submitted for the degree of Doctor of Philosophy of the Australian National University.

Department of Systems Engineering
The Australian National University

December 1988

Declaration

The contents of this thesis are the result of original research and have not been submitted for a higher degree to any other university or institution.

Much of the work in this thesis has been published or has been submitted for publication as journal papers. These papers are:

- R.A. Kennedy, and B.D.O. Anderson, "Error Recovery of Decision Feedback Equalizers on Exponential Impulse Response Channels," *IEEE Trans. on Communications,* vol.COM-35, pp.846-848, August 1987.
- R.A. Kennedy, and B.D.O. Anderson, "Recovery Times of Decision Feedback Equalizers on Noiseless Channels," *IEEE Trans. on Communications,* vol.COM-35, pp.1012-1021, October 1987.
- R.A. Kennedy, B.D.O. Anderson, and R.R. Bitmead, "Tight Bounds on the Error Probabilities of Decision Feedback Equalizers ," *IEEE Trans. on Communications,* vol.COM-35, pp.1022-1029, October 1987.
- R.A. Kennedy, G. Pulford, B.D.O. Anderson, and R.R. Bitmead, "When has A Decision-Directed Equalizer Converged?," *IEEE Trans. on Communications,* (accepted for publication).
- R.A. Kennedy, B.D.O. Anderson, and R.R. Bitmead, "Channels Leading to Rapid DFE Error Recovery," *IEEE Trans. on Communications,* (accepted for publication).
- R.A. Kennedy, B.D.O. Anderson, and R.R. Bitmead, "Blind Adaptation of Decision Feedback Equalizers: Gross Convergence Properties," *International Journal of Adaptive Control and Signal Processing,* (submitted for publication).

Papers published in Conference Proceedings, but in some cases containing material overlapping with the above are:

- B.D.O. Anderson, R.A. Kennedy, and R.R. Bitmead, "Decision Feedback Equalizers: Concepts Towards Design Guidelines," *Proc. ISSPA87,* pp.1-7, Brisbane Australia, August 1987.
- R.A. Kennedy, B.D.O. Anderson, and R.R. Bitmead, "Stochastic Analysis of Non-Adaptive Decision Feedback Equalizers," *Proc. ISSPA87,* pp.842-847, Brisbane Australia, August 1987.

- R.A. Kennedy, B.D.O. Anderson, and R.R. Bitmead, "Channels Leading to Rapid DFE Error Recovery: Passivity Analysis," *Proc. 27th IEEE Conf. on Decision and Control,* Austin, Texas, December 1988 (to appear).
- R.A. Kennedy, B.D.O. Anderson, and R.R. Bitmead, "Stochastic Dynamics of Blind Decision Feedback Equalizer Adaptation," *Proc. ACASP'89,* Glasgow, Scotland, April 1989 (to appear).
- R.A. Kennedy, "Some Difficulties with Blind Regressor Based Channel Equalizers in Digital Communications," *Proc. 1989 Australian Symposium on Signal Processing and Applications,* Adelaide, Australia, April 1989 (to appear).

The research represented in this thesis has been performed jointly with Prof. Brian D.O. Anderson, Prof. Robert R. Bitmead and Mr. Graham Pulford. The majority, approximately 75%, of this work was my own.

_____

Rodney Andrew Kennedy

Acknowledgements

The work presented in this thesis would not have been possible without the support of a number of individuals and organisations:

- My supervisors Brian Anderson and Bob Bitmead who guided me in producing this research work, gave encouragement, showed enthusiasm, and provided friendship.

- The Australian Telecommunications and Electronics Research Board (ATERB) whose stipend supplement enabled me to live above the threshold of poverty. Their partial support for a period of study overseas in Belgium is also acknowledged.

- The Laboratoire d'Automatique, de Dynamique et d'Analyse des Systèmes of the Université Catholique de Louvain at Louvain-la-Neuve, Belgium for the use of word processing facilities in the preparation of part of this thesis.

- A miscellany of sods: To my fellow students who provided friendship and ample distraction (actually). To Liz and the cats (some dearly deceased) with whom I found a second home.

- My parents for everything they have provided for me in terms of education, financial support and encouragement.

- Kris for her understanding and support.

Abstract

The central theme is the study of *error propagation* effects in decision feedback equalizers (DFEs). The thesis contains: a *stochastic analysis* of error propagation in a tuned DFE; an analysis of the effects of error propagation in a *blindly adapted* DFE; a *deterministic analysis* of error propagation through input-output stability ideas; and *testing procedures* for establishing correct tap convergence in blind adaptation. To a lesser extent, the decision directed equalizer (DDE) is also treated.

Characterizing error propagation using finite state Markov process (FSMP) techniques is first considered. We classify how the channel and DFE parameters affect the FSMP model and establish tight bounds on the error probability and mean error recovery time of a tuned DFE. These bounds are shown to be too conservative for practical use and highlight the need for imposing stronger hypotheses on the class of channels for which a DFE may be effectively used.

In *blind* DFE adaptation we show the effect of decision errors is to distort the adaptation relative to the use of a *training sequence*. The mean square error surface in a LMS type setting is shown to be a concatenation of quadratic functions exposing the possibility of false tap convergence to undesirable DFE parameter settings. Averaging analysis and simulation are used to verify this behaviour on some examples.

Error propagation in a tuned DFE is also examined in a *deterministic* setting. A finite error recovery time problem is set up as an input-output stability problem. Passivity theory is invoked to prove that a DFE can be effectively used on a channel satisfying a simple frequency domain condition. These results give performance bounds which relate well with practice.

Testing for false tap convergence in blind adaptation concludes our study. Simple statistic *output tests* are shown to be capable of discerning correct operation of a DDE. Similar tests are conjectured for the DFE, supported by proofs for the low dimensional cases.

Table of Contents

Glossary of Definitions

DFE	decision feedback equalizer
DDE	decision directed equalizer
FIR	finite impulse response
IIR	infinite impulse response
FSMP	finite state Markov process
$\mathbb{C}$	complex plane
$\mathbb{R}$	real numbers
$\mathbb{R}^{N\times P}$	real $N \times P$ matrices
$\mathbb{Z}_+$	natural numbers
$\mathbb{Z}$	integers
$\boldsymbol{A}'$	transpose of real matrix $\boldsymbol{A}$
q^{-1}	delay operator: $q^{-1}x_k \triangleq x_{k-1}$
$\widetilde{g}(z)$	Z-transform: If $g \triangleq \{g_0,\ g_1,\ g_2,\ \ldots\}$ then $\widetilde{g}(z) \triangleq \sum_{i=0}^{\infty} g_i z^{-i}$
$\mathrm{sgn}(\cdot)$	signum function: $\mathrm{sgn}(x) \triangleq 0$ for $x = 0$, $\mathrm{sgn}(x) \triangleq x/\lvert x\rvert$ for $x \neq 0$.
$\mathcal{M}$	M-ary alphabet: $\mathcal{M} \triangleq \{1-M,\ 3-M,\ \ldots,\ M-1\}$, $M \in \{2,\ 4,\ 6,\ \ldots\}$
$\mathcal{Q}_M(\cdot)$	M-ary quantizer: $\mathcal{Q}_M(x) \triangleq \sum_{k=1-M/2}^{M/2-1} \mathrm{sgn}(x+2k) \in \mathcal{M}$
$E\{\cdot\}$	expectation operator
$Pr(\cdot)$	probability function
$Re(\cdot)$	real part
$Im(\cdot)$	imaginary part
l_p	l_p-space: $x \triangleq \{x_0,\ x_1,\ x_2,\ \ldots\} \in l_p$ if $\sum_{i=0}^{\infty} \lvert x_i\rvert^p < \infty,\ p \geq 1$.
l_p^e	extended l_p-space: $x \in l_p^e$ if $\sum_{i=0}^{k} \lvert x_i\rvert^p < \infty,\ \forall k < \infty,\ p \geq 1$.
$\lVert\cdot\rVert$	l_2-norm: $\lVert x\rVert \triangleq \sqrt{\sum_{i=0}^{\infty} \lvert x_i\rvert^2}$
$\lVert\cdot\rVert_1$	l_1-norm: $\lVert x\rVert_1 \triangleq \sum_{i=0}^{\infty} \lvert x_i\rvert$
$\langle\cdot,\cdot\rangle$	real inner product: $\langle x, y\rangle \triangleq \sum_{i=0}^{\infty} x_i y_i$
$\langle\cdot,\cdot\rangle_T$	truncated real inner product: $\langle x, y\rangle_T \triangleq \sum_{i=0}^{T} x_i y_i$
$\circledast$	convolution: If $z = x \circledast y$ then $z_k \triangleq \sum_{i=0}^{k} x_{k-i} y_i$.
$O(\cdot)$	$f(x) = O\big(g(x)\big)$ as $x \to l$ if $\lim_{x\to l} \{f(x)/g(x)\} \to k$.
$o(\cdot)$	$f(x) = o\big(g(x)\big)$ as $x \to l$ if $\lim_{x\to l} \{f(x)/g(x)\} \to 0$.

CHAPTER 1. INTRODUCTION

Aim: *The dissertation contains an analysis of the effects of error propagation on the operational aspects of a decision feedback equalizer. The object of our study is to show how the non-linear recursive mechanism behind error propagation detrimentally distorts the operation of a decision feedback equalizer as a channel equalizer both during adaptation and after it is tuned.*

1.1 Preamble

We describe how intersymbol interference (ISI) arises in a dispersive channel used for digital communication, and establish the need to compensate for this effect by the use of channel equalizers (§1.2). We present, at a tutorial level, the operation of a decision feedback equalizer (DFE) as a simple non-linear (adaptive) structure that combats ISI. Our description is based on a two parameter example of a DFE which exhibits some of the key operational problems of these devices. For comparison the decision directed equalizer (DDE) is introduced. The DDE is seen to be essentially a linear structure that compensates for ISI. Adaptive equalization is also described, highlighting the important difference between training sequence adaptation and blind adaptation for both devices.

The discussions found in the following sections will also serve to introduce the terminology associated with the analysis of these equalizer structures. Keywords and concepts are emphasized. In §1.3 one may find a brief review of the literature on equalization focussing mainly on DFEs and those works from which the thesis draws. The balance of this chapter, §1.4, is composed of a summary of the contents of the

thesis on a chapter by chapter basis, and concludes, in §1.5 with a point summary of the main contributions of the thesis.

1.2 Equalization

1.2.1 Intersymbol Interference

Communication systems generally deal with the transfer of information between two separate points over some medium in the presence of disturbing influences such as noise and dispersion. Recently, and increasingly, the information format, rather than being an analogue voice signal, has taken the form which can be most easily digested by a computer. This has meant that in modern communications systems it is desirable to have both the temporal variation and the signal amplitude quantized, e.g., in the simplest case we would send binary symbols (bits) represented by pulses of plus or minus some voltage and sample our received waveforms at a regular interval of time. Naturally the channels over which these signals are propagated remain real analogue systems and typically display the *distortion* associated with non-ideal behaviour, which is characterizable in the frequency domain by either a non-constant group delay or non-constant gain (usually both). This distortion is manifested in the time domain by pulse dispersion and is labelled *intersymbol interference* (ISI). This terminology reflects the fact that sampling the output of a dispersive channel shows a contribution not only from the desired symbol but also from neighbouring symbols whose energy has been smeared in time over several sampling intervals.

Figure 1.1 shows the sampled impulse response of a representative dispersive channel. We regard the peak as the cursor, i.e., the weight bearing the information, and the remaining samples as the ISI. (Note the privileged impulse response value labelled the "cursor" is arbitrarily chosen but generally corresponds to the impulse response peak.) Such ISI may lead to incorrect decoding of the symbols sent and the system performance may suffer a high error probability as a result. As an example of an analogue channel showing ISI in digital communication we have the common telephone networks which were designed and developed for voice communication. These networks are being partially utilized to send digital signals in a variety of formats, the details of which will not concern us here. Further, we note that the increasing demands for ever higher bit rate communications only accentuate the problems of ISI and the associated enhanced error rate [1].

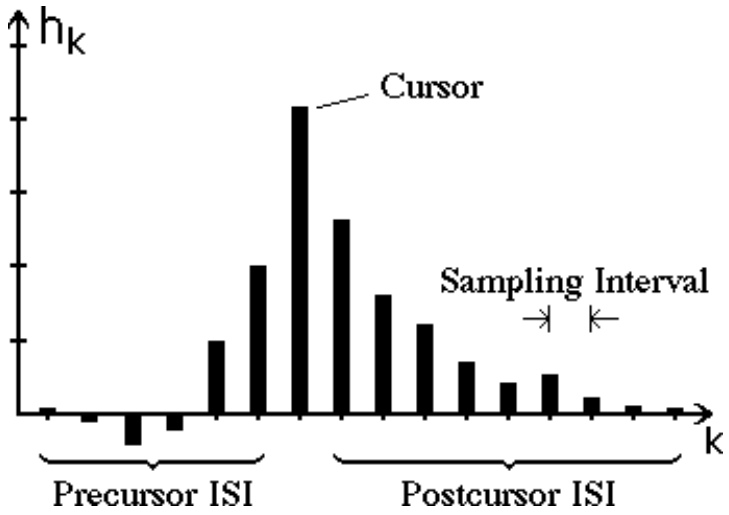

Fig.1.1 Sampled Channel Impulse Response and Intersymbol Interference

The utilization of existing analogue networks (and of course new networks) for high speed data transmission requires *compensation* for the ISI (dispersion) introduced by the channel. Such a compensation process is known as *equalization*. When the channel over which the data is sent is unknown, which is common, then one must employ *adaptive equalization*. Such adaptation is simply a merging of some channel identification scheme with equalization, and is indispensable in many applications, e.g., at speeds of 2400 bits/sec and above on switched telephone networks, because at such speeds there is a wide variation in the channel characteristics within a typical network [1].

We now turn to discuss at a tutorial level the two types of equalizer which will interest us here, after which we will move onto describing some adaptation schemes. These equalizers are the *decision feedback equalizer* (DFE) and the *decision directed equalizer* (DDE). Both are termed sub-optimum equalizers because their performance on noisy channels is inferior in an error probability sense to the use of more elaborate schemes typically based on maximum likelihood sequence estimation (usually employing the Viterbi algorithm) [1]. However, overwhelmingly, their often slight performance disadvantage is nullified by their extreme structural simplicity, which translates into great cost effectiveness.

1.2.2 Decision Feedback Equalization

This thesis deals primarily with decision feedback equalizers. To understand the basic

operation of this simple non-linear structure it suffices, we believe, to look at a simple low order example. The example consists of an idealized three tap linear sampled model of a channel given by $h_0 + h_1 q^{-1} + h_2 q^{-2}$, where q^{-1} is a one sample period delay operator. The input sequence $\{a_k\}$ takes binary values $a_k \in \{-1, +1\}$ and $k \in \{0,\ 1,\ 2,\ \ldots\}$ is the discrete time index labelling the sampling instants (in this thesis we only work in discrete time).

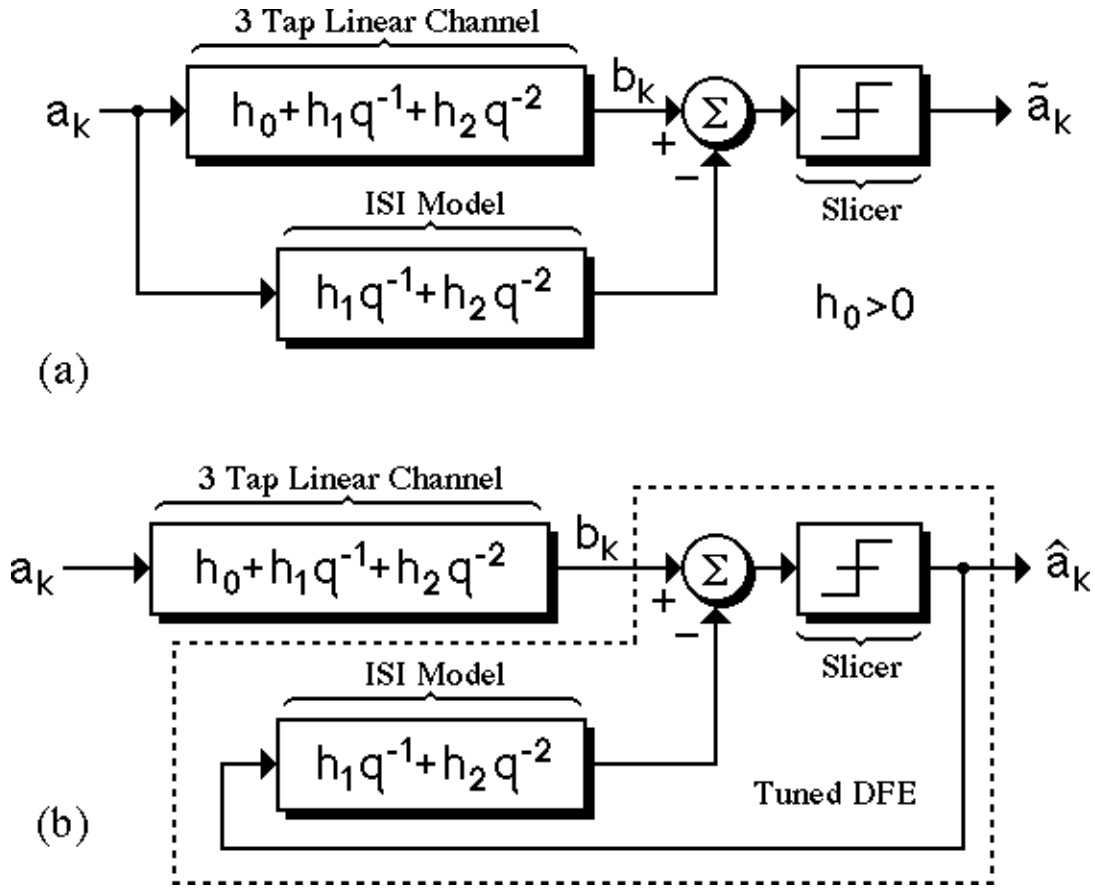

Fig.1.2 The Idea Behind Decision Feedback Equalization.

In motivating the DFE structure consider the fictitious system in Fig.1.2a. The input data a_k is passed through two linear systems, the upper being the simple three tap channel model and the lower a model of the postcursor ISI (defined in Fig.1.1) of the same channel (here we regard $h_0 > 0$ as the cursor, i.e., the weight carrying the desired information). Clearly the output of the summation will be $h_0 a_k$ after which, passing through a signum slicer, we obtain the output $\widetilde{a}_k = a_k$ (simple generalizations to multilevel, non-binary alphabets are possible). So a_k is both the input and output

(here we have made the first and hopefully the last mistake in the thesis which we will explain in the next paragraph). Given this information we could just as easily feed the postcursor ISI model $h_1q^{-1} + h_2q^{-2}$ with the system output as is done in Fig.1.2b. That part of Fig.1.2b excluding the channel (shown boxed) is precisely the perfectly tuned 2 tap DFE. (Higher order DFEs take an analogous form.) Clearly its basic action is to model and cancel channel postcursor ISI.

This example can serve to highlight some of the basic operational problems with the DFE. First we reconsider Fig.1.2a. At time periods $k = 0$ and $k = 1$ the output $\widetilde{a}_k$ need not be the same as the input a_k (as we suggested above) because the *initial conditions* (modelled at time $k = 0$) in the two tap delay line need not correspond to the initial conditions of the ISI in the channel. However such a problem does not exist for $k \geq 2$ where the output satisfies $\widetilde{a}_k = a_k,\ k \geq 2$, as is easily seen. Therefore after two time steps we can be confident the output is correct because any initial condition mismatch (error condition) is flushed out.

This initial condition problem is far more acute in Fig.1.2b and destroys our confidence that the two systems in Fig.1.2 are truly equivalent. To see this, suppose we have arbitrary initial conditions in the two tap delay line section of the DFE in Fig.1.2b. This system does not generally have the property that errors are flushed out in finite time; indeed, now the possibility arises that output errors $\widehat{a}_k \neq a_k$, which are fed back into the delay line, induce further (future) errors in a never ending recursion. This is the well-known *error propagation* mechanism and it is non-trivial to analyze [2]. It is even possible for the errors to persist after any arbitrary length of time, for some input sequences (and initial conditions), in which case we say the input sequence is *pathological* [3]. Note we may regard channel noise as being the principal potential source for a range of initial conditions in the DFE.

Further insights into the DFE can be gained from this example. Clearly what is desirable from an operational point of view is for the DFE in Fig.1.2b to act like the structure in Fig.1.2a, in the sense that any initial error condition is flushed out in a finite time. What will become clearer from this thesis is that this is precisely a *stability* notion [3] lending itself to treatment by standard techniques in input-output stability. Evidently we are faced with a *finite error recovery time* problem. More common linear notions of stability requiring the channel to be minimum phase do not make much sense when we deal with the non-linear structure of the DFE as we will see. Finally, we note that the example in Fig.1.2b also displays the tap values for a

perfectly tuned DFE, setting an ideal objective for adaptation which we will describe in §1.2.4.

1.2.3 Decision Directed Equalization

The second type of equalizer which we shall briefly consider in this thesis (and so our review here will correspondingly be short) is the decision directed equalizer (DDE) shown in Fig.1.3 (this terminology pertains more to its adaptive behaviour). The first portion of the DDE consists of a linear equalizer $d_0 + d_1 q^{-1} + d_2 q^{-2} + \ldots$ which attempts to compensate for channel ISI by approximating an inverse to the channel (the values for a tuned DDE have not been indicated). Like the DFE a slicer is employed to recover an output sequence constrained to the symbol values, in this case binary values $\widehat{a}_k \in \{-1, +1\}$. (It is possible to generalize to multilevel, non-binary alphabets.) Note that the use of a slicer relaxes the demands on the linear portion to exactly form the inverse of the channel (or the inverse with some delay if the channel is non-minimum phase). The DDE being basically a linear device is relatively simple to analyze, in comparison to the non-linear recursive DFE. From such an analysis we could describe its properties but here let us highlight just one specific defect.

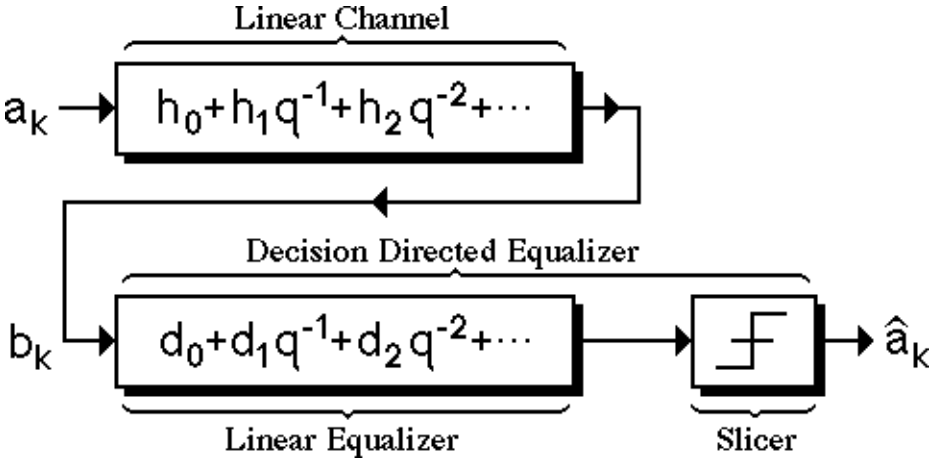

Fig.1.3 Linear Channel and Decision Directed Equalizer.

The basic operation of the DDE is to model the channel inverse. Therefore, at frequencies where the channel attenuation is high the DDE tends to enhance any channel noise and this is a serious drawback not shared by the DFE [1]. However, our analysis of the DDE in this thesis concerns more its behaviour during *adaptation* (for

comparison with the DFE) and a description of this aspect of equalization we shall briefly describe in §1.2.4.

A more common equalizer structure in fact merges the linear equalizer (Fig.1.3) and the DFE, in a sense combining the good properties of both. The linear equalizer, which precedes the DFE, functions to cancel the precursor ISI (Fig.1.1) without necessitating channel full inversion (and thus is able to avoid excessive noise enhancement). The remaining postcursor tail (Fig.1.1) is compensated for by the DFE (in a way that avoids excessive error propagation). It is generally sufficient, as we do in most of this thesis, to consider the DFE section in isolation (when considering error propagation) because the channel and linear equalizer responses can always be convolved into a single *effective* linear channel. Further, a possibility which arises in applications is for the channel to not require the preceding linear equalizer because it exhibits little precursor ISI, and so in this case the analysis is directly applicable [4].

1.2.4 Adaptive Equalization

The analysis of adaptation we perform in this thesis requires an absolute awareness of the difference between adaptation with a *training sequence* and *blind* adaptation. These are different techniques to obtain channel identification in adaptive equalization, be it with a DFE or DDE.

Channel identification utilizes in a general context both input and output channel measurements [5]. Adaptive equalization with a *training sequence* is able to utilize the input data information (knowledge of a_k) by having the transmitter send a data sequence $\{a_k\}$ known *a priori* to the equalizer for a limited time duration [1]. This is equivalent in Fig.1.2b (DFE) or Fig.1.3 (DDE) to having available both the a_k and b_k signals to identify the channel parameters. Fig.1.4 (DFE) shows the precise arrangement which is used when implementing a training sequence (the description of such adaptive systems is left to the body of the thesis) and the close relationship with Fig.1.2b is apparent. Naturally such a training process implies a loss of efficiency in terms of useful data actually sent and is also inappropriate in many practical applications. (Equally well, many applications require the use of a training sequence, especially if the channel is rapidly varying which we do not consider [6].)

In contrast to equalization with a training sequence when only the measurements available at the equalizer are used for identification, specifically b_k and $\widehat{a}_k$ in Fig.1.2b

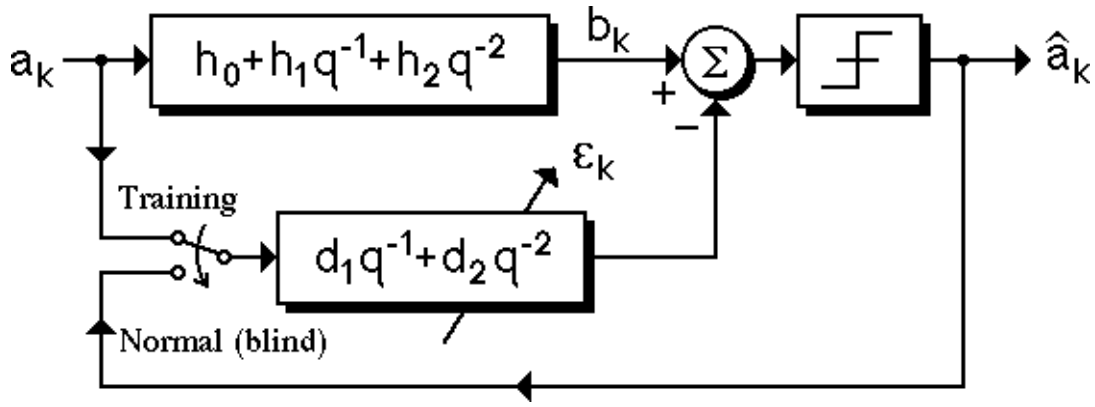

Fig.1.4 Adaptation with a Training Sequence

(DFE) or Fig.1.3 (DDE), then the standard terminology is *blind* adaptive equalization [7]. (However, *a priori* information regarding the statistics of the input a_k, e.g., the joint distribution of the symbols is implicitly used.)

Blind adaptation as opposed to adaptation with a training sequence is more in the spirit of equalization *per se* in the sense that only information at the receiver is employed for adaptation. Philosophically speaking, precise knowledge of the channel input data sequence by the receiver defeats the purpose of the equalization process. Also the use of a training sequence has the effect of completely decoupling the adaptive equalization into distinct identification and equalization modes. Blind equalization on the other hand demands greater analytical tools for its understanding, and because of this is not completely understood [8].

In blind adaptation of DFEs we note that the same output that via feedback generates error propagation (thus bursts of errors) is used as the regressor in identification. This feature serves to distinguish the DFE from the DDE and forms one focal point of the thesis. For this reason the literature contains a number of papers concerning blind adaptation of DDEs but only one (that we are aware of) on blind adaptation of DFEs [9]. We move onto a more comprehensive literature review in the next section.

1.3 Literature Review

The contents of this section are organized as follows. We begin by reviewing the various common equalizing structures which have been proposed for combatting ISI

in linear digital communication channels with the view to locating within this large set the purpose, function and advantages of the DFE. Then we move on to reviewing works most relevant to our study dealing specifically with DFEs. We remark here that it is impossible to do justice in generating a review of this form—important references may be overlooked. In any case, our main aim is to give a flavour of the style of results which may be found in the literature.

Early research efforts into developing equalizer structures concentrated on linear signal processing structures followed by a thresholding device, i.e., essentially that arrangement depicted in Fig.1.3. Such an arrangement was referred to as a linear equalizer (but we prefer to call this a decision directed equalizer or DDE). Having fixed the general structure the research concentrated on optimizing its performance. In defining a performance objective for the (tap weights of the) equalizer Tufts [10] used as a measure the mean square error (MSE) between the equalizer output sample and the corresponding input sample. In this way he jointly optimized a transmitter filter (which can be thought of as part of the channel) and the equalizer tap weights (receiver). He also obtained the optimum receiver (fixing the transmitter) for the minimum MSE (MMSE) under a zero forcing condition which demands complete elimination of the ISI. When the number of taps in the linear equalizer is finite the solution to this non-zero forcing condition for MMSE was given by Smith [11].

The main motivation for using mean square error performance measures for determining optimum equalizing structure comes from the analytical simplifications that this criterion affords. (In an adaptive context such measures also permit similar advantages [12] which we will return to discuss.) Less analytical tractability is possible if one uses as a performance measure the probability of error P_E. In this case the optimal linear equalizing structure is described by parameters obtained by solving coupled non-linear equations [13].

Naturally a broader class of equalizer structures is given by non-linear signal processors (of which the DFE in Fig.1.2b is a special case). The comprehensive consideration of such devices lies well outside the scope of this thesis but our intention is to give a small taste of the various types of receivers which have been proposed and ultimately utilized in practice. Examples of the criteria used in such devices are: (i) maximum *a posteriori* probability for a finite length input sequence; (ii) maximum *a posteriori* probability on a symbol by symbol basis; (iii) maximum likelihood symbol by symbol detectors, and the list goes on. Generally these systems tend to be very

complex non-linear systems, e.g., see [14,15].

A significant advance in terms of reducing implementation complexity within the general class of non-linear equalizer structures considered above was made by Forney [16]. In this equalizer a "whitened matched filter", as a first stage, generates at its output a sequence which theoretically contains sufficient statistics to estimate the input data sequence. Then the efficient Viterbi Algorithm is employed in estimating the maximum likelihood sequence estimate of the state and hence an estimate of the original input sequence. (In this modelling the effective channel is FIR and its output is corrupted by white gaussian noise—this enables a finite state Markov process to model the output process.)

One disadvantage of the approach in [16] is that its complexity grows quickly with the effective channel length making implementation for (effective) channels with long impulse responses difficult. Based on a suggestion of Forney some authors [17,18] presented equalizer structures which used a preliminary filter to shorten the effective channel response. One then uses a less complex Viterbi Algorithm at the expense of some loss in performance. So a trend was established which sort simpler non-linear equalizer structures in a suboptimal framework. This is where the DFE fits into the grand scheme of equalization—it is a suboptimal non-linear structure with performance advantages over the linear equalizer (DDE) but with comparable low implementation complexity (c.f., Fig.1.2b with Fig.1.3).

The research into DFEs has taken several directions. The early work concentrated on deriving the optimum taps settings using MMSE, zero forcing, or probability of error P_E criteria [19-24] under a variety of constraints ranging from: the number of feedback taps; the use of prefilters (linear equalizer as described in the end of §1.2.3); and modulation schemes employed. The interesting feature of all these works, particulary with regard to our research, is that the analyses in all these references have employed the assumption that all past decisions were error free. This assumption seemed almost essential to obtain closed form analyses but it has the effect of removing the non-linear recursive mechanism which is at the heart of the device. This assumption analytically denies the existence of error propagation, the effect we saw in the simple DFE in Fig.1.2b of §1.2.2.

This thesis weighs strongly the significance of error propagation in DFEs. Thus it is appropriate here to discuss in more detail the DFE literature dealing specifically with error propagation. Recall that error propagation is that complicated mechanism

whereby data estimation errors (output errors) recursively influence the generation of bursts of errors at later time instants (even in the absence of noise). The precise description of this propagation mechanism explicitly involves the input sequence. Consequently, given a stochastic model of the input, the standard characterization of error propagation is probabilistic. Fundamental steps in defining precisely the probabilistic model which describes error propagation were made by Zador [25], Duttweiler, Mazo and Messerschmitt [2], and Cantoni and Butler [3]. They all showed that under the usual independence assumption on the data sequence (and on the noise, if included) that the standard mathematical notion of a *finite state Markov process* (FSMP) could be used to derive performance bounds, either on the mean error recovery time, i.e., the period of time before the influence of an initial error state on the equalizer performance is completely quenched (i.e., the time it takes for Fig.1.2b to have equivalent behaviour to Fig.1.2a); or the error probability, i.e., the steady state relative frequency of making errors given channel noise. Even without the independence assumption on the driving stochastic input (the input data sequence and noise) Markov techniques may be used as approximations [26,27].

We highlight some deficiencies in these papers intending in no way to diminish the importance of these works. (Also at some of our work similar criticisms could be levelled.) The performance bounds derived in both [2] and [3] suffer from two main shortcomings. The first is that no theoretical indication is given for the tightness of the bounds; the second is that the bounds convey little practical information because they are generally hopelessly conservative (especially for DFEs with large numbers of taps). Thus the bounds do not appear to match the good performance of DFEs seen in practice. More recently, O'Reilly and de Oliveira Duarte [26,27] considered the problem of approximating the performance bounds in [2] and gave a formal procedure which reduced the dimension of the problem whilst maintaining the Markovian modelling techniques. However even with this simplification the modelling remains generally too complicated if the order of the DFE is high and the calculations become involved (this problem is certainly true of some of our work).

Another problem with the results in the literature (based on FSMPs) is that the performance bounds generally can only be calculated on a channel by channel basis. No general non-trivial condition on the types of channels which lead to satisfactory behaviour of the DFE (in terms of error propagation) is given. So this type of important practical information is lacking. (Some of the work in this thesis aims at correcting

these deficiencies.)

The second major area of interest concerning DFEs (and, of course, equalizers in general) is the analysis of adaptation. (A comprehensive review on adaptive equalization is given in Qureshi [1].) Adaptation via training sequence methods lead to classical analyses [20,21,28] and so the current theoretical interest lies with blind adaptation. Analogous results for the DDE have indicated great problems for blind adaptation exist, specifically convergence to unequalizing equilibria and related defects [29,30]. No globally converging blind algorithm has yet been found for linear equalization except when the data takes impractical input distributions [7,8]. The situation for blind DFE adaptation is less well understood and only preliminary investigations have been made [9]. One can anticipate or conjecture problems analogous to the DDE situation but an analysis, unlike the linear case, needs to contend with error propagation and the problem looks formidable. Blind adaptation for DFEs is poorly understood, so there exists a dire need to have some results in this subject area. The problem of blind adaptation is one focal point of this thesis.

1.4 Outline of the Thesis

1.4.1 Overview

This thesis studies the DFE and to a lesser extent the better understood DDE. These investigations were prompted by an applications demand which highlighted a thin theoretical coverage of some of the operational aspects of DFEs.

The subject areas (and rough chronological order) of the thesis cover a study of error propagation, the effects of noise, blind adaptation, and blind adaptation convergence tests. Some tools used in the thesis are: finite state Markov processes [2], averaging theory [31] and input-output stability [32].

The following subsection reviews what might be found in each of the four technical chapters, 2 to 5. (This discussion is often specific and may be safely skimmed over.) The final section (§1.5) gives a point summary of our main contributions.

1.4.2 Contents and Contributions of Thesis

Chapter 2: examines the behaviour of a binary DFE when its parameters are fixed at the ideal tuned values (which might have resulted after an adaptive phase of operation). The ideal values for the DFE parameters are precisely those which are identical

with the postcursor tail of the dispersive channel, see §1.2.3. Our investigation takes a classical form [2,3] and the subject of the study is error propagation. Chapter 2 partitions itself according to the two most conspicuous manifestations of the detrimental effects of error propagation: firstly, the analysis of error recovery times in the absence of noise; and secondly, the analysis of error probability performance in the presence of noise.

The now classical basis of the analysis of error propagation in DFEs [2,3,25-27] centres on applying the theory of finite state Markov processes (FSMPs). This is true also of our work here in Chapter 2. However we adopt an apparently redundant, higher dimensional model. This affords several advantages. Our first contribution is to define precisely how the channel parameters determine the stochastic dynamical properties of the DFE. It is shown that for a given length of DFE tapped delay line (modelling the significant ISI in the channel) the parameter space may be partitioned into a finite set of equivalence classes (polytopes) which can be identified in a one-to-one way with a finite set of FSMPs. This is really just the mathematical formulation of the intuitive notion that the DFE quantizer (Fig.1.2b) has insensitivity to its argument. Attention is then focussed on those equivalence classes which lead to extremes in behaviour. Indeed, we show that the conservative bounding procedures found in early works [2,3] correspond to realizing the worst case equivalence class. For example, in [2] one finds bounds on the error probability (asymptotically with small noise) which are proportional to 2^N where N is an effective channel length; in [3] the mean error recovery time is bounded in terms of the same exponential. We display channels where these bounds are actually achieved. For example, one can get a figure like 10^{10} years for a realizable mean error recovery time for a DFE which, evidently, is totally impractical. We also show minimum phaseness, as an imposition on the channel class, does not necessarily guarantee lower bounds.

In the sense that we construct equivalence classes of channel which: (i) realize the error recovery time bounds in [3], (ii) realize the error probability bounds in [2], we say that the results are *tight*. This resolves some open problems raised in [2,3]. So our analysis indicates why the results in [2,3] cannot be improved on (without imposing further hypotheses, stronger than minimum phaseness), and drives home the point that DFEs are useful devices only on some restricted class of channel models—hopefully, models matching well with physical reality. Chapter 2 also gives a detailed classification of channel models along with a low order example.

The particular model we adopt for the FSMP makes a classification of pathological input sequences (§1.2.2), i.e., those input sequences for which decision errors are always made after any arbitrary length of time, particularly transparent. These sequences, which are a function of the channel parameters, in a sense are the ones to be avoided if good/rapid error recovery performance in practice is desired. We use graphical methods to show they need not be periodic in structure. This classification is another contribution.

Statistical calculations comprise the balance of Chapter 2, e.g., we give formulae for the mean and variance of the error recovery times and an asymptotically tight bound on the probability of recovering from an arbitrary error state within a given time. Computation of error probability bounds follows a similar line. Overall our work stresses methods giving constructions rather than straight existence proofs, and highlights the need for imposing stronger hypotheses on the channel model to achieve results observed and demanded in practice. The results in Chapter 2 have been published in [33-35].

Chapter 3: looks at the *blind* adaptation of binary DFEs. We examine this simplest non-trivial system which exposes the influence of error propagation on adaptation. Comparisons are made to the simpler and better understood blind DDE [6-8,29,30]. The analysis in essence combines FSMPs (with their associated polytopes to describe the output statistics as a function of the adapting tap parameters) with averaging theory [31] (to describe the underlying drift mechanism of the adaptation). Our contribution, apart from developing the first apparently accurate model for the behaviour of this simple blind system, is to show clearly the mechanism behind the convergence of the parameter values to undesirable settings where the equalizer performs poorly in an error probability sense (even in the absence of noise). It is the output correlation statistics distorted by error propagation which lead to these undesirable equilibria. Roughly analogous results are known for the DDE (a device which, however, does not suffer from error propagation) [29,30].

Classification of equilibria is a major subject area of Chapter 3. Delay-type equilibria, i.e., those leading to output decision sequences which are a simple delay of the input (along with a possible sign-inversion) are intensively studied and characterized. The details involve fiddly questions about the structure of the underlying FSMP. However, ultimately, the conditions under which delay-equilibria exist are very simple to

state and test. These tests involve only simple sums on the channel impulse response coefficients.

Important conjectures are raised which are mathematically equivalent to questions of reachability of various closed subsets of the underlying FSMP, i.e., the manner in which input data sequence can transfer the DFE system to different states. The resolution of these conjectures is likely to be far from easy. Failed attempts to solve one of these conjectures led to the closely related results on the DDE to be found in Chapter 5 and these results are important in at least two contexts—as tests for convergence, and as implying the existence of well-behaved globally converging blind algorithms.

The latter part of Chapter 3 examines sign-error blind algorithms. Effects of quantizing the error signals on blind adaptation are investigated and these results lead to accurate predictions of the behaviour for a simple example. A closely related area of research is the use of sign-error algorithms for adaptive filtering [36]. Some of the material in Chapter 3 has been published in [37-40].

Chapter 4: returns to the error propagation problem [2] but with new techniques and a more general setting (required by our analysis of adaptation in Chapter 3). It presents a significant advance on the standard FSMP analyses met before. Firstly the techniques lend themselves readily to the non-ideal DFE where the channel is IIR (or FIR) but the DFE is only FIR. Second, the DFE parameter settings need not be close to the desired ideal values—how close they must be is precisely defined. Third, statistical models for the input are abandoned in favour of an implicit worst case analysis. So the sometimes awkward, analytically difficult stochastic modelling reflected in [2,3,33] is not needed. Therefore the recovery time bounds derived are absolute maxima regardless of the particular input sequence (driving the system) and regardless of the initial error condition (which initiates the error propagation). (This analysis is therefore valid if the input sequence is correlated which occurs in some applications.) These results are achieved by imposing stronger hypotheses on the channel model to align with what might be expected in practice (this approach is necessary as we highlight in Chapter 2). The condition we impose on the channel model has a simple description which says the real part of the channel frequency response (modulo a phase shift associated with a delay) needs to be sufficiently positive, i.e., a strictly positive real condition. Our techniques use passivity ideas [32] and the notions of stability first enunciated in [3].

Standard techniques from input-output stability (of which passivity is a special case) that we draw on are: (i) the use of loop transformations, and (ii) the theory of multipliers. The first technique enables us to cast a finite error recovery time DFE problem (§1.2.2) in the framework of control stability ideas. The use of multipliers is used to obtain explicit bounds and convergence rates from the analysis. Then we use tools related to Parseval's Theorem to put the results into the frequency domain [32].

Some of the more detailed investigations that we undertake include the study of error propagation defined for delay-like behaviour. This possibility was largely ignored in the classical references. We develop all of the necessary theory to cover this interesting case.

In Chapter 4 we compute explicit error recovery bounds and present examples throughout our analysis, including a case which has appeared in the literature [4]. Another example shows the flexibility of the general technique as demonstrated by a timing phase sensitivity study for the DFE, which can be interpreted as a robustness result. This complements a related (but different) classical result which relied on the strong assumption of the DFE never making incorrect decisions [40]. The analysis is also carried out for the M-ary case with comparable results to the binary case. Our investigations of this work in Chapter 4 have been reported in [42-44].

Chapter 5: studies the existence of convergence tests for blind adaptation. A problem identified in Chapter 3 concerns the existence of undesirable settings of the DFE parameters where blind adaptation hangs. Clearly it would be desirable to have a means of determining whether or not the equilibrium of the adaptation was one corresponding to correct operation of the equalizer. Blind adaptation demands that only signals available at the equalizer be used, and so in asking for blind convergence tests only these same signals can sensibly be used.

The M-ary DDE forms our main object for study because it is intrinsically a simpler device than the DFE and we are able to perform a complete analysis. In this case we demonstrate that simple correlation and distribution tests suffice to guarantee tap convergence to a desirable setting. In the DFE case we establish a test for a one tap binary DFE leaving the general question of existence of such blind DFE tests as a conjecture needing more advanced techniques for verification.

This theory is strongly motivated by conjectures and analysis to be found in Chapter 3. However the work also connects with ideas of the existence of blind algo-

rithms which converge globally to equalizing equilibria [7,30]. The material found in Chapter 5 has been reported in [45].

In overviewing the style of results, we see our work stressing the desire to include error propagation effects into all facets of our analysis into DFEs. This represents a considerable challenge as it is an effect born of non-linearity and recursion. To highlight that recursion is intrinsically a subject area of deep conceptual problems we need only refer the reader to [46, §1.4].

1.5 Point Summary of Contributions

A summary of the major contributions of this thesis follows. Note that each chapter includes its own more detailed summary in its conclusions.

- Refinement of stochastic modelling techniques for DFEs.
- Determination of the effects of the channel parameters on the ideal DFE performance.
- Proof of the tightness of error recovery time bounds found in the literature.
- Classification of pathological input sequences.
- Proof of the tightness of error probability bounds found in the literature.
- Analysis of blind adaptation of DFEs.
- Explanation of the mechanism behind undesirable convergence of blind adaptive DFEs.
- Classification of equilibria for blind DFE adaptation.
- Analysis of delay-like equilibria.
- Analysis of sign-error blind adaptive algorithms and generalizations.
- New techniques and improved bounds for error recovery analysis which relate well with practice.

- Proof of good properties of exponential impulse response channels.
- Proof of good properties of channels which satisfy a positive real frequency domain condition.
- Convergence rates and explicit bounds on DFE error recovery.
- Analysis of finite recovery time sensitivity to timing phase.
- Construction of blind adaptation convergence tests for DDEs and low order DFEs.

References

[1] S.U.H. Qureshi, "Adaptive Equalization," *Proc. IEEE,* vol.73, No.9, pp.1349-1387, September 1985.

[2] D.L. Duttweiler, J.E. Mazo, and D.G. Messerschmitt, "An Upper Bound on the Error Probability in Decision Feedback Equalizers," *IEEE Trans. on Information Theory,* vol.IT-20, pp.490-497, July 1974.

[3] A. Cantoni, and P. Butler, "Stability of Decision Feedback Inverses," *IEEE Trans. on Communications,* vol.COM-24, pp.1064-1075, September 1976.

[4] B.R. Clarke, "The Time-Domain Response of Minimum Phase Networks," *IEEE Trans. on Circuits and Syst.,* vol.CAS-32, No.11, pp.1187-1189, November 1985.

[5] L. Ljung, and T. Söderström, "Theory and Practice of Recursive Identification," MIT Press, Cambridge, Massachusetts 1983.

[6] D.N. Godard, "Self Recovering Equalization and Carrier Tracking in Two-dimensional data Communication Systems," *IEEE Trans. on Communications,* vol.-COM-28, pp.1867-1875, November 1980.

[7] A. Benveniste, and M. Goursat, "Blind Equalizers," *IEEE Trans. on Communications,* vol.COM-32, No.6, pp.871-883, August 1984.

[8] A. Benveniste, M. Goursat, and G. Ruget, "Robust Identification of a Non-minimum Phase System: Blind Adjustment of Linear Equalizer in Data Communications," *IEEE Trans. on Auto. Control,* vol.AC-25, No.6, pp.385-399, June 1980.

[9] A. Jennings, "Analysis of the Adaption of Decision Feedback Equalizers with Decision Errors," Internal Report Telecom Aust. Research Lab., July 1985.

[10] D.W. Tufts, "Nyquist's Problem—the Joint Optimization of Transmitter and Receiver in Pulse Amplitude Modulation," *Proc. IEEE,* vol.53, pp.248-260, March 1965.

[11] J.W. Smith, "The Joint Optimization of Transmitted Signal and Receiving Filter for Data Transmission Systems," *Bell Syst. Tech. J.,* Vol.44, pp.2363-2392, December 1965.

[12] R. Lucky, "Automatic Equalization for Digital Communication," *Bell Syst. Tech. J.,* Vol.44, pp.547-588, April 1965.

[13] M.R. Aaron, and D.W. Tufts, "Intersynbol Interference and Error Probability," *IEEE Trans. on Information Theory,* vol.IT-12, No.1, pp.26-34, January 1966.

[14] R.W. Chang, and J.C. Hancock, "On Receiver Structures for Channels Having Memory," *IEEE Trans. on Information Theory,* vol.IT-12, pp.463-468, October 1966.

[15] G. Ungerboeck, "Nonlinear Equalization of Binary Signals in Gaussian Noise," *IEEE Trans. on Communications,* vol.COM-19, pp.1128-1137, December 1971.

[16] G.D. Forney, "Maximum Likelihood Sequence Estimation of Digital Signals in the Presence of Intersymbol Interference," *IEEE Trans. on Information Theory,* vol.IT-18, pp.363-378, May 1972.

[17] S.U.H. Qureshi, and E.E. Newhall, "An Adaptive Receiver for Data Transmission Over Time-Dispersive Channels," *IEEE Trans. on Information Theory,* vol.IT-19, pp.448-457, July 1973.

[18] D.D. Falconer, and F.R. Magee, "Adaptive Channel Memory Truncation for Maximum Likelihood Sequence Estimation," *Bell Syst. Tech. J.,* Vol.52, pp.1541-1562, November 1973.

[19] M. Austin, "Decision-feedback Equalization for Digital Communication Over Dispersive Channels," M.I.T. Res. Lab Electron., Tech. Rep.461, August 1967.

[20] P. Monsen, "Adaptive Equalization of a Slow Fading Channel," *IEEE Trans. on Communications,* vol.COM-22, No.8, pp.1064-1075, August 1974.

[21] D. George, R. Bowen, and J. Storey, "An Adaptive Decision Feedback Equalizer," *IEEE Trans. on Communications,* vol.COM-19, pp.281-292, June 1971.

[22] R. Price, "Nonlinearly Feedback-Equalized PAM vs Capacity for Noisy Filter Channels," *Rec. Int. Conf. Communications,* ICC-72 (Philadelphia, PA), 1972.

[23] J. Salz, "Optimum Mean Square Decision Feedback Equalization," *Bell Syst. Tech. J.,* Vol.52, pp.1341-1373, October 1973.

[24] D.D. Falconer, and G.J. Forschini, "Theory of Minimum Mean-Square-Error QAM System Employing Decision Feedback Equalization," *Bell Syst. Tech. J.,* Vol.52, pp.1821-1849, November 1973.

[25] P.L. Zador, "Error Probabilities in Data System Pulse Regenerator with DC Restoration," *Bell Syst. Tech. J.,* vol.45, pp.979-984, July 1966.

[26] J.J. O'Reilly, and A.M. de Oliveira Duarte, "Error Propagation in Decision Feedback Receivers," *Proc. IEE Proc. F, Commun., Radar and Signal Process.,* vol.132, no.7, pp.561-566, 1985.

[27] A.M. de Oliveira Duarte, and J.J. O'Reilly, "Simplified Technique for Bounding Error Statistics for DFB Receivers," *Proc. IEE Proc. F, Commun., Radar and Signal Process.,* vol.132, no.7, pp.567-575, 1985.

[28] B. Widrow, and S.D. Stearns, "Adaptive Signal Processing ," Prentice Hall Inc., Englewood Cliffs, N.J., 1985.

[29] J.E. Mazo, "Analysis of Decision-Directed Equalizer Convergence," *Bell Syst. Tech. J.,* Vol.59, No.10, pp.1857-1876, December 1980.

[30] S. Verdú, "On the Selection of Memoryless Adaptive Laws for Blind Equalization in Binary Communication," *Proc. Sixth Intl. Conf. on Analysis and Optimization of Systems,* Nice, France, June 1984.

[31] B.D.O. Anderson, R.R. Bitmead, C.R. Johnson, Jr., P.V. Kokotovic, R.L. Kosut, I.M.Y. Mareels, L. Praly, and B.D. Riedle, "Stability of Adaptive Systems: Passivity and Averaging Analysis," MIT Press, Cambridge, Massachusetts 1986.

[32] C.A. Desoer, and M. Vidyasagar, "Feedback Systems: Input-Output Properties," Academic Press, New York 1975.

[33] R.A. Kennedy, and B.D.O. Anderson, "Recovery Times of Decision Feedback Equalizers on Noiseless Channels," *IEEE Trans. on Communications,* vol.COM-35, pp.1012-1021, October 1987.

[34] R.A. Kennedy, B.D.O. Anderson, and R.R. Bitmead, "Tight Bounds on the Error Probabilities of Decision Feedback Equalizers ," *IEEE Trans. on Communications,* vol.COM-35, pp.1022-1029, October 1987.

[35] R.A. Kennedy, B.D.O. Anderson, and R.R. Bitmead, "Stochastic Analysis of Non-Adaptive Decision Feedback Equalizers," *Proc. ISSPA87,* pp.842-847, Brisbane Australia, August 1987.

[36] C.R. Elevitch, W.A. Sethares, G. Rey, and C.R. Johnson Jr., "Quiver Diagrams For Signed Adaptive Filters ," *IEEE Trans. on Acoustics, Speech and Signal Processing,* (accepted for publication).

[37] B.D.O. Anderson, R.A. Kennedy, and R.R. Bitmead, "Decision Feedback Equalizers: Concepts Towards Design Guidelines," *Proc. ISSPA87,* pp.1-7, Brisbane Australia, August 1987.

[38] R.A. Kennedy, B.D.O. Anderson, and R.R. Bitmead, "Blind Adaptation of Decision Feedback Equalizers: Gross Convergence Properties," *International Journal of Adaptive Control and Signal Processing,* (submitted for publication).

[39] R.A. Kennedy, B.D.O. Anderson, and R.R. Bitmead, "Stochastic Dynamics of Blind Decision Feedback Equalizer Adaptation," *Proc. ACASP'89,* Glasgow, Scotland, April 1989 (to appear).

[40] R.A. Kennedy, "Some Difficulties with Blind Regressor Based Channel Equalizers in Digital Communications," *Proc. 1989 Australian Symposium on Signal Processing and Applications,* Adelaide, Australia, April 1989 (to appear).

[41] J. Salz, "Optimum Mean-Square Decision Feedback Equalization and Timing Phase," *IEEE Trans. on Communications,* vol.COM-25, pp.1471-1476, December 1977.

[42] R.A. Kennedy, and B.D.O. Anderson, "Error Recovery of Decision Feedback Equalizers on Exponential Impulse Response Channels," *IEEE Trans. on Communications,* vol.COM-35, pp.846-848, August 1987.

[43] R.A. Kennedy, B.D.O. Anderson, and R.R. Bitmead, "Channels Leading to Rapid DFE Error Recovery," *IEEE Trans. on Communications,* (accepted for publication).

[44] R.A. Kennedy, B.D.O. Anderson, and R.R. Bitmead, "Channels Leading to Rapid DFE Error Recovery: Passivity Analysis," *Proc. 27th IEEE Conf. on Decision and Control,* Austin, Texas, December 1988 (to appear).

[45] R.A. Kennedy, G. Pulford, B.D.O. Anderson, and R.R. Bitmead, "When has A Decision-Directed Equalizer Converged?," *IEEE Trans. on Communications,* (accepted for publication).

[46] R.A. Kennedy, "Operational Aspects of Decision Feedback Equalizers," PhD Dissertation, Australian National University, Canberra A.C.T., December 1988.

CHAPTER 2. DFE ERROR RECOVERY ANALYSIS

Aim: *To present a general analysis of error propagation in tuned decision feedback equalizers and establish tight theoretical bounds on their performance.*

2.1 Introduction

In the study of decision feedback equalizers (DFEs) we can identify two open problem areas. The first is the subject of investigation in this chapter (and Chapter 4). It concerns the analysis of the mechanism whereby errors in a feedback structure induce further errors under recursion and non-linearity, an effect termed *error propagation*. The second problem area concerns blind adaptation in which the analysis needs to take into account the way that error propagation distorts and interacts with adaptation. This is the subject of Chapter 3. This dependence of the analysis of blind adaptation on the study of error propagation strongly motivates our work here.

Our aim is to present some error recovery properties of DFEs in terms of the parameters describing a communication channel. We show that the non-linear decision function in the DFE receiver has the effect of partitioning the space of channel parameters into a finite number of sets when the channel can be modelled (or approximated) by a finite impulse response (FIR) filter. We show that by examining this partition one is led naturally to classify some of the important *non-adaptive* properties of DFEs namely: (i) the error recovery time statistics; (ii) the input data sequences which result in arbitrarily long recovery times; and (iii) the identification of channels which are inappropriate for the use of DFEs as equalizers.

Error recovery and error propagation effects of DFEs have been the subject of several papers and our work forms a natural extension of previous ideas. Duttweiler,

Mazo and Messerschmitt [1] determine upper bounds on the steady state *error probability* of the DFE in terms of the probability of error in the absence of past decision errors. This bound is valid for arbitrary channels but questions regarding tightness were left open. More recently, O'Reilly and de Oliveira Duarte [2,3] extended the techniques and results in [1] by developing a procedure which gives upper and lower bounds on the steady state error statistics and recovery time statistics for a given channel. They are motivated by the need to reduce the computational effort associated with doing an exact calculation. (Their results are also valid for multilevel data and correlated noise.) A different approach to the stochastic analysis of DFEs was given by Cantoni and Butler [4,5] who gave a bound on the expected *error recovery time* which is also valid for arbitrary channels and the presence of noise. They include a discussion on the input sequences which result in poor DFE recovery performance. These references all use ideas based on finite state Markov processes (FSMPs) (see also [6]). This is true also of the analysis in this chapter [7,8].

Our contribution, in the first instance, is to analyze the DFE in terms of the noiseless (high signal to noise ratio) communication channel, and to show precisely how the channel parameters affect the stochastic dynamics of DFEs [7]. We provide exact calculations for the classes of channel which in our opinion are of greatest theoretical and practical interest. We emphasize that the stochastic analysis of DFEs can be conceptually reduced to the understanding of the one-to-one correspondence between disjoint polytopes in the space of channel parameters and a set of FSMPs (or more generally a set of state transition diagrams). Our results extend, generalize and clarify the important contributions in [4].

With the inclusion of noise into the analysis our contribution is not so much to extend the techniques and results found in [1-3] but rather to contrive noisy channels which realize the upper bounds in [1], thereby settling the open questions regarding tightness [8]. (These bounds are realized by manipulating the channel parameters typically in the presence of small noise, rather than by taking the limit as the noise variance increases [4].) It is not our intention to suggest that such contrived channels will or do arise in practice (although it is not clear that they do not). Rather, the merit of our results rests in showing the need for imposing stronger hypotheses in characterizing the channel parameters for practical systems (see Chapter 4). This would enable tighter bounds on the error probability to be derived, thereby better reflecting the DFE performance to be expected in practice. However, we argue that

imposing a minimum phase property on the (high signal to noise ratio) channels does not appear strong enough to guarantee improvements on the error rate bounds in [1]. Another consequence of our analysis is the suggestion that by adding dither to a DFE one may improve its error performance. Both these latter points seem, at least initially, to be counter-intuitive [8].

Finally, the explicit use of the recovery time bound derived by Cantoni and Butler [4,5] to give a straightforward proof of an error probability bound in [1], illuminates the non-trivial but close connection between the two important early contributions to the analysis of the error propagation mechanism in DFEs.

In this chapter we work exclusively using binary input sequences. The ideas could easily be generalized to handle M-ary inputs, at least in principle (see e.g., [2-5]). Later, in Chapter 4, we treat some closely related M-ary problems. (However in Chapter 4 we will return to look at error propagation without using an analysis based on FSMPs.)

We preview the contents of this chapter by section. Section 2.2 contains our definitions and a development of FSMPs used to analyze the non-adaptive stochastic dynamics of DFEs. The $N = 2$ tap DFE is treated in §2.3. By extending the results and concepts found in §2.3, we are able to treat in §2.4 the general $N \geq 2$ tap DFE. Then in §2.5 we treat the case where we have large noise, and this is complemented in §2.6 where we treat the asymptotic high signal to noise ratio case. A summary and discussion may be found in the conclusions §2.7.

2.2 Problem Formulation

2.2.1 System Definitions

The system under consideration is shown in Fig.2.1. It shows the communication channel modelled as a finite impulse response filter (FIR) driven by an equi-probable independent binary sequence $\{a_k\}$. (In Fig.2.1, q^{-1} denotes the delay operator.) The channel will be represented by a cursor $h_0 > 0$ paired with a tail $\underline{H} \stackrel{\triangle}{=} (h_1,\ h_2,\ \ldots,\ h_N)' \in I\!R^N$ (here v' represents the transpose of v). A discussion of a wide class of physical channels (defined by those which are minimum phase), which generally consist of a dominant cursor followed, but not preceded, by a series of echoes (the tail), is given by Clarke [9]. He advocates the use of DFEs for the equalization of these channels.

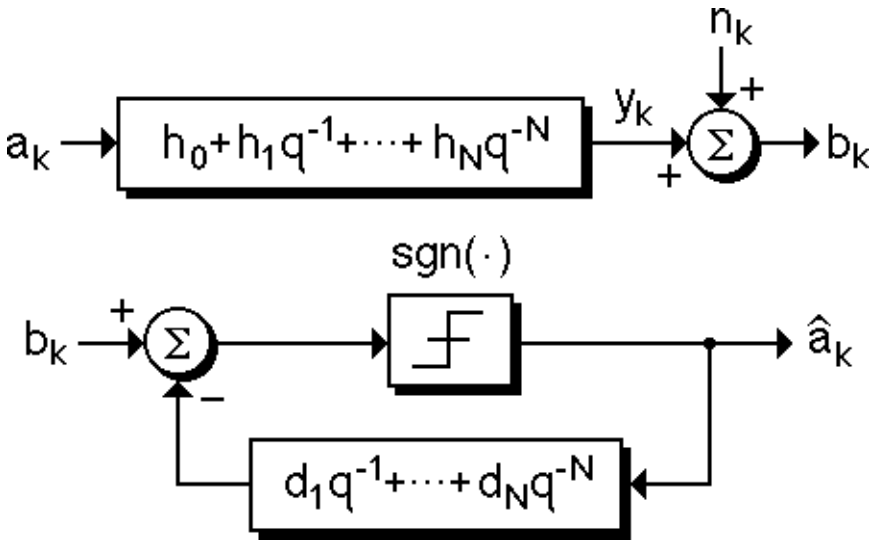

Fig.2.1 Channel and Decision Feedback Equalizer Model.

The effect of the channel tail is to introduce intersymbol interference (ISI) which corrupts the information carried with the cursor h_0, as in Fig.2.1. Additive channel noise n_k may also contaminate the received signal. The receiver structure attempts to remove the introduced ISI by modelling the channel tail with a tapped delay line which is represented by the vector of weights $\underline{D} \triangleq (d_1,\ d_2,\ \ldots,\ d_N)' \in I\!R^N$. Using estimates of the data $\widehat{a}_k$ rather than the actual data a_k, the channel ISI is reconstructed and cancelled at the receiver input b_k.

The data estimates $\widehat{a}_k$ are generated by a signum function sgn$(\cdot)$ which produces -1 for negative arguments and $+1$ otherwise (see Fig.2.1). The fundamental decision equation representing the output of the DFE is then given by

$$\widehat{a}_k = \mathrm{sgn}(h_0 a_k + \sum_{i=1}^{N} h_i a_{k-i} - \sum_{i=1}^{N} d_i \widehat{a}_{k-i} + n_k), \quad h_0 > 0. \tag{2.1}$$

This equation represents an idealization since it assumes that the length of the DFE tapped delay line equals the length of the channel tail (both N). Of course what is important in practice is that the number of taps in the DFE is sufficiently large to model the significant ISI generated by the channel. One can think of lumping any residual ISI caused by undermodelling (N too small) into the additive noise n_k implying (2.1) remains valid under suitable reinterpretation.

In a later section we treat the case where the channel noise in (2.1) is significant. In the mean time we take $n_k \equiv 0$ noting this will be a good pointer to the high signal-

to-noise ratio situation which is of greatest practical interest. Also it is well known that an attractive property of DFEs is that they provide a certain margin against noise because of the insensitivity of the signum function.

We assume the feedback tap weights take ideal tuned values, i.e., $\underline{D} = \underline{H}$, along with the noiselessness assumption. Under these conditions (2.1) simplifies to

$$\widehat{a}_k = \text{sgn}\left(h_0 a_k + \sum_{i=1}^{N} h_i(a_{k-i} - \widehat{a}_{k-i})\right), \quad h_0 > 0 \tag{2.2}$$

The idealized assumptions we have presented here can be relaxed. However, at this early stage of development we wish to keep things simple. In Chapter 4 we will see a more complete analysis but using different techniques.

Error recovery becomes an object of concern when previous decisions are incorrect since this increases the likelihood of further errors. In this situation the ISI is incorrectly cancelled and consequently an eye diagram closes [1]. This effect, termed error propagation, may result in unsatisfactory performance—typically as measured by error rates when noise is present or by the time it takes for the DFE to recover from an initial error condition (with or without noise).

Further, many DFE applications are adaptive and involve the adjustment of $\underline{D}$ on line in response to errors. It is important that the error recovery properties and the time scales of the correctly tuned DFE be understood before we can proceed with a sensible analysis of an adaptive DFE (as we will see in Chapter 3).

2.2.2 Finite State Markov Processes

Our analysis of the recovery statistics of DFEs uses the theory of finite state Markov processes (FSMPs) as have [1-6]. In modelling the DFE, we can assign a Markov state to the $2N$ binary vector of past data (channel states) and past decisions (DFE tapped delay line states) as follows:

$$X_k \triangleq (a_{k-1},\ \ldots,\ a_{k-N},\ \widehat{a}_{k-1},\ \ldots,\ \widehat{a}_{k-N})' \in \mathbb{Z}^{2N}. \tag{2.3}$$

Each component can take on two values; therefore, we have 4^N different Markov state vectors (2.3) which we refer to as *atomic states*. The complete set of atomic states will be denoted by Ω. The Markovian property arises since the input binary stream is a sequence of independent, equi-probable binary symbols, i.e., $\{a_k\}$ is a sequence of i.i.d. random variables.

We remark that this particular definition of an FSMP has not been used previously in the DFE literature. We will show that by aggregating atomic states, one obtains the FSMPs which appear in [1-5]. Further advantages of the 4^N atomic state Markov process are: (i) in the analysis of pathological input sequences (§2.3.2); and (ii) without modification it may be used to analyze the case when $\underline{D} \neq \underline{H}$ (e.g., with adaptive DFEs—Chapter 3). One advantage of aggregated FSMPs is reduced complexity because of lower dimensionality.

We introduce an ordering of the atomic states which will be particularly useful in §2.3.2. Any logical scheme can be used for this purpose, and we choose the following lexicographic rule which assigns a number $<\mathbf{i}>$ to an atomic state X_k, *viz.*,

$$<\mathbf{i}> \triangleq \frac{1}{2}\big((2^{2N-1},\ 2^{2N-2},\ \ldots,\ 4,\ 2,\ 1)\cdot X_k + 2^{2N} - 1\big), \tag{2.4}$$

e.g., with $N = 2$, $X_k = (-1,\ +1,\ +1,\ +1)'$ gets coded as $<\mathbf{i}> = 7$. In words, this cryptic formula simply gives the number associated with state X_k (2.3) considered as a $2N$-bit binary number with a_{k-1} the most significant bit, and $\widehat{a}_{k-N}$ the least significant bit (with $-1 \mapsto 0$). As a consequence $<\mathbf{i}> \in \{0,\ 1, \ldots,\ 4^N - 1\}$.

It is both convenient and computationally advantageous to aggregate the atomic states X_k into Markov states forming a new process. Such an aggregation forms an FSMP (capable of exactly modelling the transient properties of the atomic FSMP) if and only if the following properties holds (in all pairs of aggregated states $\mathcal{U}$ and $\mathcal{V}$). If the probability is p for one particular atomic state in an aggregated state $\mathcal{U}$ to transit to the set of atomic states in aggregated state $\mathcal{V}$, then all atomic states in $\mathcal{U}$ transit to $\mathcal{V}$ with the same probability p. In the DFE problem that we consider, such an aggregation is possible since the DFE tapped delay line weights correspond precisely to the channel tail. This implies that atomic states with particular past decision error patterns need not be distinguished, e.g., a correct decision when $a_k = -1$ has precisely the same effect on the distribution of future decisions as a correct decision when the data is $a_k = +1$. Using this observation, one can derive an FSMP where the states are

$$E_k \triangleq (e_{k-1},\ e_{k-2},\ \ldots,\ e_{k-N})' \in \mathbb{Z}^N \tag{2.5a}$$

where

$$e_k \triangleq a_k - \widehat{a}_k. \tag{2.5b}$$

These vectors will be referred to as E-states (short for error states). Each component of this vector can take a value in $\{-2,\ 0,\ +2\}$; hence, there are 3^N E-states. This

error model was used in [1,2,4,5] to model the stochastic dynamics of the DFE. For our purposes we introduce a yet more efficient structure which may be derived from the error model. We show that we can roughly halve the number of states in the error model by exploiting the symmetry in the a_k symbol probability density function.

The new aggregation pairs off the two E-states E_k and $-E_k$ defining a P-state (short for paired state). If $E_k = 0$, then this forms a P-state by itself. This new FSMP has $(3^N + 1)/2$ P-states, which means for $N = 2$, we can model the DFE dynamics with 5 states rather than 9 or 16. Proof that the resulting process is Markovian follows from two properties:

Property 2.1: *The input a_k takes values in $\{+1, -1\}$ with equal probability.* ❑

Property 2.2: *State E_k transits to state E_{k+1} if and only if state $-E_k$ transits to state $-E_{k+1}$ when the datum a_k is of opposite sign.* ❑

Proof: *Let $\boldsymbol{S} \in \mathbb{R}^{N\times N}$ be the shift matrix of subdiagonal ones; then from the definition of E_k (2.5a), we have the simple recursive formula [4]*

$$E_{k+1} = \boldsymbol{S}\cdot E_k + \big(a_k - \mathrm{sgn}(h_0 a_k + \underline{H}' E_k),\ 0,\ 0,\ \ldots,\ 0\big)' \tag{2.6a}$$

where we have used (2.5a) to rewrite (2.2) compactly as

$$\widehat{a}_k = \mathrm{sgn}(h_0 a_k + \underline{H}' E_k). \tag{2.6b}$$

Multiplying both sides of (2.6a) through by -1 we get

$$-E_{k+1} = \boldsymbol{S}\cdot(-E_k) + \big(-a_k - \mathrm{sgn}(h_0(-a_k) + \underline{H}'(-E_k)),\ 0,\ 0,\ \ldots,\ 0\big)' \tag{2.6c}$$

and this can be readily interpreted as Property 2.2. ❑

Hence, there is a one-to-one correspondence between an atomic state belonging to E_k and an atomic state belonging to $-E_k$. Both of these atomic states belong to the same initial P-state $\{E_k, -E_k\}$ and transit to the same destination P-state $\{E_{k+1}, -E_{k+1}\}$ (with data of the opposite sign). Because of Property 2.1, the transition probabilities are the same despite the transitions being made on data symbols with opposite signs. Hence the P-states form an FSMP as claimed.

A salient feature of both the error system and the P-state system is that the aggregation has created a single *absorbing state* corresponding to a closed set of 2^N

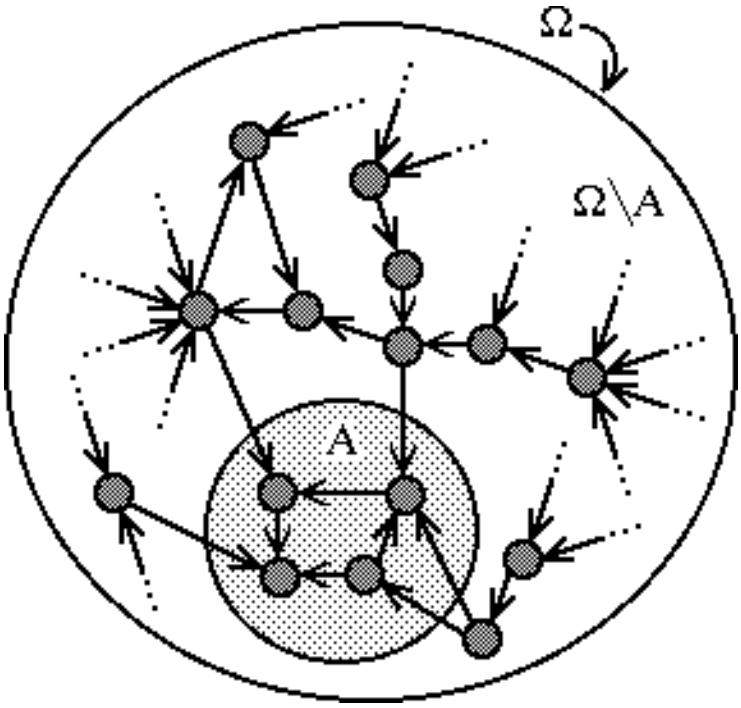

Fig.2.2 Atomic States Generic Form Representing Behaviour of DFE.

atomic states. These atomic states satisfy $\widehat{a}_{k-i} = a_{k-i}$, $\forall i \in \{0,\ 1,\ \ldots,\ N\}$, and they form a closed set since the only transitions from one such atomic state are to another in the set. We refer to this absorbing state as A (for absorbing), and it has the simple interpretation that if the system is in state A, then we have the last N decisions correct, and hence all future decisions will be correct. Naturally, once in A, the system stays in A (in the absence of further noise disturbances) and we say the DFE has *recovered*. We will denote the set of atomic states excluding A, i.e., the complement of A, by $\Omega \setminus A$. An abstract representation of these definitions is given in Fig.2.2†.

We make a further definition:

Definition: *The* ***error recovery time*** *is the first time k such that state $X_k \in A$, given some initial condition $X_0 \in \Omega \setminus A$.* ❑

(Note if $X_0 \in A$, then this is not an error state, so the error recovery time is defined as zero.) We model the initial error condition, e.g., a single noise induced error, in

† Flies feasting on a fried egg.

the DFE as an initial error distribution π_0 across the atomic states. Without loss of generality, we take the time of this disturbance as $k = 0$. For time $k > 0$, we assume the only subsequent decision errors are internally generated by the DFE through error propagation [1].

In a natural way, a distribution across the atomic states induces a distribution across the aggregated states $\overline{\pi}_0$, through a matrix $\boldsymbol{B}$,

$$\overline{\pi}_0 = \boldsymbol{B} \cdot \pi_0 \tag{2.7}$$

where $\boldsymbol{B}_{ij} \triangleq 1$ if $<\mathbf{j}>$ belongs to aggregated state i, and 0 otherwise. If we choose the P-state aggregation, $\boldsymbol{B}$ would have dimensions $(3^N + 1)/2$ by 4^N. When working with an aggregated state model, we will denote that part of the induced distribution excluding set A by $\overline{\pi}_0^*$, i.e., the partial distribution across $\Omega \setminus A$. Therefore we partition $\overline{\pi}_0$ as follows

$$\overline{\pi}_0 = \begin{pmatrix} \overline{\pi}_0^* \\ \text{----} \\ \sigma \end{pmatrix}. \tag{2.8}$$

Letting $\|\cdot\|_1$ denote the l_1-norm, we have $\sigma \triangleq 1 - \|\overline{\pi}_0^*\|_1 \in I\!R$, noting we have implicitly ordered the aggregated states with A last.

Remarks:

(i) The main restriction with aggregating atomic states is that we lose information by having our observations based on coarser objects, e.g., P-states rather than atomic states. However, in studying DFE error recovery, we are mainly concerned with observations on A and its complement $\Omega \setminus A$. These two sets are resolved by the P-states. Therefore, some of our general results can be modelled by P-states.

(ii) The P-states appear to be the lowest order FSMP for which we can exactly model the transient properties of DFEs. Lower order models appear in [1-3]. However, these are incapable of exactly modelling the nonstationary stochastic dynamics of DFEs on every channel.

2.3 Two Tap DFE

2.3.1 29 Classes of Channel

The decision equation governing the performance of the $N = 2$ tuned DFE is given

from (2.2) by

$$\widehat{a}_k = \mathrm{sgn}(h_0 a_k + h_1 e_{k-1} + h_2 e_{k-2}), \quad h_0 > 0. \tag{3.1}$$

The space of channel parameters (or equivalently, the space of tap parameters) will be called H-space, corresponding in this case to $\mathbb{R}^2$, within which lies $\underline{H} \triangleq (h_1,\ h_2)'$. (The cursor h_0 will be carried along implicitly or, equivalently, we could adopt a channel normalization.)

The set of lines in H-space given by

$$\{\underline{H} \in \mathbb{R}^2\colon\ h_1 t_1 + h_2 t_2 = h_0\} \tag{3.2}$$

where $(t_1, t_2) \in \big\{\{-2,\ 0,\ +2\} \times \{-2,\ 0,\ +2\}\big\} \setminus (0,\ 0)$, define the thresholds or switching hyperplanes of the $\mathrm{sgn}(\cdot)$ function in (3.1), and as such represent the boundaries between regions in H-space where the performance of the DFE is fixed. So the DFE performance does not depend continuously on $\underline{H}$, but varies in a quantized fashion. These regions are the intersection of half-planes with boundaries given in (3.2) and therefore represent polytopes in $\mathbb{R}^2$.

The eight boundaries of (3.2) partition H-space into the 29 polytopes of Fig.2.3. (This figure contains addition information which we will describe later. For clarity the bottom left insert shows the uncluttered polytope boundaries.) Hence, there are only 29 classes of channels to be considered, up to an arbitrary scaling factor (note how the cursor is represented in Fig.2.3).

Remarks:

(i) Two DFEs working on two different channels belonging to the same polytope, subject to the same data sequence $\{a_k\}$ and initial conditions, have indistinguishable output sequences. For example, channels $\{h_0 = 1,\ \underline{H} = (0.55, -0.03)'\}$ and $\{h_0 = 3,\ \underline{H} = (5, 1.4)'\}$ to a tuned binary DFE are equivalent.

(ii) With noise the position of the channel vector relative to the polytope boundary has a bearing on the DFE behaviour.

2.3.2 Pathological Sequences

As noted in [4], there may exist "pathological" input data sequences $\{a_k\}$, depending on the polytope, for which by definition the DFE never recovers from an initial error

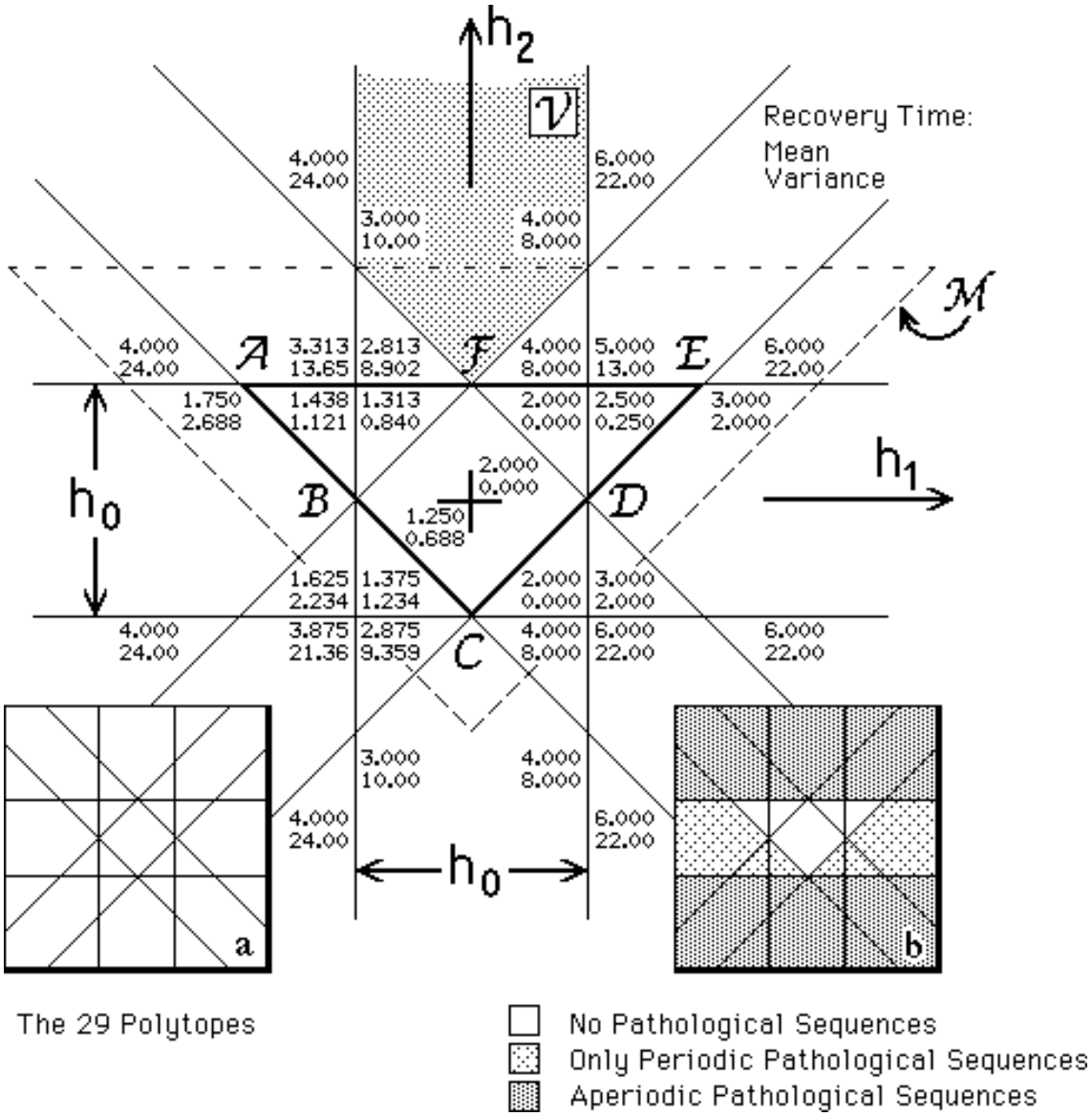

Fig.2.3 The 29 Classes of Channel for N=2 and Their Statistics.

state, i.e., the absorbing group of atomic states A is never reached. In this situation some decision errors must be made after any fixed but arbitrary time. However, from a stochastic viewpoint, it was demonstrated in [4] that these sequences have zero probability in the sense that the probability of the input sequence remaining pathological decreases to zero with time.

Our aim is to classify the pathological sequences in terms of the polytopes for $N = 2$. For brevity, our demonstration will be for one of the 29 polytopes, labelled $\mathcal{V}$

and shown shaded in Fig.2.3, which is defined by

$$\mathcal{V} \triangleq \{\, \underline{H} \in I\!R^2\colon\ \{h_0 > 2h_1\} \cap \{h_0 > -2h_1\} \cap \{h_0 < 2h_1 + 2h_2\} \\ \cap \{h_0 < 2h_2 - 2h_1\}\}. \qquad (3.3)$$

The remaining 28 polytopes may be treated in a similar fashion. (Generalizing the result for $N > 2$ proceeds analogously. However, the calculations become increasingly intractable the higher the order.)

We adopt the atomic FSMP consisting of the 16 atomic states indexed by (2.4) to classify the pathological input sequences for polytope $\mathcal{V}$. In Fig.2.4 we have shown a restricted state transition diagram where the four atomic states in the absorbing set

$$A \triangleq \{<\mathbf{0}>, <\mathbf{5}>, <\mathbf{10}>, <\mathbf{15}>\}$$

corresponding to recovery, have been deleted. Such a diagram encapsulates the complete ensemble of pathological input data sequences (by definition). We note there are an infinite number of periodic and aperiodic pathological input data sequences associated with polytope $\mathcal{V}$, e.g., we have the periodic sequence $\{+1,\ +1,\ -1,\ -1,\ +1, \ldots\}$ corresponding to the transitions $<\mathbf{1}> \rightarrow <\mathbf{8}> \rightarrow <\mathbf{14}> \rightarrow <\mathbf{7}> \rightarrow <\mathbf{1}> \ldots$, etc. The reader may wish to verify that the following sequence, when we begin in state $<\mathbf{1}>$, is pathological and deliberately aperiodic (or apparently so): $a_k \triangleq \{+1, -1, -1, -1,$ $+1, +1, -1, +1, +1, -1, -1, -1, +1, +1, -1, +1, +1, +1, -1, +1, +1, +1, -1, -1,$ $+1, -1, -1, -1, +1, -1, -1, +1, +1, -1, -1, -1, +1, +1, -1, +1, +1, -1, -1, -1,$ $+1, +1, -1, +1, +1, +1, -1, +1, +1, +1, -1, -1, +1, -1, -1, -1, +1, +1, -1, -1,$ $+1, -1, -1, -1, +1, -1, -1, +1, +1, -1, -1, -1, +1, +1, -1, +1, +1, -1, -1, -1,$ $+1, +1, -1, +1, +1, +1, -1, +1, +1, +1, -1, -1, +1, -1, -1, -1, \ldots\}$.

In Fig.2.4 we also delineate the critical (shaded) and non-critical (non-shaded) atomic states of the polytope $\mathcal{V}$. When in a non-critical state, the input datum is essentially "DON'T CARE" and the system cannot recover in one step. This defines a purely stochastic component of a pathological input sequence—the source of potential aperiodicity. In a critical state, shown shaded in Fig.2.4, we have only a probability of 1/2 of remaining pathological. For the 28 remaining polytopes we may have: (i) no pathological input sequences; (ii) only periodic pathological input sequences; or (iii) as in polytope $\mathcal{V}$, both periodic and aperiodic pathological sequences. In the next subsection we will determine to which of these three classes each of the 29 polytopes belongs.

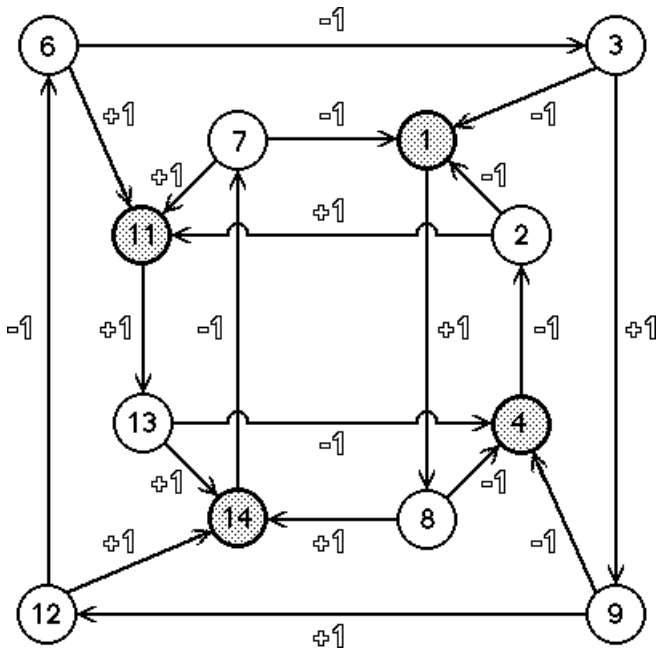

Fig.2.4 Pathological Sequence Diagram for Polytope $\mathcal{V}$.

2.3.3 Finite Recovery Time Polytopes

In the previous subsection we referred to the existence of polytopes for which the set of pathological sequences was empty. In view of the definition of pathological sequences, this implies that after some fixed time k and for all input sequences, we must have $X_k \in A$, i.e., a finite recovery time. (This recovery time is finitely bounded because there are only a finite number of atomic states.) In this subsection we determine necessary and sufficient conditions for an $N = 2$ polytope to have this property. In [4] it was shown that a necessary condition on the channel parameters for there to be no pathological sequences is that they lie in the triangle **ACE** of Fig.2.3. In the following, we demonstrate that this is also a sufficient condition.

Theorem 2.3: *A necessary and sufficient condition on the channel parameters, given by the pair* $\{h_0, \underline{H}\}$*, for the DFE to have a bounded recovery time is* $\underline{H} \in$ **ACE** *(Fig.2.3).* ❑

Proof: *Define sets:*

$$G_{01} \triangleq \{<\mathbf{1}>, <\mathbf{4}>, <\mathbf{11}>, <\mathbf{14}>\} \text{ where } e_{k-1} = 0 \text{ and } e_{k-2} \neq 0$$

$$G_{10} \triangleq \{<\mathbf{2}>, <\mathbf{7}>, <\mathbf{8}>, <\mathbf{13}>\} \text{ where } e_{k-1} \neq 0 \text{ and } e_{k-2} = 0$$

$$G_{11} \triangleq \{<\mathbf{3}>, <\mathbf{6}>, <\mathbf{9}>, <\mathbf{12}>\} \text{ where } e_{k-1} \neq 0 \text{ and } e_{k-2} \neq 0$$
$$A \triangleq \{<\mathbf{0}>, <\mathbf{5}>, <\mathbf{10}>, <\mathbf{15}>\} \text{ where } e_{k-1} = 0 \text{ and } e_{k-2} = 0.$$

In Fig.2.5 we have abstractly represented these sets along with possible (but not certain) transitions, noting it is not a FSMP because the Markovian property generally does not hold. Referring to (3.1), if we constrain $\underline{H}$ *to lie in the horizontal strip* $\mathcal{R}_0 \triangleq \{\underline{H}\colon\ |2h_2| < h_0\}$*, and let* $X_k \in G_{01}$*, then* $h_0 > |h_1 e_{k-1} + h_2 e_{k-2}|$*, whence* $X_{k-1} \in A$*, i.e., the DFE recovers (i.e., the path labelled a in Fig.2.5 is impossible for channels in* $\mathcal{R}_0$*). Now if instead we let* $X_k \in \{G_{10} \cup G_{11}\}$*, then either* $X_{k+1} \in G_{11}$ *or* $X_{k+1} \in G_{01}$*. In the latter case we get* $X_{k+2} \in A$*. Hence any pathological sequence must consist only of transitions constrained within the set* G_{11} *(ignoring the first transition). However, the only possible* $G_{11} \rightarrow G_{11} \rightarrow G_{11} \rightarrow \ldots$ *transitions are: (i)* $<\mathbf{3}> \rightarrow <\mathbf{3}> \rightarrow <\mathbf{3}> \rightarrow \ldots$ *and* $<\mathbf{12}> \rightarrow <\mathbf{12}> \rightarrow <\mathbf{12}> \rightarrow \ldots$ *for the half-plane region* $\mathcal{R}_1 \triangleq \{\underline{H}\colon\ h_0 < -2h_1 - 2h_2\}$*; (ii)* $<\mathbf{6}> \rightarrow <\mathbf{9}> \rightarrow <\mathbf{6}> \rightarrow \ldots$ *for the half-plane region* $\mathcal{R}_2 \triangleq \{\underline{H}\colon\ h_0 < 2h_1 - 2h_2\}$*. Note the region defined by* $\{\underline{H}\colon\ \mathcal{R}_0 \backslash \{\mathcal{R}_1 \cup \mathcal{R}_2\}\}$ *is identical to the triangle* **ACE** *(Fig.2.3). Therefore there are no pathological sequences inside triangle* **ACE***. Given that being in triangle* **ACE** *is a necessary condition on the channel parameters [4], then Theorem 2.3 follows.*❑

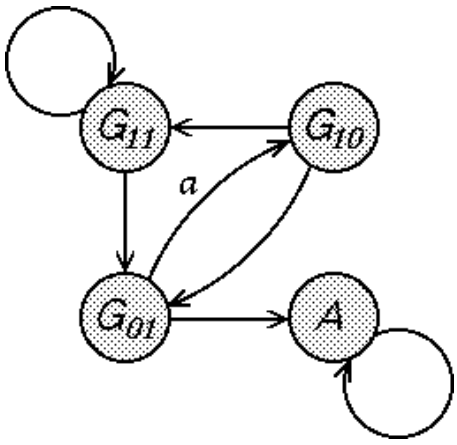

Fig.2.5 Pictorial Representation of Sets Defined in Theorem 2.3.

Remarks:

(i) Triangle **ACE** defines the union of five polytopes (see Fig.2.3) which have an empty set of pathological sequences. This region determines necessary and sufficient conditions for stability as defined in [4]. The definition of stability given in

[4] is precisely equivalent to the statement that any error recovery time is finite. In Chapter 4 we will investigate further this stability question using passivity techniques.

(ii) The six polytopes in $\{\underline{H}\colon\ \mathcal{R}_0 \setminus \{\mathbf{ACE}\}\}$ have only pathological input sequences which are periodic (see the sequences listed above in the proof of Theorem 2.3 for the two regions $\mathcal{R}_1$ and $\mathcal{R}_2$). These six polytopes are shown lightly shaded in the lower right insert in Fig.2.3.

(iii) The 18 polytopes in $\{\underline{H}\colon\ I\!R^2 \setminus \mathcal{R}_0\}$, including polytope $\mathcal{V}$ (3.3), have both periodic and aperiodic pathological sequences since the non-critical set G_{10} is reachable from set G_{01}. (Recall, a set of atomic states is critical if A is reachable in one step.) These 18 polytopes are shown heavily shaded in the lower right insert in Fig.2.3.

In Fig.2.3 we have superimposed a region labelled $\mathcal{M}$ defining the class of (second order) minimum phase channels (zeros inside the unit circle). It is interesting to note that triangle **ACE** is contained wholly within $\mathcal{M}$. We will return to relationship between our channel classification and minimum phase channels in §2.4.4.

2.3.4 Mean Error Recovery Time

Pathological sequences represent the worst case situation since arbitrarily long recovery times are possible. However, as pointed out in [4], pathological sequences have a special structure which makes their occurrence among the ensemble of sequences $\{a_k\}$ events of zero probability. This is implied by the upper bound derived in [4] for the mean error recovery time. (We will have some more to say about the probabilistic nature of pathological sequences in §2.4.5.) It therefore becomes relevant to determine the statistical error recovery properties of DFEs rather than examine improbable (pathological) behaviour.

The specific aims of this section are to demonstrate how the 29 polytopes (and hence the particular class of channel) affect the mean and variance of the recovery time and to give some general formulae for the recovery statistics. Each of the 29 polytopes defines a different probability transition matrix $\boldsymbol{P}$ which describes the stochastic dynamics of the DFE for that class of channel. The FSMP we choose for our following $N = 2$ example is the P-state system consisting of only five aggregated states.

The probability transition matrix $\boldsymbol{P}$ and the associated induced initial error distribution $\overline{\pi}_0$ can always be represented in the following generic form (valid for any of the aggregations of atomic states that we consider here):

$$\boldsymbol{P} = \left(\begin{array}{c|c} \boldsymbol{Q} & \boldsymbol{0} \\ \hline r' & 1 \end{array}\right); \qquad \overline{\pi}_0 = \left(\begin{array}{c} \overline{\pi}_0^* \\ \hline \sigma \end{array}\right). \tag{3.4}$$

where we order the aggregated states with A last, r is some positive vector, and $\boldsymbol{Q}$ is a submatrix describing transitions between aggregated states belonging to $\Omega \setminus A$ (Fig.2.2) which has eigenvalues satisfying $\left|\lambda_i(\boldsymbol{Q})\right| < 1$. This non-trivial property of the eigenvalues follows from the theory of non-negative (and stochastic) matrices [10], as we now show. Theoretically it can be shown that the dominant eigenvalue of any stochastic matrix $\boldsymbol{P}$ is unity. The multiplicity of this eigenvalue corresponds to the number of irreducible closed subsets of the FSMP [11]. As will be shown in the proof of Theorem 2.4 in §2.4.3, the state A is reachable from all atomic states in $\Omega \setminus A$, and as such, there are no closed subsets within $\Omega \setminus A$. Only state A forms a closed subset of the FSMP, and therefore the unity eigenvalue of $\boldsymbol{P}$ is simple. The remaining eigenvalues of $\boldsymbol{P}$ are common to $\boldsymbol{Q}$ and this implies the eigenvalues satisfy $\left|\lambda_i(\boldsymbol{Q})\right| < 1$.

Determining the recovery time is precisely a study of transitions made to the absorbing state A. From the generic form (3.4), let matrix $\boldsymbol{T}$ be defined as

$$\boldsymbol{T} \triangleq (\boldsymbol{I} - \boldsymbol{Q})^{-1}. \tag{3.5}$$

(Note, matrix $\boldsymbol{T}$ is non-singular because $\left|\lambda(\boldsymbol{Q})\right| < 1$.) Then the mean and variance of the absorption (recovery) time K can readily be evaluated to yield a standard result in FSMPs. Let $E\{\cdot\}$ denote the expectation operator, then from [11, pp.89-99], the mean $\mu(\pi_0) \triangleq E\{K\}$ and the variance $\sigma^2(\pi_0) \triangleq E\{K^2\} - \mu(\pi_0)^2$ rewritten in our notation become

$$\mu(\pi_0) = \boldsymbol{1}'\,\boldsymbol{T}\cdot\overline{\pi}_0^* \tag{3.6a}$$

$$\sigma^2(\pi_0) = \boldsymbol{1}'(2\,\boldsymbol{T} - \boldsymbol{I})\,\boldsymbol{T}\cdot\overline{\pi}_0^* - \mu(\pi_0)^2 \tag{3.6b}$$

where $\overline{\pi}_0^*$ is determined from π_0 by (2.7) and (2.8), and where $\boldsymbol{1}$ denotes the vector of 1's of the appropriate dimension.

We now proceed to use (3.6a) and (3.6b) in calculating the first two moments of the recovery time statistics for each of the 29 polytopes, where we assume an initial

error distribution corresponding to (i) a single noise induced error π_0^n, and (ii) a uniform error distribution across the 16 atomic states, $\pi_0^u \triangleq \frac{1}{16}\cdot\boldsymbol{1}$. These are the two cases of greatest practical interest. The first models corruptive channel noise as a rare event (a high signal to noise ratio approximation). The second models a startup of the DFE where the N tap states $\widehat{a}_{k-i},\ i \in \{1,\ \ldots,\ N\}$ take arbitrary initial values (independent of $\{a_k\}$), e.g., during a reset or during power up.

We give an outline of the calculation for polytope $\mathcal{V}$ defined in (3.3) and shown in Fig.2.3 (the remaining 28 polytopes can be handled similarly). With the indexing in (2.4) the atomic states form the following 5 P-states: $P_1 \triangleq \{<\mathbf{3}>, <\mathbf{12}>\}$, $P_2 \triangleq \{<\mathbf{2}>, <\mathbf{7}>, <\mathbf{8}>, <\mathbf{13}>\}$, $P_3 \triangleq \{<\mathbf{6}>, <\mathbf{9}>\}$, $P_4 \triangleq \{<\mathbf{1}>, <\mathbf{4}>, <\mathbf{11}>, <\mathbf{14}>\}$ and $A \triangleq \{<\mathbf{0}>, <\mathbf{5}>, <\mathbf{10}>, <\mathbf{15}>\}$. The probability transition matrix (in the above ordering of P-states) for polytope $\mathcal{V}$ along with the noise induced error distribution $\overline{\pi}_0^n$ and the uniform error distribution $\overline{\pi}_0^u$ are

$$\boldsymbol{P} = \left(\begin{array}{cccc:c} 0 & 0 & 0.5 & 0 & 0 \\ 0 & 0 & 0 & 0.5 & 0 \\ 0.5 & 0 & 0 & 0 & 0 \\ 0.5 & 1 & 0.5 & 0 & 0 \\ \hdashline 0 & 0 & 0 & 0.5 & 1 \end{array}\right), \quad \overline{\pi}_0^n \triangleq \left(\begin{array}{c} 0 \\ 1 \\ 0 \\ 0 \\ \hdashline 0 \end{array}\right), \quad \overline{\pi}_0^u \triangleq \left(\begin{array}{c} 0.125 \\ 0.25 \\ 0.125 \\ 0.25 \\ \hdashline 0.25 \end{array}\right). \tag{3.7}$$

Note that with a single noise induced error we have $a_{k-1} \neq \widehat{a}_{k-1}$ and $a_{k-2} = \widehat{a}_{k-2}$, and this codes through (2.4) as one of four states in P_2 . The uniform atomic distribution induces a P-state distribution which has components in proportion to the cardinality of the 5 P-states, i.e., 2:4:2:4:4 in the above ordering.

Substituting for $\boldsymbol{Q}$ and $\overline{\pi}_0^*$ using (3.5) and (3.6) we get $\mu_k = 4$ and $\sigma_k^2 = 8$ for the first distribution, and $\mu_k = 3$ and $\sigma_k^2 = 10$ for the second. The remaining 28 polytopes can be handled similarly and Fig.2.3 summarizes the results for both distributions. (Due to a symmetry in the recovery time statistics for both distributions with respect to a sign change in h_1, we have saved space by giving the statistics for π_0^n on the right side of the Fig.2.3 and those for π_0^u on the left. For example, to determine the statistics for π_0^n for a "left" polytope we select the numbers in the mirror image "right" polytope, etc.) We make the following comments based on Fig.2.3:

Remarks:

(i) The inner l_1-ball **BCDF** (diameter h_0) has the best recovery statistics of the 29 polytopes for the two distributions.

(ii) For the uniform distribution (left hand entries), the maximum mean recovery time of $\mu_k = 4$ is associated with 8 symmetrically placed polytopes. We generalize this observation in §2.4.3. (Note, some of the channels in these polytopes are minimum phase.)

(iii) For the noise induced distribution (right hand entries), there are 5 polytopes clustered about the origin with deterministic recovery behaviour (zero variances). This shows that certain atomic states are unreachable from $\overline{\pi}_0^*$ (unlike the uniform distribution case). Therefore, conclusions regarding DFE performance based on the single noise induced error distribution alone could be misleading.

(iv) There is a symmetry with respect to h_1 sign change but not with respect to h_2 sign change. In general, we can demonstrate that H-space displays an asymmetry in the moments of the expected recovery time (for the two distributions considered) with respect to arbitrary sign changes of the components of $\underline{H}$ for $N \geq 2$. Therefore, the appearance of symmetry for h_1 with $N = 2$ can be regarded as anomalous.

In §2.4 we will have more to say on the polytopes where the slowest and quickest recovery times have been observed, for the general $N \geq 2$ case. Also, later in Chapter 4 we will investigate further those regions of parameter space for which the recovery time is finite regardless of the initial conditions or the input $\{a_k\}$ sequence.

2.4 General N-Tap DFE

2.4.1 Subspace Results

Let $\underline{H} = (h_1,\ h_2,\ \ldots,\ h_N)'$ be a tail of a channel and consider the subspace in $\mathbb{R}^N$ formed by setting $h_i = 0$ for $i \in \{3,\ 4,\ \ldots,\ N\}$. This degenerate channel is identical to the $\underline{H} = (h_1,\ h_2)'$ channel in $\mathbb{R}^2$. Hence, we can expect all the non-trivial properties of the $N = 2$ DFE to be present in the general $N > 2$ DFE, e.g., the existence of aperiodic pathological sequences, etc.

2.4.2 Finite Class of Channels

Here we generalize the results of §2.3.1. The decision equation (2.6b) is repeated here for convenience,

$$\widehat{a}_k = \operatorname{sgn}(h_0 a_k + \underline{H}' E_k), \quad h_0 > 0. \tag{4.1}$$

The $3^N - 1$ hyperplanes which partition H-space into a finite number of polytopes are given by the thresholds of the sgn$(\cdot)$ function, as follows,

$$\{\underline{H} \in I\!R^N\colon\ \underline{H}' T_N = h_0\} \tag{4.2}$$

where $T_N = (t_1,\ t_2,\ \ldots,\ t_N)' \in Z\!\!Z^N$ such that $(t_1,\ t_2,\ \ldots,\ t_N) \in \big\{\{-2,\ 0,\ +2\} \times \{-2,\ 0,\ +2\} \times \ldots \times \{-2,\ 0,\ +2\} \setminus (0,\ 0,\ \ldots,\ 0)$. (Note the cardinality of this set is $3^N - 1$.) The word *polytope* is reserved in this work for the smallest regions in $I\!R^N$ generated by the boundaries given in (4.2).

It is a difficult problem to determine the exact number of polytopes which result in this partition of $I\!R^N$. However, the number of polytopes $\mathcal{Z}_N$, can be bounded as follows,

$$2^N \cdot N! < \mathcal{Z}_N < 3^{(3^N-1)/2}. \tag{4.3}$$

The upper bound follows by considering the $(3^N - 1)/2$ pairs of parallel hyperplanes which each divide $I\!R^N$ into three regions. We can then generate a unique ternary number corresponding to each polytope where each digit identifies in which of the three regions the polytope lies. This (conservative) upper bound simply gives the total number of combinations of $(3^N - 1)/2$ ternary digits. The lower bound is easily deduced from arguments given in the next section (see Theorem 2.4; also further details are given in [7]). The size of $\mathcal{Z}_N$ for $N \geq 3$ prohibits a complete classification of channels. Hence it is important to identify those polytopes which represent the extremes in DFE behaviour and whether these extremes are physically relevant. In the next subsection we examine precisely those restricted classes of channel which represent the best and worst in terms of the DFE mean recovery time performance.

2.4.3 Mean Recovery Time Bounds

Cantoni *et al.*, [4] address the problem of bounding the mean recovery time and by using the theory of success runs they demonstrated that an upper bound was (in their notation) $\mu(\frac{1}{2}, N) = 2(2^N - 1)$. We will show that this is the tight bound when we have the worst case class of channel (to be defined) and a single noise induced error. (This bound is tight in the sense that we define channels which realize the value of the bound.) The aims of this section are to give both the tight upper and lower bounds for the mean recovery time and to determine some of the corresponding polytopes,

i.e., classes of channel which realize these bounds. As in the previous section we will consider the two (same) initial error distributions of greatest practical interest.

We begin with some definitions before deriving our main result (Theorem 2.4). Let P_B denote the probability of a correct decision common to all atomic states belonging to some set B, e.g., if we set $B = A$ (the absorbing group of states) we have $P_A = 1$ (valid for all polytopes). We are interested in two cases:

(i) The polytopes where $P_{\Omega\setminus A} = 1$, i.e., before recovery the DFE always makes the correct decision.

(ii) The polytopes where $P_{\Omega\setminus A} = \frac{1}{2}$, i.e., before recovery the decision will be correct or incorrect with equal probability.

Theorem 2.4: *(a) There exists a single polytope where* $P_{\Omega\setminus A} = 1$.
(b) There exists at least $2^N \cdot N!$ *polytopes where* $P_{\Omega\setminus A} = \frac{1}{2}$. ❑

Proof: *(a) In polytope* $\{\underline{H} \in I\!R^N\colon\ h_0 > 2\cdot\|\underline{H}\|_1\}$ *we have* $h_0 > \max_{E_k}(\underline{H}'E_k)$, *i.e., the residual ISI can never be of sufficient magnitude to corrupt the decision. Therefore, directly from (4.1), this implies* $P_{\Omega\setminus A} = 1$. *Conversely, if the channel lies in the region* $\{\underline{H} \in I\!R^N\colon\ h_0 < 2\cdot\|\underline{H}\|_1\}$, *then there exists at least one* T_N *(4.2) such that* $|\underline{H}'E_k| > h_0$ *and so when the system is in state* $E_k = T_N$ *it makes an incorrect decision with* $a_k = -\operatorname{sgn}(\underline{H}'T_N)$.

(b) If $a_k = \operatorname{sgn}(\underline{H}'E_k)$ *then* $\widehat{a}_k = a_k$, *see (4.1). (This proves set A is always reachable in at most N steps from all atomic states. Further, this implies that matrix* $\boldsymbol{Q}$ *defined in (3.4) has all its eigenvalues bounded above in magnitude by unity, since there is always a non-zero probability of exiting from* $\Omega\setminus A$.*) Therefore,* $P_{\Omega\setminus A} = \frac{1}{2}$ *if and only if we make an incorrect decision with* $a_k = -\operatorname{sgn}(\underline{H}'E_k)$ *for all* $E_k \neq 0$. *Construct the following polytope (c.f., (4.2)),*

$$\Big\{\underline{H} \in I\!R^N\colon\ \{2h_1 > h_0\} \cap \{2h_2 > h_0 + 2h_1\} \cap \ldots \cap \{2h_N > h_0 + 2\sum_{i=1}^{N-1} h_i\}\Big\}. \quad (4.4)$$

For any channel $\underline{H}$ *in this region we have* $|\underline{H}'E_k| > h_0$ *for all* $E_k \neq 0$. *(By construction we have spaced the* h_i *sufficiently far apart; see also Theorem 2.5 later.) Therefore when* $a_k = -\operatorname{sgn}(\underline{H}'E_k)$ *we necessarily have* $\widehat{a}_k \neq a_k$. *This gives the desired result. Further, there are precisely* $2^N \cdot N!$ *polytopes of this form obtained by* 2^N *sign changes and* $N!$ *permutations of the channel vector* $\underline{H}$. *If*

$N > 2$ there are additional polytopes such that $P_{\Omega\setminus A} = \frac{1}{2}$, e.g., consider $h_0 = 2$ and $\underline{H} = (9,\ 11,\ 15)'$, where the h_i are positive and increasing but do not conform to (4.4). However, polytopes of the form (4.4) have a vertex with the least l_1-norm and in this sense are the nearest $P_{\Omega\setminus A} = \frac{1}{2}$ polytopes to the origin. ❑

We adopt the terminology "best case class of channel" and "worst case class of channel", respectively, for the two cases considered in Theorem 2.4. Clearly the terminology is justified in the former case since decision errors (in the absence of noise) are never made. In the latter case, we claim the recovery time is maximized when $P_{\Omega\setminus A} = \frac{1}{2}$. This fact can be deduced from an important and intuitively reasonable result in [5] whose proof needs a lengthy formal argument. In our notation this result takes the form,

$$Pr(X_k \in A \mid P_{\Omega\setminus A} = \frac{1}{2},\ \pi_0) \leq Pr(X_k \in A \mid \pi_0,\ n_k). \tag{4.5}$$

In words, the slowest (conceivable) recovering DFE system is precisely one where the probability of a correct decision for all atomic states before recovery is $\frac{1}{2}$. This is true for all arbitrary initial (error) distributions and whether or not noise n_k (which is independent and symmetrically distributed) is present. (In a later section we treat the noisy case where $n_k \neq 0$.)

We now evaluate the mean recovery times for the two classes of channel considered in Theorem 2.4 and thereby obtain lower and upper bounds on the mean recovery times for all channels. Clearly for $P_{\Omega\setminus A} = 1$ channels, we obtain a lower bound noting that the error recovery is deterministic. Therefore, for this case we simply note that the recovery time is bounded above by N. In fact, from elementary considerations, the "mean" recovery time realizes this bound when we have a single noise induced error.

The calculation for the $P_{\Omega\setminus A} = \frac{1}{2}$ channels, giving the upper bounds, is less straightforward than that for the lower bounds. It is possible to compute the mean recovery time bounds as a function of π_0, however, for brevity we compute the bounds for the two important practical cases. We use the theory in [4] to determine the upper bound when we start from the single noise induced error distribution π_0^n. From such a distribution we need to make N consecutive correct decisions each of probability $\frac{1}{2}$ to recover. However this mean recovery time was computed in [4] by using the theory of success runs and is given by

$$\mu(\pi_0^n) = 2(2^N - 1). \tag{4.6}$$

(This bound is also derived in [3].) However, our calculation is for an explicit channel, e.g., any channel satisfying (4.4), and not for a hypothetical one [4]. (As pointed out in [4], the bound (4.6) becomes "tight" in the low signal to noise ratio limit. As the symmetric noise variance increases, the probability of a correct decision tends to $\frac{1}{2}$, independent of the channel.)

From (4.6) we may regard a single noise induced error as being in the worst case class of initial error distributions when working on the worst case class of channel. However, for other channels the single noise induced error need not represent the worst case amongst all distributions.

The second initial error distribution of interest is the uniform atomic distribution π_0^u. In this case the mean recovery time can be shown to be

$$\mu(\pi_0^u) = 2(2^N - 1) - N \tag{4.7}$$

by an elementary but tedious calculation. A more extensive treatment of calculations involving mean recovery times, their variances and error propagation effects may be found in [2,3]. Our contribution to this style of analysis is to demonstrate that actual channels result in behaviour best described as pathological. However, the question as to the physical significance of these channels needs to be addressed. This is the subject of the next subsection.

2.4.4 Minimum Phase Channels

We make some remarks regarding whether $P_{\Omega\setminus A} = \frac{1}{2}$ polytopes contain minimum phase channels. Sensible models for physical channels should be causal and (nearly) minimum phase [9]. Note in (4.4) we have a region whose channel impulse responses increase at least exponentially. It is extremely dubious whether such a channel would exist in practice or that a DFE would be contemplated for its equalization. Channels of the form (4.4) appear to be (nearly) maximum phase. However, (4.4) represents only one of a class containing $2^N \cdot N!$ polytopes. Another, more interesting, polytope in this class is represented by

$$\Big\{ \underline{H} \in I\!R^N \colon \{2h_N > h_0\} \cap \{2h_{N-1} > h_0 + 2h_N\} \cap \ldots \cap \{2h_1 > h_0 + 2\sum_{i=2}^{N} h_i\} \Big\}. \tag{4.8}$$

When $N = 2$ this polytope intersects the triangular minimum phase region (see §2.3.3 and Fig.2.3). We conclude in this case there exist minimum phase channels with

the worst possible error recovery performance. For $N > 2$ we have been able to demonstrate that polytope (4.8) contains "nearly" minimum phase channels, i.e., those with only one zero outside the unit circle and $N-1$ zeros inside. In fact it is easy to see that channels with this property always exists (but not necessarily in polytope (4.8)) as the following calculation shows:

Theorem 2.5: *There exist $P_{\Omega\setminus A} = \frac{1}{2}$ channels $\{h_0,\ \underline{H}\}$ with at least $N-1$ stable zeros.* ❑

Proof: *Pick any $\underline{H}$ such that $h_1 + h_2 q^{-1} + \ldots + h_N q^{-N+1}$ has $N-1$ zeros inside the unit disk in the complex plane $\mathbb{C}$. Call these $\{z_i \in \mathbb{C}\colon\ |z_i| < 1\}$. If we pick the cursor $h_0 = \epsilon > 0$ then the channel*

$$\epsilon + h_1 q^{-1} + h_2 q^{-2} + \ldots + h_N q^{-N} \tag{4.9}$$

will have $N-1$ zeros approaching the $N-1$ zeros z_i as $\epsilon \to 0^+$, by continuity. Therefore for some $\epsilon_1 > 0$ (4.9) will have at least $N-1$ stable zeros whenever $0 < \epsilon < \epsilon_1$. Note the remaining zero of (4.9) will tend to be unstable because the product of all N zeros is necessarily h_N/ϵ which blows up as $\epsilon \to 0$. Now we can pick ϵ sufficiently small (in a different context) to ensure (4.9) is a $P_{\Omega\setminus A} = \frac{1}{2}$ channel. To see this, we construct $\epsilon > 0$ such that

$$\epsilon < \min_{T_N} \left| \underline{H}' T_N \right| \triangleq \epsilon_2 \tag{4.10}$$

where T_N is defined as in (4.2), and the arguments mirror those in Theorem 2.4. Equation (4.10) is subject to a mild condition $\underline{H}' T_N \neq 0,\ \forall T_N$ which can be easily avoided when choosing an $\underline{H}$. With the choice $\epsilon < \min\{\epsilon_1, \epsilon_2\}$ we guarantee at least $N-1$ stable zeros for a $P_{\Omega\setminus A} = \frac{1}{2}$ channel (4.9). ❑

We have been unable to determine, absolutely, whether there are any minimum phase channels in the class of all $P_{\Omega\setminus A} = \frac{1}{2}$ polytopes (though we do not believe there are any minimum phase channels in the $2^N \cdot N!$ $P_{\Omega\setminus A} = \frac{1}{2}$ polytopes constructed in Theorem 2.4 for $N > 2$).

We remark that discretization of continuous minimum phase channels (zeros only in the left half plane) need not result in a discrete minimum phase channel. There are two possible causes for this. Firstly sampling a continuous minimum phase channel

with clock skew can easily result in a non-minimum phase discrete channel. The second cause is a result well known in the control literature. In [12], Åström *et al.*, show that a zero-order-hold discretization of a minimum phase continuous system with a high frequency roll-off of greater than 12dB/octave always results in a non-minimum phase discrete system at sufficiently high sampling rates. Further, this may happen for quite reasonable sampling rates [12]. Therefore, for this second case, the fact that we have a worst case channel with only one zero outside the unit circle (non-minimum phase) does not negate the possibility that the continuous model of the channel is minimum phase.

2.4.5 Asymptotically Tight Recovery Time Bound

The intention here is to give an asymptotic formula for the probability of a DFE failing to recover by time k, starting from an arbitrary error distribution when we have the worst case class of channel (where $P_{\Omega \setminus A} = \frac{1}{2}$). This then forms an asymptotically tight upper bound on the DFE error recovery performance versus time, upon invoking (4.5). (The bound is asymptotically tight in the sense that there exist channels whose recovery time corresponds with the bound.)

To simplify subsequent calculations we consider a new aggregation of atomic states which reduces the order of the DFE model from 4^N atomic states to $N + 1$ aggregated states. This simpler system is defined in [3] (which is based, in turn, on ideas in [1]). The new states in Fig.2.6 are labelled according to "recovery distance" [3]. An atomic state belongs to the aggregated state i if the DFE requires i consecutive correct decisions to reach set A (also an aggregated state).

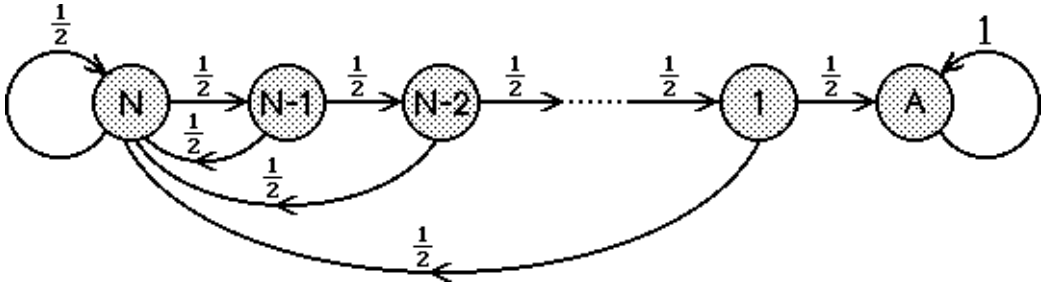

Fig.2.6 Finite State Markov Process for a Worst Case Channel.

We now describe why the fixed transition probabilities shown in Fig.2.6 are appropriate for any $P_{\Omega\setminus A} = \frac{1}{2}$ channel. As correctly pointed out in [1] the aggregation depicted in Fig.2.6 will not preserve the Markov property of the original atomic FSMP (i.e., the transition probabilities between aggregated states will not be constants, in general). So, in general, the transition probabilities between aggregated states would be quantities varying according to the particular atomic state within the aggregated state. However, for a $P_{\Omega\setminus A} = \frac{1}{2}$ channel all the atomic states within $\Omega \setminus A$ have identical probabilities of $\frac{1}{2}$, by definition. Hence the probability of transiting: (i) from aggregated state i to $i-1$ (a correct decision) is $\frac{1}{2}$; and (ii) from aggregated state i to N (an incorrect decision) is $\frac{1}{2}$. This is precisely what is represented by Fig.2.6. Therefore, Fig.2.6 represents a valid FSMP capable of exactly modelling a DFE on a $P_{\Omega\setminus A} = \frac{1}{2}$ channel.

We remark that the use in [3] of models similar to Fig.2.6 is a device for approximation that leads to upper and lower bounds on DFE performance. However, as noted in [3], if the upper and lower bounds coincide then the approximation scheme is exact. This possibility is realized by our construction of $P_{\Omega\setminus A} = \frac{1}{2}$ channels.

We need a simple preliminary lemma before we demonstrate our main results.

Lemma 2.6: *The polynomial*

$$F(z) = z^N - \sum_{i=0}^{N-1} z^i \tag{4.11}$$

has: (i) one real simple root $z_1 \in (1,2)$ approximately given by $z_1 \approx 2-(2^N-1)^{-1}$; (ii) $N-1$ simple roots $z_i \in \mathbb{C}$ such that $|z_i| < 1$ for $i = 2,\ 3,\ldots,\ N$. □

Proof: *The Schur-Cohn matrix associated with (4.11) is given by $\boldsymbol{Y} \triangleq 2\boldsymbol{1}\boldsymbol{1}' - 2\boldsymbol{I}$ which has $N-1$ eigenvalues at -2 and one at $2N-2$ [13]. This shows that $N-1$ roots lie in $|z| < 1$ and one in $|z| > 1$. Since $F(1)F(2) < 1$, there is one root lying in the interval $(1,\ 2)$. The Newton approximation is easily checked. The derivative of $(z-1)F(z)$ has roots at 0 of multiplicity $N-1$ and a simple root at $2N/(N+1)$. Neither value is a root of $F(z)$. Therefore, all roots of $F(z)$ are simple.* □

With the worst case channel (modelled in Fig.2.6) and the aggregated state ordering $\{N,\ N-1,\ \ldots,\ 1,\ A\}$, the $\boldsymbol{Q} \in \mathbb{R}^{N\times N}$ matrix of the generic form (3.4) looks

like

$$\boldsymbol{Q} = \begin{pmatrix} 0.5 & 0.5 & \dots & 0.5 & 0.5 \\ 0.5 & 0 & \dots & 0 & 0 \\ 0 & 0.5 & \dots & 0 & 0 \\ \vdots & \vdots & & \vdots & \vdots \\ 0 & 0 & \dots & 0.5 & 0 \end{pmatrix}. \tag{4.12}$$

The eigenvalues of $\boldsymbol{Q}$ and the associated right and left eigenvectors are respectively,

$$\lambda_i(\boldsymbol{Q}) = \frac{1}{2}\, z_i, \quad i \in \{1,\ 2,\ \dots,\ N\} \tag{4.13a}$$

$$\nu_i = (z_i^{N-1},\ \dots,\ z_i^2,\ z_i)' \in I\!R^N \tag{4.13b}$$

$$\omega_i = \Big(1,\ \sum_{j=1}^{N-1} z_i^{-j},\ \dots,\ z_i^{-1} + z_i^{-2},\ z_i^{-1}\Big)' \in I\!R^N \tag{4.13c}$$

where z_i are the roots defined in Lemma 2.6. (Note $F(z)$ in Lemma 2.6 is the characteristic polynomial of the companion matrix $2\,\boldsymbol{Q}$.)

Theorem 2.7: *The probability of a DFE failing to recover by time k when operating on a worst case channel (lying in a $P_{\Omega\setminus A} = \frac{1}{2}$ polytope), starting from an initial error distribution π_0, is given by*

$$Pr\big(X_k \in \Omega \setminus A \;\big|\; P_{\Omega\setminus A} = \frac{1}{2},\ \pi_0\big) = (\widehat{\omega}_1{}'\overline{\pi}_0^*)\cdot\lambda_1^k(\boldsymbol{Q}) + o(2^{-k}) \tag{4.14}$$

where $\lambda_1(\boldsymbol{Q})$ is the dominant eigenvalue of matrix $\boldsymbol{Q}$ (4.12); π_0 and $\overline{\pi}_0^*$ are related through (2.7) and (2.8) using the aggregation depicted in Fig.2.6, and

$$\widehat{\omega}_1 \triangleq \frac{1-\alpha^N}{1-N\alpha^{N+1}}\ \Big(1,\ \ \sum_{j=1}^{N-1}\alpha^j,\ \ \sum_{j=1}^{N-2}\alpha^j,\ \dots,\ \alpha+\alpha^2,\ \ \alpha\Big)' \in I\!R^N \tag{4.15}$$

with $\alpha \triangleq \frac{1}{2}\cdot\lambda_1^{-1}(\boldsymbol{Q})$. ❑

Proof: *We outline the steps in the proof. Step 1: We normalize the left and right eigenvectors (4.13b) and (4.13c) corresponding to the dominant eigenvalue $\lambda_1^{-1}(\boldsymbol{Q})$ to yield $\widehat{\nu}_1$ and $\widehat{\omega}_1$ such that $\big\|\widehat{\nu}_1\big\|_1 = 1$ and $\big\|\widehat{\omega}_1\big\|_1 = 1$. Then $\widehat{\omega}_1$ is as given in (4.15). Step 2: Choose $\omega_1 = \widehat{\omega}_1$ and $\nu_1 = \widehat{\nu}_1$ and scale $\{\omega_1\colon\ i = 2,\ 3,\ \dots,\ N\}$ in (4.13c) such that $\omega_i{}'\nu_j = \delta_{ij}$ (Kronecker delta). Step 3: By the simplicity of the roots in Lemma 2.6 the basis $\{\nu_i\}$ spans $I\!R^N$. With this basis, $\overline{\pi}_0^* \in I\!R^N$ has components $\omega_i{}'\overline{\pi}_0^*$. In particular, the component in the direction of the dominant eigenvector*

is $\omega_1{}'\overline{\pi}_0^*$. Step 4: $\widehat{\omega}_1$ is a positive vector. Therefore with $\overline{\pi}_0^*$ non-zero and non-negative, we have $\omega_1{}'\overline{\pi}_0^* \in (0,1]$ (non-degeneracy). Step 5: From Lemma 2.6 the remaining eigenvalues behave asymptotically as $o(2^{-k})$ as $k \to \infty$. Step 6: Noting $Pr\big(X_k \in \Omega \setminus A \mid P_{\Omega\setminus A} = \frac{1}{2},\ \pi_0\big) = \left\| \boldsymbol{Q}^k \overline{\pi}_0^* \right\|_1$, then (4.14) follows from standard bounding arguments. ❑

Remarks:

(i) The dominant eigenvalue $\boldsymbol{Q}$ determines the asymptotic "leakage rate" to the absorbing state A, and is approximated by $\lambda_1 \approx 1 - (2^{N+1} - 2)^{-1}$ using Lemma 2.6. So the ability of the DFE to recovery from error on a worst case channel deteriorates with N increasing.

(ii) There are two initial error partial distributions (2.8) of practical interest corresponding to a single noise induced error

$$\overline{\pi}_0^* = (1,\ 0,\ \ldots,\ 0)' \in I\!R^N$$

and the uniform distribution across the atomic states which implies

$$\overline{\pi}_0^* = 4^{-N} \cdot (2^{2N-1},\ 2^{2N-2},\ \ldots,\ 2^N)' \in I\!R^N.$$

(iii) The error term $o(2^{-k})$ decays very rapidly with time, hence, the asymptotic formula is very accurate even for small k. Figure 2.7 gives an example of the theorem for $N = 3$ and distribution $\overline{\pi}_0^* = (1,\ 0,\ 0)'$ with the asymptotic formula shown as a straight line and the true $Pr(X_k \in \Omega \setminus A)$ as a sequence of diamonds.

(iv) This result is both simpler than and intimately related to the overbound (Theorem 4.1) found in [4] (note the variable x in [4] equals our $\lambda_1^{-1}(\boldsymbol{Q})$). Our result also makes explicit the role of the initial error distribution.

(v) This result gives the worst case probability bound associated with the input sequence remaining pathological at a given time k and for general N (c.f., §2.3.2).

Corollary 2.8: *Formula (4.14) forms the asymptotically tight bound as $k \to \infty$.* ❑

Proof: *This result follows directly from (4.5).* ❑

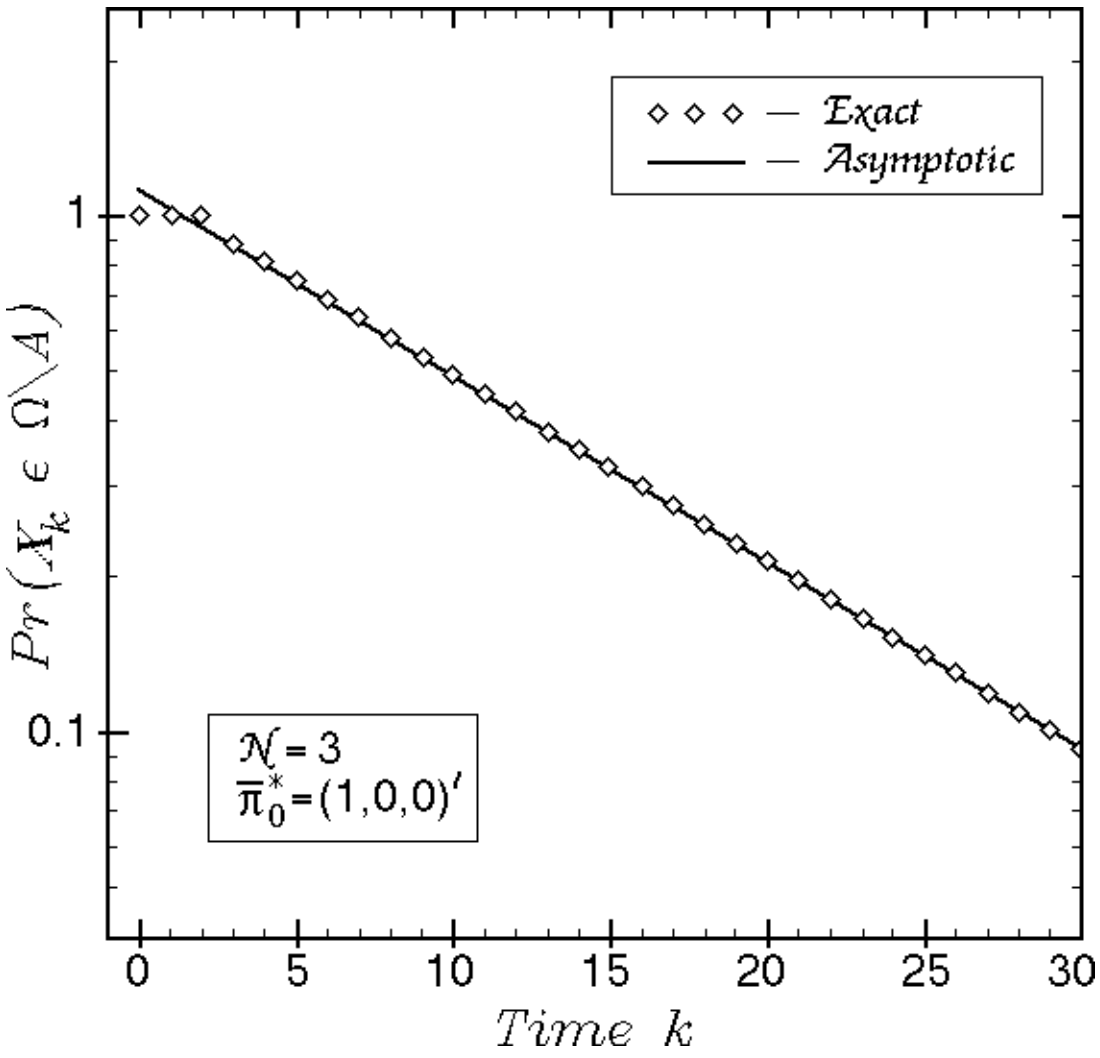

Fig.2.7 Example of Asymptotic Bound (Theorem 2.7).

Note in Corollary 2.8, the addition of noise n_k cannot make things worse in the sense that even without noise the error probability before recovery is $\frac{1}{2}$ which realizes the worst case. We will have more to say on the case where noise is significant in the next section. We conclude our discussion on the noiseless case by foreshadowing our results to be found in Chapter 4. In Chapter 4 we re-examine the noiseless error recovery problem with the objective of finding sufficient conditions on the channel parameters to ensure error recovery in a finite time, i.e., to ensure no pathological input sequences exist. The analysis to be found there also removes some of the weaknesses of the present analysis. Specifically the (implicit) assumptions regarding ideal tap settings, FIR channels and ideal modelling are relaxed. It is also possible to generate well-posed

error recovery problems for the case where errors are defined in the form

$$e_k(\delta) \triangleq a_{k-\delta} - \mathrm{sgn}(h_\delta)\widehat{a}_k$$

for some delay $\delta \in \{0,\ 1,\ \ldots,\ N\}$, rather than the error signal $e_k = a_k - \widehat{a}_k$ that we adopted in this chapter. We refer the reader to Chapter 4.

2.5 Error Recovery with Additive Noise

2.5.1 Background

In this section we study the range of performance that one can expect from a DFE as we vary across the class of noisy FIR channels used for binary transmission. We will be interested in finding a subclass of noisy channels which realize the worst possible error probability performance of the DFE. In the noiseless case, §2.4, it was meaningless to study steady state error probabilities because with probability one the DFE converges to a closed set of error-free states A. This implies the stationary error probability is zero. This situation changes with the introduction of channel noise (of sufficient amplitude) and we may observe unacceptably high error rates, reflected in a high error probability, in the DFE due to the error propagation mechanism, §2.3 [1].

In [1], Duttweiler, Mazo and Messerschmitt derive upper bounds on the stationary error probability for classes of noisy channels subject to various constraints. However, these bounds appear conservative and it seems natural to question the tightness of the bounds. Indeed, this very question is raised in the conclusions of [1]. We re-pose and solve this problem.

A significant advance on the work of Duttweiler *et al.*, [1] has appeared recently in the DFE literature. O'Reilly and de Oliveira Duarte [2,3] develop a procedure which gives upper and lower bounds on various error statistics for a given channel. (Their techniques are applicable to multi-level data sequences and correlated noise.) It is clear that this procedure produces an upper bound on the stationary error probability which cannot exceed that given in [1]. However, like [1], these results give no indication about what range of error probabilities one might expect, apart from what may be indicated by specific examples.

Our contribution to this style of analysis is not to extend the techniques and results found in [2,3] but rather to contrive noisy channels which realize the upper

bounds in [1], thereby settling the open questions regarding tightness. (These bounds are realized by manipulating the channel parameters, typically in the presence of small noise, rather than by taking the limit as the noise variance increases [4].) It is not our intention to suggest that such contrived channels will or do arise in practice (although it is not clear that they do not). Rather, the merit of our results rests in showing the need for imposing stronger hypotheses in characterizing the channel parameters for practical systems. Finally, the explicit use of the recovery time bound derived by Cantoni and Butler [4,5] to give a straightforward proof of an error probability bound in [1], illuminates the non-trivial but close connection between the two important early contributions to the analysis of the error propagation mechanism in DFEs.

We begin by filling out our previous notation from the noiseless case of the previous sections. The DFE decision equation which is central to our analysis is given by (2.1) and is repeated here for convenience (see Fig.2.1)

$$\widehat{a}_k = \mathrm{sgn}(h_0 a_k + \sum_{i=1}^{N} h_i a_{k-i} - \sum_{i=1}^{N} d_i \widehat{a}_{k-i} + n_k), \quad h_0 > 0 \tag{5.1}$$

Assuming, as in the noiseless case, correct tap weights $\underline{D} = \underline{H}$, the above equation reduces to

$$\widehat{a}_k = \mathrm{sgn}(h_0 a_k + \sum_{i=1}^{N} h_i e_{k-i} + n_k), \quad h_0 > 0 \tag{5.2}$$

which may be more compactly written,

$$\widehat{a}_k = \mathrm{sgn}(h_0 a_k + \underline{H}' E_k + n_k), \quad h_0 > 0 \tag{5.3a}$$

$$= \mathrm{sgn}(h_0 a_k + S_k + n_k) \tag{5.3b}$$

$$= \mathrm{sgn}(h_0 a_k + R_k) \tag{5.3c}$$

where we have introduced the shorthand $S_k \triangleq \underline{H}' E_k$ representing the residual intersymbol interference (ISI), and $R_k \triangleq S_k + n_k$ representing the residual ISI plus noise.

The channel noise n_k is assumed: (i) to be zero mean; (ii) to have finite variance $\sigma_n^2 < \infty$; (iii) to be independent of the data a_k and the residual ISI S_k; and (iv) to form an independent sequence. In some applications assumptions (iii) and (iv) are particularly important because they ensure one can use FSMP modelling for a noisy DFE as was done for the noiseless case in §2.3 and §2.4. Some of these assumptions are stronger than what is actually needed to derive useful results. In later subsections we will indicate when various assumptions can be dropped.

We make a simple but fundamental observation regarding (5.3c) which we state as a lemma:

Lemma 2.9: *(i) If* $a_k = \operatorname{sgn}(R_k)$ *then* $\widehat{a}_k = a_k$.
(ii) If $a_k = -\operatorname{sgn}(R_k)$ *then* $\widehat{a}_k \neq a_k$ *if and only* $\big|R_k\big| > h_0$. ❑

Most of our subsequent results centre on this simple result.

2.5.2 Global Error Probability Bound

In [1] it was established that the probability of error is always bounded above by $\frac{1}{2}$. In essence, this translates to a statement that having a DFE as a channel equalizer is generally better than not having one at all—but not always. We rederive this result because its proof will be useful in later sections, in different contexts. Using Bayes' rule, the probability of a decision error is given by

$$\begin{aligned} Pr(\widehat{a}_k \neq a_k) = Pr\big(\widehat{a}_k \neq a_k \;\big|\; a_k = \operatorname{sgn}(R_k)\big)\cdot Pr\big(a_k = \operatorname{sgn}(R_k)\big) \\ + Pr\big(\widehat{a}_k \neq a_k \;\big|\; a_k = -\operatorname{sgn}(R_k)\big)\cdot Pr\big(a_k = -\operatorname{sgn}(R_k)\big). \end{aligned} \tag{5.4}$$

Using Lemma 2.9, and the assumptions: (i) the data takes binary values with equal probability; and (ii) R_k is independent of a_k, then (5.4) reduces to

$$Pr(\widehat{a}_k \neq a_k) = \frac{1}{2}\cdot Pr(\widehat{a}_k \neq a_k \;\big|\; a_k = -\operatorname{sgn}(R_k)) \tag{5.5a}$$

$$= \frac{1}{2}\cdot Pr(\big|R_k\big| > h_0) \tag{5.5b}$$

and clearly this expression is bounded above by the global bound $\frac{1}{2}$. In §2.5.4 we construct a set of channels and a noise distribution which realize the pathological value of $\frac{1}{2}$. (This bound is realized without the assumption that the signal to noise ratio is vanishingly small in which case the error probability can be made arbitrarily close to the value $\frac{1}{2}$ [4].)

2.5.3 General Error Probability Bound

The second bound derived in [1] takes the form

$$P_E \leq \frac{\epsilon\cdot 2^N}{2\epsilon(2^N - 1) + 1} \tag{5.6}$$

where P_E is the probability of an error under stationarity, ϵ is the probability of error in the absence of past decision errors, and N is the number of taps. Our approach to demonstrating the tightness of (5.6) is simply to construct a channel and noise density which realizes the value of the bound. For simplicity and clarity we assume the channel noise magnitude can be bounded above by B_U as follows,

$$\left|n_k\right| \leq B_U < \infty. \tag{5.7}$$

(This requirement can be relaxed and Chebyshev's Inequality invoked to demonstrate the same bound in (5.6) works for unbounded noise with finite variance $\sigma_n^2 < \infty$. The analysis given in §2.6 is typical of the modification in style required to treat this more general case.)

The system we consider is given in Fig.2.8, which we shall now explain. (The state labelling and the transition probabilities marked on the arrows joining states need to be separately described. We will show subsequently that there exists a set of channels and noise densities for which Fig.2.8 represents an exact stochastic description, under suitable interpretation.) We adopt the "recovery distance" aggregated FSMP states given in [2,3]. (This set of aggregated states was also used to treat the noiseless channel case in §2.4.5.) In review, aggregated state 0 comprises the set of $2N$ atomic states which satisfy $E_k = 0$. (In §2.4.5 this set was called the set A.) Further, an atomic state X_k belongs to the aggregated state $i > 0$ if the DFE requires i consecutive correct decisions to reach aggregated state 0. Despite the fact that aggregated state 0 is no longer absorbing, as it was for the noiseless case, we will continue to refer to the DFE as having *recovered* when it is in aggregated state 0.

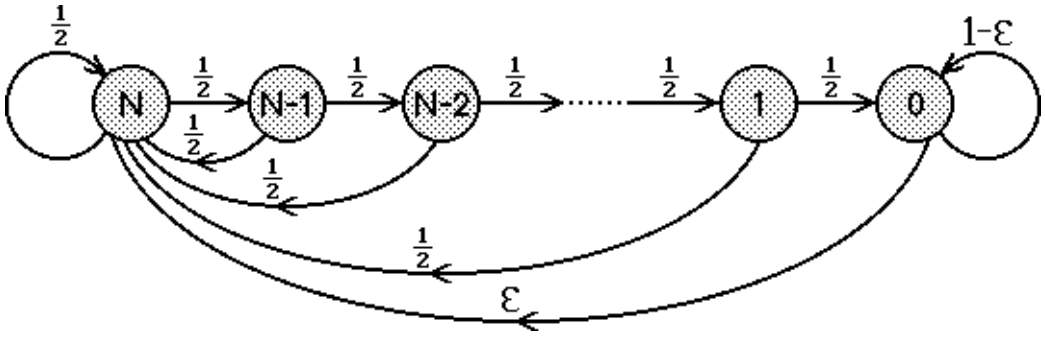

Fig.2.8 Finite State Markov Process of Bounded Noise Channel Class.

We now describe the transition probability assignments shown in Fig.2.8. When in aggregated state 0 (where $E_k = 0$) only noise can cause a decision error. With such an error the system transits to state N with probability ϵ defined by

$$\begin{aligned}\epsilon &\stackrel{\triangle}{=} Pr(\widehat{a}_k \neq a_k \mid E_k = 0) \\ &= \frac{1}{2}\cdot Pr(\left|n_k\right| > h_0) \end{aligned} \tag{5.8}$$

where we have used (5.5b) with $R_k = n_k$. Note, varying the channel tail $\underline{H}$ (keeping h_0 fixed) does not change ϵ. As will be clear from a definition of the channel given below this error probability is the same for all atomic states in aggregated state 0.

Next we consider the transitions emanating from the aggregated states N through to 1 in Fig.2.8. It is clear from the definition of recovery distance that if the DFE makes an error it transits to aggregated state N. Otherwise with each consecutive correct decision the index defining the aggregated state, i.e., the recovery distance, decrements. Now the transition probabilities shown in Fig.2.8 imply that for some *hypothetical* channel correct decisions occur with probability $\frac{1}{2}$ and incorrect decisions also with probability $\frac{1}{2}$ (in the presence of bounded noise). We realize this hypothetical channel by constructing a class of channels with the desired property.

Consider the DFE error probability *during recovery* (where $E_k \neq 0$). Then,

$$Pr(\widehat{a}_k \neq a_k \mid E_k \neq 0) = \frac{1}{2}\cdot Pr(\left|R_k\right| > h_0 \mid E_k \neq 0) \tag{5.9}$$

derived in analogy to (5.5b) except conditioned on the DFE not having recovered. To make this last expression equal to $\frac{1}{2}$ we simply need to ensure that R_k, considered as a random variable, has a conditional probability density which is zero in the interval $[-h_0,\ h_0]$. Now since the noise is assumed bounded above by B_U (5.7), it is sufficient that the random variable S_k has zero probability density in the interval $[-h_0 - B_U,\ h_0 + B_U]$. This in turn ensures that whilst the system is in the aggregated states where $E_k \neq 0$, the decision in (5.3a) is based solely on R_k, and therefore $\widehat{a}_k$ is completely uncorrelated with a_k. We can guarantee S_k has the desired property by a suitable choice of $\underline{H}$.

We assert that the non-empty region in the channel parameter space given by

$$\begin{aligned}\Big\{\underline{H} \in I\!R^N\colon\ \{2h_N > h_0 + B_U\}\ \cap\ \{2h_{N-1} > h_0 + 2h_N + B_U\}\ \cap\ \ldots \\ \cap\ \{2h_1 > h_0 + B_U + 2\sum_{i=2}^{N} h_i\}\Big\}\end{aligned} \tag{5.10}$$

defines a proper subset of the channels which have Fig.2.8 as their FSMP representation. We now show this. The formula (5.10) simply ensures the parameters $h_1 > h_2 > \ldots > h_N$ are spaced sufficiently far apart that $\left|\underline{H}'E_k\right| > h_0 + \left|n_k\right|$ for all $E_k \neq 0$. This implies, via the triangle inequality, that $\left|\underline{H}'E_k + n_k\right| > h_0$, i.e., $\left|R_k\right| > h_0$. Then using (5.9), we conclude that for all channels satisfying (5.10) one obtains $Pr(\widehat{a}_k \neq a_k \mid E_k \neq 0) = \frac{1}{2}$. Therefore, we have constructed a class of channels (5.10) where: (i) the statistical behaviour of the DFE before recovery is the same whether or not bounded channel noise is present; and (ii) Fig.2.8 is an exact stochastic description under suitable interpretation. We will now show how this property and our previous results for the noiseless case provide an elementary derivation and reinterpretation of the bound (5.6) derived in [1]. In the light of (5.8), we consider only the non-degenerate case where $Pr(\left|n_k\right| > h_0) > 0$ which ensures aggregated state 0 is non-absorbing, i.e., $\epsilon > 0$.

Example: *Let $N = 2$ and $\left|n_k\right| < 1.2$, i.e., $B_U = 1.2$ in (5.7). Then the channel $\{h_0 = 1,\ \underline{H} = (1.15,\ 2.26)'\}$ satisfies (5.10), noting that subject to $E_k \neq 0$, we have $\left|R_k\right|_{\text{MIN}} = 2 \times 2.26 - 2 \times 1.15 - 1.2 = 1.02$.*

Now consider Fig.2.8. When the system is in aggregated state 0 we can either: (i) continue normal error-free operation; or (ii) make a noise induced error. Once in aggregated state 0 the mean waiting time before a decision error is made is

$$t_1 \triangleq \epsilon^{-1} \tag{5.11}$$

from elementary considerations. With a decision error the system transits to aggregated state N. The mean time spent during recovery when we start in aggregated state N, is by construction the same as for the noiseless case (4.6), i.e.,

$$t_2 \triangleq 2(2^N - 1). \tag{5.12}$$

Now since the arrangement in Fig.2.8 depicts a FSMP, the time it takes to transit from aggregated state N to 0 is independent of the transitions which led the system to state N. Similarly for the case starting in 0 transiting to state N. Therefore under stationarity, the probability the system will be found in state 0 is given by $t_1/(t_1+t_2)$, and the probability the system is recovering (the complement event) is $t_2/(t_1 + t_2)$.

Therefore the stationary probability of error P_E for our constructed channels is simply given by Bayes' rule,

$$\begin{aligned} P_E &\triangleq Pr(\widehat{a}_k \neq a_k) \\ &= Pr(\widehat{a}_k \neq a_k \mid E_k = 0)\cdot Pr(E_k = 0) + Pr(\widehat{a}_k \neq a_k \mid E_k \neq 0)\cdot Pr(E_k \neq 0) \\ &= \epsilon\cdot\frac{t_1}{t_1 + t_2} + \frac{1}{2}\cdot\frac{t_2}{t_1 + t_2} \qquad (5.13a) \\ &= \frac{\epsilon\cdot 2^N}{2\epsilon(2^N - 1) + 1}. \qquad (5.13b) \end{aligned}$$

Expression (5.13b) is precisely the bound (5.6) derived in [1]. Hence we have established that this bound is tight, being achieved by certain noisy channels satisfying (5.7) and (5.10).

Remarks:

(i) A straightforward modification to the analysis also yields the same (supremum) bound given the assumption of unbounded channel noise with finite variance. In this case we select B_U (as a parameter rather than a bound) sufficiently large in the expression for the channel (5.10) to make P_E arbitrarily close to (5.13b). However, with larger B_U in (5.10) the resulting channels become more contrived and less likely to appear in practice.

(ii) In the high signal to noise ratio limit, i.e., as $\sigma_n^2 \to 0$, the channels that are analogous to (5.10), which yield a stationary error probability P_E that is arbitrarily close to the bound (5.6), are the $P_{\Omega\setminus A} = \frac{1}{2}$ polytopes considered in §2.4.3. (We give no formal proof of this but simply note that as $B_U \to 0$ in (5.10) we obtain a region which corresponds to a $P_{\Omega\setminus A} = \frac{1}{2}$ polytope in (4.4).) Hence, questions regarding the physical relevance of these high signal to noise ratio channels coincide with the questions raised in §2.4.4 concerning noiseless minimum phase channels.

(iii) Expression (5.13a) relates the worst case recovery time bound (5.12) derived in [4] to the error probability upper bound (5.6) derived in [1].

(iv) The independence assumption on $\{n_k\}$ is probably not needed in the above derivation because noise (by construction) only comes into play when $E_k = 0$. Provided R_k and n_k are independent the proof should carry through.

2.5.4 Range of Realizable Error Probabilities

In this subsection we contrive noise densities (distributions) which realize all values of ϵ in the interval $[0, \frac{1}{2}]$ and hence from (5.13b) all values of P_E in the interval $[0, \frac{1}{2}]$. Consider noise n_k which can be bounded above and below as follows,

$$h_0 < B_L \leq \left|n_k\right| \leq B_U. \tag{5.14}$$

Then the presence of the lower bound implies $\epsilon = \frac{1}{2}$ from (5.8). By §2.5.2, the presence of the upper bound ensures that a channel can be constructed (5.10) such that (5.13b) is realized. With $\epsilon = \frac{1}{2}$ in (5.13b) we get $P_E = \frac{1}{2}$, a most pathological situation. Constructing further noise densities yielding the remaining values in $[0, \frac{1}{2}]$ for P_E is straightforward but not of practical interest.

2.6 Asymptotically Tight Error Probability Bounds

2.6.1 Preliminary

As before let $\underline{H} \triangleq (h_1,\ h_2,\ \ldots,\ h_N)' \in I\!R^N$ and h_0 denote respectively the N-tap tail and cursor of a channel. We partition the tail $\underline{H}$ according to

$$H_n \triangleq (h_1,\ h_2,\ \ldots,\ h_n)' \in I\!R^n \quad \text{and} \quad H_d \triangleq (h_{n+1},\ h_{n+2},\ \ldots,\ h_N)' \in I\!R^{N-n}.$$

With an l_1-norm overbound on H_d given by

$$\left\|H_d\right\|_1 < \frac{1}{2}{\cdot}h_0, \tag{6.1}$$

Duttweiler *et al.*, [1], were able to demonstrate that asymptotically as $\sigma_n^2 \to 0$

$$P_E \leq \epsilon{\cdot}2^n \tag{6.2}$$

subject to mild constraints on the shape of the impulse response tail (it needs to belong to l_1) and a gaussian noise assumption. The demonstration in [1] is also valid if we let $N \to \infty$ which we will not consider here for brevity. With finite N we need no constraint on the shape of the tail. We also drop the gaussian noise assumption and require only that the noise variance is finite to demonstrate that the upper bound (6.2) is asymptotically tight. This bound is asymptotically tight in the sense that

certain noisy channels realize the value of the bound as the noise variance decreases to zero.

In the following subsection, we construct a class of channels whose stationary error probability approaches (6.2). The bound (6.2) is important because it shows that by imposing conditions on the shape of the channel, *viz.*, (6.1), corresponding to physical reality, less pessimistic error probability bounds than (5.13b) are possible.

2.6.2 Construction of a Candidate Class of Channels

The N-tap channel decision equation (2.2) is algebraically equivalent to

$$\widehat{a}_k = \mathrm{sgn}(\widetilde{h}_0(k)a_k + \sum_{i=1}^{n} h_i e_{k-i} + n_k), \quad h_0 > 0 \tag{6.3a}$$

where

$$\widetilde{h}_0(k) \triangleq h_0 + a_k \sum_{i=n+1}^{N} h_i e_{k-i} \in [h_0 - D,\ h_0 + D] \tag{6.3b}$$

and

$$D \triangleq 2 \sum_{i=n+1}^{N} \left|h_i\right| = 2 \cdot \left\|H_d\right\|_1. \tag{6.3c}$$

With constraint (6.1) we simply have

$$D < h_0 \tag{6.4}$$

and then (6.3a) can be interpreted as an equation for an n-tap channel with a random, time-varying cursor bounded to strictly positive values, i.e., $\widetilde{h}_0(k) > 0$. We note that, as mentioned in [1], condition (6.1) corresponds to the eye being open (i.e., the residual ISI satisfies $\left|S_k\right| < h_0$) after the first n taps are discarded. Therefore, in the absence of noise n_k, recovery is guaranteed if we make n rather than N consecutive correct decisions.

It is now straightforward to construct an N-tap channel $\underline{H}$ (for a given h_0) such that Fig.2.9 describes the transition probabilities between the aggregated states 0 through N when channel noise n_k is absent (these aggregated states are the same as those in Fig.2.8). (We will subsequently demonstrate that for all such channels $P_E \to \epsilon \cdot 2^n$ asymptotically for small noise where ϵ is the error probability when there is zero residual ISI (5.8).) Note from Fig.2.9 that the probability of a correct decision

is 1 for aggregated states 0 through $N-n$ because the eye is open after n or more consecutive correct decisions have been made. When the DFE is in an atomic state within any of the aggregated states $N,\ N-1,\ \ldots,\ N-n+1$, we claim we can construct a suitable $\underline{H}$ such that the probability of error is precisely $\frac{1}{2}$ (in the absence of noise). If so, then Fig.2.9 forms a valid FSMP representation of this noiseless channel.

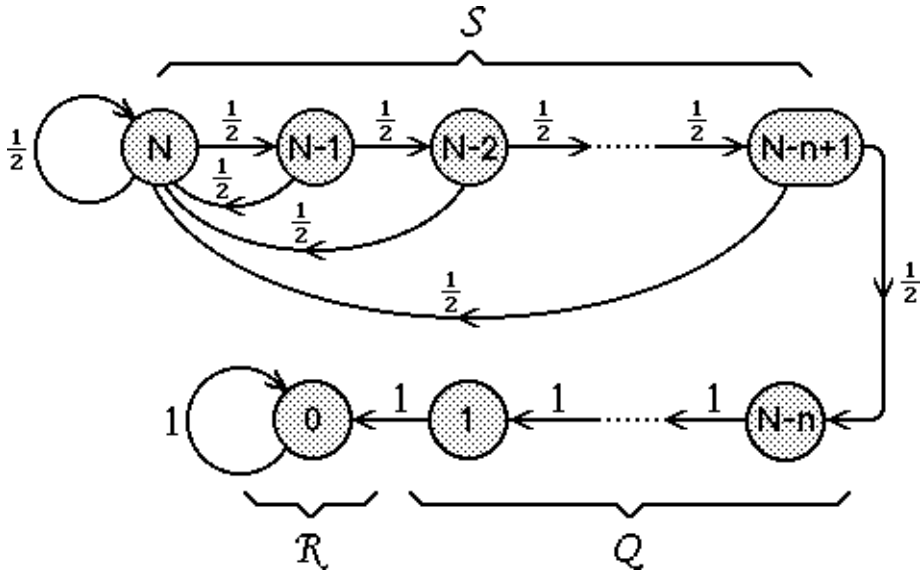

Fig.2.9 Noiseless Channel Class which Realize High SNR Bound.

We begin our construction by defining a region in the space of the first n channel parameters in terms of a positive quantity $\phi > 0$,

$$\mathcal{W}(\phi) \triangleq \Big\{ H_n \in I\!R^n\colon\ \{2h_n > \phi\} \cap \{2h_{n-1} > 2h_n + \phi\} \cap \ldots \cap \{2h_1 > 2\sum_{i=2}^{n} h_i + \phi\} \Big\}. \tag{6.5}$$

Then we assert that a sufficient condition on the N-tap channel $\underline{H}$ subject to (6.1) to have the desired behaviour in states N through $N-n+1$ is the following condition on its first n parameters,

$$H_n \in\ \mathcal{W}(h_0 + D). \tag{6.6}$$

To see this, first consider a (truncated) noiseless channel H_n with cursor $h_0 + D$. Then equation (6.6) is identical to a sufficient condition that a noiseless channel has exactly an error probability of $\frac{1}{2}$ when it has made less than n consecutive correct decisions Theorem 2.4(b). We now demonstrate that the channel pair $\{\widetilde{h}_0(k),\ H_n\}$, which has

the same fixed tail H_n but the time varying cursor of (6.3b), has this behaviour also. From the definitions (6.5) and (6.6) it is clear that for all $H_n \in \mathcal{W}(h_0 + D) \Rightarrow H_n \in \mathcal{W}(\widetilde{h}_0(k))$, i.e.,

$$\mathcal{W}(h_0 + D) \subset \mathcal{W}(\widetilde{h}_0(k)). \tag{6.7}$$

Due to the algebraic equivalence of $\{\widetilde{h}_0(k),\ H_n\}$ to $\{h_0,\ \underline{H}\}$ expressed through (5.2) and (6.3a) we have determined a subset of the class of channels $\underline{H}$, subject to (6.1) and (6.6), which have the FSMP representation of Fig.2.9. (For a more detailed account of this style of construction of noiseless channels see §2.4.3.) We now give an example of our construction.

Example: *Let $N = 7$, $n = 3$ and $h_0 = 1$. We pick any vector in $\mathbb{R}^4$ whose l_1-norm satisfies (6.1), say $H_d = (-0.3,\ 0.1,\ 0.05,\ -0.01)'$. Here $\left\|H_d\right\|_1 = 0.46$ and therefore $D = 0.92$ from (6.3c). Next we select any $H_3 \in \mathcal{W}(1.92)$ according to (6.5) and (6.6). A suitable choice is say $H_3 = (3.95,\ 2.00,\ 0.97)'$. Then we claim that the channel $\{h_0 = 1, \underline{H} = (3.95,\ 2.00,\ 0.97,\ -0.3,\ 0.1,\ 0.05,\ -0.01)'\}$, in the presence of noise n_k, will have an error probability $P_E \to 8{\cdot}\epsilon$ (6.2) as $\sigma_n^2 \to 0$, where $\epsilon \to 0$ is given by (5.8).*

2.6.3 Noise with Vanishingly Small Variance

We now include channel noise n_k in the analysis of our constructed channel. We note that the lumping of atomic states into aggregated states corresponding to "recovery distance" [2] no longer yields a FSMP (for our constructed channel) when noise is present. To see this, observe that each atomic state within a single aggregation will have different noise thresholds, implying different error probabilities. This destroys the Markov property because knowledge of the recovery distance is insufficient to deduce exact error probabilities. Fortunately, in deriving our error probability bound we do not need to use a (noisy) FSMP. However, the aggregation of atomic states into recovery distance states will be useful in deriving approximate bounds as was done in [2].

We define a further coarser partition of the set of atomic states into three sets. Set S (slow phase of recovery) is defined as the set of atomic states whose recovery distance is greater than $N - n$. Set Q (quick phase of recovery) those whose recovery distance is between (and including) $N - n$ and 1. Set R (recovery) those corresponding to

recovery. These three sets which delineate three phases of DFE recovery behaviour on our constructed channels (in the high signal to noise ratio limit) are shown in Fig.2.9. Of course with noise the transition probabilities shown in Fig.2.9 are incorrect.

To facilitate a simple and systematic derivation of the desired asymptotic formula we introduce some shorthand. The probability of error under stationarity given that the present atomic state, whatever it is, lies in a subset $X \in \Omega$ will be denoted

$$P_{E|X} \triangleq Pr(\widehat{a}_k \neq a_k \mid X). \tag{6.8}$$

Similarly, the probability that the present state X_k lies in X (again assuming stationarity) is denoted

$$\rho_X \triangleq Pr(X_k \in X). \tag{6.9}$$

Based on these definitions and noting the sets S, Q and R partition Ω, we have *under stationarity* and using Bayes' rule

$$\begin{aligned} P_E &= P_{E|R} \cdot \rho_R + P_{E|Q} \cdot \rho_Q + P_{E|S} \cdot \rho_S \\ &= \epsilon \cdot \rho_R + P_{E|Q} \cdot \rho_Q + P_{E|S} \cdot \rho_S. \end{aligned} \tag{6.10}$$

By bounding the components of the right hand side of (6.10) we will be able to determine bounds on the stationary error probability P_E for our constructed channels.

To prove the upper bound (6.2) of Duttweiler *et al.*, is tight, we will find both lower and upper bounds for our constructed channel which approach (6.2) in the high signal to noise ratio limit, i.e., as $\sigma_n^2 \to 0$.

2.6.4 Lower Asymptotic Bound

For the lower bound we have, from (6.10),

$$\begin{aligned} P_E &\geq \epsilon \cdot \rho_R + P_{E|S} \cdot \rho_S \\ &\geq \epsilon \cdot \underline{\rho}_R + \underline{P}_{E|S} \cdot \underline{\rho}_S \end{aligned} \tag{6.11}$$

where $\underline{\rho}_R$, $\underline{P}_{E|S}$, $\underline{\rho}_S$ (to be determined) are lower bounds on ρ_R, $P_{E|S}$ and ρ_S respectively.

Consider first the calculation for $\underline{\rho}_S$ in (6.11). Let ρ_i denote the probability that the DFE will be found in (recovery distance) aggregated state i under stationarity. Then by definition (see Fig.2.9), noting these sets are disjoint,

$$\rho_S = \rho_N + \rho_{N-1} + \ldots + \rho_{N-n+1} \tag{6.12a}$$

and

$$\rho_Q = \rho_{N-n} + \rho_{N-n-1} + \ldots + \rho_1. \tag{6.12b}$$

Now with every decision error the DFE transits to an atomic state whose recovery distance is N (by definition). This shows $\rho_N = P_E$. Further, by §2.5.2 the least (imaginable) probable transition from aggregated state N to $N-1$, or $N-1$ to $N-2$, etc., occurs with probability $\frac{1}{2}$. This shows $\rho_i \geq P_E(\frac{1}{2})^{N-i}$. Using (6.12a) we may then define

$$\begin{aligned} \underline{\rho}_S &\triangleq P_E + \frac{1}{2}\cdot P_E + \ldots + (\frac{1}{2})^{n-1} P_E \\ &= 2P_E(1 - 2^{-n}). \end{aligned} \tag{6.13}$$

We now compute a suitable $\underline{\rho}_R$ in (6.11). First, we give a very conservative upper bound on $\rho_S + \rho_Q$ using (6.12a) and (6.12b). Clearly, $\rho_i \leq P_E$ for $i = N,\ N-1,\ \ldots,\ 1$ because aggregated state $i \in \{1,\ 2,\ \ldots,\ N-1\}$ can only be reached from aggregated state $i+1$. Therefore

$$\rho_S + \rho_Q \leq \sum_{i=1}^{N} P_E$$

and this implies (noting $\rho_S + \rho_Q + \rho_R = 1$) that a suitable $\underline{\rho}_R$ is given by

$$\underline{\rho}_R \triangleq 1 - N\cdot P_E. \tag{6.14}$$

The calculation for $P_{E|S}$ in (6.11) can proceed by invoking Chebyshev's Inequality. Consider some particular $X_k \in S$ then from (5.5b) we have

$$Pr(\widehat{a}_k \neq a_k \mid X_k) = \frac{1}{2}\cdot Pr(\big|R_k\big| > h_0 \mid X_k), \quad X_k \in S.$$

Now for all $X_k \in S$ we have $\big|S_k\big| - h_0 > 0$ by construction (6.5). Define,

$$K_S \triangleq \min_{X_k \in S}\{\big|S_k\big| - h_0\} > 0,$$

i.e., in set S the eye is always closed by at least K_S in the absence of noise. Therefore, when $\big|n_k\big| = \big|R_k - S_k\big| < K_S$ the eye remains closed, and we deduce (outline only)

$$Pr(\widehat{a}_k \neq a_k \mid X_k) \geq \frac{1}{2}\cdot Pr(\big|R_k - S_k\big| < K_S \mid X_k), \quad \forall X_k \in S.$$

Therefore, applying Chebyshev's Inequality we obtain

$$P_{E|S} \triangleq Pr(\widehat{a}_k \neq a_k \mid S) \geq \frac{1}{2}\cdot\Big(1 - \frac{\sigma_n^2}{K_S^2}\Big),$$

i.e., anticipating the high signal to noise ratio limit and using a signed order notation,

$$\underline{P}_{E|S} \triangleq \frac{1}{2} - O(\sigma_n^2). \tag{6.15}$$

Clearly by letting $\sigma_n^2 \to 0$ we obtain the noiseless result.

A similar calculation involving Chebyshev's Inequality, for $M = Q$ or R where $h_0 - \big|S_k\big| > 0$ (eye open without noise), yields

$$P_{E|M} \leq \frac{1}{2}\cdot\frac{\sigma_n^2}{K_M^2} \tag{6.16}$$

where

$$K_M \triangleq \min_{X_k \in M}\{h_0 - \big|S_k\big|\} > 0.$$

Hence, if $M = R$ where $S_k = 0$ ($E_k = 0$) for all atomic states, we have $K_R = h_0$ which leads to

$$\epsilon \leq \frac{1}{2}\cdot\frac{\sigma_n^2}{h_0^2}. \tag{6.17}$$

This result says that (i) the probability of error *after recovery* is bounded above by the reciprocal of twice the signal to noise ratio, and (ii) $\epsilon \leq O(\sigma_n^2)$.

We can now compute the lower bound on P_E (6.11) by substituting in for (6.13), (6.14), (6.15) and (6.17):

$$\begin{aligned} P_E &\geq \epsilon\cdot\underline{\rho}_R + \underline{P}_{E|S}\cdot\underline{\rho}_S \\ &= \epsilon\cdot(1 - NP_E) + \big(\frac{1}{2} - O(\sigma_n^2)\big)\cdot 2P_E(1 - 2^{-n}) \\ &\geq \epsilon + P_E - 2^{-n}P_E - P_E\cdot O(\sigma_n^2) \\ &\geq \epsilon\cdot 2^n - O(\sigma_n^4) \end{aligned} \tag{6.18}$$

which is the desired lower bound.

2.6.5 Upper Asymptotic Bound

We now seek an upper bound on P_E. From (6.10) we may write

$$P_E \leq \epsilon\cdot\overline{\rho}_R + \overline{P}_{E|Q}\cdot\overline{\rho}_Q + \overline{P}_{E|S}\cdot\overline{\rho}_S \tag{6.19}$$

where the quantities on the right hand side of (6.19) will be shown to be given by

$$\overline{\rho}_R \triangleq 1 \geq \rho_R \tag{6.20a}$$

$$\overline{P}_{E|Q} \triangleq O(\sigma_n^2) \geq P_{E|Q} \tag{6.20b}$$

$$\overline{\rho}_Q \triangleq (N-n)2^{-n}P_E\big(1+O(\sigma_n^2)\big) \geq \rho_Q \tag{6.20c}$$

$$\overline{P}_{E|S} \triangleq \frac{1}{2} \geq P_{E|S} \tag{6.20d}$$

$$\overline{\rho}_S \triangleq 2P_E(1-2^{-n})\big(1+O(\sigma_n^2)\big) \geq \rho_S. \tag{6.20e}$$

In the above (6.20a) and (6.20d) are clearly bounded by the quantities given and it turns out that these bounds are adequate. Also we have already demonstrated (6.20b) because this is just (6.16) with $M = Q$. The remaining two terms are non-trivial to derive and we now give their proof.

First, we focus on the bound in (6.20e). We have, for the set S,

$$\rho_i \leq P_E\ (1-\underline{P}_{E|S})^{N-i}, \quad i \in \{N-n+1,\ \ldots,\ N\} \tag{6.21}$$

because $P_E = \rho_N$ and an overbound on the transition probabilities $N \to N-1$, $N-1 \to N-2$, etc., within S, is simply $(1-\underline{P}_{E|S})$. Thus from (6.12a)

$$\begin{aligned}\rho_S &\leq P_E \sum_{i=N-n+1}^{N} (1-\underline{P}_{E|S})^{N-i} \\ &= P_E \sum_{i=0}^{n-1} \Big(\frac{1}{2}\big(1+O(\sigma_n^2)\big)\Big)^i \\ &= 2P_E(1-2^{-n})\big(1+O(\sigma_n^2)\big) \triangleq \overline{\rho}_S\end{aligned} \tag{6.22}$$

which is precisely (6.20e).

Now we prove (6.20c). From (6.12b) we may write

$$\overline{\rho}_Q \leq \sum_{i=1}^{N-n} \overline{\rho}_{N-n} \tag{6.23}$$

where $\overline{\rho}_{N-n}$ is some suitable overbound on ρ_{N-n}. This formula (6.23) is based on having unity as the overbound on the transition probabilities within Q when we have correct decisions. The same old argument, this time to compute an overbound on ρ_{N-n}, yields

$$\begin{aligned}\overline{\rho}_{N-n} &\triangleq P_E\ (1-\underline{P}_{E|S})^n \\ &= 2^{-n}P_E\big(1+O(\sigma_n^2)\big),\end{aligned} \tag{6.24}$$

where we have used (6.15). Substituting (6.24) into (6.23) yields (6.20c).

Now we can compute the upper bound (6.19), by substituting in for (6.20). This leads to

$$\begin{aligned} P_E &\leq \epsilon + O(\sigma_n^2)\cdot(N-n)2^{-n}P_E\big(1+O(\sigma_n^2)\big) + \frac{1}{2}\cdot 2P_E(1-2^{-n})\big(1+O(\sigma_n^2)\big) \\ &= \epsilon + P_E - 2^{-n}P_E + P_E\cdot O(\sigma_n^2) \end{aligned}$$

which implies, after a few lines of algebra,

$$P_E \leq \epsilon\cdot 2^n + O(\sigma_n^4). \tag{6.25}$$

2.6.6 Main Result Statement

Combining (6.18) and (6.25) we have demonstrated the following theorem:

Theorem 2.10: *There exist channels satisfying* $\|H_d\|_1 < \frac{1}{2}\cdot h_0$ *(6.1) subject to additive noise* n_k *of variance* σ_n^2 *(specifically those satisfying (6.6)) which have an asymptotic error probability* $Pr(\widehat{a}_k \neq a_k)$ *given by*

$$P_E = \epsilon\cdot 2^n + O(\sigma_n^4) \quad as \quad \sigma_n^2 \to 0. \tag{6.26}$$

where $\epsilon \triangleq Pr(\widehat{a}_k \neq a_k \mid E_k = 0)$ *(5.8). Further this bound is asymptotically tight over the class of channels* $\{h_0,\ \underline{H}\}$. ❑

Remarks:

(i) Note the constituent bounds (6.20) hold over any channel $\{h_0,\ \underline{H}\}$ satisfying (6.1), and this is why we can say (6.26) is asymptotically tight.

(ii) These channels which realize (6.26) are precisely those whose stochastic dynamics in the absence of noise are described by the FSMP in Fig.2.9.

(iii) The introduction of channel noise n_k into the analysis of DFEs involves only $O(\sigma_n^2)$ modifications relative to the noiseless case. This justifies the practical relevance of studying noiseless DFEs as we have in §2.3 when the signal to noise ratio is high.

(iv) The proof is invalid if $N \to \infty$. To incorporate this case, we need to modify (6.14) by imposing a further constraint on the channel tail, e.g., an l_1-norm constraint, see [1].

(v) It is a folly to believe that with ϵ sufficiently small, (6.26) implies good DFE error behaviour because with just one decision error the error recovery time may have the worst case mean of $2(2^n - 1)$ which can be astronomically large. This point is taken up again in Chapter 4.

2.6.7 Effect of Noise on Error Recovery

Based on our results we classify the effect of channel noise on the error recovery performance of the DFE relative to the noiseless case. We distinguish three cases:

(i) **No Effect on DFE Recovery**: We have constructed a channel where, before recovery, (bounded) noise is inconsequential to DFE recovery, see (5.7) and (5.10). After recovery it is straightforward to construct (bounded) noise densities which realize any value of ϵ and hence P_E in the interval $[0, \frac{1}{2}]$, see §2.5.4.

(ii) **Noise Worsens DFE Recovery**: This might be regarded as the expected or standard case. As an example let the channel satisfy $2 \cdot \left\| \underline{H} \right\|_1 < h_0$, i.e., the eye is always open in the absence of noise. Then let $Pr(\left| n_k \right| > h_0) > 0$. Clearly with noise the eye can close.

(iii) **Noise Improves DFE Recovery**: An example of this case was obtained in §2.6.4 where by construction for the noiseless case $P_{E|S} = \frac{1}{2}$ but with noise $P_{E|S}$ may be asymptotically $\frac{1}{2} - O(\sigma_n^2)$, see (6.15).

The third case is of course counter-intuitive and the most interesting. It is a non-trivial problem to determine which classes of channels result in improved (transient) error recovery for certain noise distributions. Also it is not clear whether these channels can be expected in practice. It is also possible to contrive situations where for a particular channel parameter/channel noise distribution combination, not only is the (transient) error recovery performance improved, as indicated by (6.15), but also the stationary error probability P_E is reduced. However, it is dubious whether such channels will appear in practice.

2.7 Conclusions

2.7.1 Summary

We itemize some contributions:

(i) The class of all channels of a given tap length N can be classified into a finite number of subclasses identified with polytopes in $\mathbb{R}^N$.

(ii) Each polytope has identified with it, in a one-to-one fashion, a unique FSMP from which one may determine the error recovery statistics.

(iii) For $N = 2$, we showed how to classify the complete set of pathological input sequences, i.e., those input sequences which lead to arbitrarily long recovery times, for a given polytope. This classification generalizes to higher order systems. Graphical devices rather than algebraic relationships are the most effective for this classification.

(iv) For $N = 2$ we gave necessary and sufficient conditions on the channel parameters for a polytope to have a bounded recovery time which holds irrespective of the input data or the initial conditions. (In Chapter 4 we will return to investigate a class of channels which have such a property.)

(v) For general N we identified polytopes, i.e., those classes of channels, which represent the best and worst extremes in DFE error recovery behaviour and thus gave tight bounds on the expected recovery times (Theorem 2.4).

(vi) An asymptotic formula which gave the tight bound on the probability of a DFE failing to recover in a given time was developed (Theorem 2.7). This derivation highlights that the non-stationary or transient properties of a DFE during error recovery are dominated by the largest non-unity eigenvalues with the probability transition matrix.

(vii) One of our main contributions is to highlight that the apparently pathological upper bounds on the expected recovery times of DFEs given in [4,5] are tight in the sense that there exist channels which realize these bounds (in the absence of noise). Further, we showed that for $N = 2$ there are minimum phase channels with this property (for $N > 2$ it is known that there are nearly minimum phase channels with this property; but the same question regarding $N > 2$ minimum phase channels is open).

(viii) Our results demonstrate that DFEs are a practical option only on restricted classes of channel, else, e.g., with a $N = 64$ tap DFE running at a sampling rate of 1kHz the mean (error) recovery time can be as high as 10^{10} years, invoking (4.6). The imposition of just a minimum phase condition on the class of channels does not appear strong enough to guarantee satisfactory DFE operation.

(ix) With noise in the analysis we have shown that the most pathological conceivable DFE behaviour is realized by some channel parameter/channel noise combination. By purely constructive methods the bounds derived by Duttweiler *et al.*, [1] were shown to be tight, thereby settling the open question raised in [1].

(x) The presence of noise either: (i) has no effect on; (ii) worsens; or (iii) improves, the DFE error recovery performance relative to the noiseless case. It seems a non-trivial exercise to classify explicitly those channels which benefit from the presence of channel noise. (Naturally, the level of benefit depends also on the noise distribution.)

2.7.2 Discussion

In contriving channels and noise densities which display pathological behaviour it is not our intention to suggest they reflect behaviour to be observed in practice. (On the contrary, we would not expect or hope this to be the case.) More importantly, our results indicate the manner in which stronger hypotheses need to be imposed on the channel and noise, to further tighten the bounds on error probabilities and the like and thereby better reflect the DFE performance to be expected in practice.

We have argued that results concerning the behaviour of high signal to noise ratio DFEs can be suitably approximated by the noiseless DFE. In §2.4.4 we presented evidence that a minimum phase constraint on the channel parameters was insufficient to guarantee satisfactory error recovery behaviour. A similar conclusion thus carries over to the noisy case where it appears certain minimum phase channels may give unacceptably high error rates through error propagation, even though as a class they generally appear attractive, see [9].

In Chapter 4 we return to look at the error propagation with the objective of finding classes of channels—which turn out to satisfy a passivity constraint—which do have satisfactory error recovery behaviour. In the next chapter, having developed the basic mathematical tools in this chapter, we look at blind adaptation of DFEs.

We will see that an understanding of the error mechanism in DFEs is essential before a sensible analysis of the convergence properties can proceed.

References

[1] D.L. Duttweiler, J.E. Mazo, and D.G. Messerschmitt, "An Upper Bound on the Error Probability in Decision Feedback Equalizers," *IEEE Trans. on Information Theory,* vol.IT-20, pp.490-497, July 1974.

[2] J.J. O'Reilly, and A.M. de Oliveira Duarte, "Error Propagation in Decision Feedback Receivers," *Proc. IEE Proc. F, Commun., Radar and Signal Process.,* vol.132, no.7, pp.561-566, 1985.

[3] A.M. de Oliveira Duarte, and J.J. O'Reilly, "Simplified Technique for Bounding Error Statistics for DFB Receivers," *Proc. IEE Proc. F, Commun., Radar and Signal Process.,* vol.132, no.7, pp.567-575, 1985.

[4] A. Cantoni, and P. Butler, "Stability of Decision Feedback Inverses," *IEEE Trans. on Communications,* vol.COM-24, pp.1064-1075, September 1976.

[5] A. Cantoni, and P. Butler, "Behaviour of Decision Feedback Inverses with Deterministic and Random Inputs," Univ. Newcastle, Newcastle, Australia, Tech. Rep.EE7505, March 1975.

[6] P. Monsen, "Adaptive Equalization of a Slow Fading Channel," *IEEE Trans. on Communications,* vol.COM-22, No.8, pp.1064-1075, August 1974.

[7] R.A. Kennedy, and B.D.O. Anderson, "Recovery Times of Decision Feedback Equalizers on Noiseless Channels," *IEEE Trans. on Communications,* vol.COM-35, pp.1012-1021, October 1987.

[8] R.A. Kennedy, B.D.O. Anderson, and R.R. Bitmead, "Tight Bounds on the Error Probabilities of Decision Feedback Equalizers ," *IEEE Trans. on Communications,* vol.COM-35, pp.1022-1029, October 1987.

[9] B.R. Clarke, "The Time-Domain Response of Minimum Phase Networks," *IEEE Trans. on Circuits and Syst.,* vol.CAS-32, No.11, pp.1187-1189, November 1985.

[10] F.R. Gantmacher, "The Theory of Matrices," Vol.2, Chelsea Publishing Company, New York, 1974.

[11] D.L. Isaacson, and R.W. Madsen, "Markov Chains Theory and Applications," John Wiley and Sons Inc., 1985.

[12] K.J. Åström, P. Hagander, and J. Sternby, "Zeros of Sampled Systems," *Automatica,* vol.20, no.1, pp.31-38, 1984.

[13] E.I. Jury, "Inners and Stability of Dynamical Systems," John Wiley and Sons Inc., 1985.

CHAPTER 3. STOCHASTIC DYNAMICS OF BLIND ADAPTATION

Aim: *To determine the influence of decision errors and error propagation on the stochastic dynamics of blind adaptation in decision feedback equalization.*

3.1 Introduction

Adaptation is employed in equalization when a channel, over which data is sent, is unknown and time-invariant or the channel is slowly time-varying and needs to be tracked [1]. Standard identification schemes normally require channel input a_k and output b_k measurements to identify the channel (see Fig.3.1). Of course if we had complete knowledge of the real data a_k available at the receiver then this defeats the purpose of equalization. So what is standard in practice is to send a known *training sequence* $\{a_k\}$ for a limited time duration during which the channel parameters may be learnt. After training, with the equalizer correctly tuned, unknown data is sent and recovered at the equalizer output $\widehat{a}_k$ with a sufficiently low probability of error. Typically the adaptation during this time is left on to track slow channel variations. However, in the absence of the (knowledge of the) real data a_k, the data estimates $\widehat{a}_k$ are used in the adaptive algorithm.

Blind adaptation, in the sense that we define, represents something slightly different [2]. As in the post-training phase of standard adaptation, the data estimates $\widehat{a}_k$ are used in lieu of the real data a_k, but never is a training sequence used. So channel identification is based only on signals b_k and $\widehat{a}_k$. Therefore blind adaptation concerns *global convergence* issues when the input is unavailable and we have unreliable data estimates because the equalizer need not be tuned. There are a number of situations

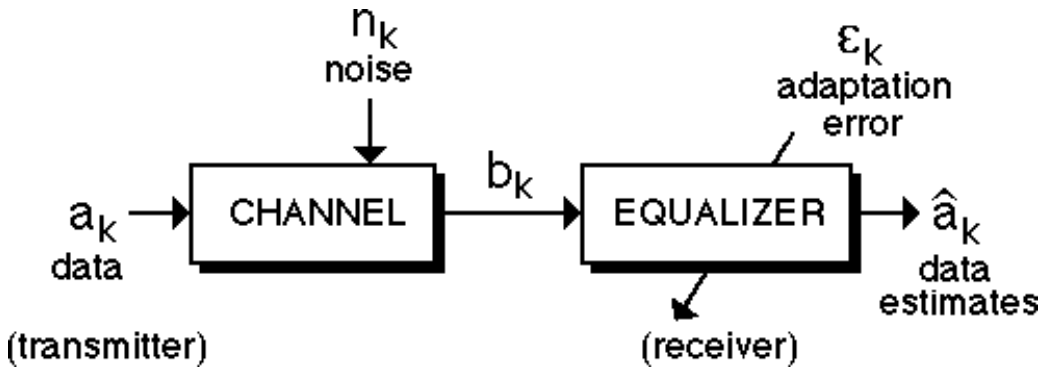

Fig.3.1 Adaptive Channel Equalization.

where blind adaptation is important in practice such as during a break in multipoint communications, see [3].

The simplest equalizer structure we could use in Fig.3.1 is the *linear equalizer* in its various guises. Typically it consists of a FIR filter cascaded with the channel [4]. However when incorporating a decision device at its output in an adaptive context it is called a *decision directed equalizer* (DDE) [5,6]. Another variation uses an IIR filter in which case it is called a recursive (linear) equalizer [7]. The theory analyzing the blind adaptation for linear equalizers is well developed, though incomplete, and contains many interesting results which we shall return to discuss, [2-4,7-9]. Because one almost always works with discrete alphabets, and hence a decision device is used, then we will use the terminology DDE rather than linear equalizer in this chapter.

The second popular type of equalizer structure is the decision feedback equalizer (DFE) which is the *non-linear* recursive filter met in Chapter 2 which utilizes past outputs $\widehat{a}_{k-1}$, $\widehat{a}_{k-2}$, ..., in its filter structure [1]. The literature is thin on the subject of blind adaptation of DFEs [10]—the principle reason being the difficulty of incorporating error propagation effects [11-17] into the analysis of adaptation. (Of course, fundamentally, an analysis of blind adaptation which excludes the effects of decision errors is not well-posed.) The problem is most acute when the DFE is poorly tuned; then decision errors are common (the error probability may be high) and its recursive nature ensures continuing poor error performance. In this situation the effects of errors will be to distort adaptation relative to the training sequence case. Our theory developed in Chapter 2 provides a partial basis to quantify such a distortion.

The other important component of any adaptation scheme, particularly in the blind case, is the choice (or design) of the algorithm. In the blind case, because the

statistics of the equalizer output govern the dynamics of adaptation rather than the actual input data, one needs to characterize the attraction points of the algorithm carefully.

For the DDE case the traditional approach to blind equalization has been to use stochastic gradient algorithms based on generalized cost functions, beginning with Sato [18]. However only when one assumes that the input distribution is subgaussian (being a one parameter family of smooth distributions with the uniform distribution as a limiting case) are global convergence results available, i.e., can it be shown that the only stable points of the algorithm correspond to the channel-equalizer combination acting as a pure delay [2]. The case when the input takes discrete values, the most common situation in practice, is not covered by the theory [9] (though one can note that discrete distributions may at least be approximated by a subgaussian distribution if the number of symbols is large [2]). Indeed Verdú [9] has shown that the Sato algorithm and its natural generalizations fail to have attractive global convergence properties for a very large class of memoryless adaptive laws when the input distribution is binary. This work throws into serious doubt the practical utility of the results in [2] (although with good cause these algorithms may be regarded as the best, most robust, available). Verdú [9], given the failure of the generalized Sato algorithms, notes in his conclusions that higher dimensional output statistics (correlations, etc.) contain information which might be exploited when devising more robust algorithms. (This observation we take up again in Chapter 5.)

Much less is known about the blind adaptation algorithms that should be employed in the DFE case which is our main focus of study here. Because a DFE is a non-linear device (with memory) the elegant results in [2] and those in [9], which rely on linearity, no longer apply. However it is our intention to say something about the *gross* convergence properties for DFEs. To keep our expectations realistic, we will focus on a Sato-like algorithm and a binary symbol alphabet. Like the DDE case we will be most interested in establishing when the channel-equalizer combination acts as a pure delay system. However, the quest for a globally convergent algorithm for which the only attraction points of the algorithm result in delay systems, like the DDE case, seems to be a distant goal (if it is achievable at all). Thus it is important to characterize the simplest case of the Sato algorithm (which has a strong similarity to the familiar LMS-type algorithms) before moving on to more esoteric schemes. A secondary problem in relation to globally convergent schemes is to be able to predict

convergence times.

A more subtle issue involved with the global convergence of DFEs is whether or not the problem is *well-posed*; after global convergence has occurred, there is no guarantee good system performance. Even with the hypothetical situation of rapid convergence to a single global minimum leading to a perfectly tuned DFE, the error propagation phenomenon can lead to appalling performance, as we have seen in Chapter 2 [15,16], suggesting that practical equalization is a channel dependent issue. A rough parallel exists with the DDE where it is known [1] that at frequencies where the channel attenuation is high the resulting ideal equalizer can lead to excessive noise enhancement.

The general aims of this chapter are to compare theoretically the blind adaptation of DDEs with the blind adaptation of DFEs, with emphasis on the latter. The points of contact and departure between these two types of equalizer will be examined. As in the DDE case our results are incomplete but not empty. Concerning the theory of blind adaptation, we see two general schools of thought. The first seeks to modify the blind adaptation algorithm to achieve global convergence, i.e., to ensure the only stable equilibria of the algorithm correspond to the channel-equalizer acting as a simple delay. This approach has been moderately successful in the DDE case [2]. However for discrete symbol distributions there have certainly been some negative results [9]. In contrast to this, our philosophy towards blind adaptation is fostered in part by the belief that the goal of achieving a globally convergent scheme is too ambitious. Our approach is more conservative in that it seeks only to classify sets of channels for which the desirable sort of global convergence is assured. Contact with reality can then hopefully be made by comparing real channels with these classes.

This chapter is organized as follows: Section 3.2 sets up a minimal DFE blind adaptive system and compares it with the better known blind DDE equalizer. Section 3.3 is a brief review of the parameter space partition which exists independently of the particular blind algorithm employed and is a mild generalization to that found in Chapter 2. Section 3.4 shows the mechanism behind the multiple equilibria of the blind algorithms. Section 3.5 gives a global picture of the blind tap convergence; classifying equilibria and establishing conditions on the channel and DFE parameters which ensure channel inversion with some delay. Section 3.6 considers the sign-error algorithm, and this is followed by §3.7 in which an analysis of the convergence of a broad class of algorithms is given. The conclusions are given in §3.8.

3.2 System Description and Notation

3.2.1 Channel and Equalizer Models

The channel we consider is shown in Fig.3.2. It will be modelled as a filter, with impulse response $\{h_0,\ h_1,\ \ldots\}$, driven by binary data $a_k \in \{-1, +1\}$ (where k denotes the discrete time index). Additive zero-mean channel noise n_k is depicted in Fig.3.2. However, mostly we will regard its influence as secondary to simplify our analysis (although the effect of noise will be briefly considered).

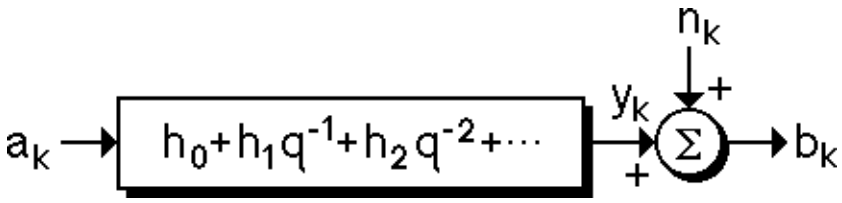

Fig.3.2 Channel Linear Model.

The DFE structure we study, shown in Fig.3.3, consists of an N-tap delay line, represented by weights $\{d_1,\ d_2,\ \ldots,\ d_N\}$ adapted to minimize the (residual) intersymbol interference (ISI). This tapped delay line is fed by past decisions or data estimates $\widehat{a}_k \in \{-1, +1\}$ and even if the d_i are correctly adjusted this can lead to problems when past decisions are incorrect, and this is the error propagation mechanism of Chapter 2 [11]. Note that in Fig.3.3, an additional weight d_0 is incorporated when forming an error signal ϵ_k to compensate for the non-unity channel term h_0. We will describe later the adaptive update mechanism which uses the error signal ϵ_k.

A more typical and indeed more general DFE structure usually consists of a FIR filter followed by the structure given in Fig.3.3. We have two motivations for considering the simpler structure. Firstly, our application demand is for subscriber-local exchange twisted pair telephone lines which measurements have shown to possess little precursor intersymbol interference thus obviating the need for the FIR cascade [20]. Secondly one of our aims is to understand the effects of error propagation on adaptation (relative to the well understood training sequence case) and Fig.3.3 is the minimal non-trivial structure to study these effects. Further in the more general structure it is sometimes possible to separate the adaptation of the FIR section from the DFE section. Then with a preliminary FIR adaptation completed the cascade of the channel and the FIR section consists of a linear system describable by the impulse response $\{h_0,\ h_1,\ \ldots\}$, effectively forming a new channel.

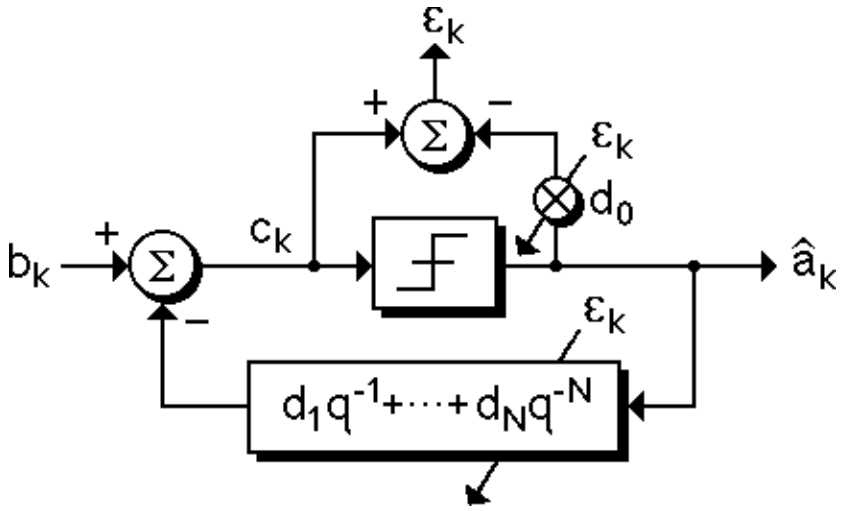

Fig.3.3 Blind Adaptive Decision Feedback Equalizer.

The fundamental binary DFE output equation describing *non-adaptive* operation, from Fig.3.2 and Fig.3.3, is given by

$$\widehat{a}_k = \mathrm{sgn}(\sum_{i=0}^{\infty} h_i a_{k-i} - \sum_{i=1}^{N} d_i \widehat{a}_{k-i} + n_k). \tag{2.1}$$

Remarks:

(i) The size of N is chosen sufficiently large so as to model adequately the ISI present in the channel in the sense that $\sum_{i=N+1}^{\infty} |h_i|$ needs to be sufficiently small. This ensures the problem is well-posed.

(ii) We refer to a decision of the form $\widehat{a}_k = \mathrm{sgn}(h_\delta)\, a_{k-\delta}$ as *correct* with the agreed convention that δ is some well defined and fixed delay. The conditions under which all this makes sense will be given later. Note that this delay should not be confused with a bulk delay representing gross propagation effects and the like, which (without loss of generality and as is standard) has been implicitly removed.

We introduce a vector convention to simplify the presentation. Let W represent a vector in $\mathbb{R}^{N+1}$. Then $\underline{W} \in \mathbb{R}^N$ is derived from $W \in \mathbb{R}^{N+1}$ by deleting the first component (i.e., by projection). For example, if we define the truncated channel impulse response vector as $H \triangleq (h_0,\ h_1,\ \ldots,\ h_N)' \in \mathbb{R}^{N+1}$, then by convention $\underline{H} \triangleq (h_1,\ h_2,\ \ldots,\ h_N)' \in \mathbb{R}^N$ (where v' denotes the transpose of v). We also define the vector of time-varying tap weights at time k as $D_k \triangleq (d_0,\ d_1,\ \ldots,\ d_N)_k{}' \in \mathbb{R}^{N+1}$

along with its associated vector $\underline{D}_k \in I\!R^N$. Further, the vectors representing the past and present data and data estimates are $A_k \triangleq (a_k,\ a_{k-1},\ \ldots,\ a_{k-N})' \in I\!R^{N+1}$ and $\widehat{A}_k \triangleq (\widehat{a}_{k-1},\ \widehat{a}_{k-2},\ \ldots,\ \widehat{a}_{k-N})' \in I\!R^{N+1}$, respectively. In our analysis, we will also be using $\underline{A}_k \in I\!R^N$ and $\underline{\widehat{A}}_k \in I\!R^N$, representing the past only data and data estimates, respectively.

With these definitions, (2.1) can be written succinctly as

$$\widehat{a}_k = \mathrm{sgn}(A_k{}'H - \underline{\widehat{A}}_k{}'\,\underline{D}_k + Q_k) \tag{2.2a}$$

where

$$Q_k \triangleq \sum_{i=N+1}^{\infty} h_i a_{k-i} + n_k. \tag{2.2b}$$

represents a perturbation to the ideal DFE system. Typically, in the high signal to noise ratio case and where N is sufficiently large, Q_k will be small except for infrequent intervals of time when the noise is significant. The form of (2.2a) with $Q_k \approx 0$ will make the partition of D_k-space, reviewed in §3.3, more transparent.

3.2.2 Blind Adaptation Schemes

Our emphasis in this chapter is with how error propagation in a DFE interacts with and distorts the stochastic dynamics of adaptation. The simplest *blind adaptation* scheme (Fig.3.3) that can be employed which updates the taps D_k, effectively identifying the channel, takes the form

$$D_{k+1} = D_k + \gamma\, \epsilon_k\, \widehat{A}_k \tag{2.3a}$$

where

$$\epsilon_k \triangleq A_k{}'H - \widehat{A}_k{}'D_k. \tag{2.3b}$$

This is a blind algorithm because we use past decisions from $\{\widehat{a}_k\}$ rather than the true data $\{a_k\}$ as the components in the regressor vector, and also in the error signal. The scalar error ϵ_k represents the discrepancy between the input and the renormalized output of the slicer (see Fig.3.3). The scalar γ in (2.3a) represents a small (time-invariant) adaptive gain.

Denote by $\psi_{\text{DFE}}(\cdot)$ the memoryless non-linearity which maps the slicer input c_k to the adaptation error signal ϵ_k, in Fig.3.3. It is given by

$$\psi_{\text{DFE}}(x) = x - d_0 \cdot \mathrm{sgn}(x). \tag{2.4}$$

By way of comparison we introduce the better studied DDE in Fig.3.4 (restricting attention to the binary case). The algorithms [2-4,8,9,18] which have been investigated for this case take the form

$$D_{k+1} = D_k - \gamma\, \epsilon_k\, B_k \tag{2.5a}$$

where

$$\epsilon_k \triangleq \psi_{\text{LE}}(c_k). \tag{2.5b}$$

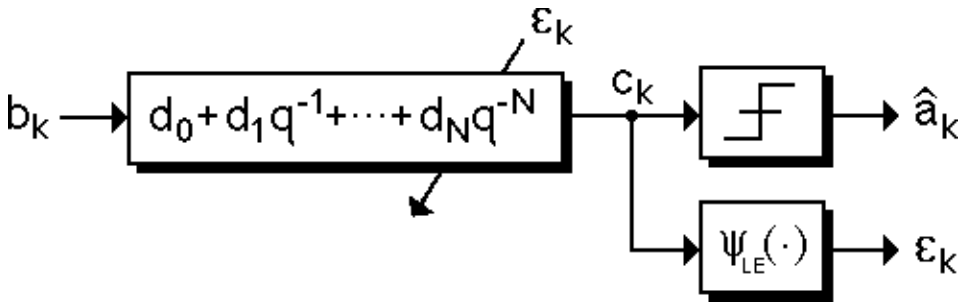

Fig.3.4 Blind Adaptive Decision Directed Equalizer.

Here $B_k \triangleq (b_k,\ b_{k-1},\ \ldots,\ b_{k-N})'$ is the regressor of channel outputs, c_k is the linear equalizer output. (The slicer input c_k and output $\widehat{a}_k$, and error ϵ_k in Fig.3.4 differ from those of Fig.3.3.) The Sato algorithm for binary communication in the DDE case is precisely (2.5) with $\psi_{\text{LE}}(\cdot)$ defined as

$$\psi_{\text{LE}}(x) = x - \text{sgn}(x). \tag{2.6}$$

So the close parallel between (2.4) and (2.6) is noted. Further the regressors in both cases (2.3a) and (2.5a) are the tapped delay line inputs. However the DFE has a computational advantage in this respect because $\widehat{a}_k$ is binary. M-ary generalizations exist [2,18] although questions regarding normalization of the input power to the quantizer need to be addressed and incorporated into the adaptation scheme [9].

Whilst the development here is fresh and in a classical setting let us briefly review the major findings in the DDE case. Benveniste, Goursat and Ruget, [2], have shown that the convergence properties of blind DDE adaptation depend on the distribution of the channel input a_k. In particular they showed that whenever the channel input distribution is *subgaussian* then a family of $\psi_{\text{LE}}(\cdot)$ (which generalize and include the Sato non-linearity (2.6)) yields ideal global convergence properties, i.e., convergence occurs

only to parameter settings leading to perfect equalization up to a delay. However for binary inputs leading to a *Bernoulli* input distribution (rather than subgaussian) Verdú [9] has shown that for a very large class of memoryless non-linearities $\psi_{\text{LE}}(\cdot)$, including those in [2], convergence to non-equalized local minima is always possible for large classes of channels. This throws into doubt the usefullness of [2], at least for small alphabets where the subgaussian approximation is poor.

Concerning the analysis of Sato algorithms for DFEs, we are interested in demonstrating the interplay between (2.2) and (2.3) given the presence of error propagation (in this respect it is a problem quite different to the DDE case). Some tools which come to our aid are averaged equations describing the mean tap trajectory of D_k (over the ensemble of input sequences), and finite state Markov processes. On the result side we will see that, like the Verdú DDE analysis (which cannot be used directly here), convergence to unequalized tap settings is possible for some channels. How the channel parameters explicitly determine some of the convergence properties is also studied. (Modifications to possibly improve the robustness of the algorithms for both decision directed and decision feedback equalization will be presented in Chapter 5.)

3.3 Parameter Space Partition

In this section we quickly generalize our results of Chapter 2 regarding the relationship between regions in parameter space and finite state Markov processes (FSMPs). We define the following hyperplanes in D_k-space (note d_0 is unconstrained):

$$\left\{D_k \in I\!R^{N+1}\colon\ A_k{}'H = \underline{\widehat{A}}_k{}'\,\underline{D}_k\right\}. \tag{3.1}$$

as we vary across all possible values taken by $A_k \in Z\!\!Z^{N+1}$ and $\underline{\widehat{A}}_k \in Z\!\!Z^N$ (here $Z\!\!Z$ denotes the integers). From (2.2) it is clear that whenever Q_k is small these hyperplanes define the manifolds in $I\!R^{N+1}$ for which the argument of the signum function in (2.2) is potentially small. These planes act as switching surfaces in the following sense. Define an atomic state

$$X_k \triangleq (\underline{A}_k{}',\ \underline{\widehat{A}}_k{}')' \in Z\!\!Z^{2N}. \tag{3.2}$$

Then from (2.2a) whenever the channel parameters satisfy (3.1) there exists an atomic state X_k and current input a_k such that an arbitrarily small perturbation in $\underline{D}_k$ (d_0 has no effect) can change a $\widehat{a}_k = +1$ to a $\widehat{a}_k = -1$ (or vice-versa). Before describing the significance of these hyperplanes to the stochastic modelling we give an example.

Example: *Let $N = 2$, $h_0 = 1$, $h_1 = 4$, and $h_2 = 3$. The $4^N = 16$ lines which partition D_k-space are given by $d_1 \pm d_2 = \zeta$, for $\zeta \in \{0, \pm 2, \pm 6, \pm 8\}$ according to (3.1). These lines are depicted in Fig.3.5. In this figure the point $(4, 3)$, representing the location of the channel tail, has been indicated by a small cross (the shading can be ignored for the moment). Notice that due to the degeneracy in this example (ζ can take the value 0) we really only have only 14 distinct lines rather than the generic 16. We will return later to consider this example in more detail.*

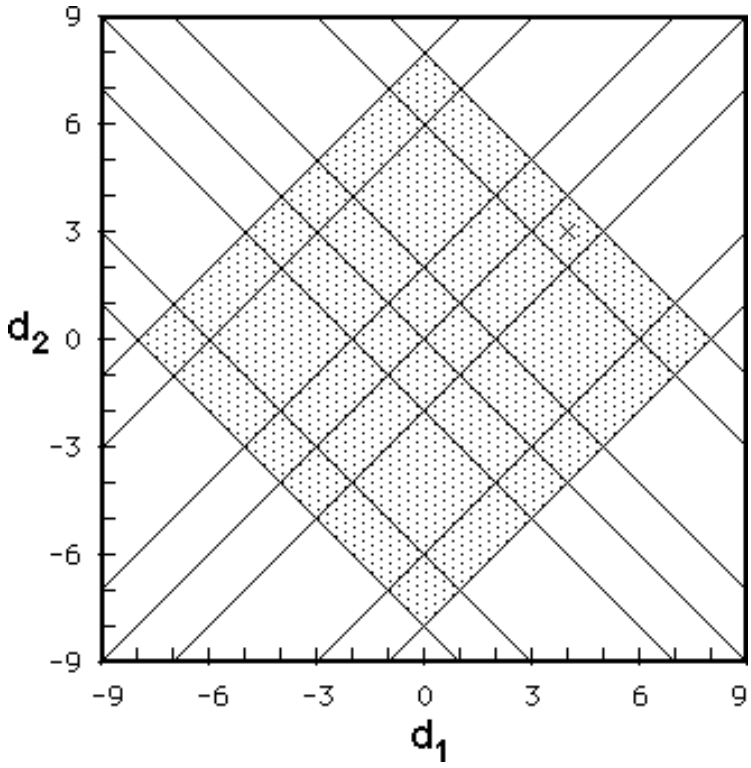

Fig.3.5 Polytopes for the H=(1,4,3)′ Channel.

Remarks:

(i) The effect of Q_k non-zero (2.2) is to blur the boundaries defined in (3.1). This means our modelling when the parameters are near the boundaries is non-ideal given the presence of channel noise or the effects of an undermodelled channel tail.

(ii) The remaining analysis will assume $Q_k = 0$ to simplify the presentation keeping in mind the significance of a non-zero Q_k.

The hyperplanes above partition D_k-space into a collection of polytopes which differ in definition from those given in Chapter 2 (naturally the generating mechanism is the same). The property of polytopes which we need here (from Chapter 2) is that one cannot distinguish between any two DFE D_k parameter settings within a given polytope based on observations of the output $\{\widehat{a}_k\}$ alone. (Nor, therefore, can any blind adaptation algorithms, including the Sato one (2.3), which uses $\widehat{a}_k$.) Next we move on to some statistical modelling.

Assumption: *The input binary sequence $\{a_k\}$ forms an equi-probable independent and identically distributed (i.i.d.) binary sequence.* ❑

Then we have a finite state Markov process describing the stochastic dynamics of the DFE, with 4^N states given by all possible values of X_k (3.2), see Chapter 2 and [15]. One can verify there is a one-to-one correspondence between polytopes and sets of FSMPs. So the conceptual picture is that as we drift through parameter space the underlying FSMP, which governs the full joint statistics of the input a_k and output $\widehat{a}_k$, changes (abruptly) only when we cross polytope boundaries. Inside a given polytope we model the $\{\widehat{a}_k\}$ process by the stationary behaviour of its associated FSMP. When the input independence assumption above does not hold and we have input correlation it is possible to still use a FSMP as an approximation device [13,14]. Alternatively we may, in most cases, extend the Markov state space and retain an exact description. Both paths could only distract our main aim to describe *gross* properties of DFE blind adaptation on the simplest non-trivial system.

Note that in principle the FSMP provides sufficient information to calculate, in our case, stationary entities of the form

$$\boldsymbol{R} \triangleq E\{\widehat{A}_k \widehat{A}_k{}'\} \quad \text{and} \quad \boldsymbol{C} \triangleq E\{\widehat{A}_k A_k{}'\} \tag{3.3}$$

which are expressible in terms of an invariant probability measure via an unilluminating calculation. (Here, $\boldsymbol{R}$ is non-negative definite, $\boldsymbol{C}$ is upper triangular by causality, and both are Toeplitz by stationarity.) Uniqueness of the invariant probability is not guaranteed, and this raises some interesting questions, but this takes us too far afield. What is important here is that we will see quantities like (3.3) provide us with sufficient information to characterize the gross convergence properties of the Sato blind adaptation algorithm (2.3).

3.4 Equilibria and Averaging Analysis

3.4.1 Wiener-Hopf Solution

Our first task is to determine the locations of the attraction points (equilibrium points) in D_k-space for the weights when the algorithm (2.3) seeks to minimize some error criterion implicit in the Sato formulation. We show that, unlike the DDE case, the criterion is locally but not globally a least squares one and this is a peculiar consequence of both the DFE structure (Fig.3.3) and the stationarity assumption on the underlying FSMPs.

Consider Fig.3.6 which simply redraws a portion of Fig.3.2 and Fig.3.3. (The definitions of the symbols in Fig.3.6 are identical to those in Fig.3.2 and Fig.3.3.) This figure suggests that $\widehat{a}_k$ can be *interpreted* as an input sequence and that y_k can be interpreted as a noiseless desired response. Thus the problem now *looks* classical (but actually the statistics of $\widehat{a}_k$ depend on D_k). As is well known, the objective of the "LMS" algorithm (2.3a) is to minimize the mean square error defined by $\xi(D_k) = E\{\epsilon_k^2(D_k)\}$ which is a quadratic function of D_k and hence uni-modal. The tap weight setting, D_{EQ} (equilibrium), which gives the minimum mean square error is the classical discrete time Wiener-Hopf formula [21] and is given by

$$D_{\text{EQ}} \triangleq E\{\widehat{A}_k \widehat{A}_k{}'\}^{-1} E\{\widehat{A}_k y_k\} \qquad (4.1a)$$

where, from (3.3) we have assumed $\det(\boldsymbol{R}) \neq 0$. Note, from this point on we consider only the case when $\boldsymbol{R}$ is non-singular. We will see that this restriction is justifiable when we come to §3.5.5.

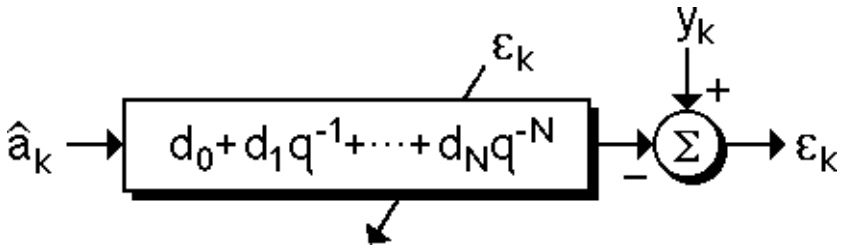

Fig.3.6 Equivalent Wiener Filter Problem.

In reality, y_k is not a user supplied sequence but simply the noiseless channel output which in our case is identified with $y_k \triangleq A_k{}'H$ (Fig.3.2). Hence (4.1a) may be

expanded to

$$D_{\text{EQ}} \triangleq E\{\widehat{A}_k \widehat{A}_k{}'\}^{-1} E\{\widehat{A}_k A_k{}'\}\ H \tag{4.2a}$$

$$= \boldsymbol{R}^{-1}\boldsymbol{C}\ H. \tag{4.2b}$$

This formula for D_{EQ} makes a qualitative and quantitative analysis more accessible. Specifically, it is clear that $D_{\text{EQ}} = \text{sgn}(h_0)\ H$ only under special circumstances and this highlights a major problem of blind adaptation with DFEs, i.e., $\text{sgn}(h_0)\ H$ (which we will see is the desired tap weight setting [11]) need not be a global attraction point for the adaptation algorithm.

The mean square error surface is quadratic with $\boldsymbol{R} = \boldsymbol{I}$ in the *training sequence* case, because the input is i.i.d., thus uncorrelated. With blind adaptation we will see that *locally* the mean square error surface is quadratic (although $\boldsymbol{R} \neq \boldsymbol{I}$ in general) given stationarity of the output $\{\widehat{a}_k\}$ process. The above analysis assumes matrices $\boldsymbol{R}$ and $\boldsymbol{C}$ are constant. We qualify this assumption for the blind DFE case later, but first we move onto another result.

3.4.2 Averaged Equation Trajectory

To characterize the attraction points for the blind algorithm (2.3) it is sufficient to define the error function implicit in the Sato formulation. A close parallel exists here with the work of Verdú [9], except he treats the DDE, in this regard. However because of the conceptual aid which it affords it is desirable to complement this error surface analysis with averaging theory to describe the mean drift of the D_k parameters.

In this section we will derive an expression for the mean trajectory for the tap weights D_k as they drift towards the equilibrium D_{EQ} given by (4.2b), assuming $\boldsymbol{R}$ and $\boldsymbol{C}$ are constant for the moment. The mean is over the ensemble of input sequences $\{a_k\}$. However, the mean trajectory is also informative in that individual realizations will tend to cluster closely about this mean, at least for sufficiently small gain γ as we will see from an example.

We now analyze the adaptation update equations (2.3). Substituting the expression for the error ϵ_k (2.3b) into the LMS tap weight update equation (2.3a) we obtain

$$D_{k+1} = \left(\boldsymbol{I} - \gamma\, \widehat{A}_k \widehat{A}_k{}'\right)\ D_k + \gamma\, \widehat{A}_k A_k{}' H. \tag{4.3}$$

If γ is sufficiently small, then the increment in going from D_k to D_{k+1} will also be small (noting that all quantities in (4.3) are bounded). Further, we might anticipate

that the matrices $\widehat{A}_k\widehat{A}_k{}'$ and $\widehat{A}_k A_k{}'$ take on a large number of (statistically) different values whilst $\{D_k\}$ evolves very little with time. Hence we might predict that the deterministic equation describing the mean tap trajectory, $\{\widetilde{D}_k\}$, takes the form,

$$\widetilde{D}_{k+1} = \Big(\boldsymbol{I} - \gamma E\big\{\widehat{A}_k\widehat{A}_k{}'\big\}\Big)\ \widetilde{D}_k + \gamma E\big\{\widehat{A}_k A_k{}'\big\}\ H + O(\gamma^2) \tag{4.4a}$$

$$= (\boldsymbol{I} - \gamma \boldsymbol{R})\ \widetilde{D}_k + \gamma \boldsymbol{C}\ H + O(\gamma^2). \tag{4.4b}$$

The formal justification that (4.4b) is indeed the correct equation as $\gamma \to 0$ may be found in the literature [22-24]; this general idea has also appeared in [2] (somewhat in disguise) and in [8]. Further study shows that the trajectories of (4.3) cluster closely about the solutions of (4.4b), e.g., see [22,24]. This property is apparent in our later example in §3.5.2.

We make some observations regarding (4.4b). It is straightforward to verify that: (a) D_{EQ} (4.2b) is indeed the equilibrium of the averaged (mean) equation (4.4b); and (b) the mean equation (4.4b) is stable if and only if $\gamma\ \lambda_{\text{MAX}}(\boldsymbol{R}) < 2$, where $\lambda_{\text{MAX}}(\boldsymbol{R})$ is the maximum eigenvalue of $\boldsymbol{R}$.

3.5 Tap Trajectories During Adaptation

3.5.1 Piecewise Constant Behaviour

With this section we bring together our previous, largely disconnected, results regarding the polytopes (§3.3), finite state Markov processes (§3.3 and §3.4.1, see also [15]), and the averaging analysis (§3.4.2). We will demonstrate that the blind LMS algorithm (2.3a) can be (but is not necessarily) attracted to undesirable regions of D_k-space where the channel is not correctly equalized and the error rates are unacceptably high (even in the absence of noise). Analogous results are of course known for the DDE [9].

The parameters which determine the dynamics of the mean equation (4.4b) are the covariance matrices $\boldsymbol{R}$ and $\boldsymbol{C}$. We also met these matrices earlier in §3.3 and we showed they could be evaluated with the assistance of FSMPs. Now, recall our one-to-one correspondence between the polytopes and FSMPs (or more generally state transition diagrams, §3.3). Hence, in D_k-space the matrices $\boldsymbol{R}$ and $\boldsymbol{C}$ will be constant only whilst the tap setting D_k remains inside any one of the D_k-space polytopes (assuming steady state of the underlying FSMP). Therefore, we have shown (albeit informally):

Proposition 3.1: *In steady state, the matrices* $\boldsymbol{R}$ *and* $\boldsymbol{C}$ *are piecewise constant functions of* D_k*, where the "pieces" are precisely the* D_k*-space polytopes bounded by the hyperplanes (3.1).* ❑

Remarks:

(i) By steady state we are specifying that the underlying FSMP has transitions only between recurrent atomic states.

(ii) To emphasize $\boldsymbol{R}$ and $\boldsymbol{C}$ are functions only of the polytope $\mathcal{P}$ for which $D_k \in \mathcal{P}$, we write $\boldsymbol{R}(\mathcal{P})$ and $\boldsymbol{C}(\mathcal{P})$.

(iii) Within each polytope the mean trajectory (4.4b) is determined by a constant coefficient, linear, deterministic difference equation. Hence, over the whole D_k-space, the averaged trajectory describing the complete adaptation is determined by a piecewise constant coefficient, linear, deterministic difference equation (see the example in §3.5.2), possibly with boundary conditions.

The next property is an embellishment on Proposition 3.1.

Proposition 3.2: *The error surface* $\xi(D_k) \triangleq E\{\epsilon_k^2(D_k)\}$ *is a piecewise (polytope-wise) quadratic function of* D_k *given by*

$$\xi(D_k \in \mathcal{P}) = E\{y_k^2\} - 2E\{\widehat{A}_k y_k\}' D_k + D_k{}' E\{A_k A_k{}'\} D_k \qquad (5.1a)$$

$$= H'H - 2H'\boldsymbol{C}(\mathcal{P})' D_k + D_k{}' \boldsymbol{R}(\mathcal{P}) D_k. \qquad (5.1b)$$

❑

Proof: *This is a trivial modification of a standard result in adaptive least squares, filtering, i.e., (5.1a) may be found in [21, eqn (2.31)]. To obtain (5.1b), we substitute both* $y_k = A_k{}'H$ *and* $E\{\widehat{A}_k y_k\} = \boldsymbol{C}(\mathcal{P})H$ *into (5.1a), and invoke the uncorrelatedness of the input sequence. Of course, we emphasize that for blind adaptation of DFEs,* $\boldsymbol{C}(\mathcal{P})$ *and* $\boldsymbol{R}(\mathcal{P})$ *are constant only within a polytope* $\mathcal{P}$*, and generally these matrices vary from polytope to polytope. Therefore, the quadratic surface is different for different polytopes, i.e., piecewise quadratic and discontinuous at the boundaries.* ❑

Remarks:

(i) The local minimum of the mean square error $\xi\big(D_{\text{EQ}}(\mathcal{P})\big)$ associated with a polytope $\mathcal{P}$, in terms of H, can be written $\xi_{\text{MIN}}(\mathcal{P}) = H'\big(\boldsymbol{I} - \boldsymbol{C}(\mathcal{P})'\boldsymbol{R}(\mathcal{P})^{-1}\boldsymbol{C}(\mathcal{P})\big)\ H$. However, if $D_{\text{EQ}}(\mathcal{P})$ lies outside $\mathcal{P}$ then this minimum need not be achievable.

(ii) Whenever $h_0 \neq 0$ we will see in §3.5.3 that the global minimum mean square error is zero at $D^{\text{OPT}} \triangleq \text{sgn}(h_0)\ H$ for the polytope which contains D^{OPT}, and is locally attainable, in the sense described in the following paragraph.

(iii) The training sequence adaptation error surface has a unique minimum. Blind DFE adaptation has potentially as many equilibria as there are polytopes!

In review, with each polytope $\mathcal{P}$ we have associated an equilibrium (potential attraction point for the blind adaptation algorithm) given by

$$D_{\text{EQ}}(\mathcal{P}) = \boldsymbol{R}(\mathcal{P})^{-1}\boldsymbol{C}(\mathcal{P})\ H.$$

It is natural to classify two types of equilibria according to whether or not the following property holds:

Definition: $D_{\text{EQ}}(\mathcal{P})$ *is* ***locally attainable*** *if* $D_{\text{EQ}}(\mathcal{P}) \in \mathcal{P}$. ❑

If $D_{\text{EQ}}(\mathcal{P})$ is locally attainable then $\{D_k\}$ will *tend* to move towards and settle down around it, whenever $D_k \in \mathcal{P}$. Otherwise, $\{D_k \in \mathcal{P}\}$ will tend to move towards the boundary $\partial\mathcal{P}$ of $\mathcal{P}$ nearest to $D_{\text{EQ}}(\mathcal{P})$ and thus head on into an adjacent polytope. So all locally attainable equilibria are real attraction points for the blind algorithm. The example in the next subsection best illustrates these ideas. This is not necessarily a channel to be expected in practice and serves merely to illustrate the concepts introduced.

3.5.2 Example of Adaptation and the Averaged Trajectory

As in §3.3 we choose the example $h_0 = 1$, $h_1 = 4$ and $h_2 = 3$. In Fig.3.7 we have plotted a large number of averaged trajectories according to (4.4b) with $\gamma = 0.01$, noting that the $\boldsymbol{R}$ and $\boldsymbol{C}$ matrices are now dependent on the polytopes (pictured in Fig.3.5). Note Fig.3.7 is a two-dimensional projection of D_k-space, therefore some of the averaged trajectories only appear to cross. The starting d_0-component for all trajectories was arbitrarily selected at zero. Naturally the mean evolution of d_0 during adaptation

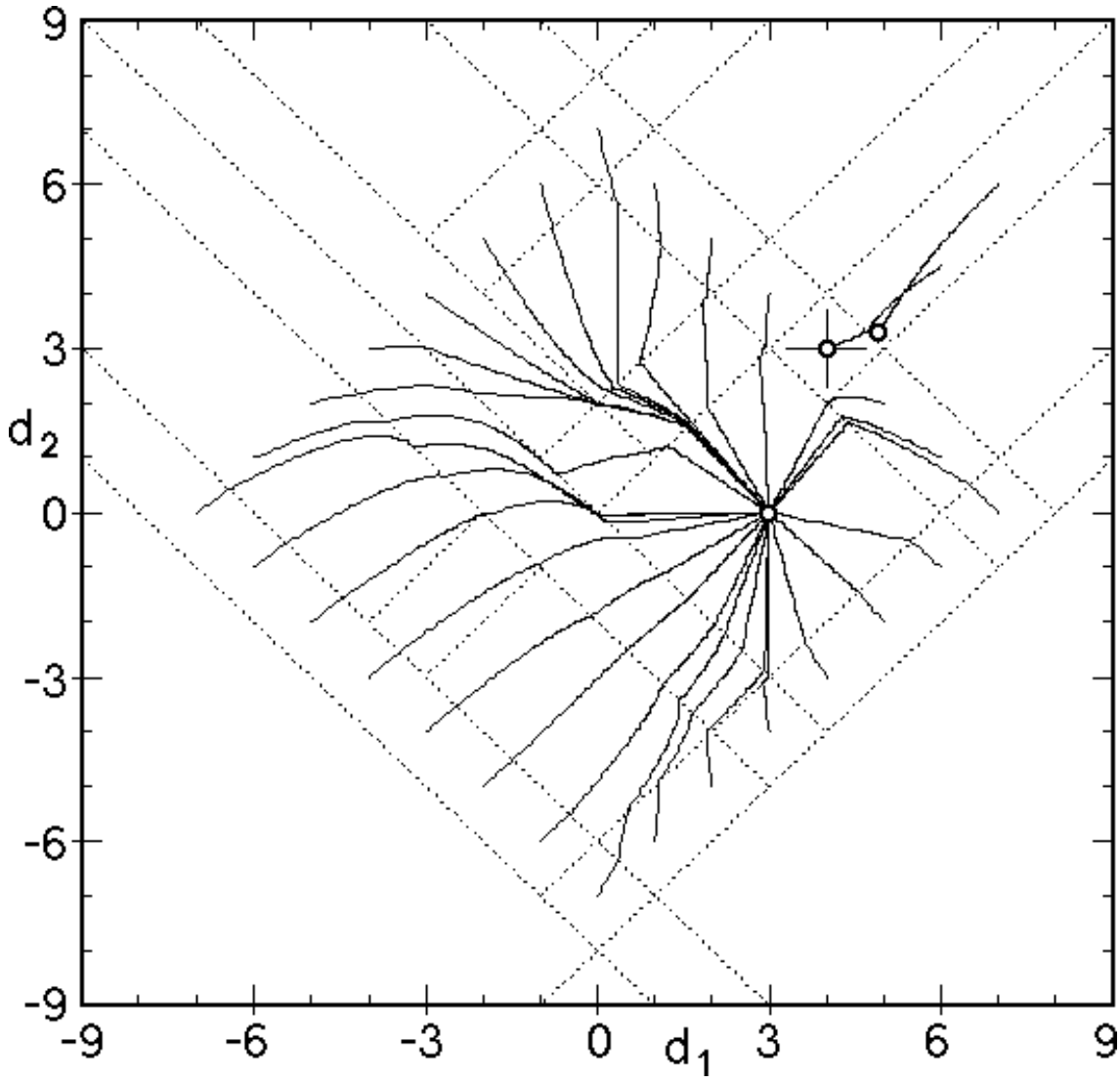

Fig.3.7 Refracting Averaged Trajectories.

cannot be discerned in such a figure. Clearly a predictable refraction phenomenon is indicated as we pass across polytope boundaries.

Figure 3.8 shows the precise sense in which to interpret Fig.3.7. It shows an insert of Fig.3.7 with a single (bold) averaged trajectory (plucked from Fig.3.7) and four realizations initialized from $(0, 7, 0)'$ (i.e., simulations according to (4.3) generated via a random number generator) which appear to cluster about the averaged trajectory. Note for this example there are only three locally attainable equilibria at $(1, 4, 3)'$, $(4, 3, 0)'$ and $(3.792, 4.833, 3.292)'$. In Fig.3.7 the 2D projections of these equilibria (depicted as small circles) are given by $(4, 3)'$, $(3, 0)'$ and $(4.833, 3.667)'$ and these

appear as (local) attraction points for the mean trajectories. The last equilibrium shows blind adaptation based on the Sato algorithm may be flawed in the sense that it does not correspond to an equalized system as we will see later (whereas the first two do—at the first, $\widehat{a}_k = a_k$, and at the second, $\widehat{a}_k = a_{k-1}$).

In Fig.3.7 we have aggregated polytopes from Fig.3.5 whenever adjacent polytopes have the same correlation statistics (more precisely when neighbouring polytopes have isomorphic sets of recurrent atomic states). In a sense this indicates that aggregations of polytopes are more important objects than the polytopes themselves for investigation and this is a lead in to some of our later results.

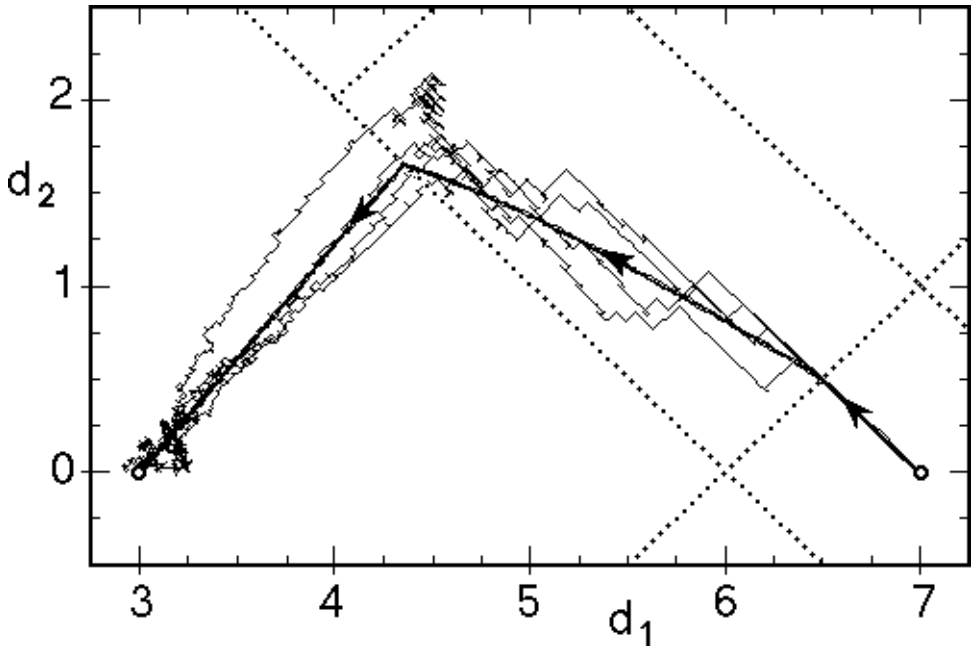

Fig.3.8 Averaged Trajectory with 4 Realizations.

3.5.3 Approximate and Exact Locally Attainable Equilibria

The equilibria predicted by the theory developed are implicitly based only on mean behaviour (4.4b). However we note that part of the driving term of the adaptation equation (2.3a) is given by ϵ_k (2.3b). Error ϵ_k in turn is only identically zero (for all k) when $D_k = D^{\text{OPT}} \triangleq \text{sgn}(h_0)\ H$ (given $h_0 \neq 0$; the proof is straightforward and omitted). So we say that only D^{OPT} is an *exact* equilibrium in the sense that $\epsilon_k(D^{\text{OPT}}) = 0$. All other locally attainable equilibria are termed *approximate* equilibria

and the physical manifestation of a locally attainable equilibrium with $\epsilon_k\big(D_{\text{EQ}}(\mathcal{P})\big) > 0$ is that the sequence $\{D_k\}$ is observed to jiggle about (but generally stay in the vicinity of) $D_{\text{EQ}}(\mathcal{P})$. This phenomenon is apparent in the lower left of Fig.3.8. The questions arise [8]:

(a) Regarded as a small noise can the variations in ϵ_k (estimating the gradient) drive $\{D_k\}$ away from $D_{\text{EQ}}(\mathcal{P})$ such that $\{D_k\}$ hits the boundary $\partial\mathcal{P}$?

(b) What is the expected time to do so?

In the stochastic process literature [22,25,26] this is known as an exit problem. These are crucial questions because if the DFE hangs at an equilibrium $D_{\text{EQ}}(\mathcal{P})$ corresponding to high error rates, e.g., $D_{\text{EQ}} = (4.667, 5.333, 3.667)'$ in Fig.3.7, then an unacceptably high exit time has serious practical consequences. On an equal footing we may ask about exit times from regions of correct equalization and consider the consequences. Also channel noise can have precisely the same effect as ϵ_k as is well known, so the above questions actually are relevant also for an exact equilibrium. These questions are the subject of current research and answers are not presented in this thesis.

3.5.4 Delay-type Equilibria Local Attainability

In this section we consider those aggregations of polytopes in D_k-space which yield a decision sequence which is a delay of the input (with an associated possible sign change) under steady state, i.e., $\widehat{a}_k = \text{sgn}(h_\delta)\, a_{k-\delta}$, $\forall k$. We derive necessary (and conjecture sufficient) conditions for attainability of the attraction points of these groups of polytopes for Sato algorithms in terms of the channel parameters. (Note in the following development all the results leading up to Theorem 3.8 are independent of the blind algorithm employed because they relate to non-adaptive properties.)

Let $\sigma_\delta \triangleq \text{sgn}(h_\delta)$, then rewriting (2.1) we have,

$$\widehat{a}_k = \text{sgn}\left(h_\delta a_{k-\delta} + U_k(\delta) + V_k(\delta)\right), \quad 0 \le \delta \le N \tag{5.2a}$$

where

$$U_k(\delta) \triangleq \sigma_\delta \sum_{i=\delta+1}^{N} d_{i-\delta}(a_{k-i} - \sigma_\delta\, \widehat{a}_{k+\delta-i}) \tag{5.2b}$$

$$V_k(\delta) \triangleq \sum_{i=0}^{\delta-1} h_i a_{k-i} + \sum_{i=\delta+1}^{N} (h_i - \sigma_\delta\, d_{i-\delta}) a_{k-i} - \sum_{i=N-\delta+1}^{N} d_i \widehat{a}_{k-i}. \tag{5.2c}$$

We also define an upper bound on (5.2c)

$$V_{\text{MAX}}(\delta) \triangleq \sum_{i=\delta+1}^{N} \big|h_i\big| + \sum_{i=\delta+1}^{N} \big|h_i - \sigma_\delta\, d_{i-\delta}\big| + \sum_{i=N-\delta+1}^{N} \big|d_i\big|. \tag{5.3}$$

The reason for the curious decomposition given by (5.2a) will become clearer later. We will see that δ corresponds to a nominal time delay and $\sigma_\delta \in \{-1, +1\}$, corresponds to an associated sign change of the channel-DFE combination.

We define two subsets of the set Ω of 4^N atomic states X_k (3.2) parametrized by $0 \le \delta < N$. (The case $\delta = N$ needs to be treated separately but fortunately is easily disposed of.) Define

$$\omega_+(\delta) \triangleq \big\{X_k \in \Omega\text{: } \widehat{a}_{k-i} = +\sigma_\delta\, a_{k-\delta-i},\ i = 1,\ 2,\ \ldots,\ N-\delta\big\}$$
$$\omega_-(\delta) \triangleq \big\{X_k \in \Omega\text{: } \widehat{a}_{k-i} = -\sigma_\delta\, a_{k-\delta-i},\ i = 1,\ 2,\ \ldots,\ N-\delta\big\}$$

both of which consist of collections of $2^{N+\delta}$ atomic states where (precisely) the $N-\delta$ most recent decisions are of the form $\widehat{a}_m = +\sigma_\delta\, a_{m-\delta}$ and $\widehat{a}_m = -\sigma_\delta\, a_{m-\delta}$, respectively.

Remarks:

(i) Note the definitions of $\omega_\pm(\delta)$ simply express that the member atomic state vectors have their $N+i$th component equal to $\pm\sigma_\delta$ times the $\delta+i$th component for $i = 1,\ 2,\ \ldots,\ N-\delta$, and thus these subsets are in effect independent of k (as the notation suggests).

(ii) We will see that whereas in the DDE case [2] $\widehat{a}_k = +a_{k-\delta}, \forall\{a_k\}$ and $\widehat{a}_k = -a_{k-\delta}$, $\forall\{a_k\}$ are *both* possible for some δ for a fixed channel, the situation for the DFE is different because only $\widehat{a}_k = +\sigma_\delta\, a_{k-\delta}, \forall\{a_k\}$ will be possible (σ_δ being fixed by the channel).

We are aiming for conditions under which only the atomic states in $\omega_+(\delta) \in \Omega$ are recurrent. The standard notion of a closed subset of Ω will considerably simplify development.

Definition: *A subset of Ω is **closed** if any transition from any one atomic state in the subset is only to another atomic state within the subset.* ❑

The following statements are equivalent: (a) Suppose $X_k \in \omega_{\pm}(\delta)$, then all future ($m \geq k$) decisions are of the form $\widehat{a}_m = \pm\sigma_\delta\, a_{m-\delta}$; and (b) $\omega_{\pm}(\delta)$ is closed. Hence to investigate channel-DFE combinations yielding simple time delay behaviour we need only to determine when a set $\omega_{\pm}(\delta)$ is closed and reachable from arbitrary states within Ω. The following proposition narrows our investigations by showing a DFE can never behave consistently according to the law $\widehat{a}_m = -\sigma_\delta\, a_{m-\delta}$ when in a steady state stochastic environment, and it also gives necessary and sufficient conditions for $\omega_+(\delta)$ closure.

Proposition 3.3: *(a) $\omega_+(\delta)$ is closed if and only if*

$$\left|h_\delta\right| > V_{\text{MAX}}(\delta). \tag{5.4}$$

(b) $\omega_-(\delta)$ is never a closed subset. □

Proof: *Suppose $\omega_{\pm}(\delta)$ is closed and that the system has been in $\omega_{\pm}(\delta)$ for some time. Then $\widehat{a}_{k-i} = \pm\sigma_\delta\, a_{k-\delta-i}$, $i \in \{1,\ 2,\ \ldots,\ N\}$. Substituting into (5.2b) and (5.2c) we obtain*

$$U_k^-(\delta) \triangleq 2\sigma_\delta \sum_{i=\delta+1}^{N} d_{i-\delta} a_{k-i}; \qquad U_k^+(\delta) \triangleq 0 \tag{5.5}$$

and

$$V_k^{\pm}(\delta) \triangleq \sum_{i=0}^{\delta-1} h_i a_{k-i} + \sum_{i=\delta+1}^{N} \big(h_i - \sigma_\delta\, d_{i-\delta}\big) a_{k-i} \mp \sigma_\delta \sum_{i=N+1}^{N+\delta} d_{i-\delta} a_{k-i}. \tag{5.6}$$

Consider first $\omega_+(\delta)$. If $\left|h_\delta\right| > V_{\text{MAX}}(\delta)$ with $U_k^+(\delta) = 0$ then this implies $\left|h_\delta\right| > \left|V_k^+(\delta)\right|$ for all $V_k^+(\delta)$, hence $\widehat{a}_k = +\sigma_\delta\, a_{k-\delta}$ by (5.2a). Then note that the a_k in (5.6) are distinct and therefore the supremum of $V_k^+(\delta)$ over $\{a_k\}$ is just $V_{\text{MAX}}(\delta)$, so (5.4) is also necessary.

Now consider $\omega_-(\delta)$. In this case we have $\widehat{a}_k = \operatorname{sgn}\big(h_\delta a_{k-\delta} + U_k^-(\delta) + V_k^-(\delta)\big)$, where by (5.5) and (5.6), $U_k^-(\delta) + V_k^-(\delta)$ is independent of $a_{k-\delta}$; and has a distribution symmetric about 0. Hence $Pr\big(\widehat{a}_k = +\sigma_\delta a_{k-\delta}\big) \geq \frac{1}{2}$, contradicting closure (noting if $\omega_-(\delta)$ were closed then $Pr\big(\widehat{a}_k = +\sigma_\delta a_{k-\delta}\big) = 0$). □

If (5.4) holds, then contriving an input sequence which visits all atomic states in $\omega_+(\delta)$ when the initial state is in $\omega_+(\delta)$ is straightforward. This shows no proper subset of $\omega_+(\delta)$ is closed assuming $\omega_+(\delta)$ itself is closed (i.e., $\omega_+(\delta)$ is a set of recurrent states). We formulate this as:

Proposition 3.4: *$\omega_+(\delta)$ is indecomposable.* ❑

The inequality (5.4) can only hold for at most one value of δ. To prove this one assumes at least two inequalities of the form (5.4) are simultaneously satisfied (say for δ_1 and δ_2) then an application of the triangle inequality establishes a contradiction. The details of the proof are omitted. We state this result as Proposition 3.5.

Proposition 3.5: *$\omega_+(\delta)$ is closed for at most one $\delta \in \{0,\ 1,\ \ldots,\ N\}$.* ❑

Proposition 3.5 can be viewed as a special case of a more general problem, now considered. Having established that only under suitable conditions $\omega_+(\delta)$ is closed and indecomposable, the crucial question arises as to whether it can be reached from an arbitrary atomic state $X_k \in \Omega \setminus \omega_+(\delta)$ by at least one input sequence. Then there are a number of side issues related to this, e.g, (a) the expected capture time by $\omega_+(\delta)$, and (b) which channels have an acceptable capture time, etc., (see [15]). A full answer to this question is not yet known. We present the following result (Proposition 3.6) and important conjecture (Conjecture 3.7).

Proposition 3.6: *Let $\left|h_\delta\right| > V_{\text{MAX}}(\delta)$ for some $0 \le \delta < N$. Then the following alternative conditions are sufficient to guarantee that there exists an input sequence such that $N-\delta$ consecutive $\widehat{a}_m = +\sigma_\delta\, a_{m-\delta}$ decisions are made:*

(i) $\delta = 0,\ 1,\ N-2,\ N-1,\ N$ *(and thus cases* $N = 1,\ 2,\ 3,\ 4$*).*

(ii) $\eta\ \text{sgn}(d_1) = \eta^2\ \text{sgn}(d_2) = \ldots = \eta^{N-\delta}\ \text{sgn}(d_{N-\delta})$ *for* $\eta \in \{+1, -1\}$.

(iii) $\eta\ \text{sgn}(h_{\delta+1}) = \eta^2\ \text{sgn}(h_{\delta+2}) = \ldots = \eta^{N-\delta}\ \text{sgn}(h_N)$ *for* $\eta \in \{+1, -1\}$. ❑

We prove this result for $\delta = 0$ and $\delta = 1$. The remaining cases are easier to prove and the proofs have been omitted.

Proof: *Let $\mathcal{F}_k = \sigma(a_k,\ a_{k-1},\ \ldots,\ \widehat{a}_k,\ \widehat{a}_{k-1},\ \ldots)$ denote the sigma algebra generated by data and decisions up to and including time k.*

(a) $\delta = 0$: From (5.2b) we note $U_k(0)$ is $\mathcal{F}_{k-1}$-measurable, hence selecting $a_k = +\sigma_0\ \text{sgn}\big(U_k(0)\big)$ gives $\widehat{a}_k = +\sigma_0\, a_k$ by (5.4) with $\delta = 0$. Apply this rule for N

consecutive k.

(b) $\delta = 1$: Suppose that for some fixed k, the DFE has been driven by the homing sequence $\{a_{k-1} = +\sigma_1;\ a_{k-j} = +\sigma_1\ \mathrm{sgn}(d_{i-j}),\ i = 2,\ 3,\ \ldots,\ N\}$. (We shall explain how a_k, a_{k+1}, etc., are to be chosen, so that $\widehat{a}_{k+j} = +\sigma_1\, a_{k+j-1},\ \forall j \geq 0$.) Then from (5.2b) we have

$$U_k(1) = \sum_{i=2}^{N} \left|d_{i-1}\right| - \sum_{i=2}^{N} d_{i-1}\widehat{a}_{k+1-i} \geq 0$$

Thus $\widehat{a}_k = +1$ independent of a_k because substituting into (5.2a) we have: (i) $h_1 a_{k-1} + U_k(1) \geq \left|h_1\right|$; and (ii) $\left|h_1\right| > \left|V_k(1)\right|$ from (5.4). Note that the $\widehat{a}_k$ decision satisfies $\widehat{a}_k = +\sigma_1\, a_{k-1}$ (with $a_{k-1} = +\sigma_1$), i.e., is one decision of desired form. We need to make the next $N-2$ also of this form. Now since $\widehat{a}_k = +\sigma_1\, a_{k-1}$ is guaranteed independent of a_k, we conclude $U_{k+1}(1)$ is $\mathcal{F}_{k-1}$-measurable. Thus we may set $a_k = +\sigma_1\ \mathrm{sgn}\big(U_{k+1}(1)\big)$ showing $h_1 a_k + U_{k+1}(1) = \mathrm{sgn}\big(U_{k+1}(1)\big)\big(\left|h_1\right| + \left|U_{k+1}(1)\right|\big)$ which dominates $V_{k+1}(1)$, by (5.4), leading to $\widehat{a}_{k+1} = \mathrm{sgn}\big(U_{k+1}(1)\big) = +\sigma_1\, a_k$, independent of a_{k+1}. Following this we conclude $U_{k+2}(1)$ is $\mathcal{F}_k$-measurable, etc., and the recipe is clear. ❑

Conjecture 3.7: *Let $\left|h_\delta\right| > V_{\text{MAX}}(\delta)$ for some $0 \leq \delta < N$. Then there exists at least one input sequence such that $N - \delta$ consecutive decisions are made of the form $\widehat{a}_m = +\sigma_\delta\, a_{m-\delta}$.* ❑

Remarks:

(i) With (5.4) satisfied, and the hypothesis of Proposition 3.6 fulfilled, $\omega_+(\delta)$ is closed, indecomposable and reachable, so that $Pr\big(X_k \in \omega_+(\delta)\big) \to 1$ exponentially fast as $k \to \infty$. Hence under stationarity the channel-DFE combination produces decisions of the form $\widehat{a}_m = +\sigma_\delta\, a_{m-\delta}$ if and only if $\left|h_\delta\right| > V_{\text{MAX}}(\delta)$ with $\omega_+(\delta)$ reachable. Note that the output forms an independent sequence under such conditions.

(ii) Given a time-invariant channel H, define the following regions (at least one does exist) of D_k-space, by rewriting (5.4):

$$\mathcal{J}(\delta) \triangleq \Big\{D_k \in I\!R^{N+1}:\ \rho_\delta > \sum_{i=\delta+1}^{N} \left|h_i - \sigma_\delta \cdot d_{i-\delta}\right| + \sum_{i=N-\delta+1}^{N} \left|d_i\right|\Big\} \qquad (5.7a)$$

where

$$\rho_\delta \triangleq \big|h_\delta\big| - \sum_{i=0}^{\delta-1} \big|h_i\big|,\ 0 \le \delta \le N. \tag{5.7b}$$

(These regions for $\delta > 0$ generalize a condition derived by Jennings [10].) Then $\widehat{a}_m = +\sigma_\delta\, a_{m-\delta}$ under steady state conditions only if $D_k \in \mathcal{J}(\delta)$ and sometimes if (according to the reachability of $\omega_+(\delta)$ and the initial conditions). Note this region may also be written $\rho_\delta > \big\|\underline{D}_k - \sigma_\delta\, \boldsymbol{S}_N^\delta\, \underline{H}\big\|_1$, where $\boldsymbol{S}_i$ denotes an $i \times i$ matrix of super-diagonal ones. Hence the projection of $\mathcal{J}(\delta)$ onto $\underline{D}_k$-space defines an l_1-ball with centre $\sigma_\delta\, \boldsymbol{S}_N^\delta\, \underline{H}$ and radius ρ_δ. (Note the d_0 component of D_k does not play a role in the constraint in (5.7a).) Region $\mathcal{J}(\delta)$ is non-empty only if $\rho_\delta > 0$. Note for our example in Fig.3.6, $\mathcal{J}(0)$ and $\mathcal{J}(1)$ are non-empty because $\rho_0 = \big|h_0\big| = 1 > 0$ and $\rho_1 = \big|h_1\big| - \big|h_0\big| = 3 > 0$, but $\mathcal{J}(2)$ is empty because $\rho_2 = \big|h_2\big| - \big|h_1\big| - \big|h_0\big| = -2 < 0$

(iii) It can be shown that each region $\mathcal{J}(\delta)$ is a *union* of polytopes whose sets of recurrent FSMP states are isomorphic.

(iv) In the case $\delta = N$, it is readily apparent that condition (5.4) is necessary and sufficient for every decision to be of the form $\widehat{a}_m = +\sigma_N\, a_{m-N}$.

Now we state the main result, which shows it is simple to check for the existence of delay-like attraction points for the Sato blind algorithm for the adaptive DFE.

Theorem 3.8: *A necessary condition for the Sato "LMS" blind adaptive algorithm*

$$D_{k+1} = D_k + \gamma\, \epsilon_k\, \widehat{A}_k$$

where

$$\epsilon_k \triangleq A_k{}' H - \widehat{A}_k{}' D_k$$

to have a locally attainable equilibrium corresponding to the channel-DFE combination producing decisions of the form $\widehat{a}_m = +\sigma_\delta\, a_{m-\delta}$ under steady state is

$$\rho_\delta \triangleq \big|h_\delta\big| - \sum_{i=0}^{\delta-1} \big|h_i\big| > 0.$$

Further, this equilibrium is given by $D_{\text{EQ}}(\mathcal{P}) \triangleq +\sigma_\delta \boldsymbol{S}_{N+1}^\delta\, H$, i.e., a simple shift of H with a possible sign flip. The condition is also sufficient when $\omega_+(\delta)$ is reachable (from all atomic states in $\Omega \setminus \omega_+(\delta)$). ❑

Proof: *Suppose* $\widehat{a}_m = +\sigma_\delta\, a_{m-\delta}\ \forall m$ *under steady state. Then it follows* $\omega_+(\delta)$ *is closed (by definition). With* $\omega_+(\delta)$ *closed it is necessary that* $\big|h_\delta\big| > V_{\text{MAX}}(\delta)$ *by Proposition 3.3. In particular, this implies*

$$\big|h_\delta\big| > \sum_{i=0}^{\delta-1} \big|h_i\big|$$

by (5.3). Hence $\rho_\delta > 0$ *(5.7b).*

Now suppose $\rho_\delta > 0$*. Then by (5.7a)* $\mathcal{J}(\delta)$ *is non-empty. Let* $D_k \in \mathcal{J}(\delta)$ *in which case* $\omega_+(\delta)$ *is closed. Now only if* $\omega_+(\delta)$ *is reachable from all initial atomic states (Proposition 3.6) can we say that transitions within* $\omega_+(\delta)$ *completely define the steady state behaviour, i.e., only if* $\omega_+(\delta)$ *is the only closed subset of* Ω *(Conjecture 3.7). Therefore only with* $\omega_+(\delta)$ *reachable does it follow from the closure property that* $\widehat{a}_m = +\sigma_\delta\, a_{m-\delta}\ \forall m$ *(given* $\rho_\delta > 0$*). So if we assume* $\omega_+(\delta)$ *is reachable, then it remains to be shown that there is an equilibrium for* $\{D_k\}$ *which is locally attainable (it turns out to be unique). Now because* $\widehat{a}_m = +\sigma_\delta\, a_{m-\delta}\ \forall m$ *it follows that: (i)* $\boldsymbol{R}(\mathcal{P}) = \boldsymbol{I}$*; and (ii)* $\boldsymbol{C}(\mathcal{P}) = +\sigma_\delta\, \boldsymbol{S}_{N+1}^{\delta}$*. Hence from (4.2b) we have* $D_{\text{EQ}}(\mathcal{P}) = +\sigma_\delta\, \boldsymbol{S}_{N+1}^{\delta}\, H$ *for all polytopes* $\mathcal{P}$ *which make up* $\mathcal{J}(\delta)$*. Then it is trivial to show from (5.5) that* $D_{\text{EQ}}(\mathcal{P}) \in \mathcal{J}(\delta)$*. (Indeed in a very real sense* $D_{\text{EQ}}(\mathcal{P})$ *is the "centre" of* $\mathcal{J}(\delta)$*, see Fig.3.7.) Hence there exists a (particular) polytope* $\mathcal{P}^* \in \mathcal{J}(\delta)$ *(say) such that* $D_{\text{EQ}}(\mathcal{P}^*) = D_{\text{EQ}}\big(\mathcal{P} \in \mathcal{J}(\delta)\big) \in \mathcal{P}^*$*, i.e.,* $D_{\text{EQ}}(\mathcal{P}^*)$ *is a locally attainable equilibrium.* ❑

Remarks:

(i) For $\delta = 0$, $D_{\text{EQ}}(\mathcal{P}) = D^{\text{OPT}} \triangleq +\sigma_0\, H$ is always locally attainable whenever $h_0 \neq 0$ and achieves the global minimum mean square error of zero, i.e., is an exact equilibrium. (If $h_0 = 0$ then trivially $D_{\text{EQ}}(\mathcal{P}) = +\sigma_1\, \boldsymbol{S}_{N+1}\, H$ is always locally attainable and exact, and so on for more degenerate cases.)

(ii) The "LMS" qualifier in the theorem statement is superfluous. The same result holds for any adaptation algorithm which seeks to minimize the mean square error (2.3b) by searching for a Wiener-Hopf solution. Hence the result holds also for blind regressor algorithms based on NLMS, RLS, etc.

3.5.5 White Equilibria

As we have earlier commented, when $\widehat{a}_k = +\sigma_\delta\, a_{k-\delta}$, the $\{\widehat{a}_k\}$ process is composed of a sequence of independent equi-probable binary random variables. Let us term any

equilibrium with the $\{\widehat{a}_k\}$ process white a *white equilibrium*. In this subsection, we shall present further results on this class and indicate some open problems.

We now give two closely related propositions which imply that adaptation should be restricted to a well defined region of D_k-space.

Proposition 3.9: *Suppose $\{\widehat{a}_k\}$ forms an independent, equi-probable binary random sequence (under steady state). Then*

$$D_k \in \Big\{ D_k \in I\!R^{N+1} \colon \big\| H \big\|_1 > \big\| \underline{D}_k \big\|_1 \Big\}. \tag{5.8}$$

❑

Proof: *If $\{\widehat{a}_k\}$ is an independent, equi-probable binary random sequence then the subsequence $\{\widehat{a}_k = -1;\ \widehat{a}_{k-i} = -\operatorname{sgn}(d_i),\ i = 1,\ 2,\ \ldots,\ N\}$ occurs with non-zero probability (for some input sequence). In (2.1) this implies $-1 = \operatorname{sgn}(A_k{}'H + \big\| \underline{D}_k \big\|_1)$ and so (5.8) follows, noting $\big\| H \big\|_1 \geq \big| A_k{}'H \big|$, $\forall A_k$.* ❑

Remarks:

(i) Taking our previous example, this region (5.8) is shown shaded as a diamond in Fig.3.5. Here $H = (1, 4, 3)'$ and we need $\big|d_1\big| + \big|d_2\big| < 8$; the output of the DFE can be independent only whilst $(d_1, d_2)'$ lies within this diamond.

(ii) The expression $\big\| H \big\|_1$ is the peak excursion of the noiseless channel output when driven by an independent binary input. Hence we can estimate $\big\| H \big\|_1$ by channel output measurements and thus impose during adaptation the requirement that $\{D_k\}$ not leave (5.8).

(iii) Closely related to the above is the following. Clearly, by the earlier definition of D^{OPT} as $\operatorname{sgn}(h_0)\, H$, we have $D^{\text{OPT}} = \big\| H \big\|_1$ (and $\big\| H \big\|_1$ can be adaptively estimated). It is obvious, yet has not been suggested in the literature, that adaptation algorithms should constrain $\{D_k\}$ only to move on the l_1-ball given by $\big\| D_k \big\|_1 = \big\| H \big\|_1$ (or progressive estimates thereof).

Proposition 3.10: *If $\det(\boldsymbol{R}(\mathcal{P})) = 0$ then $\mathcal{P} \subset \Big\{ D_k \in I\!R^{N+1} \colon \big\| \underline{D}_k \big\|_1 > \big\| H \big\|_1 \Big\}$.* ❑

Proof: *If $\det\big(\boldsymbol{R}(\mathcal{P})\big) = 0$ this implies there exists $x \triangleq (x_0,\ x_1,\ \ldots,\ x_N)' \neq 0$ such that $x'\boldsymbol{R}(\mathcal{P})x = 0$, i.e., $E\big\{(x'\widehat{A}_k)^2\big\} = 0$. Therefore, under steady state, we have*

$$x_0\widehat{a}_k + x_1\widehat{a}_{k-1} + x_2\widehat{a}_{k-2} + \ldots + x_N\widehat{a}_{k-N} = 0 \tag{5.9}$$

where at least two x_i's are non-zero. In particular, (5.9) implies $\{\widehat{a}_k\}$ is periodic because $\widehat{A}_k$ can take on only a finite number of values.

Now to obtain a contradiction, suppose that $\|\underline{D}_k\|_1 < \|H\|_1$ and consider the two input subsequences $\{a_{k-i} = +\operatorname{sgn}(h_i)\}$ and $\{a_{k-i} = -\operatorname{sgn}(h_i)\}$. Then in the two cases $A_k{}'H = +\|H\|_1$ and $A_k{}'H = -\|H\|_1$ imply (by hypothesis) that $\widehat{a}_k = +1$ and $\widehat{a}_k = -1$, respectively. However, this contradicts the periodicity of $\{\widehat{a}_k\}$. Therefore $\|\underline{D}_k\|_1 > \|H\|_1$ as claimed. ❑

Remarks:

(i) This justifies the earlier restriction that we should only consider polytopes $\mathcal{P}$ satisfying $\det(\boldsymbol{R}(\mathcal{P})) \neq 0$, because otherwise we would be considering a region of D_k-space which is complementary to the l_1-ball which, by Proposition 3.9, contains the only polytopes of interest and to which adaptation is sensibly constrained. There is some evidence which leads to the conjecture that condition (5.8) implies the stationary atomic distribution of the FSMP is unique. (For example, if (5.8) holds and $h_i > 0$ for all i, then it is provably unique). However, the general conjecture (which incidentally implies Conjecture 3.7) remains open.

(ii) When $N = 1$ and $N = 2$, or when all d_i are zero (which occurs in decision directed equalization), we can show that the only way the output $\{\widehat{a}_k\}$ can be white is for the DFE to produce decisions of the form $\widehat{a}_m = +\sigma_\delta\, a_{m-\delta}$, for some δ (only one).

Our analysis leads to the following conjecture:

(DFE) Conjecture 3.11: *Let $\{a_k\}$ be an independent sequence of random variables taking values in $\{-1, +1\}$ with equal probability. Suppose that*

$$\widehat{a}_k = \operatorname{sgn}(\sum_{i=0}^{N} h_i a_{k-i} - \sum_{i=1}^{N} d_i \widehat{a}_{k-i})$$

and the $\{\widehat{a}_k\}$ is independently distributed. Then for some $\delta \in \{0,\ 1,\ \ldots,\ N\}$, there holds

$$\widehat{a}_k = +\sigma_\delta\, a_{k-\delta}, \quad \forall\{a_k\}$$

where $\sigma_\delta \triangleq \operatorname{sgn}(h_\delta)$. ❑

If the conjecture held we would have a way of statistically testing the output of a DFE to prove it was correctly equalizing the channel up to a delay. The corresponding

question for the simpler DDE is solved in Chapter 5 where these issues are investigated further.

3.5.6 Equilibria Classification

Here we summarize our findings into the tree diagram shown in Fig.3.9. It also incorporates cases which we have not considered because they have yet to be observed in any examples, i.e., are *hypothetical*. These hypothetical cases will be treated in this section.

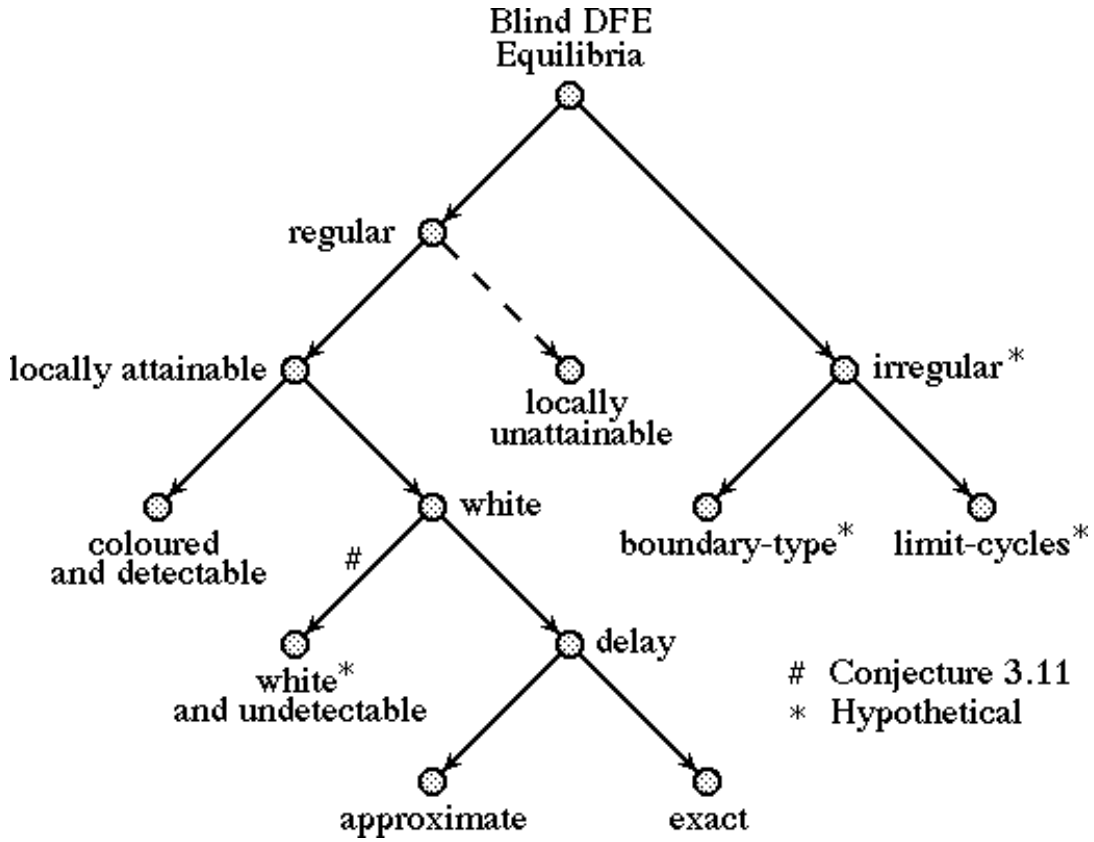

Fig.3.9 Tree Diagram for Blind DFE Equilibria.

The familiar adjectives can be found in Fig.3.9 under the first major class called "regular" which are all equilibria describable through the discrete time Wiener-Hopf formula $D_{\text{EQ}}(\mathcal{P}) = \boldsymbol{R}(\mathcal{P})^{-1}\boldsymbol{C}(\mathcal{P})\,H$: "locally obtainable" corresponding to $D_{\text{EQ}}(\mathcal{P}) \in \mathcal{P}$; "locally unobtainable" corresponding to $D_{\text{EQ}}(\mathcal{P}) \notin \mathcal{P}$ (therefore not really equilibria at all); "white" when $\{\widehat{a}_k\}$ is i.i.d.; and "coloured" otherwise. We also have "delay"

equilibria describable by $D_{\text{EQ}}(\mathcal{P}) = +\sigma_\delta \boldsymbol{S}^{\delta}_{N+1} H$; "exact" when $\epsilon_k\big(D_{\text{EQ}}(\mathcal{P})\big) \equiv 0$; and "approximate" otherwise. Note Conjecture 3.11 claims that the branch of the tree in Fig.3.9 leading to the hypothetical white and undetectable equilibria (naturally highly undesirable) does not really exist.

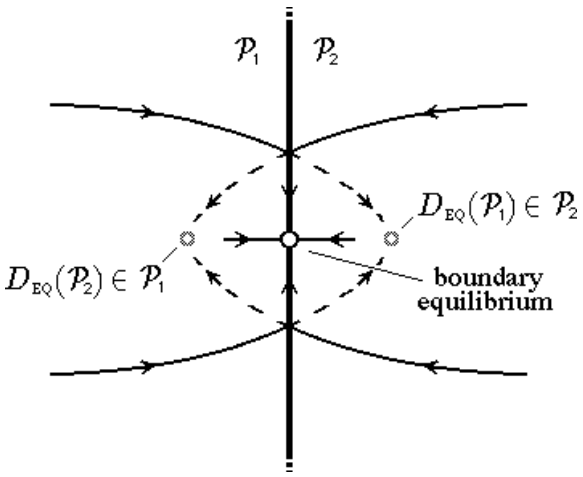

Fig.3.10 Boundary Irregular Equilibrium.

The second major class is labelled "irregular" and we can imagine two broad categories: "boundary-type" where $D_{\text{EQ}} \in \partial\mathcal{P}$ because of the mechanism depicted in Fig.3.10 (requiring two locally unattainable equilibria such that $D_{\text{EQ}}(\mathcal{P}_2) \in \mathcal{P}_1$ and $D_{\text{EQ}}(\mathcal{P}_1) \in \mathcal{P}_2$); and "limit-cycles" where mean adaptation settles down to a well-defined stable closed trajectory via a mechanism analogous to that found in Fig.3.11 (requiring at least three locally unattainable equilibria). These irregular equilibria are hypothetical constructs and given enough time one could conceivably contrive channels which support these strange behaviours. Some roughly analogous results which depict these properties are known in the adaptive filtering literature when the error signal in the adaptation is quantized [27]. (We can demonstrate that "boundary-type" equilibria do exist when the error signal in blind DFE adaptation is quantized, see §3.6.)

3.5.7 Noise Considerations

With the addition of channel noise (Fig.3.2) additional issues come to light. Firstly we note that it is standard in the DDE literature dealing with blind adaptation to work

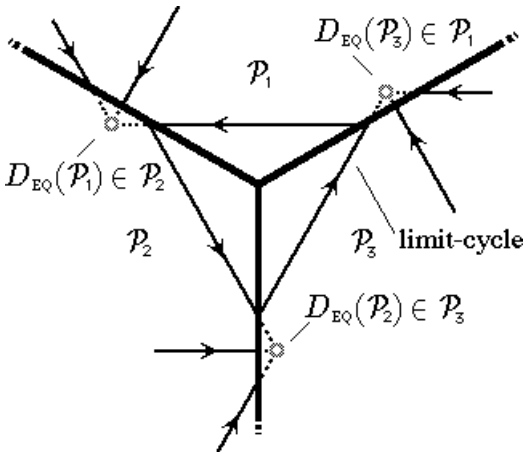

Fig.3.11 Limit-Cycle Equilibrium.

with the noiseless situation. (This is despite the realization that at frequencies where the channel attenuation is high a DDE will result in excessive noise enhancement [1].) The problem remains, of course, that even the noiseless case is not completely understood and is very difficult to analyze [2]. So our digression for the analytically more intractable DFE case will be brief.

When at a delay δ equilibrium, and assuming sufficient correct decisions have been made (in a delay sense) we obtain from (5.2) the equation

$$\widehat{a}_k = \mathrm{sgn}(h_\delta a_{k-\delta} + \sum_{i=0}^{\delta-1} h_i a_{k-i} + n_k). \tag{5.10}$$

where n_k is some zero-mean, additive channel noise (Fig.3.2). Then taking the worst case of past decisions $\{a_{k-i},\ i = 0,\ 1\ ,\ \ldots,\ \delta - 1\}$ we see that one measure of the worst case signal to noise ratio is

$$\frac{(|h_\delta| - \sum_{i=0}^{\delta-1} |h_i|)^2}{E\{n_k^2\}} = \frac{\rho_\delta^2}{E\{n_k^2\}} \tag{5.11}$$

showing the delay equilibria with the largest domain of attraction (l_1-norm radius ρ_δ) is also the best in terms of margin against noise induced decision errors (and subsequent error propagation). Thus with noise present the exact equilibrium need not be the best delay equilibrium, but rather the delay equilibrium with the largest domain of attraction is preferable by (5.11). Heuristically, we could argue that adaptation initialized near the origin would tend to select the equilibrium with the largest domain

of attraction as in Fig.3.7. Not only is it a larger target for the drifting taps but it is also closer to the origin for increasing δ because its centre is at an l_1-norm distance of $\left\|D_{\text{EQ}}\right\|_1 = \sum_{i=\delta}^{N} \left|h_i\right|$ (Theorem 3.8).

3.6 Sign-Error Algorithms

3.6.1 Problem Reformulation

Our objective here is to say something about the convergence properties of modifications of the standard blind LMS algorithms where the Sato error signal ϵ_k is quantized for reasons of numerical advantage. Further, the analysis we now present is a more algebraic description of blind convergence behaviour to complement the previous development. The model of the communication channel remains as in Fig.3.2.

When the Sato error ϵ_k is replaced by its sign, the non-linearity $\psi'_{\text{DFE}}(\cdot)$ generating the error from the decision device input c_k in the standard blind algorithm

$$D_{k+1} = D_k + \gamma\, \psi'_{\text{DFE}}(c_k)\, \widehat{A}_k \tag{6.1}$$

takes the particular form

$$\psi'_{\text{DFE}}(x) = \operatorname{sgn}\big(x - d_0 \cdot \operatorname{sgn}(x)\big). \tag{6.2}$$

The analysis techniques we will develop for the sign-error case can also be applied to algorithms where $\psi'_{\text{DFE}}(\cdot)$ is generated by

$$\psi''_{\text{DFE}}(x) = \mathcal{S}\big(x - d_0 \cdot \operatorname{sgn}(x)\big)$$

where $\mathcal{S}(\cdot)$ is a (non-trivial) sign preserving, memoryless non-linearity, and thus includes the class of standard quantizers. However to keep things specific we treat the sign case (6.2) only in detail.

A diagram of the sign-error adaptive DFE is given in Fig.3.12. It differs marginally from that given in Fig.3.3. Figure 3.12 shows the error signals, ϵ_k and $\eta_k \triangleq \operatorname{sgn}(\epsilon_k)$, that may be used to adapt the taps d_i. The sign-error η_k, from (2.3b) may be represented in various ways by

$$\eta_k \triangleq \psi'_{\text{DFE}}(c_k) \tag{6.3a}$$

$$= \operatorname{sgn}(A_k{}'H - \widehat{A}_k{}'D_k) \tag{6.3b}$$

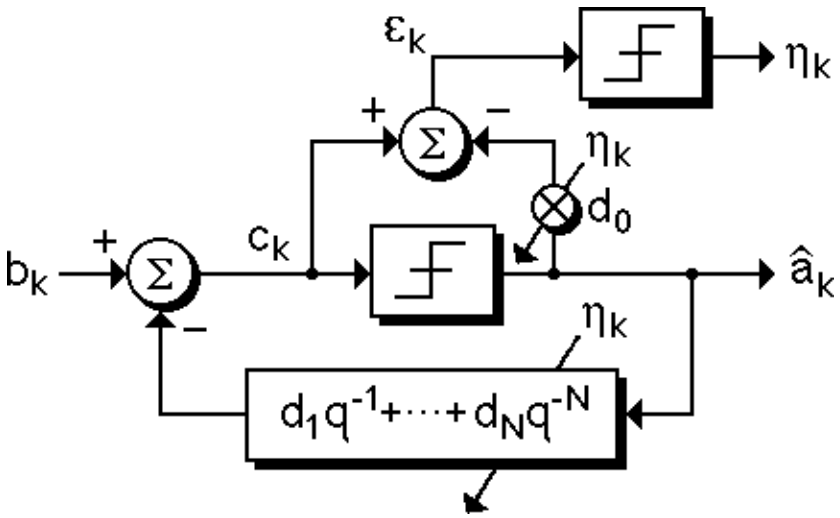

Fig.3.12 Sign-Error Adaptive Decision Feedback Equalizer Model.

where $H \triangleq (h_0,\, h_1,\, \ldots,\, h_N)'$, $D_k \triangleq (d_0,\, d_1,\, \ldots,\, d_N)_k{}'$, $A_k \triangleq (a_k,\, a_{k-1},\, \ldots,\, a_{k-N})'$ and $\widehat{A}_k$ similarly, as before. Recall that the introduction of the d_0 tap in Fig.3.12 is essential if we are to null ϵ_k because it compensates for a non-unity magnitude h_0 (or a non-unity magnitude h_δ if we are near a delay equilibrium).

An attractive property of (6.1) is that to update D_k no multiplications are necessary, as $\eta_k \widehat{A}_k$ is a vector of ± 1's; thus (6.1) is ideal for practical implementation from the viewpoints of lack of complexity and speed. However letting $\|\cdot\|$ denote the l_2-norm, it is clear that

$$\left\|\gamma\, \eta_k\, \widehat{A}_k\right\| = \sqrt{N+1}\cdot\gamma$$

implying the mapping $D_k \rightarrow D_{k+1}$ cannot have a fixed point, leading to a modified concept of convergence [28]. The effect of quantizing the error signal as in (6.3) is to cause a degree of insensitivity of the incremental properties of the algorithm to the parameter values D_k. Predictably this insensitivity is manifest by regions in parameter space not unlike the polytopes encountered earlier in §3.3. To avoid confusion, because as we will see there are two sets of superimposed polytopes, we call the polytopes generated by the previous mechanism in §3.3, $\widehat{a}_k$-polytopes. Also we reserve the symbol $\mathcal{P}$ for a typical $\widehat{a}_k$-polytope.

3.6.2 New Parameter Space Partitions

We begin by introducing some further notation. Let $\mathbb{B} \triangleq \{-1, +1\}$, then $\mathbb{B}^{N+1}$ is the set of all vectors with $N+1$ binary entries. Our intention here is to give a direct

comparison between the polytopes generated by the quantization effect present in forming decisions (§3.3) and the polytopes generated by the quantization effect due to taking the signum function of the error signal ϵ_k (6.3a). This is straightforward because the set of switching hyperplanes for the sign-error (6.3b) is almost identical to the familiar $\widehat{a}_k$-polytope equation (3.1) and clearly takes the form

$$\{D_k \in I\!R^{N+1}\colon\ A_k{}'H = \widehat{A}_k{}'D_k\}. \tag{6.4}$$

The set of switching hyperplanes is generated as we vary across all possible values taken by A_k and $\widehat{A}_k$ in $I\!B^{N+1}$. Note this time d_0 is constrained unlike (3.1). Let us designate as η_k-polytopes the resulting disjoint regions in D_k-space. (Recall this parameter space is the same space in which the $\widehat{a}_k$-polytopes are found.) These regions have the following fundamental property:

Property of η_k-polytopes: *Let $D_1, D_2 \subset \mathcal{N}$ where $\mathcal{N} \in I\!R^{N+1}$ is an arbitrary η_k-polytope. Then*

$$\eta_k(D_1, H, A_k, \widehat{A}_k) = \eta_k(D_2, H, A_k, \widehat{A}_k) \quad \forall A_k \in I\!B^{N+1},\ \forall \widehat{A}_k \in I\!B^{N+1}. \tag{6.5}$$

❑

The modified notation makes it clear on which quantities η_k depends, see (6.3b). We reserve the symbol $\mathcal{N}$ for a typical η_k-polytope.

Remarks:

(i) The signal $\eta_k = \mathrm{sgn}(\epsilon_k)$ is a fixed function of A_k and $\widehat{A}_k$ for the η_k-polytope $\mathcal{N}$, for a given channel.

(ii) If $\widehat{A}_k$ is given, then $\forall D_k \in \mathcal{N}$ the increment direction and magnitude in (6.1) is fixed.

(iii) Despite their superficial similarity, the two sets of hyperplanes (3.1) and (6.4) are quite distinct.

The next step is straightforward. We now consider the regions of D_k-space called $\mathcal{F}$-polytopes (fine polytopes) which are generated by both sets of hyperplanes (3.1) and (6.4). Naturally, each $\widehat{a}_k$-polytope is a disjoint union of $\mathcal{F}$-polytopes as is each η_k-polytope. Within each $\mathcal{F}$-polytope the FSMP is fixed *and* the sign of the error is

independent of $D_k \in \mathcal{F}$. This leads, as we will see, to a very simple picture of the mean behaviour of the blind adaptation of the sign-error DFE (simpler indeed than unsigned error adaptation).

3.6.3 Averaging Theory of Blind Sign-Error Adaptation

From (6.1) we can generate of an averaged equation, as we have for the unsigned error case, describing the mean tap evolution $\{\widetilde{D}_k\}$ when the adaptation gain γ is small. (The mean is in the sense of the ensemble of input sequences.) We formally write the averaged equation as

$$\widetilde{D}_{k+1} = \widetilde{D}_k + \gamma\, \Delta_{\text{AVG}}(D_k, H) \tag{6.6}$$

where $\Delta_{\text{AVG}}(D_k, H)$ acts as the average of $\eta_k \widehat{A}_k = \widehat{A}_k \operatorname{sgn}(A_k{}'H - \widehat{A}_k{}'D_k)$ in (6.1) according to the statistics of A_k and $\widehat{A}_k$. The statistics of A_k and $\widehat{A}_k$ are completely determined by the relevant FSMP. In turn, the FSMP is a function only of the $\widehat{a}_k$-polytopes §3.3.

Our quest to calculate $\Delta_{\text{AVG}}(D_k, H)$ is eased by the finiteness of the number of Markov states. Given the right initial distribution across the Markov states, corresponding to stationarity, we have,

$$\Delta_{\text{AVG}}(D_k, H) = \sum_{(X,Y)\in \mathbb{B}^{N+1}\times\mathbb{B}^{N+1}} \operatorname{sgn}(X'H - Y'D_k) Y \cdot Pr(A_k = X \ \cap\ \widehat{A}_k = Y \ \big|\ D_k). \tag{6.7}$$

This formula is easily explained. The first non-probabilistic portion under the double summation represents a specific value taken on by $\eta_k \widehat{A}_k$ when $A_k = X$ and $\widehat{A}_k = Y$. The second (probabilistic) portion weights the first according to the joint relative frequency (calculable from the FSMP). The conditioning simply recognizes the coarse D_k-dependence of the FSMP.

Now as alluded to above, $\Delta_{\text{AVG}}(D_k, H)$ will actually be constant for extended regions of D_k-space and will not vary continuously with D_k. To see this let $\widehat{D} \in \mathcal{F}$ be arbitrary, where $\mathcal{F}$ is the $\mathcal{F}$-polytope containing D_k. Note both $\operatorname{sgn}(X'H - \widehat{Y}'\widehat{D})Y$ and $Pr(A_k = X \ \cap\ \widehat{A}_k = Y \ \big|\ \widehat{D})$ are fixed for all $\widehat{D} \in \mathcal{F}$ because by construction $\mathcal{F}$ is wholly contained within an $\widehat{a}_k$-polytope and an η_k-polytope, respectively. We rewrite (6.7) as,

$$\Delta_{\text{AVG}}(D_k \in \mathcal{F}, H) = \sum_{(X,Y)\in \mathbb{B}^{N+1}\times\mathbb{B}^{N+1}} \Big\{ \operatorname{sgn}(X'H - Y'\widehat{D}) Y \cdot Pr(A_k = X \ \cap\ \widehat{A}_k = Y \ \big|\ \widehat{D}) \Big\} \tag{6.8}$$

for all $\widehat{D} \in \mathcal{F}$, i.e., the mean adaptive update for all points in an $\mathcal{F}$-polytope is a fixed vector (invariant in $\mathcal{F}$). Thus:

Property of $\mathcal{F}$-polytopes: *With each $\mathcal{F}$-polytope we associate a unique fixed vector (6.8) which when scaled by γ represents the mean adaptive tap update in (6.1) in the sense of (6.6).* ❑

Remarks:

(i) This is very similar in appearance to the "Quiver Diagram" concept found in [27]. However, the difference in our analysis is that we use an informal argument leading to stochastic averaging and the regions (polytopes) in our problem are generated by two mechanisms: (i) the blind regressor generating a coarse parameter space dependence of the FSMP; and (ii) the quantized error which causes the mean parameter update direction to be a coarse function of the parameter space. In [27] only the second mechanism is present.

(ii) Mean adaptation takes place in piecewise linear sections rather than the "steepest descent" curves of standard (unsigned error) blind LMS.

(iii) In blind sign error LMS (6.1) we can regard the taps as moving along a mean square error surface composed of hyperplanes rather than the piecewise quadratic surface arising in the Sato blind unsigned-error LMS (2.3), or the unimodal quadratic surface in standard (training sequence) LMS [21]. Hence any "equilibrium" for $\{D_k\}$ must lie on the boundary between $\mathcal{F}$-polytopes. For similar considerations including: the presence of chattering, limit cycles, etc., see [27].

(iv) The stationarity assumption on the FSMP is essential for tractability of the analysis when looking at case studies. Without it the amount of computation required is substantial. Also it would be a nightmare trying to justify any other assumption. See our example in §3.6.4 where we use the stationarity assumption.

(v) It is possible (as a later example shows) for the stationary distribution of the FSMP to be initial condition dependent in the sense that there may be more than one closed subset (i.e., the unity eigenvalue of the probability transition matrix is not simple [15]). Therefore the stationary probability distribution (invariant probability measure) need not be unique, a possibility overlooked in (6.8). In this situation we would expect to associate two or more $\Delta_{\text{AVG}}(D_k \in \mathcal{F}, H)$ vectors with each $\mathcal{F}$-polytope with only one being appropriate for a given set of initial conditions (and subsequent input $\{a_k\}$).

(vi) For stationarity to hold we are really requesting that a certain time-scale constraint be satisfied—with any transients (of the distribution) having died away. This time-scale for securing stationarity must be necessarily shorter than any time-scale that is associated with the evolution $\{D_k\}$ if our analysis is to be valid. That the time-scale for stationarity is closely related to the largest non-unity magnitude eigenvalue of the FSMP probability transition matrix can be inferred from the work in [15].

3.6.4 Example of Sign-Error Adaptation

Our illustration is with the simplest possible example. We take $N = 1$ and let $h_0 > h_1 > 0$. Figure 3.13 actually displays the case where $h_0 = 4$ and $h_1 = 1$ (it can be shown, but it is not obvious, that all cases where $h_0 > h_1 > 0$ are "isomorphic" to this). Despite the low order the example is a good demonstration of the ideas that we have presented. Incidentally this channel is minimum phase; equally well we could have selected a non-minimum phase example.

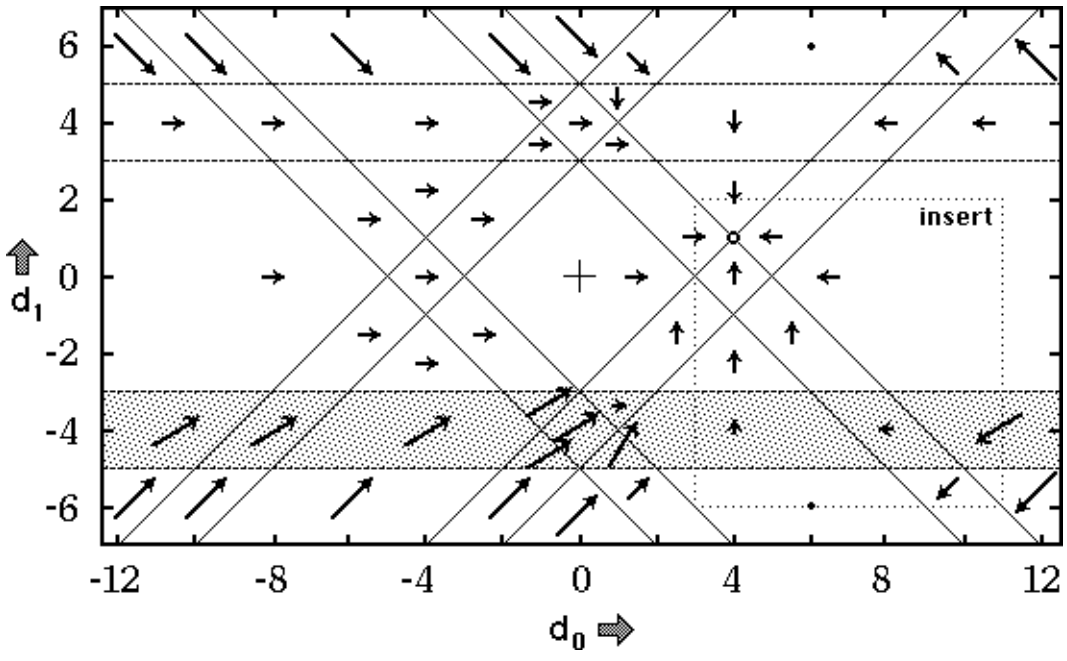

Fig.3.13 $\mathcal{F}$-Polytopes and Quiver Arrows for H=(4,1)′.

Let us explicitly label the elements of $\mathbb{B}^2$ when $N = 1$ as follows,

$$\alpha_1 = \begin{pmatrix} -1 \\ -1 \end{pmatrix}, \quad \alpha_2 = \begin{pmatrix} +1 \\ -1 \end{pmatrix}, \quad \alpha_3 = \begin{pmatrix} -1 \\ +1 \end{pmatrix}, \quad \alpha_4 = \begin{pmatrix} +1 \\ +1 \end{pmatrix},$$

i.e., $\mathbb{B}^2 = \{\alpha_1, \alpha_2, \alpha_3, \alpha_4\}$ (or simply $\mathbb{B}^2 = \{1, 2, 3, 4\}$). (This ordering scheme is slightly different to that seen in Chapter 2, but is necessary to avoid non-standard indexing of matrix entries.) Now we have the following: (i) $X_k \triangleq (a_{k-1}, \widehat{a}_{k-1})'$, the state representing past information at time k, (ii) $A_k = (a_k, a_{k-1})'$, and (iii) $\widehat{A}_k = (\widehat{a}_k, \widehat{a}_{k-1})'$, i.e., each of X_k, A_k and $\widehat{A}_k$ take values in $\mathbb{B}^2$.

Now there are 5 $\widehat{a}_k$-polytopes in this example, whose boundaries (3.1) are the 4 horizontal lines in Fig.3.13, being given by $d_1 = -5, d_1 = -3, d_1 = +3$, and $d_1 = +5$. Let us concentrate on one such $\widehat{a}_k$-polytope, specifically the one satisfying $-5 < d_1 < -3$ (lightly shaded in Fig.3.13). The 4×4 probability transition matrix $\boldsymbol{P}$ for this region is defined by $\boldsymbol{P}_{ij} \triangleq Pr(X_{k+1} = \alpha_i \mid X_k = \alpha_j),\ i, j \in \{1, 2, 3, 4\}$ and is explicitly,

$$\boldsymbol{P} = \begin{pmatrix} \frac{1}{2} & \frac{1}{2} & \frac{1}{2} & 0 \\ \frac{1}{2} & 0 & 0 & 0 \\ 0 & 0 & 0 & \frac{1}{2} \\ 0 & \frac{1}{2} & \frac{1}{2} & \frac{1}{2} \end{pmatrix} \tag{6.9}$$

This matrix defines the FSMP for this $\widehat{a}_k$-polytope (see also Fig.3.14, which we will explain later). The corresponding stationary probability density π_s, defined by $\pi_s = \boldsymbol{P}\pi_s$, is $\pi_s = (\frac{1}{3}, \frac{1}{6}, \frac{1}{6}, \frac{1}{3})'$ and is unique. For the general $N = 1$ matrix $\boldsymbol{P}$, we represent the components of π_s by $(\pi_1, \pi_2, \pi_3, \pi_4)'$. To compute the averaged equation (6.8) we assume stationarity. The joint probability density function $Pr(A_k = \alpha_i \cap \widehat{A}_k = \alpha_j),\ i, j \in \{1, 2, 3, 4\}$ used in (6.8) can be represented by a 4×4 matrix $\boldsymbol{U}$ with components $\boldsymbol{U}_{ij} \triangleq Pr(A_k = \alpha_i \cap \widehat{A}_k = \alpha_j)$. Without proof we give $\boldsymbol{U}$ expressed in terms of the general $N = 1$ state transition matrix $\boldsymbol{P}$ and its invariant probability measure π_s:

$$\boldsymbol{U} = \begin{pmatrix} \boldsymbol{P}_{11}\pi_1 & \boldsymbol{P}_{31}\pi_1 & \boldsymbol{P}_{13}\pi_3 & \boldsymbol{P}_{33}\pi_3 \\ \boldsymbol{P}_{21}\pi_1 & \boldsymbol{P}_{41}\pi_1 & \boldsymbol{P}_{23}\pi_3 & \boldsymbol{P}_{43}\pi_3 \\ \boldsymbol{P}_{12}\pi_2 & \boldsymbol{P}_{32}\pi_2 & \boldsymbol{P}_{14}\pi_4 & \boldsymbol{P}_{34}\pi_4 \\ \boldsymbol{P}_{22}\pi_2 & \boldsymbol{P}_{42}\pi_2 & \boldsymbol{P}_{24}\pi_4 & \boldsymbol{P}_{44}\pi_4 \end{pmatrix} \tag{6.10}$$

which for our example (where $-5 < d_1 < -3$ and $\boldsymbol{P}$ is given by (6.9)) leads to

$$\boldsymbol{U} = \begin{pmatrix} \frac{1}{6} & 0 & \frac{1}{12} & 0 \\ \frac{1}{6} & 0 & 0 & \frac{1}{12} \\ \frac{1}{12} & 0 & 0 & \frac{1}{6} \\ 0 & \frac{1}{12} & 0 & \frac{1}{6} \end{pmatrix}. \tag{6.11}$$

Again this is understood only in the sense of stationarity.

The boundaries of the η_k-polytopes in Fig.3.13 are those eight 45° lines given by $d_0 \pm d_1 = \pm h_0 \pm h_1$, see (6.4). This leads to 25 η_k-polytopes. The $\mathcal{F}$-polytopes are those regions resulting from both the horizontal lines ($\widehat{a}_k$-polytopes) and 45° lines (η_k-polytopes), and total 57.

Now for every $\mathcal{F}$-polytope in our shaded $\widehat{a}_k$-polytope we give an expression for $\Delta_{\text{AVG}}(D_k, H)$, see (6.8). Incorporating the numbers found in (6.11) we can evaluate (6.8), after taking into account symmetry, as

$$\begin{aligned}\Delta_{\text{AVG}}(D_k, H) =& \frac{1}{6}\Big\{2\ \text{sgn}(-5 + d_0 + d_1) + 2\ \text{sgn}(3 + d_0 + d_1) \\ &+ \text{sgn}(-3 + d_0 + d_1)\Big\}\begin{pmatrix}-1\\-1\end{pmatrix} + \frac{1}{6}\ \text{sgn}(5 - d_0 + d_1)\begin{pmatrix}+1\\-1\end{pmatrix}. \quad (6.12)\end{aligned}$$

Then, as an example, substituting $d_0 = 8$ and $d_1 = -4$ gives

$$\Delta_{\text{AVG}}(D_k, H) = (-\tfrac{1}{3}, 0)',$$

and we can find this "left arrow" at point $(8, -4)'$ in a rhombus shaded $\mathcal{F}$-polytope in Fig.3.13. The remaining 10 $\mathcal{F}$-polytopes inside our given shaded $\widehat{a}_k$-polytope can be evaluated similarly using (6.9). The 4 remaining $\widehat{a}_k$-polytopes can be treated similarly and clearly the calculation is quite tedious.

In Fig.3.13, in each of the 57 $\mathcal{F}$-polytopes, we have placed a scaled arrow representing $\Delta_{\text{AVG}}(D_k, H)$ which is an invariant for all $D_k \in \mathcal{F}$. Those regions with a dot instead of an arrow have $\Delta_{\text{AVG}}(D_k, H) = 0$, i.e., adaptation undergoes a random walk. Naturally these arrows scale through γ when forming the true mean update in (6.6).

In Fig.3.14 we have shown the 5 FSMPs for the $\widehat{a}_k$-polytopes in Fig.3.13 (which has been symbolically indicated). Further explanation of Fig.3.13 and Fig.3.14 will be covered in a series of remarks.

Remarks:

(i) Note that in Fig.3.13 the $\mathcal{F}$-polytopes only weakly affect $\Delta_{\text{AVG}}(D_k, H)$ in the sense that crossing a boundary need not necessarily lead to a change in it. This is not a deficiency in the theory but just the stationarity assumption coming into play. If transient stochastic dynamics were to be analyzed (a grotesque problem) then all boundaries indicated, and no more, would be important. The fact that we clearly have properties common to many regions *under stationarity* (thus facilitating an aggregation) is implicitly studied in §3.7.2.

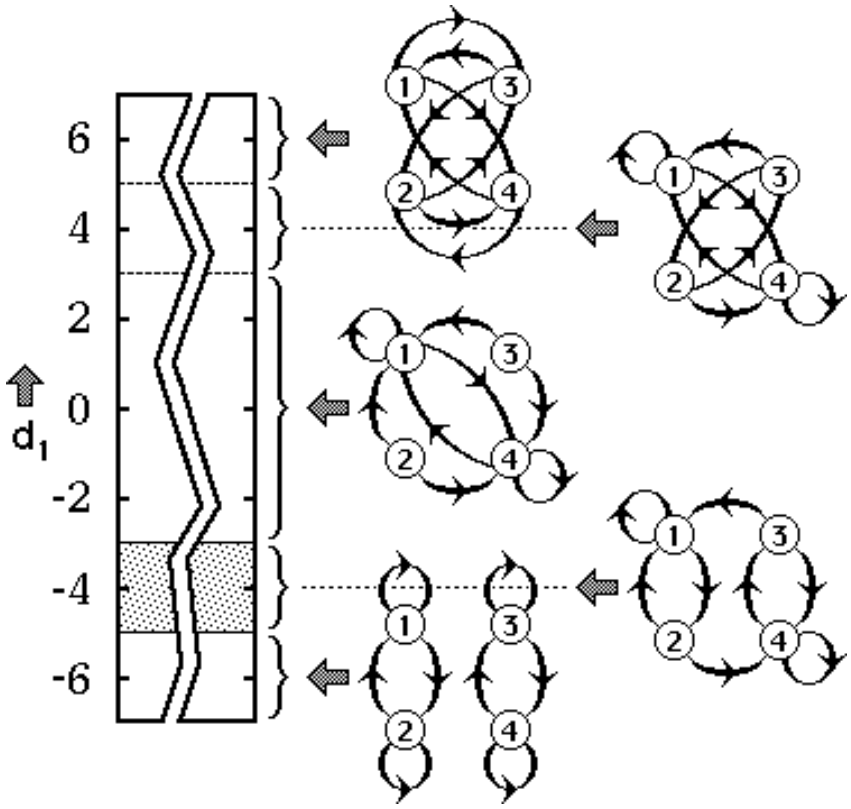

Fig.3.14 The 5 FSMPs and Their Associated $\widehat{a}_k$-Polytopes.

(ii) Observe from Fig.3.13 that the desired tap setting (assuming $h_0 > 0$) lies on the boundaries of 4 η_k-polytopes, a fact obvious from (6.4), setting $D_k = H$ (valid for general N).

(iii) In Fig.3.14 we have indicated 5 FSMPs whose transitions between states $X_k \in \mathbb{B}$ which occur with probability $\frac{1}{2}$.

(iv) The FSMP associated with the bottom $\widehat{a}_k$-polytope, where $d_1 < -5$, has two closed subsets, i.e., the stationary probability density is non-unique, a possibility discussed earlier. When in this particular region we have either $\widehat{a}_k = +1\,\forall k$ (states $\{\alpha_3, \alpha_4\}$) or $\widehat{a}_k = -1\,\forall k$ (states $\{\alpha_1, \alpha_2\}$), i.e., deterministic behaviour once given the initial conditions. Remarkably this dichotomy, as discussed earlier, does not carry over to $\Delta_{\text{AVG}}(D_k, H)$ which is the same in the two cases. More generally we would not expect this.

(v) The top $\widehat{a}_k$-polytope, where $d_1 > +5$, leads to a deterministic behaviour (once given the initial conditions) where the $\{\widehat{a}_k\}$ sequence alternates.

In Fig.3.15, which is an insert of Fig.3.13, we have tried to clarify the meaning of the averaged trajectory equation (6.6). It shows the (discrete) evolution of the DFE taps D_k beginning from $d_0 = 10$ and $d_1 = -4$ for a single input sequence $\{a_k\}$ realization, with $\gamma = 0.01$. The averaged equation (6.6), along with (6.8), implies that adaptation tends along a straight line until it hits an $\mathcal{F}$-polytope boundary and then it abruptly changes direction. This behaviour is confirmed in Fig.3.15. We make some further observations regarding Fig.3.15:

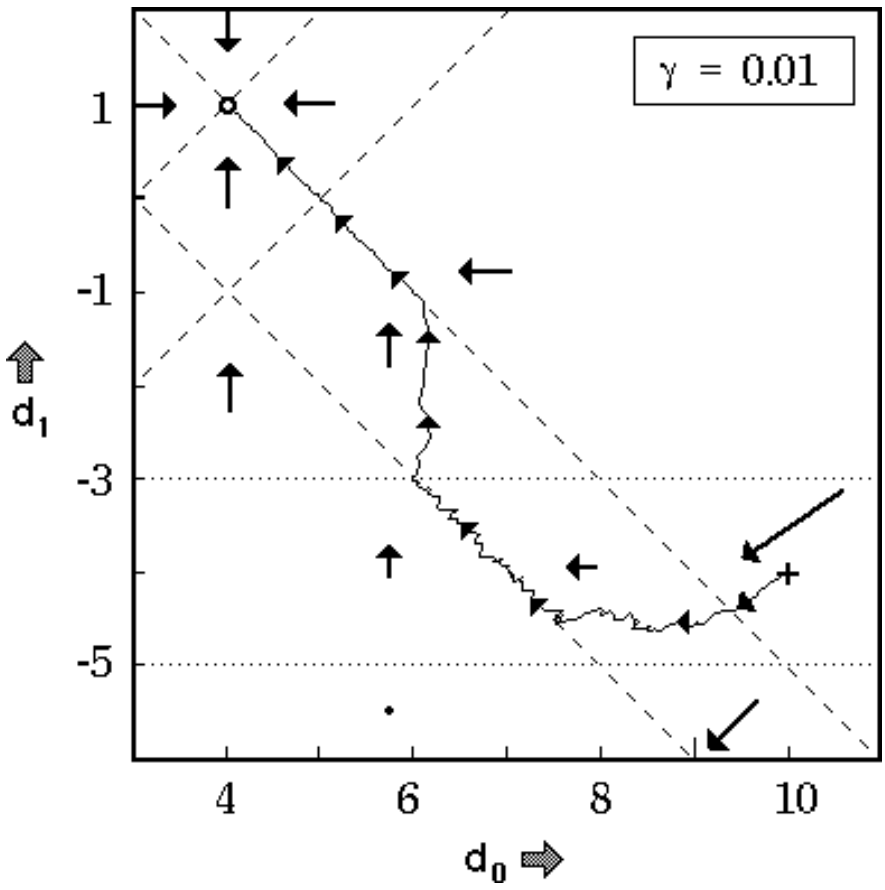

Fig.3.15 Single Adaptation Realization and Polytopes.

Remarks:

(i) For this initial starting position we have convergence to the desired tap setting. For almost all other initial conditions this is also true, see Fig.3.13. That bad behaviour occurs for $|d_1| > 5$ is not of great concern because, as discussed in

§3.5.5, adaptation is sensibly constrained to the region

$$\{D_k \in \mathbb{R}^{N+1}\colon\ \|\underline{D}_k\|_1 < \|H\|_1\}.$$

(ii) A chattering phenomenon is taking place along some boundaries.

(iii) The averaged trajectory not only makes sense in terms of the mean over the ensemble of input sequences but also in terms of a single realization as this example shows. This is true when γ is small and the details are concerned with the law of large numbers [22].

(iv) To avoid confusion we have not drawn-in the averaged trajectory (6.6) in on Fig.3.14. It is clearly that piece-wise linear path parallel to the arrows which the single realization so nearly follows.

3.7 Local Convergence of Blind Sign-Error LMS

3.7.1 Sign-Error Training Sequence Adaptation

Here we quickly review the simple standard training sequence adaptation case because we can utilize this calculation later in a different context. With a training sequence in sign-error adaptation the tap update takes the form,

$$D_{k+1} = D_k + \gamma\ \mathrm{sgn}\left(A_k(H - D_k)\right) A_k, \tag{7.1}$$

when $h_0 > 0$. In terms of the analysis in §3.6.3 this is equivalent to setting $\widehat{A}_k = A_k\ \forall k$ along with a suitable modification of the joint probability density function term. Hence, it can be shown that the mean update akin to (6.8) takes the form,

$$\Delta_{\text{AVG}}(D_k \in \mathcal{N}, H) = \frac{1}{2^{N+1}} \sum_{X \in \mathbb{B}^{N+1}} \mathrm{sgn}((H - \widehat{D})'X)\cdot X, \quad \forall \widehat{D} \in \mathcal{N} \tag{7.2}$$

where: (i) $Pr(A_k = X) = \frac{1}{2^{N+1}}$ replaces $Pr(A_k = X\ \cap\ \widehat{A}_k = Y \mid \widehat{D} \in \mathcal{F})$, and (ii) we have $\widehat{D} \in \mathcal{N}$ rather than $\widehat{D} \in \mathcal{F}$ because the tapped delay line is artificially fed with the known training sequence, equal to $\{a_k\}$. Hence the $\widehat{a}_k$-polytopes play no role in training sequence adaptation. (Indeed, (7.1) is completely independent of $\widehat{a}_k$.) However, with the η_k-polytopes, we see that the maximum number of partitioning hyperplanes reduces from 2^{2N+1} to 2^{N+1}, as setting $\widehat{A}_k = A_k$ in (6.4) shows. This

leads to an aggregation of (the old) η_k-polytopes into coarser (new) η_k-polytopes, i.e., $\mathcal{N}$ above can and should actually be understood as an aggregation of η_k-polytopes. This then aligns with some known results—our coarser η_k-polytopes are isomorphic to the "cones" described in [8], and also derived in [5] (arising in the simpler decision directed equalizer context).

3.7.2 Local Stability of Blind Sign-Error Adaptation

Our aim in this section is to show that the sign-error algorithm (6.1) has the right dynamical properties in the vicinity of the desired tap setting where $D_k = H$ ($h_0 > 0$ is assumed). In particular we wish to show that if the tap weights are perturbed away from $D_k = H$ then there is a general restoring force back to the desired tap setting.

Our first task will be to show that the stochastic dynamics of the DFE in the vicinity of the desired tap setting H take a particularly simple form if we impose stationarity, allowing us to draw on the results in §3.7.1.

In §3.5.4 it was shown that the region in D_k-space given by

$$\mathcal{J}(0) \triangleq \{D_k \in I\!R^{N+1}\colon\ h_0 > \sum_{i=1}^{N} \big|h_i - d_i\big|\} \tag{7.3}$$

has the following properties which are easily verified: (i) it is a union of $\widehat{a}_k$-polytopes, (ii) every FSMP identified with each $\widehat{a}_k$-polytope in $\mathcal{J}(0)$ has precisely one closed subset. In this closed subset all decisions will be correct, i.e., of the form $\widehat{a}_k = a_k$. This says all the FSMPs in $\mathcal{J}(0)$ share a common substructure. This closed subset property means that the stationary behaviour is characterized by $\widehat{a}_k = a_k$, $\forall k > K$, for some finite K a.s. Hence under stationarity we have $\widehat{A}_k = A_k$, $\forall D_k \in \mathcal{J}(0)$. Thus we see that (6.8) degenerates to (7.2) when $D_k \in \mathcal{J}(0)$.

We have shown that, under stationarity and for $D_k \in \mathcal{J}(0)$,

$$\Delta_{\text{AVG}}(D_k, H) = \frac{-1}{2^{N+1}} \sum_{X \in I\!B^{N+1}} \operatorname{sgn}(X'(D_k - H))X \tag{7.4}$$

by drawing on (7.2). Then we observe from (7.4) that

$$\begin{aligned}\Delta_{\text{AVG}}(D_k, H)'(D_k - H) &= \frac{-1}{2^{N+1}} \sum_{X \in I\!B^{N+1}} \operatorname{sgn}\big(X'(D_k - H)\big)X'(D_k - H) \\ &= \frac{-1}{2^{N+1}} \sum_{X \in I\!B^{N+1}} \big|X'(D_k - H)\big| < 0, \quad D_k \neq H \end{aligned} \tag{7.5}$$

where the last line follows from the $\mathbb{R}^{N+1}$ spanning property of $\mathbb{B}^{N+1}$ (this is actually a persistence of excitation condition, see [29]).

Result (7.5) says that the euclidean distance of D_k from H decreases in the mean $\forall D_k$ excluding a neighbourhood of H (which scales in proportion to γ). Thus the mean behaviour of $\{D_k\}$ will be to close in on H until it is roughly within an euclidean distance of $\sqrt{N+1}\cdot\gamma$ (§3.6.1) where the fixed step size disrupts further convergence, see [28]. This is a simple geometric argument which shows the sign-error algorithm has a form of local convergence, at least in $\mathcal{J}(0)$ centering on H. Note $\mathcal{J}(0)$ (7.3) can typically be quite large, e.g., for those channels in [20].

Remarks:

(i) Taking up a suggestion in [30] any switching from unsigned error LMS to sign-error LMS inside $\mathcal{J}(0)$ will tend to maintain $D_k \in \mathcal{J}(0)$ and thus $\widehat{a}_k = a_k$, $\forall k > K$ for some finite K a.s. The effect of taking the sign of the error ϵ_k in forming η_k (6.3b) is effectively to increase the adaptive gain relative to unsigned error LMS and thus presumably provide superior tracking of H if it is slowly time varying (for fixed γ).

(ii) The analysis shows that when $D_k \in \mathcal{J}(0)$ the blind adaptation is identical to training sequence adaptation apart from some stochastic transient which exists before the FSMP achieves steady state or stationarity. The equivalence between blind and training sequence adaptation whenever $D_k \in \mathcal{J}(0)$ is independent of the adaptive algorithm employed because it is a manifestation only of equation (2.2).

(iii) Let $N = 1$, then $\mathcal{J}(0)$ (7.3) is $\left|h_1 - d_1\right| < h_0$, i.e., $-3 < d_1 < 5$, and we can identify this in Fig.3.13 as the union of two $\widehat{a}_k$-polytopes. Note the form taken on by the two FSMPs (see Fig.3.14) alluded to above (existence of an invariant closed subset, i.e., $\{\alpha_1, \alpha_4\}$ which is reached in finite time a.s.).

(iv) Consider the case where $\eta_k = \mathrm{sgn}(\epsilon_k)$ in (6.3c) is replaced by $\mathcal{S}(\epsilon_k)$ where $\mathcal{S}(\cdot)$ is any (saturating) memoryless non-linearity, not necessarily a quantizer, which preserves the sign of ϵ_k. Then (7.5) will still hold with obvious scaling modification, implying local convergence for the algorithm,

$$D_{k+1} = D_k + \gamma\, \mathcal{S}(\epsilon_k)\widehat{A}_k.$$

This property was eluded to in §3.6.1.

3.7.3 Local Stability of Delay-Type Equilibria

Up to this point we have concentrated on the local properties of sign-error adaptation when in the vicinity of the desired tap setting $D_k = H$. This is the most important case for our application in mind [20]. This desired tap setting is an attraction point for all reasonable algorithms, blind or otherwise. However, with blind unsigned error LMS algorithms (2.3) multiple equilibria are possible having typically non-ideal properties §3.5.6. Of these the so-called "delay-type equilibria" are the most interesting and of greatest practical interest. Here we wish to study the corresponding delay-type equilibria (if they exist) for the sign-error LMS algorithm (6.1).

In unsigned error LMS (2.3), when the tap weights move within a vicinity of a delay-type equilibrium all decisions $\widehat{a}_k$ will be of the form $\widehat{a}_k = +\sigma_\delta\, a_{k-\delta}$ (for some delay parametrized by $\delta \in \{0,\ 1,\ \ldots,\ N\}$) under stationarity. The desired tap setting is such an equilibrium when we set $\delta = 0$. This delay type behaviour is only a consequence of the non-adaptive properties of the DFE, i.e., equation (2.2), and hold independent of the adaptive algorithm employed. (It is a property only of the $\widehat{a}_k$-polytopes and is independent of the η_k-polytopes.) We now show that the delay-type equilibria will have the same local convergence properties as has the desired tap setting where $\delta = 0$ provided an additional inequality involving the h_i parameters is satisfied.

In §3.5.4 it was shown that a necessary condition for $\widehat{a}_k = +\sigma_\delta\, a_{k-\delta}\ \forall k\ \forall\{a_k\}$ is

$$\mathcal{J}(\delta) \triangleq \{D_k \in I\!R^{N+1}\colon\ \big|h_\delta\big| > \sum_{i=0}^{\delta-1}\big|h_i\big| + \sum_{i=\delta+1}^{N}\big|h_i - \sigma_\delta{\cdot}d_{i-\delta}\big| + \sum_{i=N-\delta+1}^{N}\big|d_i\big|\}. \quad (7.6)$$

To simplify proceedings we assume that this condition is also sufficient when we have stationarity. (This is true for $\delta \in \{0, 1\}$ as well as for many channels of interest, and is the basis of Conjecture 3.11.) One thinks of (7.6) as defining and generalizing a region in D_k-space like $\mathcal{J}(0)$ (7.3). Indeed (7.6) is a domain of attraction for an equilibrium located at

$$D_{\text{EQ}}(\delta) = \sigma_\delta\ (h_\delta,\ h_{\delta+1},\ \ldots,\ h_N,\ 0,\ \ldots,\ 0)'. \quad (7.7)$$

in the unsigned error case (2.3), see §3.5.4. (Note with $D_k = D_{\text{EQ}}(\delta)$ the last two summations in (7.6) are identically zero.) We now show that with the sign-error blind algorithm there is always a general restoring force if the taps are perturbed away from a small region containing $D_{\text{EQ}}(\delta)$.

We begin by studying (6.8), when (7.6) is in force. Then whenever

$$X = A_k \triangleq (a_k,\ a_{k-1},\ \ldots,\ a_{k-N})'$$

we have

$$Y = \widehat{A}_k = \sigma_\delta \left(a_{k-\delta},\ a_{k-\delta-1},\ \ldots,\ a_{k-\delta-N}\right)'$$

under stationarity. It is clear that X and Y are highly correlated because they share $N-\delta+1$ components. Under these conditions we can simplify (6.8) to

$$\Delta_{\text{AVG}}(D_k, H) = \frac{1}{2^{N+1+\delta}} \sum_{I\!B^{N+\delta+1}} \text{sgn}\left(X'H - Y'D_k\right) Y \tag{7.8a}$$

noting

$$X'H - Y'D_k = \sum_{i=0}^{\delta-1} h_i a_{k-i} + \sum_{i=\delta}^{N} (h_i - \sigma_\delta \cdot d_{i-\delta}) a_{k-i} - \sigma_\delta \sum_{i=N-\delta+1}^{N} d_i a_{k-\delta-i} \tag{7.8b}$$

where $I\!B^{N+\delta+1}$ is the set of all possible values of $\{a_k,\ a_{k-1},\ \ldots,\ a_{k-\delta-N}\}$, noting $\left|I\!B^{N+\delta+1}\right| = 2^{N+1+\delta}$, and $Pr(Z) = \frac{1}{2^{N+1+\delta}}$, $\forall Z \in I\!B^{N+\delta+1}$. In analogy with §3.7.2 we examine the following projection

$$\Delta_{\text{AVG}}(D_k, H)'\left(D_k - D_{\text{EQ}}(\delta)\right) \tag{7.9}$$

and attempt to show it is strictly negative, thus implying convergence in the appropriate sense. First we define $\mathcal{H}(Z \in I\!B^{N+\delta+1}) \triangleq Y'\left(D_k - D_{\text{EQ}}(\delta)\right)$, i.e.,

$$\mathcal{H}(Z \in I\!B^{N+\delta+1}) \triangleq -\sum_{i=\delta}^{N} (h_i - \sigma_\delta d_{i-\delta}) a_{k-i} + \sigma_\delta \sum_{i=N-\delta+1}^{N} d_i a_{k-\delta-i} \tag{7.10a}$$

and

$$\mathcal{G}(Z \in I\!B^{N+\delta+1}) \triangleq \sum_{i=0}^{\delta-1} h_i a_{k-i}. \tag{7.10b}$$

So substituting (7.8a) into (7.9) and utilizing (7.10) we obtain

$$\Delta_{\text{AVG}}(D_k, H)'\left(D_k - D_{\text{EQ}}(\delta)\right) = \frac{1}{2^{N+1+\delta}} \sum_{Z \in I\!B^{N+\delta+1}} \text{sgn}\left(\mathcal{G}(Z) - \mathcal{H}(Z)\right) \mathcal{H}(Z) \tag{7.11}$$

noting (7.11) reduces to (7.5) when $\delta = 0$. However when $\delta > 0$, we need to be concerned with when $\mathcal{H}(Z)$ dominates $\mathcal{G}(Z)$, i.e., with the argument of the sgn$(\cdot)$ function in (7.11). This leads us to consider a region in D_k-space, an inequality alluded to earlier, defined by the following condition,

$$\inf_{\{a_k\}} \left|\sum_{i=0}^{\delta-1} h_i a_{k-i}\right| > \sum_{i=\delta}^{N} \left|h_i - \sigma_\delta \cdot d_{i-\delta}\right| + \sum_{i=N-\delta+1}^{N} \left|d_i\right| \tag{7.12a}$$

$$= \left\|D_k - D_{\text{EQ}}(\delta)\right\|_1 \tag{7.12b}$$

noting, to make things clearer, that the left hand side of (7.12) is the minimum value achievable by $\mathcal{G}(Z)$ in (7.10b), whilst the right hand side is the maximum value achievable by $\mathcal{H}(Z)$ in (7.10a).

Now suppose (7.12) is satisfied, then by construction it follows that $\operatorname{sgn}\big(\mathcal{G}(Z) - \mathcal{H}(Z)\big) = \operatorname{sgn}\big(\mathcal{G}(Z)\big)\ \forall Z \in \mathbb{B}^{N+\delta+1}$ which means (7.11) becomes $\Delta_{\text{AVG}}(D_k, H)'\big(D - D_{\text{EQ}}(\delta)\big) = 0$ by the independence of $\mathcal{H}(Z)$ and $\mathcal{G}(Z)$. In fact $\Delta_{\text{AVG}}(D_k, H)$ in this case just becomes

$$\Delta_{\text{AVG}}(D_k, H) = \frac{1}{2^{N+1+\delta}} \sum_{Z \in \mathbb{B}^{N+\delta+1}} \operatorname{sgn}\big(\mathcal{G}(Z)\big)\ Y(Z) = 0$$

because $\mathcal{G}(Z)$ and $Y(Z)$ are independent. This shows that for a small l_1-ball region about $D_{\text{EQ}}(\delta)$, i.e., (7.12), the adaptation performs a random walk. We might say that the error surface is flat within an l_1-ball (7.12) around a delay equilibrium.

Now suppose (7.12) is not satisfied, i.e., D_k is exterior to the l_1-ball (7.12) and its boundary (the boundary is excluded because of our general disclaimer regarding the unlikely occurrence of zero arguments in sgn$(\cdot)$ functions). Then it is straightforward to verify there exists $Z \in \mathbb{B}^{N+\delta+1}$ with non-zero probability such that

$$\operatorname{sgn}\big(\mathcal{G}(Z) - \mathcal{H}(Z)\big) = -\operatorname{sgn}\big(\mathcal{H}(Z)\big) = -\operatorname{sgn}\big(\mathcal{G}(Z)\big)$$

and

$$\big|\mathcal{H}(Z)\big| = \sum_{i=\delta}^{N} \big|h_i - \sigma_\delta \cdot d_{i-\delta}\big| + \sum_{i=N-\delta+1}^{N} \big|d_i\big| > 0.$$

This implies that $-\mathcal{H}(Z)$ agrees in sign or dominates $\mathcal{G}(Z)$ for more than half of the elements of $Z \in \mathbb{B}^{N+\delta+1}$, whence we have the desired strict inequality in (7.9):

$$\Delta_{\text{AVG}}(D_k, H)'\big(D_k - D_{\text{EQ}}(\delta)\big) < 0.$$

This shows that the D_k-taps converge towards the l_1-ball (7.12) which is centered on $D_{\text{EQ}}(\delta)$ and within which the adaptation performs a random walk. This analysis hinges on hypothesis (7.6) being satisfied. This then raises the question of whether (7.12) is wholly contained within region (7.6). The condition under which this can only occur is the inequality:

$$\big|h_\delta\big| - \sum_{i=0}^{\delta-1} \big|h_i\big| > \inf_{\{a_k\}} \big|\sum_{i=0}^{\delta-1} h_i a_{k-i}\big| \tag{7.13}$$

To prove this we first rewrite (7.6) as

$$\big|h_\delta\big| - \sum_{i=0}^{\delta-1} \big|h_i\big| + \big|h_\delta - \sigma_\delta\ d_0\big| > \big\|D_k - D_{\text{EQ}}(\delta)\big\|_1$$

and then compare this with (7.12) in the form,

$$\inf_{\{a_k\}} \big|\sum_{i=0}^{\delta-1} h_i a_{k-i}\big| > \big\|D_k - D_{\text{EQ}}(\delta)\big\|_1.$$

Equation (7.13) is then a direct consequence when we have the critical case $h_\delta = +\sigma_\delta\ d_0$.

Recapitulating, when $\delta > 0$ the region (7.6) acts as a domain of attraction for the sign-error algorithm (6.1) if and only if (7.13) holds. (Condition (7.13) automatically holds for $\delta = 0$.) This is in contrast with the unsigned error case (2.3) where (7.6) is the unconditional domain of attraction. Violation of (7.13) means that it is possible the taps D_k undergo a (zero-drift) random walk which may take it out of region (7.6), i.e., with little effort. Of course even with (7.13) in force the taps may leave (7.6), since (7.13) is only a condition on average behaviour. However, to do so it would be a rare event (analyzable through large deviations theory) and it is this distinction we wish to draw when we refer to convergence.

Finally, we note an even more detailed analysis than that carried out in this section necessitates the introduction of the polytope ideas of §3.6.2. Indeed, it is possible to see that the fundamental region (7.12) has boundaries precisely of the form (6.4) which define the η_k-polytopes. In other words the l_1-ball (7.12) is a union of η_k-polytopes, as we must expect.

3.8 Conclusions

3.8.1 Summary

We itemize some contributions:

(i) The parameter space partition which was shown to be useful in the study of error recovery for DFEs (whose parameter settings matched those of the channel, Chapter 2) has been extended to the case where we do not have matching to cover the case where the taps are being adapted.

(ii) The effect of using a blind regressor was shown to cause the DFE parameter space to be tiled where each tile is a polytope and within each tile the error surface is a quadratic function of the DFE parameters. This error surface is discontinuous at the boundaries in general.

(iii) A general mechanism whereby the blind adaptive algorithm may get hung at an undesirable setting of the DFE parameters was shown. We also gave an example where this behaviour is demonstrated.

(iv) A discrete averaged equation which provides information about the mean drift of the DFE taps was given and this verified our predictions regarding the behaviour of the DFE as the boundary of a polytope is traversed. A predicted refraction phenomenon was observed.

(v) The various convergence points for the blind DFE algorithm were classified, focussing on the most important δ-delay equilibria where the DFE output sequence is a δ time sample delay of the input with an associated possible sign inversion. These results differ from the blind DDE case where all possible delays are possible and both signs are possible. With a DFE only a finite number of delays (generally well less than the number of tap parameters) are possible and only one sign is associated with each delay.

(vi) The conditions under which delay equilibria exist were presented in a theorem and are interpreted as a simple condition on the channel impulse response values.

(vii) A signum quantization of the error signal (and standard coarse quantization) leads to an additional set of polytopes to characterize blind DFE adaptation which need to be superimposed on those polytopes originating from the FSMP classification.

(viii) An averaging theory was developed for sign-error blind adaptation and this lead to accurate predictions of the behaviour of the evolving DFE taps as shown by an example.

(ix) A local stability analysis was performed when the DFE taps are in a well-defined vicinity of a delay equilibrium. When a sign-error is used in blind adaptation one obtains a dead region (where the taps perform a random walk) in a small neighbourhood of a delay equilibrium which may disrupt convergence. This dead region is not related to the well-known effect where the taps cannot converge because a minimum step size (both effects are present).

3.8.2 Discussion

We have demonstrated that an analysis of blind adaptation in decision feedback equalization is possible—the principal difficulty being how to incorporate the effects of decision errors into the picture. We have shown it is possible to build a conceptual model for the behaviour of the equalizer during blind adaptation, and based on this we can understand why the taps may hang at equilibria leading to poor performance. These investigations more than anything build and aid our intuition, for example, we can view standard blind adaptation as evolving on a mean square error surface composed of a tiling (the polytopes) of quadratic functions. When it so happens that the minimum of one of these quadratic functions for a given tile lies within the tile we have a locally attainable minimum, i.e., an attraction point for the adaptation. Also we can use our theory to predict with sufficient precision the adaptive behaviour of a blind DFE on a given channel, via tedious calculations.

However the difficulty remains of extracting useful practical information from these sorts of investigations. Here we have limited success, e.g., a simple condition on the channel parameters provides information on the *possibility* of the algorithm being found at an equilibrium giving delay-like behaviour. Still, the likelihood of obtaining broad sweeping statements relating to the guarantee of ideal blind convergence attributes seems a distant goal (and the same problem exists for linear equalization, although we have the remarkable results in [2] for a special case). Our work has value in showing just how difficult such a general theory giving useful practical information would need to be, and perhaps in highlighting what simplifying assumptions might be valid.

The results in this chapter stand in contrast to the simplicity of the systems and algorithms proposed and under study. In fact it becomes apparent from our work that if one tries to simplify the algorithm from a practical viewpoint, e.g., use the sign of the error (rather than full precision), then the theory can very easily get more complicated (and obscure). Our useful results in this case show that there is a general tendency for the adapting taps to stay in the vicinity of a delay equilibrium (for both the standard and sign-error algorithms).

We note that to secure our theory we need to make a stationarity assumption on the underlying FSMPs. This is a reasonably strong assumption. It is equivalent to a time-scale separation idea, meaning that given an non-ideal initial starting distribution of the FSMP (arbitrary initial conditions in the DFE) we need to stipulate

that the adapting taps not move too far before the invariant distribution is established (with reasonable probability). So the fast time-scale is associated with the transient dynamics of the FSMP and a slow time-scale is associated with the adaptation algorithm, i.e., the adaptive gain γ needs to be sufficiently small. Clearly a theory which could deal with both timescales being of comparable orders would be ambitious, to say the least.

Finally, we have some comments on the system under study. Our general aim was to show how decision errors, which may be common, distort adaptation relative to the training sequence case. To achieve this understanding we chose, sensibly, the simplest non-trivial system. This system can be used on channels exhibiting limited pre-cursor intersymbol interference, and has limited but non-empty practical application. A more general DFE structure requires the use of a linear equalizer as the first stage and its taps may be simultaneously (blindly) adapted with the simpler structure we have studied. This is a different, more complicated problem and our techniques may be partially employed in performing an analysis of this more complex system. We are confident such an analysis is possible but we have made no attempt in this direction. A second comment is that blind adaptation has restricted practical application. In the case of rapidly time-varying channels training sequences would appear to be indispensable, and more robust techniques of channel identification perhaps using coding, etc., would be required.

References

[1] S.U.H. Qureshi, "Adaptive Equalization," *Proc. IEEE,* vol.73, No.9, pp.1349-1387, September 1985.

[2] A. Benveniste, M. Goursat, and G. Ruget, "Robust Identification of a Non-minimum Phase System: Blind Adjustment of Linear Equalizer in Data Communications," *IEEE Trans. on Auto. Control,* vol.AC-25, No.6, pp.385-399, June 1980.

[3] D.N. Godard, "Self Recovering Equalization and Carrier Tracking in Two-dimensional data Communication Systems," *IEEE Trans. on Communications,* vol.-COM-28, pp.1867-1875, November 1980.

[4] A. Benveniste, and M. Goursat, "Blind Equalizers," *IEEE Trans. on Communications,* vol.COM-32, No.6, pp.871-883, August 1984.

[5] O. Macchi, and E. Eweda, "Convergence Analysis of Self Adaptive Equalizers," *IEEE Trans. on Information Theory,* vol.IT-30, No.2, pp.161-176, March 1984.

[6] R. Kumar, "Convergence of a Decision-Directed Equalizer," *Proc. 1983 Conf. on Decision and Control,* pp.1319-1324.

[7] A. Benveniste, "A Gain and Phase Identification Procedure: Blind Adjustment of a Recursive Equalizer," *"Optimization Tech."* 7th IFIF Conf., Würzburg, FRG, 1978 Springer V. LNCIS vol.6-7.

[8] J.E. Mazo, "Analysis of Decision-Directed Equalizer Convergence," *Bell Syst. Tech. J.,* Vol.59, No.10, pp.1857-1876, December 1980.

[9] S. Verdú, "On the Selection of Memoryless Adaptive Laws for Blind Equalization in Binary Communication," *Proc. Sixth Intl. Conf. on Analysis and Optimization of Systems,* Nice, France, June 1984.

[10] A. Jennings, "Analysis of the Adaption of Decision Feedback Equalizers with Decision Errors," Internal Report Telecom Aust. Research Lab., July 1985.

[11] D.L. Duttweiler, J.E. Mazo, and D.G. Messerschmitt, "An Upper Bound on the Error Probability in Decision Feedback Equalizers," *IEEE Trans. on Information Theory,* vol.IT-20, pp.490-497, July 1974.

[12] A. Cantoni, and P. Butler, "Stability of Decision Feedback Inverses," *IEEE Trans. on Communications,* vol.COM-24, pp.1064-1075, September 1976.

[13] J.J. O'Reilly, and A.M. de Oliveira Duarte, "Error Propagation in Decision Feedback Receivers," *Proc. IEE Proc. F, Commun., Radar and Signal Process.,* vol.132, no.7, pp.561-566, 1985.

[14] A.M. de Oliveira Duarte, and J.J. O'Reilly, "Simplified Technique for Bounding Error Statistics for DFB Receivers," *Proc. IEE Proc. F, Commun., Radar and Signal Process.,* vol.132, no.7, pp.567-575, 1985.

[15] R.A. Kennedy, and B.D.O. Anderson, "Recovery Times of Decision Feedback Equalizers on Noiseless Channels," *IEEE Trans. on Communications,* vol.COM-35, pp.1012-1021, October 1987.

[16] R.A. Kennedy, B.D.O. Anderson, and R.R. Bitmead, "Tight Bounds on the Error Probabilities of Decision Feedback Equalizers ," *IEEE Trans. on Communications,* vol.COM-35, pp.1022-1029, October 1987.

[17] R.A. Kennedy, and B.D.O. Anderson, "Error Recovery of Decision Feedback Equalizers on Exponential Impulse Response Channels," *IEEE Trans. on Communications,* vol.COM-35, pp.846-848, August 1987.

[18] Y. Sato, "A Method of Self-Recovering Equalization for Multilevel Amplitude Modulation," *IEEE Trans. on Communications,* vol.COM-23, pp.679-682, June 1975.

[19] R.A. Kennedy, G. Pulford, B.D.O. Anderson, and R.R. Bitmead, "When has A Decision-Directed Equalizer Converged?," *IEEE Trans. on Communications,* (accepted for publication).

[20] B.R. Clarke, "The Time-Domain Response of Minimum Phase Networks," *IEEE Trans. on Circuits and Syst.,* vol.CAS-32, No.11, pp.1187-1189, November 1985.

[21] B. Widrow, and S.D. Stearns, "Adaptive Signal Processing ," Prentice Hall Inc., Englewood Cliffs, N.J., 1985.

[22] M.I. Freidlin, and A.D. Wentzell, "Random Perturbations of Dynamical Systems," Springer-Verlag New York Inc., 1984.

[23] R.R. Bitmead, B.D.O. Anderson, and T.S. Ng, "Convergence Rate Determination for Gradient Based Adaptive Estimators," *Automatica,* vol.22, no.2, pp.185-191, 1986.

[24] B.D.O. Anderson, R.R. Bitmead, C.R. Johnson, Jr., P.V. Kokotovic, R.L. Kosut, I.M.Y. Mareels, L. Praly, and B.D. Riedle, "Stability of Adaptive Systems: Passivity and Averaging Analysis," MIT Press, Cambridge, Massachusetts 1986.

[25] J. Zabczyk, "Exit Problem and Control Theory," *Systems and Control Letters,* no.6, pp.165-172, 1985.

[26] M. Cottrell, J.C. Fort, and G. Malgouyres, "Large Deviations and Rare Events in the Study of Stochastic Algorithms," *IEEE Trans. on Auto. Control,* vol.AC-28, No.9, pp.907-920, September 1983.

[27] C.R. Elevitch, W.A. Sethares, G. Rey, and C.R. Johnson Jr., "Quiver Diagrams For Signed Adaptive Filters ," *IEEE Trans. on Acoustics, Speech and Signal Processing,* (accepted for publication).

[28] A. Gersho, "Adaptive Filtering with Binary Reinforcement," *IEEE Trans. on Information Theory,* vol.IT-30, No.2, pp.191-199, March 1984.

[29] W.A. Sethares, "Quantized State Adaptive Algorithms," PhD Dissertation, Cornell University, Ithaca NY, August 1987.

[30] C.R. Johnson Jr., "Lectures on Adaptive Parameter Estimation," Prentice Hall Inc., Englewood Cliffs, N.J., 1987.

CHAPTER **4.**

NON-ADAPTIVE DFE PASSIVITY ANALYSIS

Aim: *To determine sufficient conditions on the channel frequency response that guarantee the rapid error recovery of non-ideal decision feedback equalizers via a stability analysis.*

4.1 Introduction

Decision feedback equalizers (DFEs) have been seen to be simple hardware devices designed to cancel intersymbol interference (ISI) generated by a distorting channel. However, the major problem identified with their non-adaptive operation was error propagation [1] which we have analyzed in a stochastic setting in Chapter 2.

We saw in Chapter 2 that the presence of error propagation means that DFE operation in practice may be unsatisfactory, in the sense that the time for the DFE to recover from any error condition may be unacceptably long [2,3]. In fact, we showed that over the class of all finite impulse response (FIR) channels of length N the mean error recovery time may be of order 2^N data periods (even for some which are minimum phase or near minimum phase), which evidently is totally impractical. Our previous analysis established the problem of identifying *stronger hypotheses* on the channel model for which the error recovery time is sufficiently short, as judged by practical standards. For these channels we can say then that a DFE is a practical option. Determining such a class of channels is the aim of this chapter. (Some generalizations of the notion of error recovery prompted by the investigations into adaptation found in Chapter 3 are also treated.)

In general we can classify two classes of channel which are acceptable from a practical point of view—the distinction is not great. The first class needs some statistical model of the input sequence for its definition. To define the class, one then simply

requests that the expected or mean time for error recovery for all initial error states is sufficiently short—this was the approach of Chapter 2. However, this leaves open the possibility of the existence of pathological input sequences [2,4] for which errors are made after any arbitrary length of time even in the absence of noise. In a well defined sense, however, these sequences are probability zero events [2,4]. The second class of channels are those for which the error recovery time is finite for all possible input sequences and initial conditions. In this case the statistical model of the input is largely irrelevant. Further, this means that pathological input sequences are non-existent, i.e., one can never be so unlucky as to have an input sequence for which the DFE never performs satisfactorily—a most attractive property. In this chapter we find a broad and robust class of channels for which the error recovery time is finite. As such we are defining a class of channels suffering from significant ISI for which a DFE may be effectively used. This class captures a range of practical channels as we will see from an example.

In the literature there has been very little written about the error recovery properties of DFEs. In fact only in [2,5,6] has it been indicated theoretically that there are some non-trivial channels for which the DFE operates satisfactorily. In contrast, the two prominent early references analyzing error propagation in DFEs [1,4] both give no comfort to the practicing engineer who finds the practical simplicity of DFEs appealing. In [1,4] the given bounds on recovery time and error probability actually correspond to the *worst* realizable channel models as was demonstrated in Chapter 2 (reported in [2,3]). Because the DFE has such deplorable performance when operating on channels with these bounds, the results are not very useful in practice (but of theoretical importance and interest). We note here also the work in [7,8] which strives to reduce these bounds given explicit, i.e., specific, knowledge of the channels. In contrast, here we give a broad general condition on the channel parameters—specifically the coefficients satisfy a passivity constraint or equivalently a simple frequency response condition—to ensure good DFE error recovery performance. This condition is satisfied by a class of practical channels as we will show.

The major sections are organized as follows. In §4.2 we define the DFE system of interest and we define our finite error recovery time problem. In §4.3 we use Lyapunov techniques to show that exponential impulse response channels have a quantifiable maximum recovery time. In §4.4 we give the necessary background on the passivity theorem, sufficient for our needs. It also gives our basic main result which establishes

that whenever the channel satisfies a simple frequency domain constraint, the error recovery time of an ideal DFE is always finite. We also include four applications of this theorem including analysis of a real channel. In §4.4 we move away from purely existential results to establish convergence rates and explicit bounds given an exponential overbound on the channel impulse response. It also contains the results of serious practical interest because we relax most of the major idealized assumptions to be found in Chapter 2 and those of §4.2. We also give the result for M-ary data and relate the error recovery time bound back to the binary case. For high signal to noise ratio channels satisfying a passivity constraint we give a formula for the error probability, §4.5. In §4.6 we examine a timing phase problem. The conclusions as well as a useful summary are given in §4.7.

4.2 Problem Formulation and Definitions

A communication channel and general non-adaptive decision feedback equalizer (DFE) are shown in Fig.4.1. The communication channel is modelled as a linear, time-invariant filter with impulse response,

$$h \triangleq \{h_0,\ h_1,\ h_2,\ \ldots\} \tag{2.1}$$

of possibly infinite dimension. This channel is driven by an input binary sequence $\{a_k\}$, where k is the discrete time index. No statistical model of $\{a_k\}$ is assumed nor needed. The M-ary $\{a_k\}$ case will also be treated in a later section. We note that in a more general context h could be thought of as the cascade (convolution) of the linear channel and a linear equalizer preceding the DFE.

The distorted output of the linear channel is b_k and is assumed noiseless. By studying the noiseless case we are creating a pointer to the important practical situation of a high signal to noise ratio channel. (In a later section we will introduce an additive noise signal into the analysis but only treat the asymptotic case as the noise variance tends to zero.) At the receiving end we have a DFE consisting of a tapped delay line with impulse response

$$d \triangleq \{0,\ d_1,\ d_2,\ \ldots\} \tag{2.2}$$

fed by a binary output decision sequence $\{\widehat{a}_k\}$ as described by Fig.4.1.

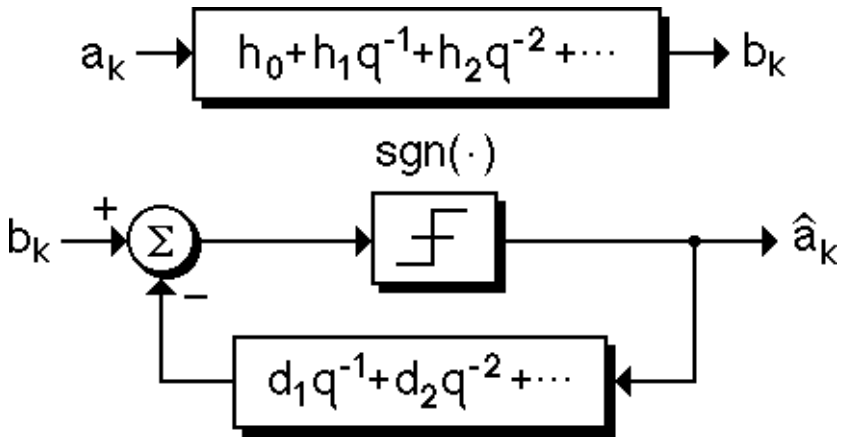

Fig.4.1 Channel and Decision Feedback Equalizer Models.

The algebraic formulation of the system depicted in Fig.4.1 is given by

$$\widehat{a}_k = \mathrm{sgn}(h_0 a_k + \sum_{i=1}^{\infty} h_i a_{k-i} - \sum_{i=1}^{\infty} d_i \widehat{a}_{k-i}); \quad h_0 \geq 0 \tag{2.3}$$

where ideally we would like $d_i = h_i$, $\forall i > 0$. Note also that we assume without loss of generality that $h_0 \geq 0$ (if $h_0 = 0$, see §4.4.5). Hence the study of error propagation under these ideal conditions leads to the equation,

$$\widehat{a}_k = \mathrm{sgn}(h_0 a_k + r_k) \tag{2.4a}$$

where

$$r_k \triangleq \sum_{i=1}^{\infty} h_i e_{k-i} \tag{2.4b}$$

and

$$e_k \triangleq a_k - \widehat{a}_k. \tag{2.4c}$$

Most of the ideal assumptions represented in (2.4) will be relaxed in §4.4.5. Here it is convenient to treat the ideal case first so that we may focus on the technique employed and not get lost in a labyrinth of unimportant detail.

We now define what we mean by error recovery:

Definition: *The DFE has* ***recovered from error*** *at time K if*

$$\widehat{a}_k = a_k \quad \text{, or equivalently,} \quad e_k = 0 \quad \forall k \geq K, \quad \forall \{a_k\}.$$

□

This definition is the most natural one but differs from the definition of error recovery time given in Chapter 2. The condition in Chapter 2 is stronger than what is actually needed—it is sufficient but not necessary for guaranteed error free behaviour. Explicitly, the definition in Chapter 2 identifies error recovery with an error vector $E_k \triangleq (e_{k-1},\ e_{k-2},\ \ldots,\ e_{k-N})'$ being identically zero. Clearly in terms of error recovery what is more important is that r_k in (2.4b) is sufficiently small (rather than $E_k = 0$) and this is precisely what the new definition attempts to reflect. In both cases the definitions are convenient for the style of analysis being performed.

Now if we rewrite (2.4) as

$$\widehat{a}_k = \operatorname{sgn}\big((h_0 + r_k a_k)\ a_k\big)$$

then it is clear that $h_0 > \big|r_k\big|$ ensures $h_0 + r_k a_k > 0$ and thus a sufficient condition for DFE recovery at time K is

$$h_0 > \big|r_k\big| \quad \forall k \geq K, \quad \forall\{a_k\}. \tag{2.5}$$

However, this condition (2.5) is also necessary because the definition for error recovery stipulates no errors can be made when we consider all possible input sequences. So that particular input sequence which is generated by $a_k = -\operatorname{sgn}(r_k) \ \ \forall k \geq K$ must give no errors, and the desired conclusion follows.

From (2.5) it is clear that the ISI term r_k is crucial in understanding the error propagation and error recovery mechanisms. We investigate this signal further. We complete this section with a simple but fundamental lemma which is a mild generalization of the above analysis and so we omit a proof (if ever one were needed).

Lemma 4.1: *Let r_k in (2.4b) denote the ISI and h_0 the cursor. Then:*

(i) $\big|r_k\big| < h_0$ *or* $a_k = +\operatorname{sgn}(r_k) \ \Rightarrow\ \widehat{a}_k = +a_k \iff e_k = 0.$

(ii) $\big|r_k\big| > h_0$ *and* $a_k = -\operatorname{sgn}(r_k) \ \Rightarrow\ \widehat{a}_k = -a_k \iff e_k = -2\ \operatorname{sgn}(r_k).$

❑

The next two sections investigate two different approaches to providing quantitative and qualitative statements on the times to recovery for DFEs—we begin with a Lyapunov analysis in §4.3 and follow this by a passivity analysis in §4.4.

4.3 Exponential Impulse Response Channels

As a preliminary to the more general passivity analysis, which is to follow, we examine the special situation where the channel impulse response is exponential [6]. Thus we consider channels of the following form:

$$h_m = \beta^m \cos(\omega m), \quad m \geq 0 \tag{3.1}$$

where $0 \leq \beta < 1$ and $0 \leq \omega < 2\pi$. We may represent this channel by

$$h_m = \frac{1}{2}\left(\alpha^m + (\alpha^*)^m\right) \tag{3.2}$$

where $\alpha \triangleq \beta \exp(j\omega) \in \mathcal{C}$ (the complex plane), and α^* denotes the complex conjugate of α. From (3.2) we will focus on a quantity B_k, closely related to r_k (2.4b), defined as follows

$$B_k \triangleq \sum_{m=1}^{\infty} e_{k-m}\alpha^m \tag{3.3}$$

where $e_k \triangleq a_k - \widehat{a}_k$, as usual. We will see that $\{|B_k|\}$ is a candidate Lyapunov function. Writing the DFE output equation in terms of B_k we get

$$\widehat{a}_k = \operatorname{sgn}(a_k + \sum_{m=1}^{\infty} \beta^m \cos(m\omega) e_{k-m}) \tag{3.4a}$$

$$= \operatorname{sgn}(a_k + Re(B_k)) \tag{3.4b}$$

noting $r_k \triangleq Re(B_k)$ for this special channel. However $\{B_k\}$, by the nature of the exponential character of the channel, evolves in time according to

$$B_{k+1} = \alpha \cdot (B_k + e_k) \tag{3.5}$$

as is easily verified from (3.3).

In view of Lemma 4.1 we see:

$$B_{k+1} = \begin{cases} \alpha \cdot B_k, & \text{if } \widehat{a}_k = a_k; \\ \alpha\{B_k - 2\operatorname{sgn}(Re(B_k))\}, & \text{if } \widehat{a}_k \neq a_k, \end{cases}$$

in either case we claim $\{|B_k|\}$ is a Lyapunov function, explicitly:

Lemma 4.2: *Let the channel $\{h_m\}$ be given by (3.1) and B_k be given by (3.3), then*

$$\left|B_{k+1}\right| \leq \beta \cdot \left|B_k\right|, \quad \forall k \geq 0 \tag{3.6}$$

❑

Proof: *From (3.5) if $\widehat{a}_k = a_k$ then (3.6) is automatic recognizing $\left|\alpha\right| = \beta$. In the case $\widehat{a}_k = -a_k$ one is led to conclude $\left|r_k\right| > 1$ (Lemma 4.1) which is the same as the statement $\left|Re(B_k)\right| > 1$. By symmetry we need only to consider $Re(B_k) > 1$, then $B_{k+1} = \alpha(B_k - 2)$. Whence*

$$\begin{aligned}\left|B_{k+1}\right|^2 = Im^2(B_{k+1}) + Re^2(B_{k+1}) &= \left|\alpha\right|^2\big((Re(B_k) - 2)^2 + Im^2(B_k)\big) \\ &= \left|\alpha\right|^2\big(Re^2(B_k) - 4Re(B_k) + 4 + Im^2(B_k)\big) \\ &< \left|\alpha\right|^2 \left|B_k\right|^2\end{aligned}$$

which completes the proof. ❑

Remarks:

(i) $\{\left|B_k\right|\} \rightarrow 0$ at least as fast as $\left|\alpha\right|^k = \beta^k$, i.e., decays to zero at a rate commensurate to the channel parameter β.

(ii) The result is independent of the modulation parameter ω in (3.1).

We complete the analysis by determining an explicit upper bound on the error recovery time using a worst case analysis. This involves finding a bound on $\left|B_0\right|$ which models an initial, arbitrary error state. From (3.3) we see that

$$\left|B_0\right| \leq 2\sum_{i=0}^{\infty}\left|\alpha\right|^i = \frac{2\beta}{1-\beta}. \tag{3.7}$$

Then to determine a bound on the worst case recovery time we need to find the least integer K which satisfies $\left|B_K\right| < 1$ (guaranteeing $\widehat{a}_k = a_k$ from (3.4b)), since then the monotonicity of $\left|B_k\right|$ with respect to k (3.6), implies all decisions for $k \geq K$ are correct. The calculation is simple. Using (3.6) and (3.7) we obtain

$$\left|B_K\right| \leq \beta^K \cdot \left|B_0\right| \leq \frac{2 \cdot \beta^{K+1}}{1-\beta} < 1 \tag{3.8}$$

noting $\left|B_k\right| < 1$ guarantees $\widehat{a}_k = a_k$ (3.4b). After a little manipulation on (3.8) we obtain K as the least integer satisfying

$$K > \log_\beta \left\{ \frac{1-\beta}{2\beta} \right\}, \quad \frac{1}{3} < \beta < 1 \tag{3.9}$$

noting whenever $0 \leq \beta < \frac{1}{3}$ the ISI can never be large enough to ever cause an error.

It is possible to relate the bound K with a number J which we interpret as a measure of the channel time constant [6]. Define J as the number for which $\beta^J = 0.01$, i.e., the period of time that it takes the impulse response to die to a hundredth of its initial peak. Thus

$$J \triangleq \log_\beta\{0.01\}$$

which may be compared with (3.9). Figure 4.2 shows a plot of K versus J as β ranges from 0.33 through 0.99. It shows that for exponential impulse response channels where $\beta < 0.99$, the time required for error recovery is less than the order of the channel time constant. Note that because one can find initial conditions and a suitable input sequence $\{a_k\}$ which realizes the worst case recovery, then, in this sense, the error recovery time bound is tight.

Remarks:

(i) Paradoxically, the calculation leading to Lemma 4.2 shows that the slowest error recovery results when the output sequence consists entirely of correct decisions. With decision errors, recovery is sped.

(ii) The above results may be generalized to M-ary symbols rather than binary symbols using the same style of analysis. Later, for a more general class of channels, we will derive results for the M-ary case using passivity ideas.

4.4 General Passivity Analysis

4.4.1 Background

The idea of reformulating the error recovery problem as a stability problem originated with Cantoni *et al.*, [4]. Our analysis in this chapter takes up this concept and it is natural to investigate the use of stability ideas in proving that under certain conditions a DFE has a finite recovery time (for all initial conditions and for all input

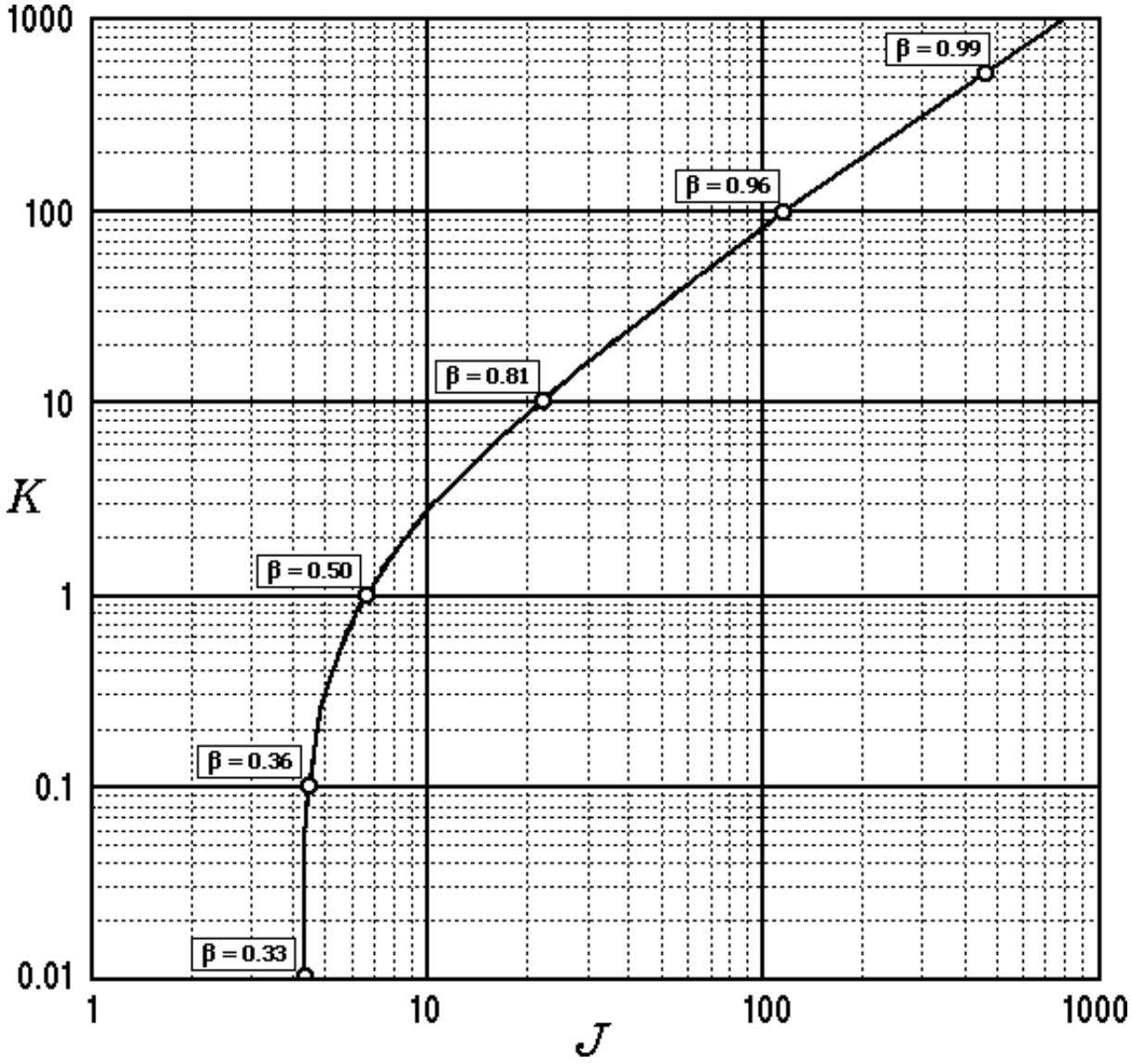

Fig.4.2 Recovery Time K vs Channel Time Constant J.

sequences). The ideas we need have their origins within circuit theory. Our main result uses Passivity Theory [9] to give an easily checked frequency domain condition that guarantees a finite recovery time [10].

We begin our passivity analysis by re-examining Lemma 4.1 from §4.2. Lemma 4.1 is significant because it characterizes the error propagation mechanism. Figure 4.3 is a pictorial representation of Lemma 4.1. The upper block in Fig.4.3 is just a block representation of equation (2.4b). It is modelled by a strictly causal convolutional operator $\underline{\mathcal{H}}$ which maps the error sequence $e \stackrel{\Delta}{=} \{e_k,\ k \geq 0\}$ to the ISI sequence $r \stackrel{\Delta}{=} \{r_k,\ k \geq 0\}$

in accordance with (2.4b), i.e., $r = \underline{\mathcal{H}}e \triangleq \underline{h} \circledast e$ where $\underline{h} \triangleq \{0,\ h_1,\ h_2,\ \ldots\}$ (which differs from (2.1)). The lower block $\mathcal{L}$ in Fig.4.3 consists of two parts. The first is a stochastic multiplier, to account for the stochastic input a_k, defined by,

$$m_k \triangleq \begin{cases} 1 & \text{if } \ a_k = -\operatorname{sgn}(r_k); \\ \\ 0 & \text{if } \ a_k = +\operatorname{sgn}(r_k), \end{cases} \tag{4.1}$$

whose function is clear from Lemma 4.1(i), i.e., if $m_k = 0 \ \Rightarrow \ a_k = \operatorname{sgn}(r_k) \ \Rightarrow \ e_k = 0$. Otherwise m_k does nothing, i.e., m_k takes the value unity (4.1). The second part of the lower block is a time-invariant non-linearity which maps $\{m_k r_k\}$ into the sequence $z \equiv -e$. Note whenever the input $m_k r_k$ is less in magnitude than h_0 the output $z_k = -e_k$ is zero (as in Lemma 4.1(i)). Otherwise the output conforms to Lemma 4.1(ii). Note that in this block the stochastic multiplier and the non-linearity may be commuted. The point of introducing the summation block to perform the inversion of z to e is that the blocks then form the standard arrangement of a feedback system suggesting the use of stability arguments.

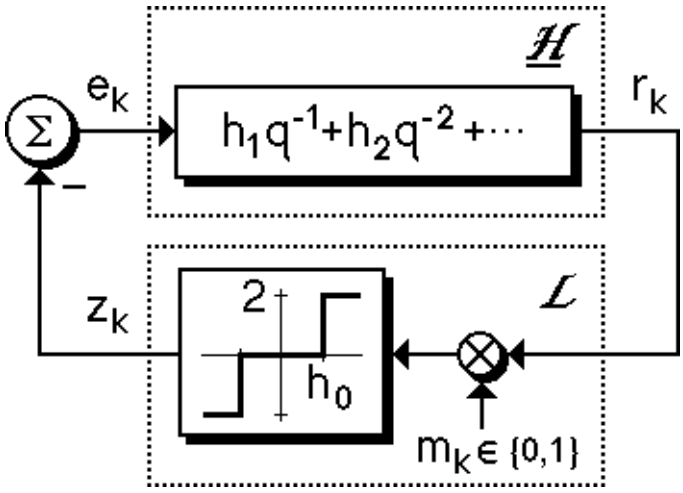

Fig.4.3 Error Propagation (Feedback) Block Diagram.

A significant observation we make concerning the lower block $\mathcal{L}$ in Fig.4.3 is that it is a memoryless (stochastically time-varying) sector-bounded non-linearity. We see that whenever the output is non-zero it preserves the sign of the input and therefore is a passive operator in the circuit theoretic sense [9] (when $h_0 = 0$ or indeed is just very small then our analysis in §4.4.5 applies). Our first task will be to transform the

system in Fig.4.3 such that the upper block $\underline{\mathcal{H}}$ becomes a strictly passive operator whilst the lower block $\mathcal{L}$ remains passive. Then we utilize some standard results from input-output stability to show the DFE has a (quantifiable) bounded recovery time. In the next section we present the minimal set of definitions and notation needed to develop the general input-output (passivity) stability result.

4.4.2 Definitions and Passivity Theorem

We begin with some definitions which are standard in input-output stability theory [9]. We focus on a Hilbert space structure composed of real valued sequences indexed by $k \in \mathbb{Z}_+$ (non-negative integers). Then if we have two sequences $x \triangleq \{x_0,\ x_1,\ \ldots\}$ and $y \triangleq \{y_0,\ y_1,\ \ldots\}$ their inner product will be defined as

$$\langle x, y \rangle \triangleq \sum_{i=0}^{\infty} x_i y_i. \tag{4.2}$$

where it is clear that $\langle x, y \rangle = \langle y, x \rangle$. This inner product (4.2) induces a natural euclidean norm defined by

$$\|x\| \triangleq \langle x, x \rangle^{\frac{1}{2}} = \Big(\sum_{i=0}^{\infty} {x_i}^2 \Big)^{\frac{1}{2}}. \tag{4.3}$$

We define the discrete function space l_2 which consists of all sequences satisfying

$$x \in l_2 \iff \|x\| < \infty. \tag{4.4}$$

Similarly we have the space l_1 which consists of all sequences satisfying

$$x \in l_1 \iff \|x\|_1 \triangleq \sum_{i=0}^{\infty} |x_i| < \infty.$$

The space l_2 is generally too restrictive an arena for deriving results, so we introduce the standard concept of an extended space l_2^e [9], defined by

$$x \in l_2^e \iff \|P_T x\| < \infty, \quad \forall T \in \mathbb{Z}_+ \tag{4.5}$$

where P_T is a truncation operator parametrized by $T \in \mathbb{Z}_+$ in turn defined by

$$(P_T x)(k) \triangleq \begin{cases} x_k, & \text{if } k \le T; \\ 0, & \text{if } k > T. \end{cases}$$

Note (4.5) just says that $x \in l_2^e$ if and only if $\left|x_k\right| < \infty \ \forall k$, i.e., x does not have a finite escape time. So for example if $x \triangleq \{x_k = 2^k, \ \forall k \in \mathbb{Z}_+\}$ then $x \in l_2^e$ but clearly $x \notin l_2$.

From definitions (4.4) and (4.5) it is apparent that $l_2 \subset l_2^e$. In our work all signals considered will lie in the extended space l_2^e (because we stipulate only that $h \in l_1$). However it is of great interest to show that particular signals also lie in the subset l_2. For example with the error signal, it is our aim to show $e \in l_2$. Then because $e_k \in \{-2, 0, +2\}$ we have the following fundamental observation,

$$e \in l_2 \iff e_k = 0, \quad \forall k \geq K \qquad K < \infty \tag{4.6}$$

i.e., by our previous definition, the DFE has recovered from error at time K.

Now define $x_t \triangleq P_T x$ and $\left\|x\right\|_T \triangleq \left\|P_T x\right\|$. In relating l_2 and l_2^e we note the following important properties of the inner product and its induced norms which we will use later without explicit reference:

(i) $\forall x \in l_2^e$, the mapping $T \mapsto \left\|x\right\|_T$ is monotonically increasing.

(ii) $\forall x \in l_2$, $\lim_{T \to \infty} \left\|x\right\|_T = \left\|x\right\|$.

(iii) $\forall x, y \in l_2^e, \ \forall T \in \mathbb{Z}_+$, we have $\left\langle x_T, y_T \right\rangle = \left\langle x_T, y \right\rangle = \left\langle x, y_T \right\rangle \triangleq \left\langle x, y \right\rangle_T$.

This nomenclature leads to the crucial definitions of passivity.

Definition: *An operator $\mathcal{H}: l_2^e \mapsto l_2^e$ is* ***passive*** *if $\exists$ constant β such that*

$$\left\langle \mathcal{H}x, x \right\rangle_T \geq \beta, \quad \forall x \in l_2^e \ \forall T \in \mathbb{Z}_+. \tag{4.7}$$

❑

If $\mathcal{H}$ were linear then β could be taken as zero [9].

Definition: *An operator $\mathcal{H}: l_2^e \mapsto l_2^e$ is* ***strictly passive*** *if $\exists \delta > 0$ and $\exists \beta$ such that*

$$\left\langle \mathcal{H}x, x \right\rangle_T \geq \delta \cdot \left\|x\right\|_T^2 + \beta, \quad \forall x \in l_2^e \ \forall T \in \mathbb{Z}_+. \tag{4.8}$$

❑

Again if $\mathcal{H}$ were linear then β could be taken as zero. We label δ as the *degree of passivity.*

As an example of passivity (but not strict passivity), which will be important later, let us check the claim at the end of §4.4.1 concerning the lower block $\mathcal{L}$ of Fig.4.3. Suppose $x \in l_2^e$ is the input to an operator $\widehat{\mathcal{H}}$ with output $y \triangleq \widehat{\mathcal{H}}x$, which satisfies $y_k x_k \geq 0$, $\forall k \in \mathbb{Z}_+$ (a sign preserving operator). Then trivially

$$\langle \widehat{\mathcal{H}}x, x \rangle_T = \sum_{k=0}^{T} y_k x_k \geq 0, \quad \forall x \in l_2^e \ \ \forall T \in \mathbb{Z}_+, \tag{4.9}$$

showing $\widehat{\mathcal{H}}$ is passive according to definition (4.7) with $\beta = 0$. That is, if $\widehat{\mathcal{H}}$ is a non-linearity constrained to the first and third quadrants then it is passive (even if it is time-varying or has memory).

Our second example which we state as a lemma will be important later and relates to the definition of strict passivity (4.8) applied to linear operators.

Lemma 4.3: *Suppose the linear operator* $\mathcal{G}$*:* $l_2^e \mapsto l_2^e$ *defined by* $\mathcal{G}u = g \circledast u$*, where* $g \triangleq \{g_0,\ g_1,\ \ldots\} \in l_1$*. Let the input* $u \in l_2^e$*. Then*

$$\langle \mathcal{G}u, u \rangle_T \geq \delta \cdot \|u\|_T^2,\ \forall u \in l_2^e \ \ \forall T \in \mathbb{Z}_+ \iff Re\big(\widetilde{g}(e^{j\theta})\big) \geq \delta, \ \ \forall \theta \in [0, 2\pi] \tag{4.10}$$

where $\widetilde{g}(z) \triangleq \sum_{i=0}^{\infty} g_i z^{-i}$ *is the Z-transform of the impulse response* g*, and* $\delta > 0$*.* ❑

The proof follows from Parseval's Theorem (see [9]). Lemma 4.3 says that a linear convolutional operator is strictly passive if and only if its Nyquist plot belongs to

$$\{z \in \mathbb{C}\colon\ Re(z) \geq \delta\}.$$

We now come to the main passivity theorem. Figure 4.4 defines the signals and operators of interest. In it e and v are the input sequences to the operators $\mathcal{H}_1$ and $\mathcal{H}_2$ and $y = \mathcal{H}_1 e$ and $z = \mathcal{H}_2 v$ are the respective output sequences. There is a single external signal u. All signals shown are assumed to lie in l_2^e. The following theorem and proof are an adaptation of a more general result in [9,p.182].

(Passivity) Theorem 4.4: *Suppose: (i) Operator* $\mathcal{H}_1$ *is linear and strictly passive, i.e.,*

$$\langle \mathcal{H}_1 e, e \rangle_T \geq \delta_1 \cdot \|e\|_T^2, \quad \forall e \in l_2^e \ \ \forall T \in \mathbb{Z}_+ \tag{4.11}$$

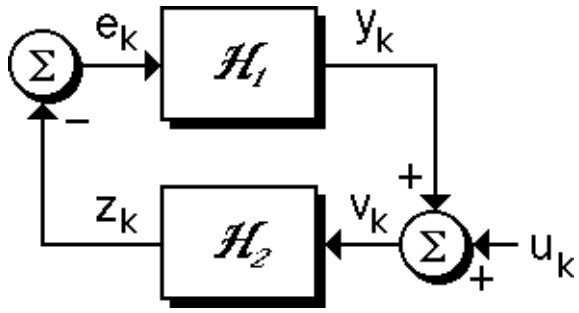

Fig.4.4 Passivity Theorem Block Diagram.

where $\delta_1 > 0$; and (ii) operator $\mathcal{H}_2$ is a non-linearity confined to the first and third quadrant, implying

$$\langle \mathcal{H}_2 v, v \rangle_T \geq 0, \quad \forall v \in l_2^e \;\; \forall T \in \mathbb{Z}_+ \tag{4.12}$$

by (4.7), and is thus passive. Then $u \in l_2 \;\Rightarrow\; e \in l_2$ ❑

Proof: *We show $e \in l_2$ by determining upper and lower bounds on $\langle \mathcal{H}_1 e, e \rangle_T + \langle \mathcal{H}_2 v, v \rangle_T$ which may be thought of as the total energy dissipated by the system in Fig.4.4 from time 0 to time T. First we determine a lower bound. Using (4.11) and (4.12) we clearly have*

$$\langle \mathcal{H}_1 e, e \rangle_T + \langle \mathcal{H}_2 v, v \rangle_T \geq \delta_1 \cdot \|e\|_T^2 \;\; \forall T \in \mathbb{Z}_+ \tag{4.13}$$

where, recall, $\delta_1 > 0$ is the constant associated with the degree of passivity of the $\mathcal{H}_1$ operator. An upper bound on (4.13) follows from the following simple calculation, using Fig.4.4,

$$\begin{aligned} \langle \mathcal{H}_1 e, e \rangle_T + \langle \mathcal{H}_2 v, v \rangle_T &= \langle \mathcal{H}_1 e, e \rangle_T + \langle -e, v \rangle_T = \langle -e, v - \mathcal{H}_1 e \rangle_T \\ &= \langle -e, u \rangle_T \leq \|e\|_T \cdot \|u\|_T, \quad \forall T \in \mathbb{Z}_+ \end{aligned} \tag{4.14}$$

where the last line is an application of the Cauchy-Schwartz inequality. Then combining (4.13) with (4.14) we obtain $\|e\|_T \leq \delta_1^{-1} \|u\|_T \;\; \forall T \in \mathbb{Z}_+$ whenever $\|e\|_T > 0$. Letting $T \to \infty$ we find

$$\|e\| \leq \delta_1^{-1} \|u\| \tag{4.15}$$

i.e., $u \in l_2 \;\Rightarrow\; e \in l_2$ as desired. ❑

4.4.3 Sufficient Conditions for a Finite Recovery Time

In this section we transform the system in Fig.4.3 so that we may apply the general passivity theorem of the last section. This involves two steps. The first step is to apply a feedforward path around the upper block in Fig.4.3 to attempt to turn it into a strictly passive operator, which currently it is not. To compensate for this distortion we need also to apply an identical feedback path about the lower block. The second step is to model the effects of initial conditions at time $k = 0$, i.e., an initial (arbitrary) error state, by an external signal u as in the passivity theorem. This latter point, which will be treated in more detail later, is based on the equivalence of non-zero initial conditions and zero external input in Fig.4.3 to zero initial conditions and non-zero external input in Fig.4.5 at time $k = 0$.

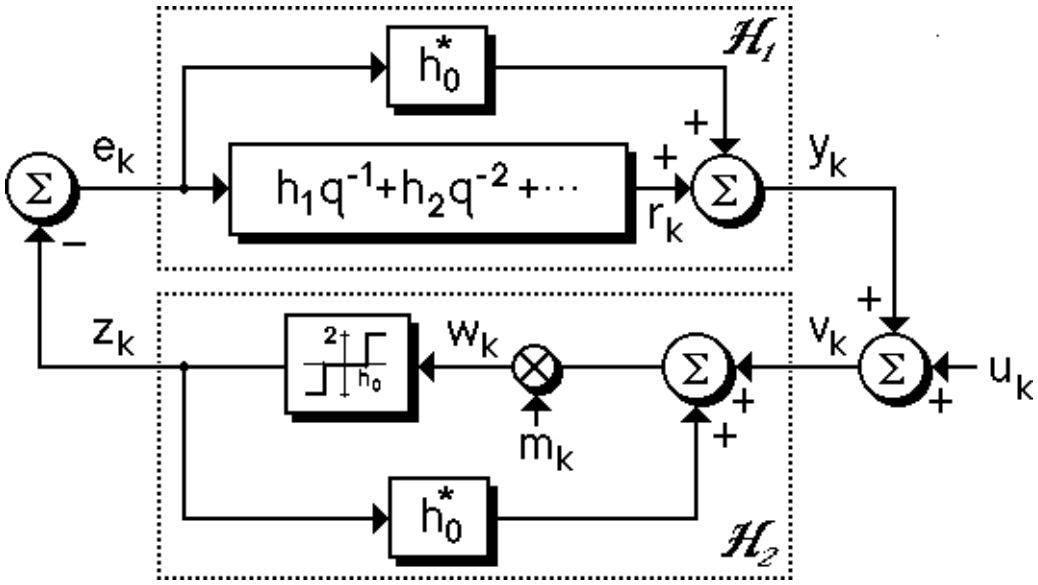

Fig.4.5 Loop Transformation.

We apply a loop transformation [9] to the system in Fig.4.3 to obtain the new system shown in Fig.4.5. Note that the effect of the newly introduced feedforward and feedback paths with gains h_0^* is to cancel exactly. The upper block labelled $\mathcal{H}_1$ has impulse response given by

$$\{h_0^*,\ h_1,\ h_2,\ \ldots\} \tag{4.16}$$

where h_0^* is a finite gain associated with the feedforward path. For the passivity theorem to apply we need (4.16) strictly passive, i.e., h_0^* sufficiently positive, and we have available Lemma 4.3 as a test in the frequency domain.

In the lower block labelled $\mathcal{H}_2$, which includes the positive feedback of gain h_0^*, we need to be concerned that we have not destroyed the passivity of the original lower block (Fig.4.3). The following lemma with proof now applies. The symbol definitions are given in Fig.4.5.

Lemma 4.5: *If* $0 \leq h_0^* \leq \frac{h_0}{2}$ *then* $\mathcal{H}_2$ *(Fig.4.5) is passive.* ❑

Proof: *The* $\mathcal{H}_2$ *block has input* v_k *and output* $z_k \in \{-2, 0, +2\}$. *We attempt to show* $v_k z_k \geq 0,\ \forall k$ *which is known to ensure passivity. From Fig.4.5 the input* w_k *to the sector non-linearity within the* $\mathcal{H}_2$ *block is given by* $w_k = m_k(v_k + h_0^* z_k)$ *from which we have after multiplying through by* z_k,

$$m_k v_k z_k = (w_k - m_k h_0^* z_k) z_k, \quad \forall k \in \mathbb{Z}_+. \tag{4.17}$$

We have three cases according to the values taken by $z_k \in \{-2, 0, +2\}$ *(see Fig.4.5): (i)* $z_k = +2 \ \Rightarrow \ m_k = 1$ *and* $w_k \geq h_0$, *which implies from (4.17) that* $v_k z_k = 2(w_k - 2h_0^*) \geq 2(h_0 - 2h_0^*) \geq 0$, *given* $0 \leq h_0^* \leq \frac{h_0}{2}$, *i.e.,* $v_k z_k \geq 0$; *(ii)* $z_k = -2 \ \Rightarrow$ $m_k = 1$ *and* $w_k \leq -h_0$ *leading to* $v_k z_k \geq 0$ *by symmetry; and (iii)* $z_k = 0$ *which gives* $v_k z_k = 0$ *because* $v \in l_2^e$, *i.e.,* $\left|v_k\right| < \infty\ \forall k$. *Therefore* $v_k z_k \geq 0\ \forall k$ *in every case, implying* $\mathcal{H}_2$ *is passive by (4.9).* ❑

Another condition which needs to be fulfilled in Theorem 4.4 is $u \in l_2$. This condition will necessitate some hypothesis on the channel h to be fulfilled. The signal u for our application will model the effects of *initial conditions* in the $\mathcal{H}_1$ block since all our sequences are defined only for $k \geq 0$, whereas the real system may have been operating from the distant past, i.e., $k = -\infty$. Note that this signal u, as shown in Fig.4.5, is unaffected by the introduction of h_0^*. From Fig.4.3 we use superposition on the upper $\underline{\mathcal{H}}$ linear operator of impulse response $\{0,\ h_1,\ h_2,\ \ldots\}$ to represent the effects of arbitrary initial conditions, i.e., an arbitrary initial error state via the signal

$$u_k \triangleq \sum_{i=k+1}^{\infty} h_i e_{k-i}, \quad k \in \mathbb{Z}_+ \tag{4.18}$$

where values $e_{-1},\ e_{-2},\ e_{-3},\ \ldots$, taking values in $\{-2, 0, +2\}$ define the initial state at time $k = 0$. To ensure $u \in l_2$ we impose some sufficient conditions on the channel h.

Lemma 4.6: *Suppose $h \in l_2^e$ satisfies $\left|h_m\right| = O(m^{-\eta})$ as $m \to \infty$ where η is constant. Then:*

$$(i) \quad \eta > 1 \;\Rightarrow\; h \in l_1, \tag{4.19a}$$

$$(ii) \quad \eta > \frac{3}{2} \;\Rightarrow\; u \in l_2. \tag{4.19b}$$

❑

Proof: *(i) Is elementary. (ii) By using continuous approximations to the summations it is easy to show that from (4.18) $\left|u_k\right| \leq 2\sum_{i=k+1}^{\infty}\left|h_i\right| = O(k^{-\eta+1})$ as $k \to \infty$. Then $p_k \stackrel{\Delta}{=} u_k^2 = O(k^{-2\eta+2})$ as $k \to \infty$. However, $u \in l_2$ if and only if $p \in l_1$. Using part (i) on p this implies $2\eta - 2 > 1$, i.e., $\eta > \frac{3}{2}$.* ❑

We state our first main DFE result.

Theorem 4.7: *Suppose a channel $h \stackrel{\Delta}{=} \{h_0,\ h_1,\ \ldots\}$ used for binary transmission of symbols $\{a_k\}$ satisfies $\left|h_m\right| = O(m^{-\frac{3}{2}-\epsilon})$ as $m \to \infty$ where $\epsilon > 0$. Suppose $\exists \delta > 0$ such that*

$$Re\Big(\widetilde{h}(e^{j\theta}) - \frac{h_0}{2}\Big) \equiv \frac{h_0}{2} + \sum_{m=1}^{\infty} h_m \cos(m\theta) \geq \delta, \quad \forall \theta \in [0, 2\pi]. \tag{4.20}$$

where $\widetilde{h}(z)$ denotes the Z-transform of h.

Given an ideal DFE output sequence $\{\widehat{a}_k\}$ generated through

$$\widehat{a}_k = \operatorname{sgn}\left(h_0 ak + \sum_{i=1}^{\infty} h_i(a_{k-i} - \widehat{a}_{k-i})\right)$$

then for some $K < \infty$, we have $\widehat{a}_k = a_k,\ \forall k \geq K$. ❑

Proof: *By Lemma 4.6(i) the constraint on the channel implies $h \in l_1$, thus $\widetilde{h}(e^{j\theta})$ exists, and we can use Lemma 4.3. Set $h_0^* = \frac{h_0}{2}$ in Fig.4.5. By Lemma 4.3 we have $Re\big(\widetilde{h}(e^{j\theta}) - \frac{h_0}{2}\big) \geq \delta$, $\forall \theta \in [0, 2\pi]$ if and only if operator $\mathcal{H}_1$ in Fig.4.5 is linear and strictly passive. Operator $\mathcal{H}_2$ in Fig.4.5, on the other hand, is passive by Lemma 4.5. By Lemma 4.6(ii) the constraint on the channel implies $u \in l_2$, therefore Theorem 4.4 applies and we deduce $e \in l_2$. However by (4.6) $e \in l_2$ if and only if $e_k = 0,\ \forall k > K$ for some $K < \infty$, which proves the result.* ❑

A somewhat clearer and conceptually simpler result takes the form:

Corollary 4.8: *DFEs with weights correctly adjusted to match the coefficients of an exponentially stable channel h whose frequency response $\widetilde{h}(e^{j\theta})$ satisfies*

$$Re\Big(\widetilde{h}(e^{j\theta})\Big) > \frac{h_0}{2} \quad \forall\theta \in [0, 2\pi]$$

have finite error recovery times, regardless of the initial conditions and regardless of the input sequence. ❑

An explicit bound on the error recovery time is the subject of §4.4.4. Note, a finite recovery time means there are not any pathological input sequences [2,4]. Now we look at some applications of Theorem 4.7.

Example (i) *Suppose (4.19b) is satisfied, $\exists\delta' > 0$ and*

$$\frac{h_0}{2} \geq \sum_{i=1}^{\infty} \big|h_i\big| + \delta'. \tag{4.21}$$

Then it follows that (4.20) is satisfied. In fact condition (4.21) is equivalent to $h_0 > \big|r_k\big|$, $\forall k \in \mathbb{Z}_+$. In this case the DFE has always recovered by equation (2.5), i.e., it never makes errors (in the absence of noise).

Example (ii) *Let the channel be FIR with impulse response $\{h_0,\ h_1,\ h_2,\ 0,\ 0,\ \ldots\}$ (such that $h_0 > 0$). Then condition (4.20) is simply*

$$\frac{h_0}{2} + h_1\cos\theta + h_2\cos 2\theta \geq \delta, \quad \forall\theta \in [0, 2\pi]. \tag{4.22}$$

This defines a region as $\delta \to 0$ in (h_1, h_2)-space shown shaded in Fig.4.6 (see [11]). Note this ice-cream cone region consists of two straight boundaries which are tangent to an ellipse at points $(\pm\frac{2}{3}h_0, \frac{1}{6}h_0)$. This region is shown sandwiched between two other regions: (i) an inner diamond which is (4.21); and (ii) an outer triangle which is the region which defines the necessary and sufficient conditions for a finite recovery time (demonstrated in [2], see Chapter 2 also). This highlights that the converse of Theorem 4.7 is false (for more on this, see §4.4.6).

Example (iii) *As in §4.3 let $h \triangleq \{h_m = \beta^m\cos(m\omega),\ \forall m \in \mathbb{Z}_+\}$, where $0 \leq \beta < 1$ and $\omega \in [0, 2\pi]$. Then $\widetilde{g}(z) \triangleq \widetilde{h}(z) - \frac{1}{2}$ is given by*

$$\widetilde{g}(z) = \frac{\frac{1}{2}(z^2 - \beta^2)}{z^2 - 2\beta\cos\omega\ z + \beta^2}.$$

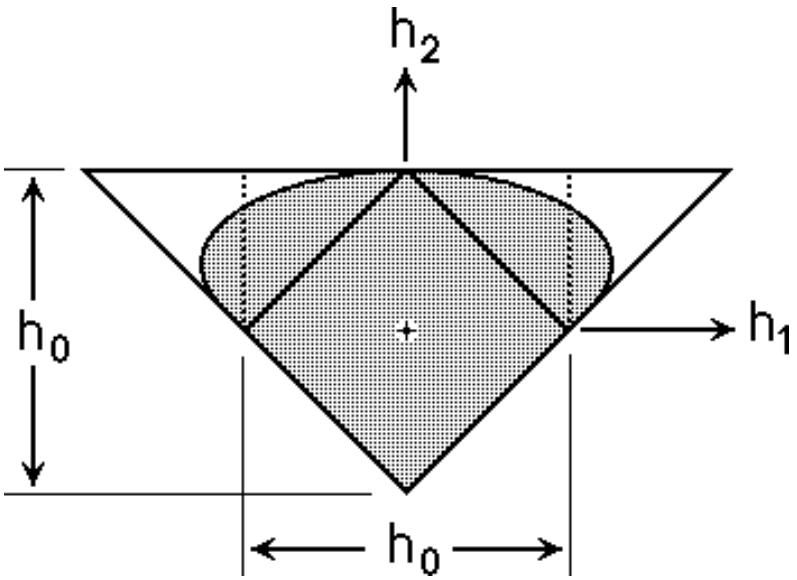

Fig.4.6 3 Tap FIR Channel Regions.

We need $\widetilde{g}(e^{j\theta})$ to have positive real part and this can be shown to be equivalent to checking

$$Re\big((e^{j2\theta}-\beta^2)(e^{-j2\theta}-2\beta\cos\omega\ e^{-j\theta}+\beta^2)\big)\geq\widetilde{\delta},\quad\forall\theta\in[0,\pi], \tag{4.23}$$

for some $\widetilde{\delta}>0$ which is not the same as but is related to the δ which appears in (4.20). But the left hand side of (4.23) can be decomposed as follows:

$$\begin{aligned}1-2\beta\cos\omega\cos\theta+2\beta^3\cos\omega\cos\theta-\beta^4&=(1-\beta^2)\big((1-\beta)^2+2\beta(1-\cos\theta\cos\omega)\big)\\&\geq(1-\beta^2)(1-\beta)^2>0\end{aligned}$$

Thus all decaying exponential channels with impressed sinusoidal oscillation (of the appropriate phase) have a finite recovery time. This is essentially the same result as that which can be found in §4.3 (and [6]). Note that one can extend this result to $h\triangleq\{h_m=\beta^m\cos(m\omega+\phi),\ \forall m\in\mathbb{Z}_+\}$ to conclude that one can trade-off β against ϕ and maintain $\widetilde{g}(z)$ strictly passive provided ϕ remains close to zero, see §4.6.

Example (iv) *Figure 4.7 shows the measured impulse response of a 3km twisted pair copper cable which is the line between a subscriber and a local exchange [12]. Figure 4.8 shows the Nyquist plot of the same channel. Since the closed Nyquist*

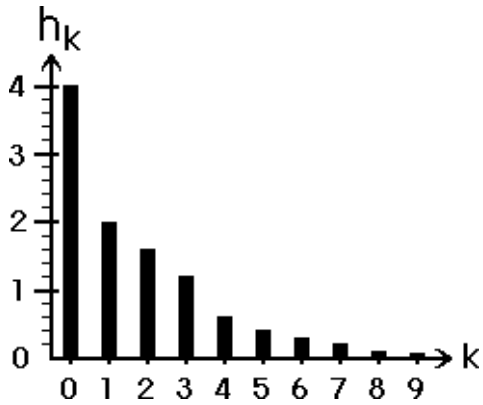

Fig.4.7 3km Twisted Pair Cable Response.

curve lies completely to the right of the line $Re\big(\widetilde{h}(e^{j\theta})\big) = h_0/2$ *(shown dashed) then Theorem 4.7 establishes any error recovery time is finite. Also shown in Fig.4.8 is a geometrical interpretation of* δ *in Theorem 4.7. With some further analysis we will indicate that this type of channel is ideal for the use of a DFE.*

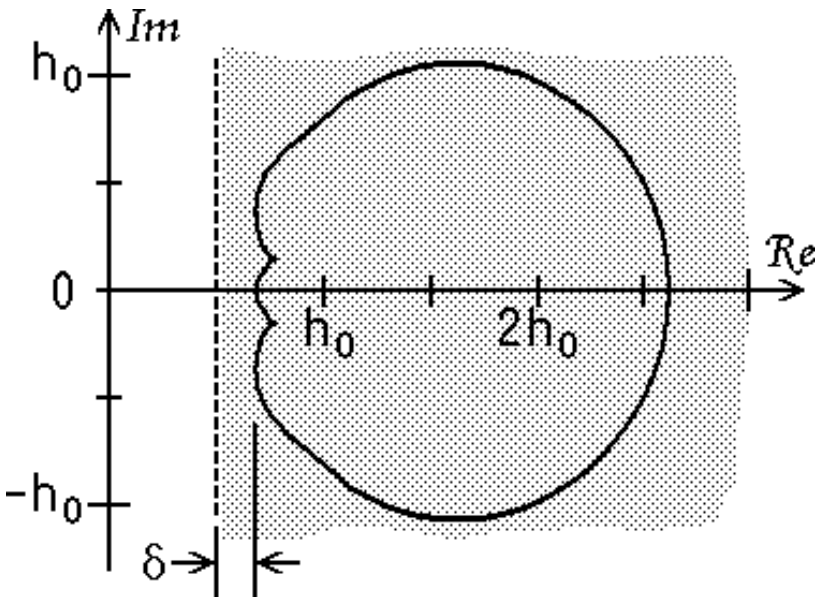

Fig.4.8 Nyquist Plot for Twisted Pair Cable.

4.4.4 Convergence Rates and Explicit Bounds

Theorem 4.7 gives no indication of the maximum time one needs to wait before the

DFE returns to an error-free mode. Intuitively the more dissipative the upper block $\mathcal{H}_1$ is in Fig.4.4, i.e., the greater is δ_1, the more rapidly the error signal should go to zero. We investigate this intuitive insight further.

Consider Fig.4.9 which shows the use of multipliers [9] to transform Fig.4.4. The signals $e_k,\ y_k,\ u_k,\ v_k$ and z_k are identical to those in Fig.4.4, being unaffected by the introduction of the multipliers. We will be applying Theorem 4.4 to the new starred system where $\mathcal{H}_1^*$ maps $e_k^* = \rho^k e_k$ to $y_k^* = \rho^k y_k$, and $\mathcal{H}_2^*$ maps $v_k^* = \rho^k v_k$ to $z_k^* = \rho^k z_k$. The new external signal is now $u_k^* = \rho^k u_k$. We take the multiplier $\rho > 1$.

Now since we take $\rho > 1$ we trivially have $\mathrm{sgn}(v_k) = \mathrm{sgn}(v_k^*)$ and $\mathrm{sgn}(z_k) = \mathrm{sgn}(z_k^*)$. Thus $\mathcal{H}_2^*$ is passive since $\mathcal{H}_2$ is so. To check that $\mathcal{H}_1^*$ is strictly passive is simplified by linearity. It is an elementary calculation to show that the Z-transforms of $\mathcal{H}_1^*\colon e_k^* \mapsto y_k^*$ and $\mathcal{H}_1\colon e_k \mapsto y_k$ are related through

$$\widetilde{h}_1^*(z) = \widetilde{h}_1(z{\cdot}\rho^{-1}). \tag{4.24}$$

This implies that more stringent conditions need to be enforced on the channel h than those given by Lemma 4.6 if the starred signals are to belong to l_2 and then other conditions need to be checked for passivity. Appealing to Lemma 4.6, the most natural and only sensible condition for stability takes the following form:

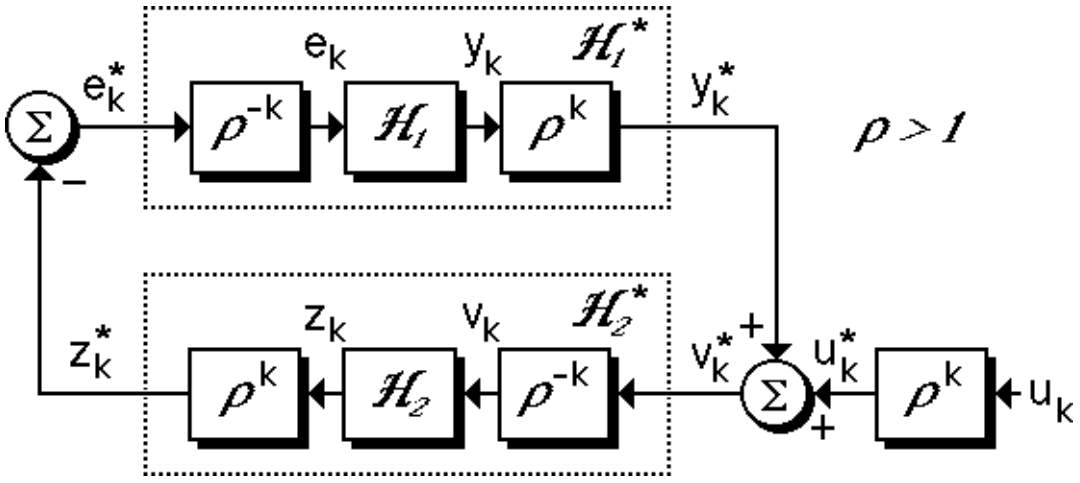

Fig.4.9 Convergence Rates via Multiplier Transformation.

Assumption: *For some* $0 < \gamma < 1$, $\left|h_i\right| < B{\cdot}\gamma^i,\ \forall i \in \mathbb{Z}_+$. (4.25)

This assumption ensures $\widetilde{h}_1^*(z)$ has an impulse response in l_1. Then $\mathcal{H}_1^*$ is strictly passive if and only if

$$Re\Big(\widetilde{h}_1^*(e^{j\theta}) - \frac{h_0}{2}\Big) \geq \delta_1^*, \quad \forall\theta \in [0, 2\pi] \tag{4.26}$$

for some $\delta_1^* > 0$. This shows how the degree of passivity trades off against the degree of exponential stability because if we increase the ρ in (4.24) too far then (4.26) will only hold if δ_1^* is negative, and then we cannot use the stability theorem.

The main stumbling block remaining before we can invoke the Theorem 4.4 is to show $u^* \in l_2$. Using (4.25) we may prove the following, noting $u_k^* = \rho^k u_k$,

$$\begin{aligned}\big\|u^*\big\|^2 \triangleq \sum_{k=0}^{\infty}\Big\{\rho^{2k}\big|\sum_{i=k+1}^{\infty} h_i e_{k-i}\big|^2\Big\} &\leq 4B^2\sum_{k=0}^{\infty}\Big\{\rho^{2k}\ \big|\sum_{i=k+1}^{\infty}\gamma^i\big|^2\Big\} \\ &= \frac{4B^2\gamma^2}{(1-\gamma)^2}\sum_{k=0}^{\infty}(\rho\gamma)^{2k} \\ &= \frac{4B^2\gamma^2}{(1-\gamma)^2(1-(\rho\gamma)^2)}\end{aligned} \tag{4.27}$$

provided $\big|\rho\gamma\big| < 1$, i.e., $\big\|u^*\big\| < \infty$. Thus with an exponential overbound of the channel and $\big|\rho\gamma\big| < 1$, Theorem 4.4 applies to the starred system in Fig.4.9 and we conclude from (4.15) that

$$\begin{aligned}\big\|e^*\big\|^2 \triangleq \sum_{k=0}^{\infty}\big|e_k^*\big|^2 &\leq \delta_1^{*-2}\big\|u^*\big\|^2 \\ &\leq \delta_1^{*-2}\frac{4B^2\gamma^2}{(1-\gamma)^2(1-(\rho\gamma)^2)}\end{aligned} \tag{4.28}$$

i.e., $e^* \in l_2$ (provided $\big|\rho\gamma\big| < 1$). This provides an exponential rate of decay on $\big|e_k\big| = \rho^{-k}\big|e_k^*\big| \leq \rho^{-k}\big\|e^*\big\|$. However e_k is restricted to the set $\{-2, 0, +2\}$ and therefore must be zero after some time $K(\rho) \in \mathbb{Z}_+$ which is the least integer satisfying

$$2 > \frac{2B\gamma}{\delta_1^*}\frac{\rho^{-K(\rho)}}{(1-\gamma)\sqrt{(1-(\rho\gamma)^2)}}, \tag{4.29}$$

i.e., the least integer such that,

$$K(\rho) \geq \log_\rho(B\gamma) - \log_\rho\left(\delta_1^*(1-\gamma^2)\right) - \frac{1}{2}\log_\rho(1-(\rho\gamma)^2); \quad K(\rho) \in \mathbb{Z}_+. \tag{4.30}$$

This $K(\rho)$ is an explicit error recovery time bound that we desired. We will not elaborate further but rather give an example which makes the above analysis clearer and shows how to determine a suitable multiplier ρ, at least in principle.

We consider the special case of the third example given in §4.4.3 by setting $\omega = 0$, i.e., $h_i = \gamma^i,\ \forall i \in \mathbb{Z}_+$ for some $0 < \gamma < 1$ (this case is very similar to Fig.4.7). This channel trivially satisfies (4.25) with $B = 1$. For this channel it can be shown using elementary analysis that

$$Re\Big(\widetilde{h}^*(e^{j\theta}) - \frac{1}{2}\Big) = \frac{\frac{1}{2}\big(1-(\rho\gamma)^2\big)}{1 - 2\rho\gamma\cos\theta + (\rho\gamma)^2} \tag{4.31}$$

where ρ is chosen such that $\gamma < \rho\gamma < 1$. (Note also $h_i^* = (\rho\gamma)^i,\ \forall i \in \mathbb{Z}_+$, by (4.24)) From (4.31) the δ_1^* associated with strict passivity of $\mathcal{H}_1^*$ is given by $\delta_1^* = \frac{1}{2}(1-\rho\gamma)/(1+\rho\gamma)$, being the minimum of (4.31) achieved when $\theta = \pi$. We can now use (4.30) to compute the bound on the error recovery time for various $\rho > 1$. To obtain the tightest bound we can optimize over $1 < \rho < \frac{1}{\gamma}$, noting $K(\rho) \to \infty$ whenever $\rho \to \frac{1}{\gamma}$ or $\rho \to 1$. We give three numerical examples: (i) $\gamma = 0.50$ then using (4.30) we can determine an optimum $\rho \approx 1.642$ yielding $\delta_1^* = 0.0492$ leading to $K_{\text{opt}} \approx K(1.642) = 8$; (ii) $\gamma = 0.81$ with optimum $\rho \approx 1.194$ yielding $\delta_1^* = 0.0083$ leading to $K_{\text{OPT}} \approx K(1.194) = 43$; and (iii) $\gamma = 0.95$ with $\rho \approx 1.047$ yielding $\delta_1^* = 0.0014$ leading to $K_{\text{OPT}} \approx K(1.047) = 258$.

Table 4.1: Error Recovery Time Bounds

Analysis Technique	$\gamma = 0.50$	$\gamma = 0.81$	$\gamma = 0.95$
Passivity Theory (5.7)	8	43	258
Exponential Results [6]	2	11	71
Markov Processes [1-4]	6^*	4094^*	$5 \times 10^{21\,*}$

* These bounds are on the mean not the maximum recovery time.

These bounds are conservative by the nature of the analysis. In §4.3 equation (3.9), for the cases examined here, it is shown that tighter bounds on the maximum error recovery times are 2, 11 and 71, respectively. It is interesting to compare both sets of bounds (see the first two rows of Table 4.1) with mean error recovery time bounds which can be deduced from the DFE literature based on Markov Processes [1-4]. Of course being statistical bounds we need a statistical model of the input sequence $\{a_k\}$—an independent, equiprobable binary distribution being standard. This does

not invalidate the comparison because the error recovery time bound $K(\rho)$ in (4.30) always overbounds the true mean error recovery time.

To compute the mean error recovery time bounds based on the work in [1] we define an effective channel length n for the exponential channel, Chapter 2 §2.6.1. This is given by the minimum n such that

$$2\sum_{i=n+1}^{\infty}\gamma^i = \frac{2\gamma^{n+1}}{1-\gamma} < 1. \tag{4.32}$$

The meaning attached to the quantity n is simply that the DFE needs to make n consecutive correct decisions to recover from any error state with $\widehat{a}_{k-1} \neq a_{k-1}$ (k being the present instant of time). Equation (4.32) has the simple interpretation: the LHS is the maximum residual ISI (2.4b) given n consecutive correct decisions have been made; the RHS is just the amplitude of the cursor $h_0 = 1$. Now for the worst case channels implicitly considered in [1-4], subject to (4.32), the probability of making an error is precisely $\frac{1}{2}$ for every decision before recovery (i.e., before n consecutive correct decisions have been made). By the theory of success runs [4] the mean recovery time is given by $2(2^n-1)$. Looking at our three examples we have: (i) $\gamma = 0.50$ implying $n = 2$ and thus a mean recovery time of 6; (ii) $\gamma = 0.81$ implying $n = 11$ and thus a mean recovery time of 4094; and (iii) $\gamma = 0.95$ implying $n = 71$ and thus a mean recovery time of 5×10^{21}. These three bounds are displayed in the third row of Table 4.1.

Remarks:

(i) Table 4.1 shows that using the theory of Markov Processes one may get ridiculously conservative results, even though we have (minimally) exploited some structural assumptions (4.32). Also note that here the Markov techniques are incapable of telling us directly that the recovery time is finite. (In principle, however, one could answer this by examining the topology of an infinite dimensional graph associated with the Markov Process.)

(ii) Equation (4.32) is identical to (3.8), noting γ is identifiable with β. Thus for exponential channels (without ω-modulation) we see that the worst case error recovery time bound K (3.8) is identical to the effective channel length n (4.32). This coincidence is easily explained. We know that if n consecutive correct decisions are made then the DFE recovers. However from §4.3 we also know that for exponential impulse response channels, with the worst case initial conditions, a

sequence of correct decisions characterizes the slowest recovery, and so the result is not so surprising.

(iii) The mean bounds in Table 4.1 can presumably be improved on by the techniques in [7,8]. However the amount of computation that would be necessary looks formidable (also the IIR channel would need to be approximated).

4.4.5 Error Recovery Under Imperfect Equalization

This subsection represents a threefold generalization of the previous results. These modifications involve, in part, relaxation of some of the previous assumptions regarding the model of the system under study. The analysis we perform here will be carried out up to the point where it is obvious the same techniques as before can be used. This saves repetition. The generalizations are as follows: (i) the DFE tapped delay line is assumed to be FIR of length N rather than IIR, whilst the channel may be IIR; (ii) the assumption that $d_i = h_i,\ \forall i \geq 1$ is relaxed to a condition which stipulates the d_i are sufficiently close but not necessarily equal to some ideal values (how close and what the ideal values are will be precisely defined); and (iii) the results are generalized to the situation where error-free behaviour is characterized by $\widehat{a}_k = \mathrm{sgn}(h_\delta)a_{k-\delta},\ \forall k \geq K$ for some fixed delay $\delta \in \{0,\ 1,\ \ldots,\ N\}$ rather than $\widehat{a}_k = a_k,\ \forall k \geq K$ (which is the special case where $\delta = 0$, recalling $h_0 > 0$). All these generalizations will be treated in parallel. A key feature of the analysis performed in this subsection is showing explicitly the close relationship between eye diagrams and rates of error recovery.

As some motivation to studying delay-type behaviour, alluded to above, consider the situation where a DFE has its taps adapted blindly, i.e., without a training sequence. In this case, it was shown in Chapter 3 that the DFE taps may adapt not only to an (ideal) equilibrium where $d_i = h_i,\ i \in \{1,\ 2,\ \ldots,\ N\}$ but also to a delay equilibrium where $d_i = \mathrm{sgn}(h_\delta)h_{i+\delta},\ i \in \{1,\ 2,\ \ldots,\ N\}$ provided certain conditions are met. We will show that when in the vicinity of a *delay equilibrium*, after some finite time K, all decisions will be of the form $\widehat{a}_k = \mathrm{sgn}(h_\delta)a_{k-\delta}\ \forall k \geq K$, hence the terminology.

To analyze non-ideal behaviour we take (2.3) and set $d_i = 0$ for $i > N$, i.e., the tapped delay line is FIR of length N rather than IIR. Define

$$\sigma_\delta \triangleq \mathrm{sgn}(h_\delta).$$

We can decompose (2.3) as follows:

$$\widehat{a}_k = \operatorname{sgn}\big(\sum_{i=0}^{\infty} h_i a_{k-i} - \sum_{i=1}^{N} d_i \widehat{a}_{k-i}\big) \tag{4.33a}$$

$$= \operatorname{sgn}(h_\delta a_{k-\delta} + r_k(\delta) + s_k(\delta) + t_k(\delta)) \tag{4.33b}$$

where

$$r_k(\delta) \triangleq \sum_{i=\delta+1}^{N+\delta} h_i(a_{k-i} - \sigma_\delta \cdot \widehat{a}_{k+\delta-i}) \tag{4.33c}$$

$$s_k(\delta) \triangleq \sum_{i=0}^{\delta-1} h_i a_{k-i} + \sigma_\delta \sum_{i=\delta+1}^{N+\delta} (h_i - \sigma_\delta \cdot d_{i-\delta}) \widehat{a}_{k+\delta-i} \tag{4.33d}$$

and

$$t_k(\delta) \triangleq \sum_{i=N+\delta+1}^{\infty} h_i a_{k-i}. \tag{4.33e}$$

In (4.33): (i) $r_k(\delta)$ acts as the basic residual ISI term (note if we let $\delta = 0$ and $N \to \infty$ then (4.33c) becomes (2.4b)); (ii) $s_k(\delta)$ is a term which generally gets smaller as the taps $(d_1,\ d_2,\ \ldots,\ d_N)'$ approach the δ-delay equilibrium $+\sigma_\delta(h_{\delta+1},\ h_{\delta+2},\ \ldots,\ h_{\delta+N})'$, and includes any precursor; and (iii) $t_k(\delta)$ is that part of the tail of the channel which cannot be modelled by the DFE because the tapped delay line is FIR.

Beginning with $t_k(\delta)$ in (4.33e), it is clear that we need

$$\big|t_k(\delta)\big| \le \sum_{i=N+\delta+1}^{\infty} \big|h_i\big| \triangleq \Phi,\ \forall k \in \mathbb{Z}_+ \tag{4.34}$$

with Φ sufficiently small else the DFE problem is not well-posed, i.e., N, the number of DFE taps, needs to be chosen large enough in the first place so that the DFE can effectively cancel the ISI.

Now when in the vicinity of a delay equilibrium we claim $\widehat{a}_k = +\sigma_\delta \cdot a_{k-\delta},\ \forall k \ge K$ provided certain conditions are met, which we now determine. Define new (delay) errors

$$e_k(\delta) \triangleq a_{k-\delta} - \sigma_\delta \cdot \widehat{a}_k \tag{4.35}$$

then the basic residual ISI term $r_k(\delta)$ (4.33c) may be written

$$r_k(\delta) \triangleq \sum_{i=\delta+1}^{N+\delta} h_i e_{k+\delta-i}(\delta) \tag{4.36}$$

and will be zero whenever we make N consecutive correct δ-delay decisions. Now suppose

$$\Delta_{\text{MIN}}(\delta) \triangleq \big|h_\delta\big| - \sum_{i=0}^{\delta-1}\big|h_i\big| - \sum_{i=\delta+1}^{N+\delta}\big|h_i - \sigma_\delta{\cdot}d_{i-\delta}\big| - \sum_{i=N+\delta+1}^{\infty}\big|h_i\big| > 0. \tag{4.37}$$

Then some perusal will show that whenever N consecutive correct decisions are made, all future decisions will be correct (in the delay sense) because $r_k(\delta) = 0$ and h_δ is larger in magnitude than $s_k(\delta) + t_k(\delta)$ can ever be, see (4.33b). This defines a new form of error recovery, i.e., (4.37) is a sufficient condition for all decisions to be (delay) correct whenever N consecutive δ-delay decisions have been made. Note that if all decisions are to be of the form $\widehat{a}_k = \sigma_\delta{\cdot}a_{k-\delta}$ for all input sequences, given N consecutive correct decisions have been made, then condition (4.37) is also a necessary condition (see [13] which treats a similar problem).

Define $\Delta_k(\delta) \triangleq \big(h_\delta a_{k-\delta} + s_k(\delta) + t_k(\delta)\big)\sigma_\delta{\cdot}a_{k-\delta}$, noting $\Delta_k(\delta) \geq \Delta_{\text{MIN}}(\delta) > 0$ by (4.37). We can write (4.33b) as $\widehat{a}_k = \text{sgn}\big(\sigma_\delta{\cdot}a_{k-\delta}\ \Delta_k(\delta) + r_k(\delta)\big)$. Then clearly the analogue of Lemma 4.1 is:

Lemma 4.9: *Suppose condition (4.37) holds. Then*

(i) $\big|r_k(\delta)\big| < \Delta_k(\delta)$ *or* $a_{k-\delta} = +\sigma_\delta{\cdot}\,\text{sgn}(r_k(\delta)) \Rightarrow \widehat{a}_k = +\sigma_\delta{\cdot}a_{k-\delta}$.

(ii) $\big|r_k(\delta)\big| > \Delta_k(\delta)$ *and* $a_{k-\delta} = -\sigma_\delta{\cdot}\,\text{sgn}(r_k(\delta)) \Rightarrow \widehat{a}_k = -\sigma_\delta{\cdot}a_{k-\delta}$.

□

Thus we have the picture in Fig.4.10 which differs marginally from Fig.4.3. Note the lower block is sector bounded within the 1st and 3rd quadrants whilst $\Delta_{\text{MIN}}(\delta) > 0$. The critical value at which $r_k(\delta)$ causes a change from $z_k = 0$ to $z_k = +2$ is $\Delta_k(\delta)$ and is thus time-varying (but bounded below by $\Delta_{\text{MIN}}(\delta)$)—we have depicted this behaviour by a shading or fuzziness of the switching value in the non-linearity in Fig.4.10. The generalization of Theorem 4.7 is then clearly:

(Imperfect Equalization) Theorem 4.10: *Suppose a channel* $h \triangleq \{h_0,\ h_1,\ \ldots\}$ *and the DFE tapped delay line* $d \triangleq \{0,\ d_1,\ d_2,\ \ldots\}$ *satisfy*

$$\Delta_{\text{MIN}}(\delta) \triangleq \big|h_\delta\big| - \sum_{i=0}^{\delta-1}\big|h_i\big| - \sum_{i=\delta+1}^{N+\delta}\big|h_i - \sigma_\delta{\cdot}d_{i-\delta}\big| - \sum_{i=N+\delta+1}^{\infty}\big|h_i\big| > 0. \tag{4.38}$$

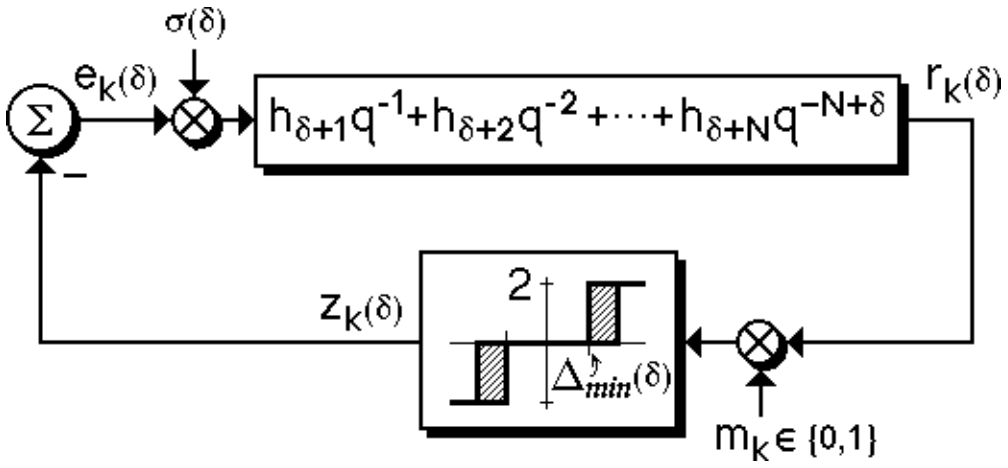

Fig.4.10 Imperfect Equalization Error Propagation Block Diagram.

for some (at most one) delay $\delta \in \{0,\ 1,\ \ldots,\ N\}$ *and* $\sigma_\delta \triangleq \mathrm{sgn}(h_\delta)$. *Further, suppose* $\exists \xi > 0$ *such that*

$$\frac{\Delta_{\text{MIN}}(\delta)}{2} + \sigma_\delta \sum_{m=1}^{N} h_{m+\delta} \cos(m\theta) \geq \xi, \quad \forall \theta \in [0, 2\pi].$$

Given a non-ideal DFE output sequence $\{\widehat{a}_k\}$ *generated through*

$$\widehat{a}_k = \mathrm{sgn}\,\big(\sum_{i=0}^{\infty} h_i a_{k-i} - \sum_{i=1}^{N} d_i \widehat{a}_{k-i})\big)$$

then for some $K < \infty$, *we have* $\widehat{a}_k = +\sigma_\delta \cdot a_{k-\delta},\ \forall k \geq K$. ❑

Remarks:

(i) The asymptotic condition on h in the previous Theorem 4.7, in reality, controls the behaviour of the tail of the ideal DFE tap setting, not the tail of the channel. That is why such a condition does not appear in Theorem 4.10. (It is implicit in the sense that (4.38) implies $h \in l_1$.)

(ii) Note condition (4.38) stipulates that the d_i need to be sufficiently close to the $\sigma_\delta \cdot h_{i+\delta}$ (in an l_1-norm sense) if a certain operator is to be strictly passive. Note that the worse the mismatch, the less $\Delta_{\text{MIN}}(\delta)$ will be. This forms a convenient geometrical picture to replace the messy algebra.

(iii) Note $\Delta_{\text{MIN}}(\delta)$ may be interpreted precisely as the amount that a certain eye diagram is open (after recovery). Thus the wider the post-recovery eye can be, the more rapid one can expect recovery to be. Theorem 4.10 is saying that given the eye is initially closed (an arbitrary error state) it will always open after at most some finite time K (again this is quantifiable).

4.4.6 Comparison with the Exact Theory

An exact theory treating error recovery capable (in principle) of providing necessary and sufficient conditions on the system parameters for finite error recovery times and related problems can be found in Chapter 2, (see also [2]). One conclusion of Chapter 2 is that if inclusion in a certain region of the channel parameter space is a necessary and sufficient condition for a (guaranteed) finite error recovery time then that region is, without exception, a union of a (countable) number of polytopes, i.e., the region is bounded by hyperplanes. In contrast, the region determined in Theorem 4.7 has in general some curved boundaries (see Fig.4.6). Thus we can see immediately that Theorem 4.7 can only be a sufficiency result—a conclusion we arrived at earlier. However, it is quite easy to strengthen Theorem 4.7 such that the region appearing in (4.22) is replaced by a suitable union of polytopes (of the form defined in Chapter 2) which contains the region (4.22). For example in Fig.4.6 the passivity analysis ice-cream cone region can in fact be replaced by the outer triangle in the theorem statement. The reason is the following. The property which defines the polytopes in [2] is that all points interior to a given polytope have indistinguishable error recovery properties (a manifestation of the sgn$(\cdot)$ quantization in (2.3)). Let us refer to all points inside a given polytope as *isomorphic*, then we have the following straightforward extension of Theorem 4.7:

(Extended) Theorem 4.11: *All channels h which are isomorphic to at least one channel satisfying the passivity constraint in (4.20) have a guaranteed finite recovery time.* ❑

Remarks:

(i) For example in Fig.4.6 the outer triangle is composed of five polytopes (see also [2]) each of which intersect with the passivity region in (4.22). Therefore, e.g., $h = \{2,\ 1.5,\ 0.75\}$ violates (4.22) (e.g., at $\theta = 135°$) but is isomorphic to $h = \{2,\ 1.1,\ 0.5\}$ which satisfies (4.22).

(ii) The degree of passitivity $\delta_1 > 0$ that we can associate with any channel h can be maximized by searching over all channels which are isomorphic to h, thus giving a tighter overbound on the error recovery rate, e.g., $h = \{2,\ 0,\ 0.9\}$ has $\delta_1 = 0.1$ but is isomorphic to $h = \{2,\ 0,\ 0\}$ with $\delta_1 = 1$. This may explain why the passivity theory does not give the tight result of [6] in Table 4.1.

(iii) For FIR channels with less than four parameters, Theorem 4.11 provides both necessary and sufficient conditions for a guaranteed finite recovery time. It is not known whether this property holds for higher dimensions.

4.4.7 M-ary Results

The theory developed for binary systems can be extended to larger alphabets where M symbols are used. We outline some of the important differences. For brevity we restrict attention to zero delay systems. Let $\{a_k\} \in \{1-M,\ 3-M,\ \ldots,\ M-1\}$ where M is positive and even. The standard decision function $\mathcal{Q}_M(\cdot)$ which replaces $\mathrm{sgn}(\cdot)$ in the binary analysis is defined by

$$\mathcal{Q}_M(x) \triangleq \sum_{k=1-M/2}^{M/2-1} \mathrm{sgn}(x+2k). \tag{4.39}$$

The M-ary version of (2.4a), where we have ideal equalization, becomes

$$\widehat{a}_k = \mathcal{Q}_M(h_0 a_k + r_k), \quad h_0 > 0 \tag{4.40}$$

where r_k is as in (2.4b) with the exception that $e_k \in \{0,\ \pm 2,\ \ldots,\ \pm 2(M-1)\}$. Now suppose we had no residual ISI, i.e., $r_k = 0$, then (4.40) reduces to

$$\widehat{a}_k = \mathcal{Q}_M(h_0 a_k) \tag{4.41}$$

from which it is clear that (with $M \geq 4$) we need $h_0 \approx 1$ for error-free behaviour. (This differs from the binary case, $M = 2$, where it was only necessary that $h_0 > 0$.) Elaborating, we have

Lemma 4.12: *Given $e_{k-i} = 0,\ \forall i \in \mathbb{Z}_+$, and $M \geq 4$ even, then*

$$\widehat{a}_k = a_k, \quad \forall a_k \iff \frac{M-2}{M-1} < h_0 < \frac{M-2}{M-3}. \tag{4.42}$$

□

Proof: *(Outline): If h_0 exceeds the upper bound in (4.42) then $a_k = M-3$ gets decoded as $\widehat{a}_k = M-1$ in (4.41). Similarly if h_0 is less than the lower bound in (4.42) then $a_k = M-1$ gets decoded as $\widehat{a}_k = M-3$. These symbols define the critical cases.* □

So, in summary, we require the right-hand condition in (4.42) to be in force if the M-ary error recovery problem is to be *well-posed*. (Note, with an obvious redefinition of e_k an analogous result for $h_0 < 0$ can be generated.)

Consider the error propagation mechanism for the well-posed M-ary problem. We now verify that the operator $\mathcal{L}$ which maps r to $z = -e$ (the residual ISI to the negative of the errors) is passive, indeed sector bounded.

We will adopt a slightly different approach to the M-ary analysis from the binary analysis. In the binary analysis, recall, we included a stochastic multiplier to compensate for the event where the residual ISI r_k and data a_k had the same sign (leading to zero error). It is possible, and preferable in the M-ary case, to include the stochastic effects of the input a_k into the sector non-linearity as a time variation. Lemma 4.13 provides the mathematical details. However, before presenting Lemma 4.13 let us determine the conditions on residual ISI r_k and data a_k which lead to $e_k = 0$ in the M-ary case.

Zero error simply means $\widehat{a}_k = a_k$ which may be written

$$\widehat{a}_k = \mathcal{Q}_M(h_0 a_k + r_k) = a_k.$$

This implies in view of the quantizer definition (4.39)

$$a_k - 1 < h_0 a_k + r_k < a_k + 1, \quad \forall a_k \in \{3-M,\ \ldots,\ M-3\}$$

$$a_k - 1 < h_0 a_k + r_k, \quad \text{for } a_k = M-1$$

and

$$h_0 a_k + r_k < a_k + 1, \quad \text{for } a_k = 1-M.$$

Therefore the conditions under which the residual ISI r_k is harmful vary according to a_k, and are most lax with the extreme symbols. Now onto the lemma statement and proof.

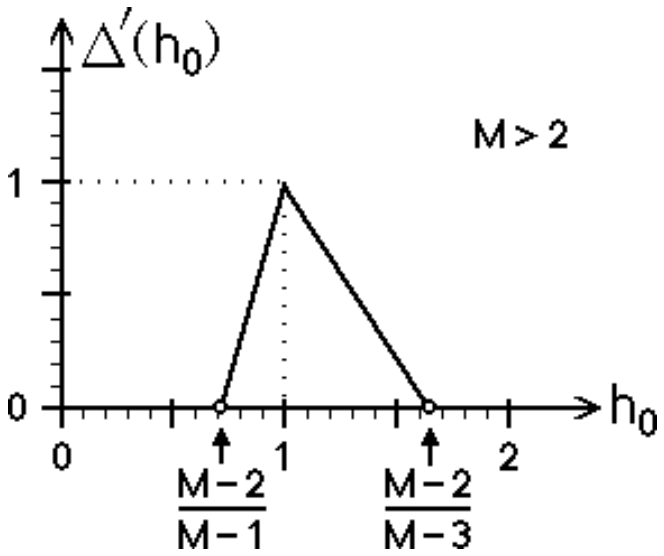

Fig.4.11 M-ary $\Delta'(h_0)$ Function.

Lemma 4.13: *Let* $r_k \triangleq \sum_{i=1}^{\infty} h_i e_{k-i}$ *and* $z_k \triangleq -e_k = \widehat{a}_k - a_k$. *Then the operator* $\mathcal{L}$: $r \mapsto z$ *is sector bounded according to*

$$0 \leq \frac{z_k}{r_k} \leq \frac{2}{\Delta'(h_0)} \tag{4.43}$$

where (see Fig.4.11)

$$\Delta'(h_0) \triangleq \begin{cases} (M-1)h_0 - (M-2) & \text{if } h_0 \leq 1; \\ -(M-3)h_0 + (M-2) & \text{if } h_0 \geq 1, \end{cases} \tag{4.44}$$

provided the M-ary error recovery problem is well-posed, i.e., h_0 *satisfies*

$$\frac{M-2}{M-1} < h_0 < \frac{M-2}{M-3}.$$

❑

Proof: *That* z_k/r_k *is non-negative will be implicit in the following development. To compute the upper bound we search over all possible values of* $z_k \in \{0, \pm 2, \ldots, \pm 2(M-1)\}$. *Note we can restrict attention to the set* $\{2, 4, \ldots, 2(M-1)\}$ *by symmetry (and discarding the zero error case). We begin with* $z_k = 2$. *By definition this implies*

$$z_k = 2 \iff \widehat{a}_k = \mathcal{Q}_M(h_0 a_k + r_k) = a_k + 2$$

which in turn implies

$$a_k + 1 < h_0 a_k + r_k < a_k + 3, \quad \forall a_k \in \{1 - M, \ \ldots, \ M - 5\} \tag{4.45a}$$

and

$$a_k + 1 < h_0 a_k + r_k, \quad \text{for} \ \ a_k = M - 3. \tag{4.45b}$$

With $z_k = 2$ fixed, the two critical inequalities which minimize r_k (in the light of (4.43)) are: (i) the LHS of (4.45a) with $a_k = 1 - M$; and (ii) (4.45b) where $a_k = M - 3$. Imposing further that $r_k > 0$ (i.e., stipulating that the non-linearity lies in the 1st quadrant) leads to the two line segments which define $\Delta'(h_0)$ (4.44), shown in Fig.4.11. (Note that the condition in (4.42) is equivalent to the condition $r_k > 0$ whenever $z_k = 2$.) However we need to verify that other values of z_k do not yield higher values for z_k/r_k. Let us consider $z_k = 4$. By definition this implies

$$z_k = 4 \iff \widehat{a}_k = \mathcal{Q}_M(h_0 a_k + r_k) = a_k + 4$$

which in turn implies

$$a_k + 3 < h_0 a_k + r_k < a_k + 5, \quad \forall a_k \in \{1 - M, \ \ldots, \ M - 7\} \tag{4.46a}$$

and

$$a_k + 3 < h_0 a_k + r_k, \quad \text{for} \ \ a_k = M - 5. \tag{4.46b}$$

The two critical inequalities which minimize r_k are: (i) the LHS of (4.46a) with $a_k = 1 - M$; and (ii) (4.46b) where $a_k = M - 5$. However it is easy to check geometrically that these two inequalities do not yield higher values for z_k/r_k. This conclusion holds true for $z_k \geq 4$ as a tedious calculation shows (ordering arguments can be employed here). Thus when $z_k = 2$ we can achieve the maximum z_k/r_k. Then (4.44) arises from (4.45a) with $a_k = 1 - M$ and (4.45b) where $a_k = M - 3$.□

Figure 4.11 shows the function $\Delta'(\cdot)$ versus h_0. At a conceptual level $\Delta'(\cdot)$ may be thought of as an effective cursor replacing h_0. Note $\Delta'(\frac{M-2}{M-1}) = 0$, $\Delta'(\frac{M-2}{M-3}) = 0$ and $\Delta'(1) = 1$ (the maximum). Figure 4.12 shows the error propagation diagram for the M-ary case, noting it depicts the sector bound property of Lemma 4.13 in the block $\mathcal{L}$. Then in analogy to Theorem 4.7 (and Fig.4.3), we have the M-ary result where $M \geq 4$ is even:

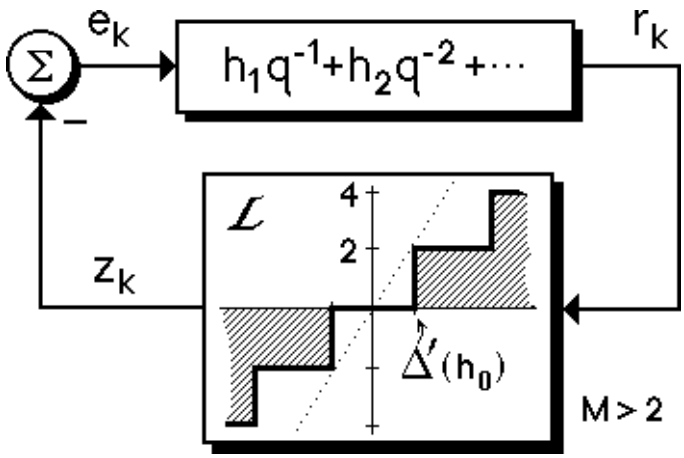

Fig.4.12 M-ary Error Propagation Block Diagram.

(M-ary) Theorem 4.14: *Suppose* $a_k \in \{1-M,\ 3-M,\ \ldots,\ M-1\}$ *is the input to a linear channel* $h \triangleq \{h_0,\ h_1,\ \ldots\}$ *which satisfies*

$$\frac{M-2}{M-1} < h_0 < \frac{M-2}{M-3}$$

(to be well-posed) and $|h_m| = O(m^{-\frac{3}{2}-\epsilon})$ *as* $m \to \infty$ *where* $\epsilon > 0$. *Suppose* $\exists \delta > 0$ *such that*

$$\frac{\Delta'(h_0)}{2} + \sum_{m=1}^{\infty} h_m \cos(m\theta) \geq \delta, \quad \forall \theta \in [0, 2\pi] \tag{4.47}$$

where $\Delta'(h_0)$ *is given by (4.44) (Fig.4.11). Given an ideal DFE output sequence* $\{\widehat{a}_k\}$ *generated through*

$$\widehat{a}_k = \mathcal{Q}_M\big(h_0 a_k + \sum_{i=1}^{\infty} h_i(a_{k-i} - \widehat{a}_{k-i})\big)$$

then for some $K < \infty$, *we have* $\widehat{a}_k = a_k,\ \forall k \geq K$. □

Remarks:

(i) Theorems relating the rates of convergence and robustness for the M-ary case can be generated by analogy with the binary case.

(ii) The error recovery rate is most rapid with $h_0 = 1$ which implies $\Delta'(h_0) = 1$ because this makes (4.47) the most strictly passive, which is in accord with intuition. If h_0 differs from 1 there will be a diminishing of passivity and hence

a drop in the rate of error recovery (this is represented graphically in Fig.4.11). This highlights the crucial role that gain compensation plays in the M-ary case (not a consideration for the binary case).

(iii) Normalized channels where h is scaled such that $h_0 = 1$ (e.g., if we had ideal gain compensation in the DFE), which result in a finite recovery time for binary symbols will also have a finite recovery time for the M-ary case because then conditions (4.47) and (4.20) are identical. The explicit error recovery times, however, will be different as we now indicate. Letting $K_M(\rho)$ denote the error recovery time bound for the M-ary case, in analogy to (4.30), then this is related to the binary error recovery time bound $K(\rho)$ via

$$K_M(\rho) = K(\rho) + \log_\rho(M-1).$$

To prove this note that in a calculation which mimics (4.27) the factor of 4 (the maximum binary error squared) is replaced by $4(M-1)^2$ (the maximum M-ary error squared).

4.5 Noise and Asymptotic Error Probability Bounds

In Chapter 2 §2.5.3 (see also [3]) it is shown how the mean error recovery time is related to the error probability in the most important case of a high signal to noise ratio channel. This material, in fact, showed the close relationship between the two fundamental early contributions to the analysis of error propagation, [1,4]. To calculate an error probability bound we include additive channel noise with variance σ_n^2 into the analysis, and following [1] we define the fully open eye error probability as

$$\epsilon \triangleq Pr(\widehat{a}_k \neq a_k \mid r_k = 0)$$

where r_k is the residual ISI (2.4b), and $\epsilon = O(\sigma_n^2)$ (see Chapter 2 §2.5.3 and [3]). (For this calculation it is not necessary to assume the noise forms an independent sequence, as is done for simplicity in [3].) We can then use the techniques in [3] to bound the stationary error probability $P_E \triangleq Pr(\widehat{a}_k \neq a_k)$ for channels satisfying the conditions (4.25) and (4.26), via

$$P_E < \frac{\epsilon}{2}\cdot(K(\rho)+2) \quad \text{as} \quad \sigma_n^2 \to 0, \tag{5.1}$$

where $K(\rho)$ is the passivity analysis error recovery time bound which appears in (4.30). From Table 4.1, bound (5.1) may be anything up to a factor of 10^{20} tighter than the oft-cited result in [1] which says $P_E \leq \epsilon \cdot 2^n$ (effectively derived by replacing $K(\rho)$ in the above formula by $2(2^n - 1)$ which is the worst case mean error recovery time implicit in [1]).

Rather than derive (5.1), we will give a simple heuristic which demonstrates the concepts involved that lead to a proof. To compute the probability of error P_E we will consider two distinct phases of DFE operation corresponding to before and after recovery.

In the limit as $\sigma_n^2 \to 0$ the probability of significant, i.e., harmful, noise becomes increasingly rare. Consequently for channels satisfying (4.25) and (4.26) the time taken to recovery from a worst case error approaches that of the noiseless calculation, i.e., $K(\rho)$ (4.30). The probability of error during this phase we take as $\frac{1}{2}$, the upper bound. Once in the post-recovery phase only noise can induce an error and, given the asymptotics on the noise variances, we see that the interval of time one must wait typically will be exceedingly long. During this time the ISI will continue to decrease (exponentially) in accordance with the exponential overbound (4.25) on the channel tail. Thus when the rare noise induced error event does occur it almost always will be when the ISI is effectively zero and we can say that the post-recovery error probability will be effectively ϵ (the zero residual ISI error probability). Also by elementary considerations the time we will need to wait before such an error will have asymptotic mean approaching $\frac{1}{\epsilon}$.

So in summary, the ratio of time spent before:after recovery will be asymptotically $K(\rho) : \frac{1}{\epsilon}$, and the corresponding error probabilities $\frac{1}{2} : \epsilon$ (asymptotically). Here it is useful to note that $\epsilon = O(\sigma_n^2)$. Hence an overbound of the overall error probability takes the form:

$$\begin{aligned} P_E &\leq \frac{K(\rho)\cdot\frac{1}{2} + \frac{1}{\epsilon}\cdot\epsilon}{K(\rho) + \frac{1}{\epsilon}} \quad \text{as } \epsilon \to 0 \\ &= \frac{\epsilon}{2}\cdot\left(\frac{K(\rho)+2}{1+\epsilon\cdot K(\rho)}\right) \quad \text{as } \epsilon \to 0, \end{aligned}$$

and this is compatible with (5.1). Naturally, our result is tighter than that given in [1] because we are imposing stronger structural assumptions on the channels to be subject to equalization.

4.6 Timing Phase Sensitivity Analysis

4.6.1 Background

An important question which arises in practice concerns determining the best (continuous) time instant to serve as the discrete time reference point for the sampling. Naturally it is of interest to determine the penalty incurred when the optimum sampling is not achieved. An analysis of these problems can take several directions. In [14] Salz studies a DFE timing phase problem where a particular phase is determined in the sampling operation to optimize the mean square error between the quantizer input and the actual data. However to implement this analysis it is necessary to assume that all decisions are correct. (This incidentally turns the problem into a linear one.) In comparison, the problem we study concerns the effects on error recovery with variations in the timing phase (a non-linear problem). Our approach to this problem will be to analyze a relatively simple class of channels which appear to represent reasonable models of some communications channels [12]. We formulate a precise statement of our problem in the next subsection.

4.6.2 Problem Formulation and Solution

We analyze the following somewhat idealistic problem. Suppose the discrete time representation of the communication channel is generated by a sampled impulse discretization [15] leading to

$$h_m \triangleq \beta^m \cos(m\omega + \phi) \tag{6.1}$$

i.e., the continuous time representation of the channel is an exponentially decaying sinusoid. In (6.1), $-\pi < \omega \leq \pi$ and $0 < \beta < 1$ are parameters relating the time constant of the channel to the discrete sampling interval, and $-\frac{\pi}{2} < \phi < \frac{\pi}{2}$ is some sampling phase perturbation which ideally should be zero. (Note also that a zero-order-hold discretization [15] of the same continuous time channel leads to (6.1). In this case ϕ also represents in a complicated way the delay implicit in the hold circuit.) Note for our analysis we will just consider delay $\delta = 0$ systems where $e_k \triangleq a_k - \widehat{a}_k$ requiring $h_0 > 0$ (the condition on ϕ ensures this). We pose the question:

> How do perturbations in the sampling phase ϕ trade off against β and ω when one stipulates that the error recovery time is to remain finite?

For the unperturbed system where $\phi = 0$ the error recovery time is indeed finite, §4.4.3. To apply the passivity results (Theorem 4.7) one simply needs to ensure, as a function of ϕ, the following holds:

$$Re\big(\widetilde{h}(e^{j\theta}) - \frac{\cos\phi}{2}\big) > 0 \quad \forall\theta \in [0, 2\pi] \tag{6.2}$$

where $\widetilde{h}(z)$ denotes the Z-transform of (6.1) and $h_0 = \cos\phi$ is the cursor. We now evaluate (6.2) for the channel (6.1).

Noting the following Z-transforms,

$$\Big\{\beta^m \cos(m\omega)\Big\} \leftrightarrow \frac{z(z - \beta\cos\omega)}{z^2 - 2\beta\cos\omega z + \beta^2},$$

$$\Big\{\beta^m \sin(m\omega)\Big\} \leftrightarrow \frac{\beta\sin\omega z}{z^2 - 2\beta\cos\omega z + \beta^2},$$

one obtains, after a simple calculation

$$\widetilde{h}(z) - \frac{\cos\phi}{2} = \frac{\cos\phi\,\frac{1}{2}(z^2 - \beta^2) - \sin\phi\,(\beta z\sin\omega)}{z^2 - 2\beta\cos\omega z + \beta^2}. \tag{6.3}$$

The poles of (6.3) are inside the unit circle thus the denominator of (6.3) is bounded away from zero on the unit circle. Thus realizing the denominator of (6.3) then taking the real part, when computing (6.2), leads to the equivalent condition

$$\cos\phi\ \frac{(1-\beta^2)}{2}\Big((1-\beta)^2 + 2\beta(1 - \cos\theta\cos\omega)\Big) + \sin\phi\ \beta\sin\omega\Big(2\beta\cos\omega - (1+\beta^2)\cos\theta\Big) > 0, \quad \forall\theta \in [0, 2\pi] \tag{6.4}$$

noting we recover the result of the third example in §4.4.3 as a special case when $\phi = 0$.

Now clearly the $\cos\phi$ term in (6.4) is positive for all parameter values, recalling $-\frac{\pi}{2} < \phi < \frac{\pi}{2}$. The $\sin\phi$ term, on the other hand, is negative or zero for at least one value of θ. Indeed it is easy to see that (6.4) takes its extreme values when $\theta = 0$ or $\theta = \pi$. In view of this we define, from (6.4),

$$u_\pm \triangleq \frac{(1-\beta^2)}{2}\big((1-\beta)^2 + 2\beta(1 \mp \cos\omega)\big) > 0 \tag{6.5a}$$

$$v_\pm \triangleq -\beta\sin\omega\big(2\beta\cos\omega \mp (1+\beta^2)\big), \tag{6.5b}$$

the subscripts indicating whether or not $\cos 0 = +1$ or $\cos \pi = -1$ applies. It is not difficult to see also $v_+ v_- \leq 0$. Now (6.4), in the two cases of interest and for the threshold of passivity (positivity), takes the form

$$\cos\phi\, u_+ - \sin\phi\, v_+ = 0,$$
$$\cos\phi\, u_- - \sin\phi\, v_- = 0.$$

Then viewing β and ω as parameters we can determine the critical values of ϕ in the two cases as

$$\phi_1 = \tan^{-1}\left(\frac{u_+}{v_+}\right) \quad \text{and} \quad \phi_2 = \tan^{-1}\left(\frac{u_-}{v_-}\right)$$

where one of these ϕ's lies in $-\frac{\pi}{2} < \phi < 0$ and the other in $0 < \phi < \frac{\pi}{2}$. In fact $\phi_1 = -\phi_2$, allowing us to concentrate on just $\phi > 0$. Figure 4.13 plots these functions of β vs ϕ for various ω (note the curves for ω, $-\omega$, $\pi - \omega$ and $\omega - \pi$ are identical, up to symmetry). As is suggested by the figure the worst case choice of ω appears to be $\omega = \frac{\pi}{2}$ for $\phi > 0$. This is easy to verify analytically. Further comments based on this figure and the above analysis will be covered in a series of remarks.

Remarks:

(i) Figure 4.13 shows lines corresponding to the thresholds of passivity. For a given ω it is the values of $\beta > 0$ below and $\phi \geq 0$ to the left of the line for which a finite error recovery time is guaranteed.

(ii) The case $\omega = \frac{\pi}{2}$ for $\phi > 0$ leads to the following algebraic relationship

$$\phi = \tan^{-1}\left(\frac{1-\beta^2}{2\beta}\right) \tag{6.6}$$

mapping $\phi \in [0, \frac{\pi}{2})$ from $\beta \in (0, 1]$.

(iii) The opposite extreme for the choice of ω which allows the greatest slop in $\phi > 0$ for a given β is clearly $\omega = 0$. This is clear from (6.1) because then (whenever $\phi < \frac{\pi}{2}$) we recover the results of §4.4.3. Letting instead $\phi < 0$ admits $\omega = \pi$ as the most attractive case by similar arguments.

(iv) Globally the results indicate that the DFE exhibits a great deal of robustness to phase timing errors. Figure 4.13 forms a neat summary and (6.6) defines the worst case.

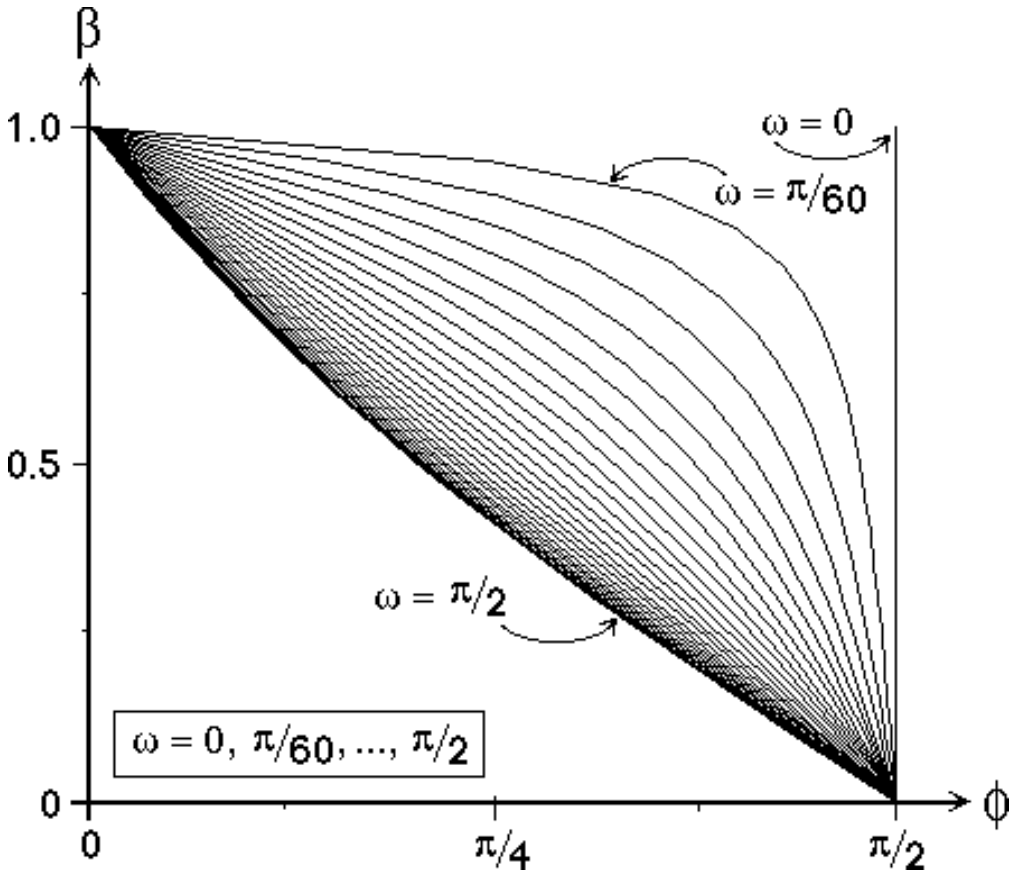

Fig.4.13 Timing Phase Sensitivity.

(v) The results are not restricted to clean channel models of the form (6.1). In principle the passivity results permit a similar analysis (numerical in the simplest manifestation) of timing phase sensitivity for more general parametrized classes of models.

4.7 Conclusions

4.7.1 Summary

We make a list of the main contributions of this chapter:

(i) Any channel satisfying the Nyquist condition in Theorem 4.7 (or its variants Theorem 4.10 and Theorem 4.14) will have a finite recovery time regardless of the initial conditions and regardless of the particular input sequence. These channels possess no pathological input sequences.

(ii) The maximum time to recover from error can be bounded in terms of the degree of strict passivity of a operator derived from the channel parameters. This degree of passivity is intimately related to a post error recovery eye diagram opening and an overbound on the rate of recovery.

(iii) With imperfect equalization this (post recovery) eye closes in proportion to an l_1-norm measure between the ideal DFE tapped delay line parameters and the actual values. The eye also closes when we use too few tap parameters in the DFE.

(iv) In the absence of ideal equalization, it is possible for the DFE to exhibit nice error recovery properties in a delay sense, i.e., the DFE output always settles down in a finite time to a fixed delay of the input with a possible (fixed) sign inversion. The conditions under which this behaviour is possible are stringent and have been determined.

(v) The techniques extend naturally to M-ary systems. Under ideal gain compensation (scaling of h such that $h_0 = 1$) any channel which behaves satisfactorily for binary signals will be satisfactory for M-ary signals (and vice-versa) because the conditions for passivity will then be identical.

(vi) A bound on the error probability for high signal to noise ratio channels has been given based on the passitivity techniques.

(vii) Passivity ideas were utilized to give an analysis of the effects of timing phase on error recovery properties.

4.7.2 Discussion

Up until now there has been scant theoretical justification that non-trivial, non-adaptive DFEs behave satisfactorily because of error propagation, perhaps only [5,6] being relevant. This is in stark contrast with the purported popularity of DFEs in practice. Previous theoretical work [1,4,7,8] concentrated on bounds which turn out to be hopelessly conservative in the majority of cases. These latter bounds will not be improved without relying heavily on explicit knowledge of the channel to be equalized—this was emphasized in [2,3] and [6]. In this chapter we have determined some non-trivial broad classes of channels for which a DFE can be effectively used (the results in [5,6] are very narrow and are subsumed by our present analysis). This

class, motivated by the work in [6], includes channels which have near exponential impulse responses which may either be overdamped or underdamped—thus capable of modelling twisted pair cable [12]. This provides some theoretical justification to the (controlled) use of DFEs in practice.

As well as defining a non-trivial class of channels for which the DFE behaves satisfactorily, the passivity analysis appears to provide an opportunity to clarify the role and function of a DFE. Recently the intuition that sensibly the DFE can only be used on minimum phase channels was shown to be misguided [2]. In [2] it is highlighted that minimum phaseness or near minimum phaseness of

$$h = \{h_0,\ h_1,\ h_2,\ \ldots\} \tag{7.1}$$

is not enough to imply satisfactory DFE error recovery. In comparison we have shown that the stronger notion of strict passivity of the object (or its generalizations)

$$\{\frac{h_0}{2},\ h_1,\ h_2,\ \ldots\} \tag{7.2}$$

is a concept which leads to a sensible decision feedback equalization problem (for both binary and M-ary alphabets). Naturally strict passivity of (7.2) implies strict passivity and thus minimum phaseness of (7.1) (but not vice versa). If the channel fails the passivity condition it is our contention that a linear equalizer preceding the DFE must be used. Note that our analysis covers the case of a cascade of a linear equalizer with a DFE because we can interpret h as being not just the channel impulse response but alternatively as the convolution of the channel impulse response with the linear equalizer. We interpret the function of the linear equalizer as being to transform the channel into a passive object which aligns well with the intuition that the linear equalizer is needed to remove precursor ISI. We believe this may be a fruitful new way of viewing the digital equalization problem and these investigations are a natural extension to the present work.

References

[1] D.L. Duttweiler, J.E. Mazo, and D.G. Messerschmitt, "An Upper Bound on the Error Probability in Decision Feedback Equalizers," *IEEE Trans. on Information Theory,* vol.IT-20, pp.490-497, July 1974.

[2] R.A. Kennedy, and B.D.O. Anderson, "Recovery Times of Decision Feedback Equalizers on Noiseless Channels," *IEEE Trans. on Communications,* vol.COM-35, pp.1012-1021, October 1987.

[3] R.A. Kennedy, B.D.O. Anderson, and R.R. Bitmead, "Tight Bounds on the Error Probabilities of Decision Feedback Equalizers ," *IEEE Trans. on Communications,* vol.COM-35, pp.1022-1029, October 1987.

[4] A. Cantoni, and P. Butler, "Stability of Decision Feedback Inverses," *IEEE Trans. on Communications,* vol.COM-24, pp.1064-1075, September 1976.

[5] P.L. Zador, "Error Probabilities in Data System Pulse Regenerator with DC Restoration," *Bell Syst. Tech. J.,* vol.45, pp.979-984, July 1966.

[6] R.A. Kennedy, and B.D.O. Anderson, "Error Recovery of Decision Feedback Equalizers on Exponential Impulse Response Channels," *IEEE Trans. on Communications,* vol.COM-35, pp.846-848, August 1987.

[7] J.J. O'Reilly, and A.M. de Oliveira Duarte, "Error Propagation in Decision Feedback Receivers," *Proc. IEE Proc. F, Commun., Radar and Signal Process.,* vol.132, no.7, pp.561-566, 1985.

[8] A.M. de Oliveira Duarte, and J.J. O'Reilly, "Simplified Technique for Bounding Error Statistics for DFB Receivers," *Proc. IEE Proc. F, Commun., Radar and Signal Process.,* vol.132, no.7, pp.567-575, 1985.

[9] C.A. Desoer, and M. Vidyasagar, "Feedback Systems: Input-Output Properties," Academic Press, New York 1975.

[10] R.A. Kennedy, B.D.O. Anderson, and R.R. Bitmead, "Channels Leading to Rapid DFE Error Recovery," *IEEE Trans. on Communications,* (accepted for publication).

[11] L. Ljung, "On Positive Real Transfer Functions and the Convergence of Some Recursive Schemes," *IEEE Trans. on Auto. Control,* vol.AC-22, No.4, pp.539-551, August 1977.

[12] B.R. Clarke, "The Time-Domain Response of Minimum Phase Networks," *IEEE Trans. on Circuits and Syst.,* vol.CAS-32, No.11, pp.1187-1189, November 1985.

[13] R.A. Kennedy, B.D.O. Anderson, and R.R. Bitmead, "Blind Adaptation of Decision Feedback Equalizers: Gross Convergence Properties," *International Journal of Adaptive Control and Signal Processing,* (submitted for publication).

[14] J. Salz, "Optimum Mean-Square Decision Feedback Equalization and Timing Phase," *IEEE Trans. on Communications,* vol.COM-25, pp.1471-1476, December 1977.

[15] K.J. Åström, and B. Wittenmark, "Computer Controlled Systems Theory and Design," Prentice Hall Inc., Englewood Cliffs, N.J., 1984.

CHAPTER 5. TESTING CONVERGENCE OF BLIND ADAPTATION

Aim: *To construct testing procedures on an equalizer output to verify correct convergence of blind adaptation, for both decision directed and decision feedback equalizers.*

5.1 Introduction

It has been established that in the case of linear equalization [1-4] and in the case of decision feedback equalization [5] (Chapter 3) that blind adaptation may lead to convergence of the filter parameters to undesirable settings where the equalizer does not correctly compensate for the channel dispersion. This is potentially a serious problem, so in the design of practical systems means to avoid this situation need to be addressed. Because equalization is blind, knowledge of the true input data sequence is lacking. Therefore a procedure testing correct operation of the equalizer *using only the output data* must be devised. In certain situations testing could be quite straightforward (at least for a human), e.g., if the input data stream were text or pictures then the reproduced data would immediately reflect the accuracy of equalization process—pictures would be scrambled, words would be muddled. Often, however, the data might not represent something to which a human could directly relate. Clearly high level subjective tests are beyond the capabilities of a simple equalizer, so the quest for a simple, low-level procedure to detect correct equalization, despite apparent equalizer parameter convergence, is highly desirable. This chapter is devoted to the demonstration that suitable testing procedures exist.

The general problem setting can be described as follows. The equalizer filter parameter values are fixed in the vicinity of a local minimum of some cost function which governs the adaptation phase of operation. The output data estimates are

necessarily being used in lieu of the real data in implementing the equalization. The data estimates need not correspond to the actual data (or a delay thereof), but some form of stationarity will be assumed of the output $\{\widehat{a}_k\}$ process. The tests we propose, and in a sense are the only sensible ones, are *statistical tests* on the output. These split into two categories: (a) distributional tests, i.e., the output should have the same distribution of symbols as the input; and (b) correlation tests, i.e., the properties of the output sequence with respect to delayed versions of itself should mimic those of the input. (Our usage of the terms "distribution" and "correlation" are not in the rigorous technical senses of these words but merely reflect the general concepts we need. The following detailed development does not suffer from this vagueness.) Foreshadowing the analysis to follow we will see that the simplicity of the proposed tests stands in stark contrast to the complexity of the proofs (when available).

In the literature we can see clear precursors to the present results. For the linear equalizer case Benveniste, Goursat and Ruget [2], quote a theorem which states that if the output distribution equals the input distribution then the linear channel-linear equalizer combination is equivalent to an overall delay, or the symbol distributions are gaussian. The situation where the input distribution is gaussian is practically irrelevant—typically input distributions are discrete and finite—thus we have a test on the output (at least when the distribution is not continuous). Unfortunately these results do not apply to the decision directed equalizer (DDE) because the combination of linear equalizer with quantizer is non-linear. (Indeed the results do not apply to any non-linear filter including the decision feedback equalizer (DFE).) The quantizer is desirable for a number of reasons, e.g., it provides tolerance to parameter variations, and it provides a limited protection against noise.

More recently, Verdú [4] suggested that the additional information present in the correlation of the output signal could be exploited to extend the result in [2]. This is precisely the direction one must head if we do not have the somewhat idealistic linearity situation as we will show. The proof of a theorem which in essence extends the theorem in [2] to the DDE case has been proven by us in [6]. In [6] a complete proof of the binary $M = 2$ case can be found, but it contains only an outline of the M-ary proof which we present here.

The first technical section §5.2 is devoted to the M-ary DDE for which relatively complete results have been found. In the second technical section §5.3 we look at the binary DFE case. Proofs that certain simple tests suffice are presented only for the

cases of low order DFEs. In principle we can extend our methods in the DFE case to determine conclusively whether or nor the proposed tests are adequate (to conclude correct convergence) because only a finite number of cases needs be checked for a given order of channel. However, the sheer dimensionality of the resulting proof restricts a demonstration to the low order cases. In §5.4 we look at some implications of our tests for achieving the long sought after blind adaptive algorithm which converges only to equalizing parameter settings. Finally §5.5 contains the conclusions. An appendix has been included containing the proofs of some non-trivial properties required for our main DDE theorem.

5.2 Decision Directed Equalizer Convergence Tests

5.2.1 Lead In

The behaviour of DDEs after adaptation, or with the adaptation mechanism switched off, can be described as follows (see Fig.5.1). The input sequence $\{a_k\}$ to the channel is a sequence of independent random variables taking values in an M-ary alphabet with equal probability. The channel has impulse response $\{h_0,\ h_1,\ \ldots\}$ and we shall assume that $h_j = 0$ for $j > N_1$. (Extensions to the infinite impulse response case could also be considered.) The noiseless ($n_k = 0$) channel output sequence $\{b_k\}$ is accordingly given by

$$b_k = \sum_{i=0}^{N_1} h_i a_{k-i}. \tag{2.1}$$

This noiseless output drives the equalizer, which is a finite impulse response filter with response $\{d_0,\ d_1,\ \ldots,\ d_{N_2}\}$ followed by a quantizer. (Note, in practice, one would choose N_2 sufficiently large, i.e., conservatively, on physical grounds.) Thus the quantizer input sequence $\{c_k\}$ is

$$c_k = \sum_{j=0}^{N_2} d_j b_{k-j}, \tag{2.2}$$

and the equalizer output is

$$\widehat{a}_k = \mathcal{Q}_M(c_k). \tag{2.3a}$$

where $\mathcal{Q}_M(\cdot)$ is the standard M-ary quantizer [7] given by

$$\mathcal{Q}_M(x) \triangleq \sum_{k=1-M/2}^{M/2-1} \operatorname{sgn}(x + 2k). \tag{2.3b}$$

(In (2.3b) we suppose x can only take those values such that the argument of all the sgn(·) functions can never be zero. This assumption is not crucial; also one could argue this situation occurs with zero probability.) Correct operation of the equalizer is characterized by

$$\widehat{a}_k = a_k \ \forall k \quad \text{or} \quad \widehat{a}_k = -a_k \ \forall k \tag{2.4a}$$

or, for some fixed integer $\delta > 0$,

$$\widehat{a}_k = a_{k-\delta} \ \forall k \quad \text{or} \quad \widehat{a}_k = -a_{k-\delta} \ \forall k. \tag{2.4b}$$

We note that in practical operation, noise n_k must usually be added into (2.1) as in Fig.5.1. However, one property of this form of equalizer is that it provides a certain margin against the noise, i.e.,

$$\mathcal{Q}_M(\sum_{j=0}^{N_2} d_j y_{k-j}) = \mathcal{Q}_M\big(\sum_{j=0}^{N_2} d_j (y_{k-j} + n_{k-j})\big)$$

for many specific noise sequences. We defer consideration of noisy channels until §5.2.6. Until then we will take $n_k \equiv 0$.

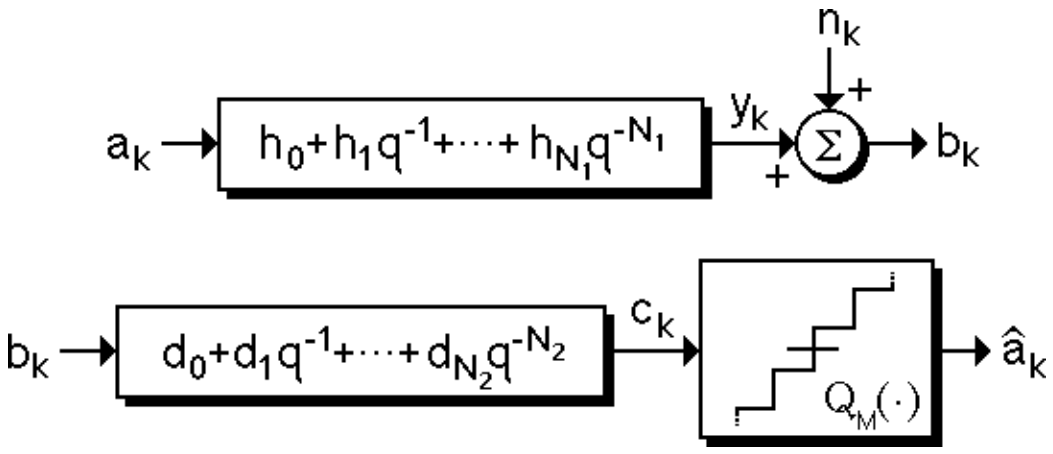

Fig.5.1 Channel and M-ary DDE Models.

In DDEs, the coefficients $\{d_j\}$ are adjusted by an adaptive algorithm, the details of which have been reported elsewhere [1-3]. One key property of these algorithms is however that convergence of the $\{d_k\}$ can occur to an undesirable setting; finite step-size effects in the adaptive algorithm mean that eventually such a setting should be

left, but it would clearly be helpful to have some way of knowing whether the output of an equalizer which had appeared to converge was or was not correct.

This leads us to formulate the following problem. Let $\{l_0,\ l_1,\ \ldots,\ l_N\}$, where $N = N_1 + N_2$, be the convolution of $\{h_j\}$ and $\{d_j\}$. Given measurements $\{\widehat{a}_k\}$ generated by

$$\widehat{a}_k = \mathcal{Q}_M(\sum_{j=0}^{N} l_j a_{k-j})$$

where the l_j are unknown but fixed, the $\{a_k\}$ are unmeasured, but known to be independent and taking values in an M-ary alphabet with equal probability, is there a test on the $\{\widehat{a}_k\}$ which would determine whether or not (2.4) held?

Obviously, if (2.4) holds, then the $\{\widehat{a}_k\}$ sequence is itself independent, so that independence of the measurements is a necessary condition for (2.4) to hold for some $\delta \in \{0,\ 1,\ \ldots,\ N\}$. Our main result is that an independence property is also sufficient for (2.4) to hold.

Notice that independence is a property that can, at least approximately, be readily checked. In this problem, as we will see, it is a non-trivial fact that checking just a finite number of terms of the form $Pr(\widehat{a}_{k+p} = i\ \cap\ \widehat{a}_k = j)$, for some $i, j, p \in \mathbb{Z}_+$ implies full independence, thus considerably simplifying the testing. We also briefly expand the ideas to consider the effects of channel noise in §5.2.6.

5.2.2 Generalized Eye Conditions

The first result we bring to bear on the DDE problem is what we call a generalized eye condition and it takes the following form.

Theorem 5.1: *Let $\{a_k\}$ be an input sequence taking values in an M-ary alphabet $\mathcal{M} \triangleq \{1-M,\ 3-M,\ \ldots,\ M-1\}$ with M even, such that all finite subsequences have non-zero probability. Let $\{\widehat{a}_k\}$ be the DDE output sequence generated by*

$$\widehat{a}_k = \mathcal{Q}_M(\sum_{i=0}^{N} l_i a_{k-i}) \tag{2.5a}$$

$$= \mathcal{Q}_M\big(l_\delta\ a_{k-\delta} + r_k(\delta)\big), \tag{2.5b}$$

where $l_0,\ l_1,\ \ldots,\ l_N$ are constants and

$$r_k(\delta) \triangleq \sum_{\substack{i=0 \\ i\neq\delta}}^{N} l_i a_{k-i}. \tag{2.5c}$$

Then there exists precisely one $\delta \in \{0,\ 1,\ \ldots,\ N\}$ *such that*

$$\widehat{a}_k = \mathrm{sgn}(l_\delta)\ a_{k-\delta},\ \forall\{a_k\}$$

if and only if

$$R(\delta) < \big|l_\delta\big| \qquad \text{for } M = 2 \tag{2.6a}$$

$$\frac{M-2+R(\delta)}{M-1} < \big|l_\delta\big| < \frac{M-2-R(\delta)}{M-3} \qquad \text{for } M = 4,\ 6,\ 8,\ \ldots \tag{2.6b}$$

where

$$R(\delta) \triangleq \max_{\{a_k\}} \big\{r_k(\delta)\big\} = (M-1)\sum_{\substack{i=0\\ i\neq\delta}}^{N} \big|l_i\big|. \tag{2.7}$$

□

Proof: *Define the quantizer intervals of (2.3b), indexed by the symbol to which they correspond, by*

$$\mathcal{I}(m) \triangleq (m-1,\ m+1), \quad \forall m \in \mathcal{M}\backslash\{1-M,\ M-1\}, \tag{2.8a}$$

$$\mathcal{I}(M-1) \triangleq (M-2,\ \infty), \quad \text{and} \quad \mathcal{I}(1-M) \triangleq (-\infty,\ 2-M). \tag{2.8b}$$

These conditions are equivalent to

$$x \in \mathcal{I}(m) \iff \mathcal{Q}_M(x) = m.$$

$\forall x \in \mathbb{R}$ *and* $\forall m \in \mathcal{M}$. *The linear equalizer is operating correctly when the output sequence is a delayed version of the input sequence, with possible inversion. This may be characterized by*

$$\sum_{i=0}^{N} l_i\ a_{k-i} \in \mathcal{I}\big(\mathrm{sgn}(l_\delta)\ a_{k-\delta}\big), \quad \forall\{a_k\} \tag{2.9}$$

where $\delta \in \{0,\ 1,\ \ldots,\ N\}$ *is some fixed delay. We see a decoding error will occur only if (2.9) is violated. With the definition of* $r_k(\delta)$ *in (2.5c) and letting* $a_{k-\delta}$ *range through the values in* $\mathcal{M}$ *gives the system of inequalities which must be satisfied for correct operation of the DFE, as follows:*

$$\begin{aligned}
0 &< r_k(\delta) + \big|l_\delta\big| < 2\\
&\ \ \vdots\\
M-6 &< r_k(\delta) + (M-5)\ \big|l_\delta\big| < M-4\\
M-4 &< r_k(\delta) + (M-3)\ \big|l_\delta\big| < M-2 \qquad (2.10a)\\
M-2 &< r_k(\delta) + (M-1)\ \big|l_\delta\big| \qquad (2.10b)
\end{aligned}$$

Firstly, for $M \geq 4$, inequalities (2.10a) and (2.10b) yield the tightest bounds on $|l_\delta|$; it can be shown that if they are satisfied $\forall\{a_k\}$ then the remaining inequalities also hold. Combining (2.10a) and (2.10b) we obtain the requirement

$$\frac{M-2+r_k(\delta)}{M-1} < |l_\delta| < \frac{M-2-r_k(\delta)}{M-3} \qquad \forall\{a_k\}. \tag{2.11}$$

Now inequality (2.11) must hold for all input sequences $\{a_k\}$, thus in particular we need

$$\max_{\{a_k\}} \left\{ \frac{M-2+r_k(\delta)}{M-1} \right\} < |l_\delta| < \min_{\{a_k\}} \left\{ \frac{M-2-r_k(\delta)}{M-3} \right\}. \tag{2.12}$$

However by (2.7) this is precisely condition (2.6b). For any $|l_\delta|$ outside the interval (2.12) an error will occur for some input sequence. The result for $M = 2$ only involves a single inequality, i.e., (2.10b), which, by the same arguments, leads to (2.6a). ❑

Remarks:

(i) Theorem 5.1 is saying that for the output to be a δ-delay of the input, then $|l_\delta|$ must be the overwhelmingly dominant l_i because the left hand inequality in (2.6) implies

$$\sum_{\substack{i=0 \\ i\neq\delta}}^{N} |l_i| < |l_\delta|.$$

(ii) Note $|l_\delta| \to 1$ as $M \to \infty$, i.e., the larger the alphabet the tighter the conditions on the l_i parameters have to be.

(iii) As is well known [2], indeed is obvious, there is no restriction on the sign of l_δ. So if one setting of the DDE parameters leads to $\widehat{a}_k = +a_{k-\delta}$ $\forall\{a_k\}$ then the negative of the setting leads to $\widehat{a}_k = -a_{k-\delta}$ $\forall\{a_k\}$. This situation is at odds with the DFE case where only one sign is possible (independent of the DFE parameter setting) as we have seen in Chapters 3 and 4.

(iv) Theorem 5.1 holds for the case when the input is independent and identically distributed, and the support of the distribution is all the M symbols.

Theorem 5.1 provides no clue as to how an observer of an equalizer might infer that it is decoding correctly (in a delay sense), given only output measurements, because the l_i

are not directly measurable by the observer. A means to get around this problem—by using statistical tests on the output—is investigated in the next section.

5.2.3 Main Result Statement

Our main result is the following (we assume M is even, noting that the less interesting case of M odd could be approached in a similar way):

Theorem 5.2: *Let $\{a_k\}$ be an M-ary independent sequence taking values in the set $\mathcal{M}$ with equal probability. Let $\{a_k\}$ be the input to the system given by*

$$\widehat{a}_k = \mathcal{Q}_M(\sum_{i=0}^{N} l_i a_{k-i}). \tag{2.13}$$

where $l_0,\ l_1,\ \ldots,\ l_N$ are constants. Suppose that: (i) $\{\widehat{a}_k\}$ take values in $\mathcal{M}$ with equal probability

$$Pr(\widehat{a}_k = s) = \frac{1}{M} \quad \forall s \in \mathcal{M}; \tag{2.14a}$$

and (ii) the $\widehat{a}_k$ are pairwise independent in the sense that

$$Pr(\widehat{a}_{k+p} \geq s_1 \mid \widehat{a}_k \geq s_2) = Pr(\widehat{a}_{k+p} \geq s_1) \tag{2.14b}$$

$\forall p \in \mathbb{Z}_+$ and $\forall s_1, s_2 \in \mathcal{M}$. Then for precisely one $\delta \in \{0,\ 1,\ \ldots,\ N\}$ there holds

$$\widehat{a}_k = \mathrm{sgn}(l_\delta)\ a_{k-\delta},\ \forall \{a_k\}. \tag{2.15}$$

□

We give a brief discussion before presenting our proof (which terminates in §5.2.5). If the output $\{\widehat{a}_k\}$ is not a trivial delay-like mapping of the input $\{a_k\}$, as in (2.15), then we claim that this will be reflected in either as a form of output correlation or the output distribution will differ from the input distribution. This seems perfectly reasonable. To highlight the importance of the underlying hypotheses of the theorem we consider two examples.

Example (i) *(Mazo [1]) Suppose $\widehat{a}_k = \mathcal{Q}_4(1000\ a_k)$, implying $\widehat{a}_k = 3\ \mathrm{sgn}(a_k)$, then $\{\widehat{a}_k\}$ is a sequence of independent random variables. However $Pr(\widehat{a}_k = -1) = Pr(\widehat{a}_k = +1) = 0$ and $Pr(\widehat{a}_k = -3) = Pr(\widehat{a}_k = +3) = 0.5$, i.e., $\widehat{a}_k$ has a non-uniform distribution. Thus (2.14b) holds but (2.14a) does not. Then Theorem 5.2 tells us, as we know, that (2.15) does not hold.*

Example (ii) *Suppose instead of (2.13) the system was* $\widehat{a}_k = \mathcal{Q}_2(a_k\ a_{k-1})$ *where* $\mathcal{M} = \{-1, +1\}$. *Then* $\{\widehat{a}_k\}$ *is an independent sequence and the output distribution is uniform, i.e., both (2.14a) and (2.14b) hold. However, (2.15) does not hold for any* δ. *(Theorem 5.2 does not apply here because the system is not described by (2.13).) This example will be important later because it indicates structural assumptions need to be employed in proving the validity of any convergence test.*

For didactic purposes the reader may prefer to see the proof of the binary ($M = 2$) result in [6] before proceeding further with the full M-ary proof presented here.

5.2.4 Preliminary Results

To prove Theorem 5.2 we need a number of preliminary results which extract the subtle way correlation is reflected in the output when (2.13) is not a simple overall delay system.

Define integers $I \leq J \in \{0,\ 1,\ \ldots,\ N\}$ by the following requirements:

$$\mathcal{Q}_M(\sum_{i=I}^{J} l_i a_{k-i}) = \mathcal{Q}_M(\sum_{i=0}^{N} l_i a_{k-i}) \triangleq \widehat{a}_k, \quad \forall\{a_k\} \tag{2.16a}$$

$$\mathcal{Q}_M(\sum_{i=I}^{J-1} l_i a_{k+J-I-i}) \neq \widehat{a}_{k+J-I}, \text{ for some } \{a_k\} \tag{2.16b}$$

$$\mathcal{Q}_M(\sum_{i=I+1}^{J} l_i a_{k-i}) \neq \widehat{a}_k, \text{ for some } \{a_k\} \tag{2.16c}$$

In terms of the problem statement in §5.2.3 one can regard $l_0,\ l_1,\ \ldots,\ l_{I-1}$ as very small precursors, and $l_{J+1},\ l_{J+2},\ \ldots,\ l_N$ as very small postcursors in the combined channel-equalizer impulse response. Equations (2.16b) and (2.16c) guarantee that $\widehat{a}_{k+J-I}$ and $\widehat{a}_k$ depend nontrivially on a_{k-I}, and that a_{k-I} is the only symbol on which both $\widehat{a}_{k+J-I}$ and $\widehat{a}_k$ can depend. Because of this we expect that there is some correlation between $\widehat{a}_{k+J-I}$ and $\widehat{a}_k$. Observe that if $I = J$ in (2.16a) then

$$\widehat{a}_k = \mathcal{Q}_M(l_I a_{k-I}),\ \forall\{a_k\} \tag{2.17}$$

and we have:

Lemma 5.3:

$$\left.\begin{array}{r} Pr(\widehat{a}_k = M-1) = \dfrac{1}{M} \\ \widehat{a}_k = \mathcal{Q}_M(l_I a_{k-I}),\ \forall\{a_k\} \end{array}\right\} \ \Rightarrow\ \widehat{a}_k = \mathrm{sgn}(l_I)\ a_{k-I}\ \forall\{a_k\} \tag{2.18}$$

❑

Proof: *Suppose* $\left|l_I\right| < \frac{M-2}{M-1}$, *then substituting* $a_{k-I} = \mathrm{sgn}(l_I)\ (M-1)$ *into (2.17) implies* $\widehat{a}_k < M-1$. *Therefore* $Pr(\widehat{a}_k = M-1) = 0$ *(regardless of the distribution of* a_{k-I}*). On the other hand if* $\left|l_I\right| > \frac{M-2}{M-3}$ *then both* $a_{k-I} = \mathrm{sgn}(l_I)\ (M-1)$ *and* $a_{k-I} = \mathrm{sgn}(l_I)\ (M-3)$ *give* $\widehat{a}_k = M-1$, *and consequently* $Pr(\widehat{a}_k = M-1) \geq \frac{2}{M}$ *(by the uniformity of the input distribution). Hence* $Pr(\widehat{a}_k = M-1) = \frac{1}{M}$ *implies*

$$\frac{M-2}{M-1} < \left|l_I\right| < \frac{M-2}{M-3}. \tag{2.19}$$

From (2.17), Theorem 5.1 may now be applied with $R(\delta) \equiv 0$ *(because (2.17) is a special case of (2.5b) where* $r_k(\delta) \equiv 0$*) to show the desired delay behaviour.* ❑

In what follows it will be shown that, assuming the output distribution is uniform (2.14a), $I < J$ contradicts the pairwise independence of the $\{\widehat{a}_k\}$ sequence, by evaluating the conditional probability denoted by

$$\xi(s_1, s_2) \triangleq Pr(\widehat{a}_{k+J-I} \geq s_1 \mid \widehat{a}_k \geq s_2) \tag{2.20}$$

when symbols s_1 and s_2 take carefully selected values s_1^* and s_2^*, respectively.

Applying Bayes' rule to (2.20) yields

$$\xi(s_1, s_2) = \sum_{m \in \mathcal{M}} Pr(\widehat{a}_{k+J-I} \geq s_1 \mid \widehat{a}_k \geq s_2\ \cap\ a_{k-I} = m) \cdot Pr(a_{k-I} = m \mid \widehat{a}_k \geq s_2). \tag{2.21}$$

The conditioning $\widehat{a}_k \geq s_2$ in the first term of (2.21) is redundant given $a_{k-I} = m$ because $\widehat{a}_{k+J-I}$ and $\widehat{a}_k$ only have a_{k-I} in common. To see this more clearly consider the following. The conditioning in question is equivalent to the event

$$\begin{aligned} \left\{\widehat{a}_k \geq s_2\ \cap\ a_{k-I} = m\right\} &\equiv \left\{\sum_{i=I}^{J} l_i a_{k-i} \geq s_2 - 1\ \cap\ a_{k-I} = m\right\} \\ &\equiv \left\{\sum_{i=I+1}^{J} l_i a_{k-i} + l_I m \geq s_2 - 1\ \cap\ a_{k-I} = m\right\} \end{aligned}$$

and this first event is independent of $\widehat{a}_{k+J-I}$.

We can further simplify (2.21) by reversing the second term in the following sense. Define the function $f\colon \mathcal{M} \mapsto \mathbb{Z}_+$ by $f(m) \triangleq \frac{1}{2}(M+1-m)$ which gives the number of symbols in the M-ary alphabet greater than or equal to a given symbol m, e.g., $f(1-M) = M$ and $f(M-1) = 1$. Thus $Pr(a_k \geq m) = Pr(\widehat{a}_k \geq m) = \frac{f(m)}{M}$. Therefore we may write

$$\begin{aligned} Pr(a_{k-I} = m \mid \widehat{a}_k \geq s_2) &= \frac{Pr(a_{k-I} = m \ \cap \ \widehat{a}_k \geq s_2)}{Pr(\widehat{a}_k \geq s_2)} \\ &= M \cdot \frac{Pr(a_{k-I} = m \ \cap \ \widehat{a}_k \geq s_2)}{f(s_2)} \\ &= \frac{1}{f(s_2)} \cdot Pr(\widehat{a}_k \geq s_2 \mid a_{k-I} = m) \end{aligned}$$

because $Pr(a_k = s_2) = Pr(\widehat{a}_k = s_2) = \frac{1}{M}$, and so (2.21) may be re-expressed more simply as

$$\xi(s_1, s_2) = \frac{1}{f(s_2)} \sum_{m \in \mathcal{M}} Pr(\widehat{a}_{k+J-I} \geq s_1 \mid a_{k-I} = m) \cdot Pr(\widehat{a}_k \geq s_2 \mid a_{k-I} = m). \quad (2.22)$$

We aim to show that $\xi(s_1, s_2)$ in (2.22) is not equal to

$$Pr(\widehat{a}_{k+J-I} \geq s_1) = \frac{f(s_1)}{M} \quad (2.23)$$

for a certain $s_1 = s_1^*$, which would be the case if $\{\widehat{a}_k\}$ satisfied a pairwise independence property (2.14b) (implying the conditioning in (2.20) could be dropped, yielding (2.23)). With this in mind, the following definitions are made:

For all $m \in \mathcal{M}$, and $\forall s_1, s_2 \in \mathcal{M}$

$$Pr(\widehat{a}_{k+J-I} \geq s_1 \mid a_{k-I} = m) \triangleq \frac{f(s_1)}{M}\big(1 + \mathrm{sgn}(l_J)\ \epsilon(m, s_1)\big) \quad (2.24a)$$

$$Pr(\widehat{a}_k \geq s_2 \mid a_{k-I} = m) \triangleq \frac{f(s_2)}{M}\big(1 + \mathrm{sgn}(l_I)\ \eta(m, s_2)\big) \quad (2.24b)$$

for suitable functions $\epsilon(\cdot,\cdot)$ and $\eta(\cdot,\cdot)$ whose domain is $\mathcal{M} \times \mathcal{M}$. Note any departure from pairwise independence will be reflected in $\epsilon(m, s_1)$ or $\eta(m, s_2)$ being non-zero. We now establish the existence of symbols $s_1^*, s_2^* \in \mathcal{M}$ such that four crucial properties regarding the functions $\epsilon(\cdot, s_1^*)$ and $\eta(\cdot, s_2^*)$ hold. The proofs of these four properties are relegated to an appendix. (Note the symbols $s_1^*, s_2^* \in \mathcal{M}$ defined by the first property are the same symbols used in the remaining three properties.)

Property 5.4: $\exists s_1^*, s_2^* \in \mathcal{M}$ *such that* $\epsilon(M-1, s_1^*) > 0$ *and* $\eta(M-1, s_2^*) > 0$. ❑

Property 5.5: $\forall m_1 < m_2 \in \mathcal{M}$, $\epsilon(m_1, s_1^*) \leq \epsilon(m_2, s_1^*)$ *and* $\eta(m_1, s_2^*) \leq \eta(m_2, s_2^*)$. ❑

Property 5.6: $\sum_{m\in\mathcal{M}} \epsilon(m, s_1^*) = 0$ *and* $\sum_{m\in\mathcal{M}} \eta(m, s_2^*) = 0$. ❑

Property 5.7: $\sum_{m\in\mathcal{M}} \epsilon(m, s_1^*)\ \eta(m, s_2^*) > 0$. ❑

For our purposes in what follows we need only Property 5.6 and Property 5.7. However the first two properties are needed for the proof of the last two, and in this sense are implicitly used.

5.2.5 Proof of Main Result

With the previous results in hand the remainder of the proof of the main result, Theorem 5.2, is straightforward.

Proof: *From (2.22) along with definitions (2.24a) and (2.24b), setting* $s_1 = s_1^*$ *and* $s_2 = s_2^*$, *we get*

$$\begin{aligned}\xi(s_1^*, s_2^*) &= \frac{1}{f(s_2^*)} \sum_{m\in\mathcal{M}} \frac{f(s_1^*)}{M}\frac{f(s_2^*)}{M}\big(1+\operatorname{sgn}(l_J)\ \epsilon(m, s_1^*)\big)\big(1+\operatorname{sgn}(l_I)\ \eta(m, s_2^*)\big) \\ &= \frac{f(s_1^*)}{M^2}\Big\{M + \operatorname{sgn}(l_J)\sum_{m\in\mathcal{M}} \epsilon(m, s_1^*) + \operatorname{sgn}(l_I)\sum_{m\in\mathcal{M}} \eta(m, s_2^*) \\ &\qquad + \operatorname{sgn}(l_J l_I)\sum_{m\in\mathcal{M}} \epsilon(m, s_1^*)\ \eta(m, s_2^*)\Big\} \qquad (2.25)\end{aligned}$$

In (2.25) the middle terms in the brackets vanish by Property 5.6, and Property 5.7 guarantees that the sum of the products $\epsilon(m, s_1^*)\ \eta(m, s_2^*)$ *is non-zero. We therefore have*

$$\xi(s_1^*, s_2^*) \triangleq Pr(\widehat{a}_{k+J-I} \geq s_1^* \mid \widehat{a}_k \geq s_2^*) \neq \frac{f(s_1^*)}{M} = Pr(\widehat{a}_{k+J-I} \geq s_1^*) \qquad (2.26)$$

which contradicts the pairwise independence of the output sequence (2.14b). It follows that the hypothesis $I < J$ *is flawed and thus we must have* $I = J$. *However, by Lemma 5.3 with* $\delta = I$, *equation (2.15) is implied, and this ends the proof of Theorem 5.2.* ❑

Remarks:

(i) The converse of Theorem 5.2 is trivial, for if the output sequence $\{\widehat{a}_k\}$ satisfies (2.15), then both the input and output sequences have the same statistical properties.

(ii) We only require the pairwise independence of the $\widehat{a}_k$ over a finite interval because $\widehat{a}_k$ and $\widehat{a}_{k+N+i}$ for $i > 1$ are independent by (2.5).

(iii) In effect the equivalence of the following has been established: (a) $\widehat{a}_k, \widehat{a}_j$ pairwise independent for $1 \leq \left|k-j\right| \leq N$, and $\widehat{a}_k \in \mathcal{M}$ equi-probable; (b) $\widehat{a}_k = \text{sgn}(l_\delta)\, a_{k-\delta}$ some $\delta \in \{0,\ 1,\ \ldots,\ N\}$; and (c) generalized eye conditions are satisfied (Theorem 5.1).

(iv) A slightly simpler test than that indicated by (2.26) takes the form

$$Pr(\widehat{a}_{k+J-I} = t_1^* \ \cap\ \widehat{a}_k = t_2^*) \neq \frac{1}{M^2} = Pr(\widehat{a}_{k+J-I} = t_1^*) \cdot Pr(\widehat{a}_{k+J-I} = t_2^*) \quad (2.27)$$

for some $t_1^*, t_2^* \in \mathcal{M}$, not necessarily equal to $s_1^*, s_2^* \in \mathcal{M}$, respectively. To derive this from (2.26) involves a trivial manipulation with Bayes' Rule and is therefore not presented.

5.2.6 Additive Noise Effects

We turn our attention now to the behaviour of the DDE with additive channel noise. To avoid needless complications we will treat only the binary case (and our development will be partly heuristic). We consider the system

$$\widehat{a}_k = \text{sgn}(\sum_{j=0}^{N} l_j a_{k-j} + n_k) \quad (2.28)$$

where $\{n_k\}$ is the extraneous noise (Fig.5.1).

Initially, we shall assume that $\{n_k\}$ and $\{a_k\}$ are individually independent sequences which are mutually independent. More realistically if n_k is correlated over time, as is the case for a moving average signal

$$n_k = \sum_{i=0}^{N_2} d_i \nu_{k-i}$$

with $\{\nu_k\}$ independent, then the independence of $\{\widehat{a}_k\}$ will be violated by dint of this mechanism. We shall return to consideration of such noise signals later as they represent a typical class of noise arising in the output of an equalized channel.

We constrain our attention to the situation where occasional noise bursts are capable of altering the equalized signal but this signal is more usually decoded correctly. To analyse this case we repeat the arguments of the preceding subsections, suitably amended.

Denote by $\mathcal{F}_k$ the sigma-algebra of events generated by $\{a_k,\ a_{k-1},\ \ldots\}$ and define the integers I (maximal) and J (minimal), subject to $I < J$, by the following conditional distributions:

$$Pr\big(\operatorname{sgn}(\sum_{i=I}^{J} l_i a_{k-i} + n_k) = +1 \bigm| \mathcal{A}\big) = Pr\big(\widehat{a}_k = +1 \bigm| \mathcal{A}\big) \quad \forall \mathcal{A} \in \mathcal{F}_k, \tag{2.29a}$$

$$Pr\big(\operatorname{sgn}(\sum_{i=I}^{J-1} l_i a_{k+J-I-i} + n_k) = +1 \bigm| \mathcal{B}\big) = Pr\big(\widehat{a}_{k+J-I-i} = +1 \bigm| \mathcal{B}\big) \tag{2.29b}$$

for some $\mathcal{B} \in \mathcal{F}_{k+J-I-i}$, and

$$Pr\big(\operatorname{sgn}(\sum_{i=I+1}^{J} l_i a_{k-i} + n_k) = +1 \bigm| \mathcal{C}\big) = Pr\big(\widehat{a}_k = +1 \bigm| \mathcal{C}\big) \tag{2.29c}$$

for some $\mathcal{C} \in \mathcal{F}_k$. To avoid a degenerate problem we make the mild assumption on the amplitude of the noise:

$$Pr(\sum_{i=0}^{N} \big|l_i\big| > \big|n_k\big|) > 0. \tag{2.30}$$

Then an identical argument to that of the previous section leads to the conclusion that the above definition of I and J, $I < J$ and $\widehat{a}_k, \widehat{a}_{k+p}$ being pairwise independent $\forall p \in \mathbb{Z}_+ \setminus 0$ are incompatible. To recapitulate, we have:

Theorem 5.8: *Let $\{a_k\}$ be an independent sequence of random variables taking the values ± 1 with equal probability. Let $\{n_k\}$ be a sequence of independent random variables independent from $\{a_k\}$. Suppose that for some constants $l_0,\ l_1,\ \ldots,\ l_N$*

$$\widehat{a}_k = \operatorname{sgn}(\sum_{j=0}^{N} l_j a_{k-j} + n_k) \tag{2.31}$$

and further that the distribution of $\{n_k\}$ *satisfies (2.30) and is such that the occurrence of a zero argument of the sign function in (2.31) is a probability zero event.*

Then, if $\{\widehat{a}_k\}$ *defined by (2.31) is itself composed of pairwise independent random variables, then there holds*

$$Pr(\widehat{a}_k = +1 \mid \mathcal{A}) = Pr(\text{sgn}(l_\delta\ a_{k-\delta} + n_k) = +1 \mid \mathcal{A}), \quad \forall \mathcal{A} \in \mathcal{F}_k. \tag{2.32}$$

for some $\delta \in \{0,\ 1,\ \ldots,\ N\}$. ❑

This theorem demonstrates that the non-noisy result carries over to the case of additive independent noise, subject to a mild condition (2.30). That is, uncorrelatedness of $\{\widehat{a}_k\}$ implies that its distribution is centered on $\text{sgn}(l_\delta)\ a_{k-\delta}$ for some $\delta \in \{0,\ 1,\ \ldots,\ N\}$.

Unfortunately, as remarked earlier, the more realistic assumption for an equalized channel is that $\{n_k\}$ is not independent but a moving average (or m-dependent) process of order N_2, i.e., with a correlation length given by the number of taps in the equalizer component. In a well-designed system, the channel noise should be well below the signal level for a great proportion of the time. Thus the probability of noise-induced decision error will be small. The moving average nature of n_k will, however, cause these noise-induced errors to persist for periods of the order of the equalizer length as the infrequent event of a large noise sample shifts through the tapped-delay line structure.

The net effect of small additive channel noise will be not to affect the decision and therefore not to affect the correlation test for convergence except in infrequent intervals where bursts of errors, and therefore presumably correlated decisions, occur.

5.3 Decision Feedback Equalizer Convergence Tests

5.3.1 Lead In

The behaviour of DFEs after adaptation, or with the adaptation mechanism switched off, has already been studied in detail (Chapters 2 and 4). As in the DDE case we wish to indicate that convergence tests exist, at least for low order DFEs. The more general problem, of finding tests for arbitrary order DFEs, remains open. The principle differences between the DFE and DDE cases constitute the source of the technical difficulties and so it is appropriate to foreshadow these now.

The DFE is a recursive device; therefore, to obtain an understanding of the statistics of the output $\{\widehat{a}_k\}$ one must unravel the subtleties of error propagation. The exact description of the output process is conveniently provided by FSMPs. However, generally these are high dimensional and become unwieldy. Further, to obtain a sensible problem formulation one needs to impose stationarity assumptions on the output process because, for example, the statistics of the output process during say error recovery (non-stationary behaviour) are typically entirely different to those after recovery. However, to characterize the stationary behaviour corresponds to determining closed sets of non-transient atomic states of the FSMP which describes the stochastic dynamics of a given channel (polytope of channels), and this problem is entirely non-trivial. A better understanding of some of these issues can obviously be gained by looking at the low order proofs that we now provide. The formulation will constrain itself to the binary case given the apparent complexity of the problem.

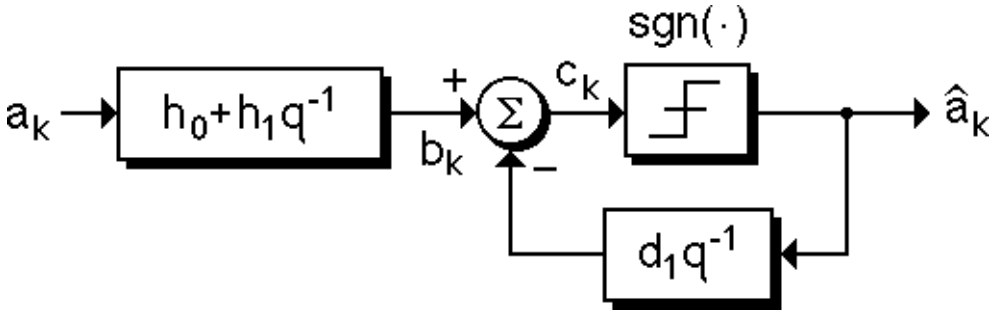

Fig.5.2 N=1 Binary DFE and Channel Model.

5.3.2 The N=1 Case

With $N = 1$ the DFE equation can be written (see Fig.5.2)

$$\widehat{a}_k = \mathrm{sgn}(h_0 a_k + h_1 a_{k-1} - d_1 \widehat{a}_{k-1}). \tag{3.1}$$

The type of test for convergence we propose for the DFE is quantitatively similar to that given for the DDE (2.27). It involves only a correlation type test and not a distributional test, of which the latter is degenerate in the binary case.

Theorem 5.9: *Let $\{a_k\}$ be an equiprobable independent binary process, and let $\{\widehat{a}_k\}$ be the stationary output process of an $N = 1$ DFE, viz.,*

$$\widehat{a}_k = \mathrm{sgn}(h_0 a_k + h_1 a_{k-1} - d_1 \widehat{a}_{k-1}).$$

Then $\forall \alpha, \beta \in \{-1, +1\}$ we have

$$Pr(\widehat{a}_k = \alpha \ \cap \ \widehat{a}_{k-1} = \beta) = \frac{1}{4}, \ \Rightarrow \ \widehat{a}_k = +\mathrm{sgn}(h_\delta)\, a_{k-\delta} \tag{3.2}$$

for precisely one $\delta \in \{0, 1\}$. ❑

(The stationarity assumption ensures the FSMP governing the DFE behaviour can only be found in recurrent and not transient atomic states. Our second proof makes this point clearer.)

Proof: *We proceed by contradiction. We assume that the channel-DFE combination cannot act as a delay $\delta = 0$ or delay $\delta = 1$ system. From Chapter 3 §3.5.4 we have the equivalent conditions which ensure this, viz.,*

$$\big|h_0\big| < \big|h_1 - \sigma_0 \cdot d_1\big|, \tag{3.3a}$$

$$\big|h_1\big| < \big|h_0\big| + \big|d_1\big|. \tag{3.3b}$$

where we are defining

$$\sigma_0 \triangleq \mathrm{sgn}(h_0), \quad \sigma_1 \triangleq \mathrm{sgn}(h_1), \quad \tau_1 \triangleq \mathrm{sgn}(d_1).$$

Alternatively it is relatively straightforward to see that (3.3a) and (3.3b) deny delay $\delta = 0$ and delay $\delta = 1$ behaviour for all input sequences, given stationarity, because only a few cases need to be checked.

Beginning from the hypothesis in (3.2), consider the following calculation:

$$\begin{aligned}
\frac{1}{4} = \quad & Pr\big(\widehat{a}_k = +1 \ \cap \ \widehat{a}_{k-1} = -\tau_1\big) && (3.4a)\\
= \quad & Pr\big(\widehat{a}_k = +1 \ \cap \ \widehat{a}_{k-1} = -\tau_1 \ \cap \ a_k = +\sigma_0 \ \cap \ a_{k-1} = +\sigma_1\big) \\
& + Pr\big(\widehat{a}_k = +1 \ \cap \ \widehat{a}_{k-1} = -\tau_1 \ \cap \ a_k = +\sigma_0 \ \cap \ a_{k-1} = -\sigma_1\big) \\
& + Pr\big(\widehat{a}_k = +1 \ \cap \ \widehat{a}_{k-1} = -\tau_1 \ \cap \ a_k = -\sigma_0 \ \cap \ a_{k-1} = +\sigma_1\big) \\
& + Pr\big(\widehat{a}_k = +1 \ \cap \ \widehat{a}_{k-1} = -\tau_1 \ \cap \ a_k = -\sigma_0 \ \cap \ a_{k-1} = -\sigma_1\big). && (3.4b)
\end{aligned}$$

But the argument of (3.1) can take, in general, only 4 values if we fix $\widehat{a}_{k-1} = -\tau_1$. *Then we have the following*

$$h_0 a_k + h_1 a_{k-1} - d_1 \widehat{a}_{k-1} = \begin{cases} +\big|h_0\big| + \big|h_1\big| + \big|d_1\big| & \Rightarrow\ \widehat{a}_k = +1 \quad \textit{by positivity.} \\ +\big|h_0\big| - \big|h_1\big| + \big|d_1\big| & \Rightarrow\ \widehat{a}_k = +1 \quad \textit{by (3.3b).} \\ -\big|h_0\big| + \big|h_1\big| + \big|d_1\big| & \Rightarrow\ \widehat{a}_k = +1 \quad \textit{by (3.3a).} \\ -\big|h_0\big| - \big|h_1\big| + \big|d_1\big| & \Rightarrow\ \widehat{a}_k = -1 \quad \textit{by Theorem 3.7.} \end{cases}$$

Thus in the four terms of (3.4b) the value of $\widehat{a}_k$ *is completely determined and so (3.4b) may be reduced to*

$$\begin{aligned} \frac{1}{4} = \quad & Pr\big(\widehat{a}_{k-1} = -\tau_1 \ \cap\ a_k = +\sigma_0 \ \cap\ a_{k-1} = +\sigma_1\big) \\ & + Pr\big(\widehat{a}_{k-1} = -\tau_1 \ \cap\ a_k = +\sigma_0 \ \cap\ a_{k-1} = -\sigma_1\big) \\ & + Pr\big(\widehat{a}_{k-1} = -\tau_1 \ \cap\ a_k = -\sigma_0 \ \cap\ a_{k-1} = +\sigma_1\big). \end{aligned} \tag{3.5}$$

However a_k *is independent of* a_{k-1} *and, by causality, independent of* $\widehat{a}_{k-1}$. *Therefore the* $a_k = +\sigma_0$ *and* $a_k = -\sigma_0$ *events factor out as a multiplicative factor of* $\frac{1}{2}$ *and collecting common terms we get*

$$\begin{aligned} \frac{1}{4} &= Pr\big(\widehat{a}_{k-1} = -\tau_1 \ \cap\ a_{k-1} = +\sigma_1\big) + \frac{1}{2} Pr\big(\widehat{a}_{k-1} = -\tau_1 \ \cap\ a_{k-1} = -\sigma_1\big) \\ &= \frac{1}{2} Pr\big(\widehat{a}_{k-1} = -\tau_1\big) + \frac{1}{2} Pr\big(\widehat{a}_{k-1} = -\tau_1 \ \cap\ a_{k-1} = +\sigma_1\big) \\ &= \frac{1}{4} + \frac{1}{2} Pr\big(\widehat{a}_{k-1} = -\tau_1 \ \cap\ a_{k-1} = +\sigma_1\big), \end{aligned} \tag{3.6}$$

showing

$$Pr\big(\widehat{a}_{k-1} = -\tau_1 \ \cap\ a_{k-1} = +\sigma_1\big) = 0 \tag{3.7}$$

and by symmetry

$$Pr\big(\widehat{a}_{k-1} = +\tau_1 \ \cap\ a_{k-1} = -\sigma_1\big) = 0. \tag{3.8}$$

Equations (3.7) and (3.8) imply $\widehat{a}_{k-1} = \sigma_1 \tau_1\ a_{k-1}$, $\forall k$ *under stationarity. This is a delay* $\delta = 0$ *system which contradicts (3.3a). Hence the assumption that the channel-DFE combination cannot act as a delay is false and the theorem follows.*❑

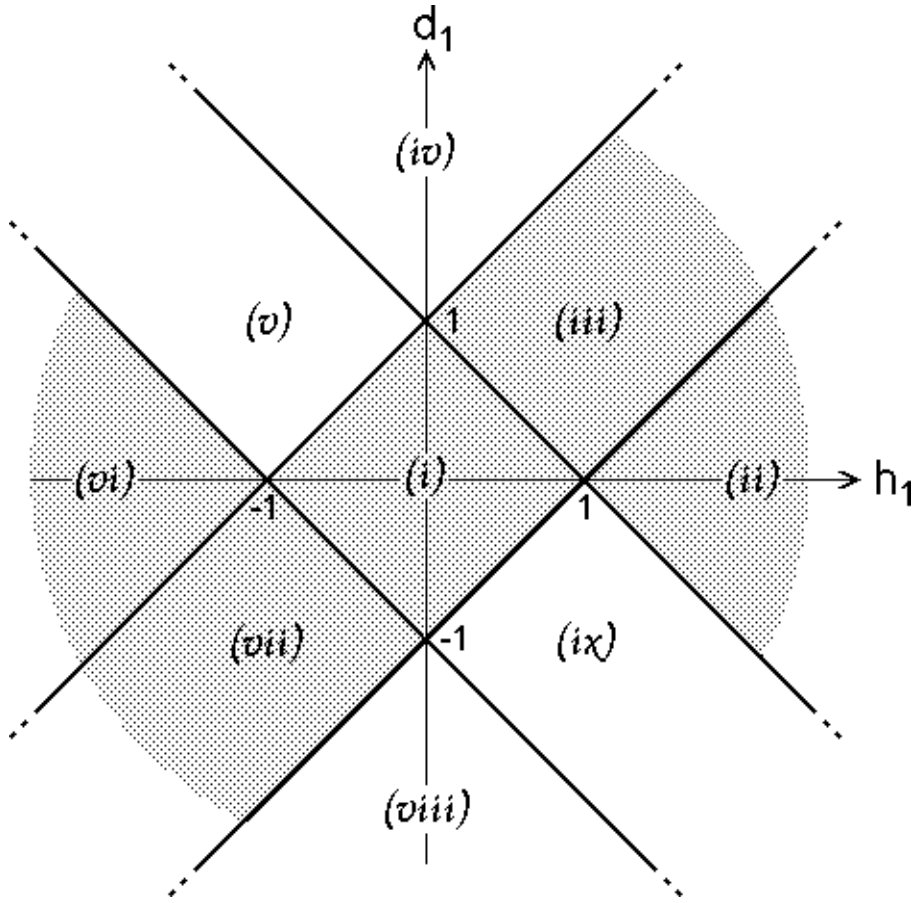

Fig.5.3 The 9 Polytopes for N=1.

It is instructive to give an alternate proof of this theorem using a different approach. We will see that the appeal in using the new approach is that, in principle, it provides a methodology to resolve whether an analogue of Theorem 5.9 holds for general finite $N > 1$. However, in practice the generalization involves too much calculation.

Proof: *Without loss of generality we take* $h_0 = +1$ *(because the input and output distributions are symmetric and zero mean, and* $\mathrm{sgn}(\cdot)$ *is insensitive to the magnitude of its argument). From our work in Chapters 2 and 3 we may determine the polytopes which define the finite set of classes to which every channel can be assigned.*

Figure 5.3 depicts the polytopes in $(h_1, d_1)'$*-space which concern us. Remarkably, it is clear that there are only nine equivalence classes into which* $N = 1$ *channels are partitioned. Thus every channel is equivalent to precisely one of 9 channels represented in Table 5.1. The FSMPs associated with each equivalence*

Table 5.1: The 9 Channel Equivalence Classes

Class	h_0	h_1	h_2	**Recurrent State Behaviour**
(i)	1	0	0	$\widehat{a}_k = a_k \ \forall k \in \mathbb{Z}_+$
(ii)	1	2	0	$\widehat{a}_k = a_{k-1} \ \forall k \in \mathbb{Z}_+$
(iii)	1	1	1	$\widehat{a}_k = a_k \ \forall k > K, \ K < \infty$ a.s.
(iv)	1	0	2	$\widehat{a}_k = -\widehat{a}_{k-1} \ \forall k \in \mathbb{Z}_+$
(v)	1	-1	1	$Pr(\widehat{a}_k = +1 \mid \widehat{a}_{k-1} = +1) = \frac{1}{4} \ \forall k \in \mathbb{Z}_+$
(vi)	1	-2	0	$\widehat{a}_k = -a_{k-1} \ \forall k \in \mathbb{Z}_+$
(vii)	1	-1	-1	$\widehat{a}_k = a_k \ \forall k > K, \ K < \infty$ a.s.
(viii)	1	0	-2	$\widehat{a}_k = \widehat{a}_{k-1} \ \forall k \in \mathbb{Z}_+$
(ix)	1	1	-1	$Pr(\widehat{a}_k = -1 \mid \widehat{a}_{k-1} = +1) = \frac{1}{4} \ \forall k \in \mathbb{Z}_+$

class have state vectors

$$X_k \triangleq \begin{pmatrix} a_{k-1} \\ \widehat{a}_{k-1} \end{pmatrix} \tag{3.9}$$

along with Markov (atomic) states

$$<\mathbf{0}> \triangleq \begin{pmatrix} -1 \\ -1 \end{pmatrix} \quad <\mathbf{1}> \triangleq \begin{pmatrix} -1 \\ +1 \end{pmatrix} \quad <\mathbf{2}> \triangleq \begin{pmatrix} +1 \\ -1 \end{pmatrix} \quad <\mathbf{3}> \triangleq \begin{pmatrix} +1 \\ +1 \end{pmatrix}. \tag{3.10}$$

The FSMPs corresponding to each of the nine cases considered above are given in Fig.5.4. In it we see that systems (i), (ii) and (vii) all have the same recurrent atomic state structure, i.e., transitions are only between states $<\mathbf{0}>$ *and* $<\mathbf{3}>$*, with* $<\mathbf{1}>$ *and* $<\mathbf{2}>$ *being recurrent. Looking up* $<\mathbf{0}>$ *and* $<\mathbf{3}>$ *in (3.10) we see that under the coding (3.9) the steady state behaviour is governed by* $\widehat{a}_k = a_k$*, i.e., a delay-0 system. Continuing in this fashion we can establish the relationships represented by the last column in Table 5.1. In it we see that only cases (i), (ii), (iii), (vi), (vii) give* $\{\widehat{a}_k\}$ *as an independent process because the output is a delay of the input (under stationarity). The polytopes corresponding to these cases have been shaded in Fig.5.3.* ❑

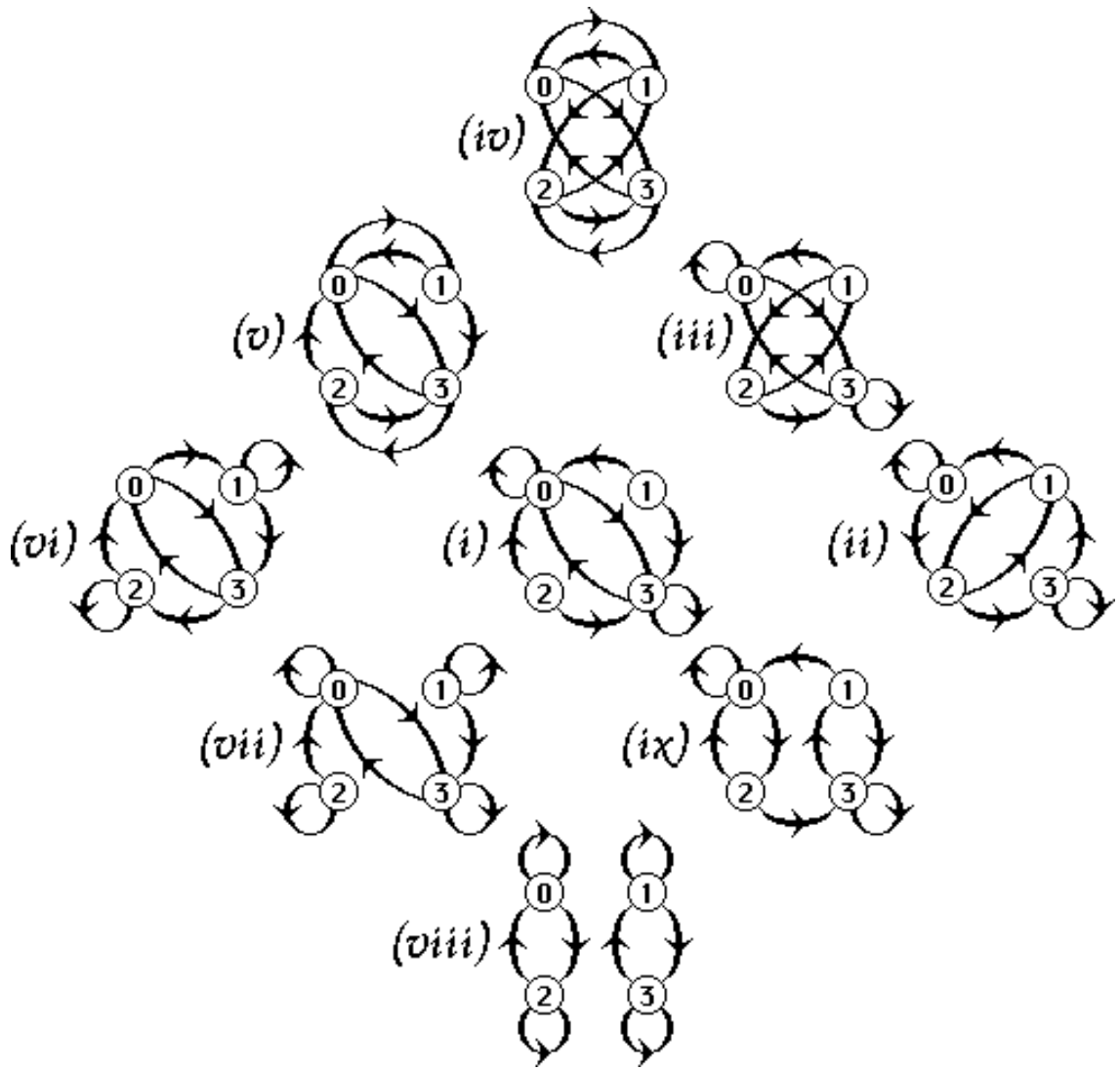

Fig.5.4 The 9 FSMPs for N=1.

5.4 Second Generation Blind Algorithms

Here we briefly reflect on some further consequences of the convergence tests for both types of equalizer (DDE and DFE). In the DDE case, blind adaptive laws (Chapter 3, §3.2.2) which operate in a memoryless way on the raw output c_k of the DDE tapped delay line (see Fig.5.5) take the form [2,4,9]

$$D_{k+1} = D_k - \gamma\, \psi_{\text{LE}}(c_k) B_k \tag{4.1}$$

where, $\psi_{\text{LE}}(\cdot)$ is a memoryless non-linearity, γ some small constant (or time-varying) gain, the regressor is $B_k \triangleq (b_k,\ b_{k-1}\ \ldots,\ b_{k-N})'$, and $D_k \triangleq (d_0,\ d_1,\ \ldots,\ d_N)_k{}'$ with

the remaining symbols defined in Fig.5.5. It is known that wide classes of $\psi_{\text{LE}}(\cdot)$, including all those proposed in the literature [2,8] fail to have nice global convergence properties in the binary case (presumably also in the M-ary case), i.e., there exist non-equalizing equilibria for the blind algorithm [4]. To overcome this fundamental problem, the possibility of incorporating more than the most recent tapped delay line output c_k as in (4.1) was suggested by Verdú [4]. In other words algorithms which incorporate the 2-dimensional or higher $\{c_k\}$-sequence distribution (e.g., correlation information) were proposed as a means of achieving global convergence to equalizing parameter settings (satisfying Theorem 5.1).

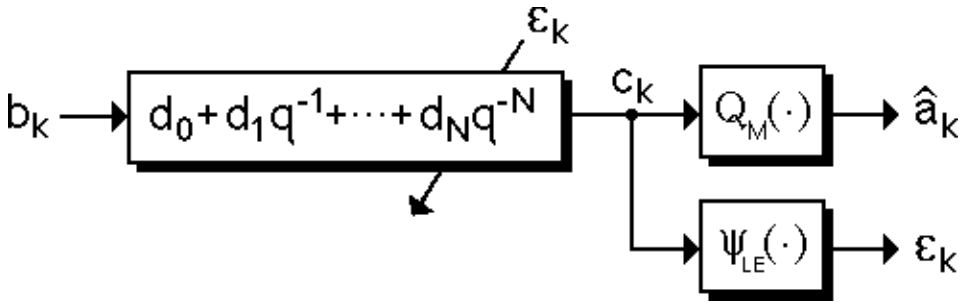

Fig.5.5 Blind DDE Adaptation Scheme.

Theorem 5.2 suggests that the 2-dimensional output $\{\widehat{a}_k\}$ distribution contains sufficient information that could be exploited by a "second generation blind algorithm". Note it is the distribution of $\widehat{a}_k = \mathcal{Q}_M(c_k)$ (a simple discrete object) rather than c_k itself that contains enough information for detectability of correct equalization. The precise form of such a new algorithm, if one exists, remains an interesting question. A possible candidate seems to be

$$D_{k+1} = D_k - \gamma\, \psi^*_{\text{LE}}(\widehat{a}_k, \widehat{a}_{k-1}) B_k \tag{4.2}$$

where $\psi^*_{\text{LE}}(\cdot,\cdot)$ is some admissible class [4] of memoryless non-linear functions of $\widehat{a}_k$ and $\widehat{a}_{k-1}$. Presumably similar results are possible for the DFE but the resolution of Theorem 5.9 for $N > 1$ would seem to be a necessary preliminary step.

5.5 Conclusions

5.5.1 Summary

We record here an outline of the main contributions to be found in this chapter. In

the case of a decision directed equalizer (DDE), acting on a FIR channel driven by equi-probable independent M-ary symbols, we have the following results:

(i) Theorem 5.1 gives necessary and sufficient conditions for a linear channel-DDE combination to act as a simple overall delay for some nominal delay δ. These conditions have the interpretation as eye conditions in the sense that satisfaction of the conditions is equivalent to an eye diagram being open (and thus decoding is error-free in a delay sense).

(ii) Theorem 5.2 shows one can detect in a statistic sense that a DDE is decoding correctly (for some undetectable delay) using only output measurements. The minimal testing procedure involves both a distributional-type test and a correlation-type test.

(iii) A simple pairwise independence property suffices for the output to be shown to be independently distributed and this constitutes the test.

(iv) Meaningful results were inferred for the case where additive (correlated) noise corrupts the signal at the input of the DDE. However these results are valid only in the small noise (small variance) limit which ensures noise-induced decision errors are infrequent. Extension to IIR channels were also indicated, given a suitable (e.g., exponential) bound on the behaviour of the channel tails.

Preliminary investigations were also made in this chapter towards analogous convergence tests for the detection of correct operation of a decision feedback equalizer (DFE), whose task it was to equalize a FIR channel driven by independent binary symbols. We summarize some conclusions reached regarding this case:

(v) The recursive nature of the DFE means a considerable complication to prove concrete results relative to the DDE case. Two proofs that a simple pairwise independence test suffices for the $N = 1$ binary DFE were given.

(vi) Relative to the DDE case we need also to impose a stationarity constraint on the output process and this is not straightforward to achieve mathematically.

(vii) In principle it was indicated that proof that pairwise independence of the output process implies correct convergence for any finite order N is possible. The basis of this observation was that the polytope classification of Chapters 2 and 3 indicate that only a finite number of explicit channels needs be checked for any given N.

5.5.2 Discussion

The current results assume the input consists of a sequence of independent random variables. In some practical applications redundancy is introduced into the data sequence to implement error correction (line codes). This means the input sequence is correlated and our previous results are not applicable. Clearly it would be desirable to have analogous tests for the correlated input case to cover such cases, if they exist.

The introduction of noise into the analysis presents problems. It is not a sensible problem formulation to have large noise because neither the DDE nor the DFE are geared for this application (both are used primarily as intersymbol interference compensators). However a better understanding of how correlated noise effects the tests proposed would be desirable from both the theoretical and practical viewpoints.

The DFE results are clearly incomplete despite most of our effort being directed to this case. (Note the DDE mathematical statement can be interpreted as a special case of the DFE problem where the DFE tap weights are all set to zero and the channel model is reinterpreted.) The first direction in which we can take our present results is to prove some results for the range of N (the number of DFE taps) of practical interest by numerical techniques, i.e., by looking at explicit channels and computing stationary probabilities and their output statistics. (This has been done for the $N = 2$ case where it has been shown that pairwise independence tests do indeed exist as hoped. However, this involves a very long and tedious calculation coupled with a computer check and cannot be reproduced here, and certainly not in the margin.) This approach is anticipated to escalate in computational effort as N increases in the same way that the FSMP approach of Chapter 2 became difficult to work with. One advantage of a numerical search though is that counterexamples may be found which indicate suitable output statistical tests need not exist. A general theoretical proof is greatly desired (including generalization to the M-ary situation) but necessarily these will need to incorporate structural assumptions and further difficulties remain.

The existence of convergence tests for blind adaptation clearly has important practical consequences. For the case of linear equalizers, arguably the simplest case (over the class of equalizer structures), the results in [2,3] appear to be a sufficiently general characterization and classification to exhaust one's theoretical interest. Of greater practical utility and interest are the non-linear equalizers of which the DDE and DFE are examples. That in general one can show that statistical convergence tests do *not* exist for arbitrary non-linear equalizers is afforded by the simple binary example

given in §5.2.3, i.e., $\widehat{a}_k = a_k\ a_{k-1}$. Hence the existence of simple tests for the DDE [6] may come as a surprise, at least when viewed form this direction. Similarly the low order result for DFEs may register surprise. Of course where these results depart from the more general non-linear results is in structural properties incorporated as assumptions. Specifically despite being non-linear both the DDE and DFE have a linear substructure.

In a global setting one can see that it is necessary to abandon broad general proofs that might appear in the standard mathematical literature, particularly information theoretic varieties, and concentrate on proving results on an equalizer by equalizer basis (which is less attractive but apparently necessary). We stress here, as we have before, that the difficulties one encounters in proving various results is largely irrelevant to the practical consequences because the tests we seek are intrinsically simple and easy to implement.

References

[1] J.E. Mazo, "Analysis of Decision-Directed Equalizer Convergence," *Bell Syst. Tech. J.,* Vol.59, No.10, pp.1857-1876, December 1980.

[2] A. Benveniste, M. Goursat, and G. Ruget, "Robust Identification of a Non-minimum Phase System: Blind Adjustment of Linear Equalizer in Data Communications," *IEEE Trans. on Auto. Control,* vol.AC-25, No.6, pp.385-399, June 1980.

[3] A. Benveniste, and M. Goursat, "Blind Equalizers," *IEEE Trans. on Communications,* vol.COM-32, No.6, pp.871-883, August 1984.

[4] S. Verdú, "On the Selection of Memoryless Adaptive Laws for Blind Equalization in Binary Communication," *Proc. Sixth Intl. Conf. on Analysis and Optimization of Systems,* Nice, France, June 1984.

[5] R.A. Kennedy, B.D.O. Anderson, and R.R. Bitmead, "Blind Adaptation of Decision Feedback Equalizers: Gross Convergence Properties," *International Journal of Adaptive Control and Signal Processing,* (submitted for publication).

[6] R.A. Kennedy, G. Pulford, B.D.O. Anderson, and R.R. Bitmead, "When has A Decision-Directed Equalizer Converged?," *IEEE Trans. on Communications,* (accepted for publication).

[7] A. Cantoni, and P. Butler, "Stability of Decision Feedback Inverses," *IEEE Trans. on Communications,* vol.COM-24, pp.1064-1075, September 1976.

[8] Y. Sato, "A Method of Self-Recovering Equalization for Multilevel Amplitude Modulation," *IEEE Trans. on Communications,* vol.COM-23, pp.679-682, June 1975.

[9] J.C. Willems, and R.W. Brockett, "Some New Rearrangement Inequalities Having Application in Stability Analysis," *IEEE Trans. on Auto. Control,* vol.AC-13, No.5, pp.539-549, October 1968.

APPENDIX A
Proofs of Properties 5.4 to 5.7

This appendix contains the proofs of the four properties stated in §5.2.4 required in the proof of the main DDE convergence test Theorem 5.8.

Proof: *(Property 5.4) Let* $\{a_j^*\}$ *be defined as any sequence for which*

$$\widehat{a}_j = \mathcal{Q}_M(r_j^*(\delta) + l_\delta a_{j-\delta}^*) \neq Q_M\big(r_j^*(\delta)\big) \tag{A1}$$

where $a_{j-\delta}^* > 0$ *without loss of generality (by symmetry). (The existence of at least one such sequence will be verified later.) By the monotonicity of* $\mathcal{Q}_M(\cdot)$ *one can see that if* $a_{j-\delta}^*$ *were to increase to the maximum value* $M-1$*, and* $r_j^*(\delta)$ *were to stay the same, then inequality (A1) would still hold. In view of this, we restrict attention to the following conditional probability density* $Pr\big(\widehat{a}_j = s \;\big|\; a_{j-\delta} = M-1\big)$ *where the conditioning ensures that (A1) comes into play at least for some realizations. This density can be rewritten*

$$\begin{aligned} Pr\big(\widehat{a}_j = s \;\big|\; a_{j-\delta} = M-1\big) &= \frac{Pr\big(\widehat{a}_j = s \;\cap\; a_{j-\delta} = M-1\big)}{Pr\big(a_{j-\delta} = M-1\big)} \\ &= M{\cdot}Pr\big(Q_M(r_j(\delta) + (M-1)l_\delta) = s \;\cap\; a_{j-\delta} = M-1\big) \\ &= Pr\big(Q_M(r_j(\delta) + (M-1)l_\delta) = s\big) \end{aligned}$$

where the last step uses the independence of $\{a_j\}$ *recalling the definition of* $r_j(\delta)$ *in (2.5c). The corresponding conditional mean of* $\widehat{a}_j$ *is given by*

$$E\{\widehat{a}_j \;\big|\; a_{j-\delta} = M-1\} = \sum_{x\in\mathcal{R}} \mathcal{Q}_M\big(x + (M-1)\; l_\delta\big){\cdot}Pr\big(r_j(\delta) = x\big)$$

where $\mathcal{R}$ *denotes the set of all possible values of* $r_j(\delta)$*. From (A1) we see that because there exists at least one* $x \in \mathcal{R}$ *such that* $\mathcal{Q}_M(x + (M-1)\big|l_\delta\big|) \neq \mathcal{Q}(x)$*, and* $\mathcal{Q}(\cdot)$ *is monotonic, then*

$$E\{\widehat{a}_j \;\big|\; a_{j-\delta} = M-1\} \neq \sum_{x\in\mathcal{R}} \mathcal{Q}_M(x)\; Pr\big(r_j(\delta) = x\big) \equiv 0. \tag{A2}$$

The right hand side of (A2) is identically zero because $\mathcal{Q}_M(\cdot)$ *is an odd function and* $r_j(\delta)$ *is a symmetrically distributed random variable. Simply, (A2) implies the conditional probability in question is non-uniformly distributed, indeed its mass is*

biased in a direction determined by $\mathrm{sgn}(l_\delta)$. *This, in turn, implies there exists at least one* $s^* \in \mathcal{M}$ *such that*

$$Pr\big(\widehat{a}_j \geq s^* \;\big|\; a_{j-\delta} = M-1\big) = \frac{f(s^*)}{M}\big(1 + \mathrm{sgn}(l_\delta)\;\xi\big)$$

where $\xi > 0$. *(To see this, note* $\xi \equiv 0\ \forall s^* \in \mathcal{M} \iff$ *the random variable* $\widehat{a}_j \big| a_{j-\delta} = M-1$ *is uniformly distributed.) We apply this result to our two special cases: (i)* $j = k + J - I,\ \delta = J$, *then* $\exists s^* = s_1^*$ *such that* $\xi = \epsilon(M-1, s_1^*) > 0$, *noting (2.16b) is equivalent to the hypothesis of the existence of a sequence with the property (A1); and (ii)* $j = k,\ \delta = I$, *then* $\exists s^* = s_2^*$ *such that* $\xi = \eta(M-1, s_2^*) > 0$ *this time with (2.16c) being relevant.* □

Proof: *(Property 5.5) By Bayes' Rule and the independence of* $\{a_j\}$ *we have, for our generic symbols,* $s^*,\ \delta$ *defined in the proof of Property 5.4,*

$$Pr\big(\widehat{a}_j \geq s^* \;\big|\; a_{j-\delta} = m\big) = Pr\Big(Q_M\big(\sum_{\substack{i=0\\ i\neq\delta}}^{N} l_i a_{j-i} + m\; l_\delta\big) \geq s^*\Big),\quad \forall m \in \mathcal{M}.$$

Suppose $m_1 < m_2$, *then by the monotonicity of* $Q_M(\cdot)$ *for* $l_\delta > 0$

$$Pr\big(\mathcal{Q}_M\big(\sum_{\substack{i=0\\ i\neq\delta}}^{N} l_i a_{j-i} + m_1 l_\delta\big) \geq s^*\big) \leq Pr\Big(\mathcal{Q}_M\big(\sum_{\substack{i=0\\ i\neq\delta}}^{N} l_i a_{j-i} + m_2 l_\delta\big) \geq s^*\Big) \qquad \text{(A3)}$$

and the reverse inequality applies if $l_\delta < 0$. *Choosing* $s^* = s_1^*,\ j = k + J - I$, *and* $\delta = I$ *we can rewrite (A3), using (2.24a), as*

$$\frac{f(s_1^*)}{M}\big(1 + \epsilon(m_1, s_1^*)\big) \leq \frac{f(s_1^*)}{M}\big(1 + \epsilon(m_2, s_1^*)\big)$$

which demonstrates the ordering property on the function $\epsilon(\cdot, s_1^*)$. *The same result holds when* $l_\delta < 0$, *and a similar one for* $\eta(\cdot, s_2^*)$. *(Note the ordering property holds also for* $\epsilon(\cdot, s)$ *and* $\eta(\cdot, s)\ \ \forall s \in \mathcal{M}$, *not just for* s_1^* *and* s_2^*.*)* □

Proof: *(Property 5.6) Under the assumption of uniform input and output distributions,*

$$\begin{aligned} Pr(\widehat{a}_j \geq s^*) = \frac{f(s^*)}{M} &= \sum_{m\in\mathcal{M}} Pr(\widehat{a}_j \geq s^* \;\big|\; a_{j-\delta} = m)\cdot Pr(a_{j-\delta} = m) \\ &= \frac{1}{M}\sum_{m\in\mathcal{M}} Pr(\widehat{a}_j \geq s^* \;\big|\; a_{j-\delta} = m) \end{aligned}$$

So from (2.24a) it is simple to see that with $s^* = s_1^*$, $j = k + J - I$, $\delta = J$

$$\frac{f(s_1^*)}{M} = \frac{1}{M}\sum_{m\in\mathcal{M}} \frac{f(s_1^*)}{M}\big(1 + \epsilon(m, s_1^*)\ \operatorname{sgn}(l_J)\big)$$
$$= \frac{f(s_1^*)}{M^2}\big\{M + \operatorname{sgn}(l_J)\sum_{m\in\mathcal{M}} \epsilon(m, s_1^*)\big\}$$

which implies the epsilon summation is zero. The eta summation is similarly proven using (2.24b). ❑

Proof: *(Property 5.7) To simplify the notation we write* ϵ_m *for* $\epsilon(m, s_1^*)$ *and* η_m *for* $\eta(m, s_2^*)$. *Because* ϵ_m *and* η_m *are monotonic in* m *(Property 5.5), the theory of rearrangement inequalities [9] tells us*

$$\sum_{m\in\mathcal{M}} \epsilon_m\eta_m \geq \sum_{m\in\mathcal{M}} \epsilon_{\pi(m)}\eta_m \tag{A4}$$

where $\pi(\cdot)$ *is any element of the group of permutations of the symbols in* $\mathcal{M}$. *Noting that the sequences* $\{\epsilon_m\}$ *and* $\{\eta_m\}$ *are non-constant and monotonically non-decreasing (Property 5.4, Property 5.5 and Property 5.6), consider the permutation* $\tilde{\pi}(\cdot)$ *which only swaps symbols* $M - 1$ *and* $1 - M$. *Then*

$$\sum_{m\in\mathcal{M}} \epsilon_m\eta_m = \sum_{m\in\mathcal{M}} \epsilon_{\tilde{\pi}(m)}\eta_m + \big(\epsilon_{M-1} - \epsilon_{1-M}\big)\big(\eta_{M-1} - \eta_{1-M}\big)$$
$$> \sum_{m\in\mathcal{M}} \epsilon_{\tilde{\pi}(m)}\eta_m \tag{A5}$$

where the last line follows from Property 5.4 and Property 5.5. Now take the coset generated by $\tilde{\pi}_1(m) \triangleq \tilde{\pi}(m)$ *denoted by* $\{\tilde{\pi}_i(m)\colon\ i = 1,\ \ldots,\ M\}$ *whose elements are just cyclic permutations of* $\tilde{\pi}(m)$. *Then using (A4)*

$$M\sum_{m\in\mathcal{M}} \epsilon_m\eta_m > \sum_{i=1}^{M}\sum_{m\in\mathcal{M}} \epsilon_{\tilde{\pi}_i(m)}\eta_m \tag{A6a}$$
$$= \sum_{m\in\mathcal{M}} \eta_m\Big(\sum_{p\in\mathcal{M}} \epsilon_p\Big) = 0 \tag{A6b}$$

where the strict inequality in (A6a) is a manifestation of (A4) and (A5), and (A6b) is just an application of Property 5.6. This establishes Property 5.7. ❑

CHAPTER 6. CONCLUSIONS AND FUTURE RESEARCH

Aim: *To summarize the thesis contents and findings, and highlight possible directions for future research.*

6.1 Conclusions

This thesis has considered the effects of *error propagation* on the operational properties of a decision feedback equalizer (DFE). Generally, error propagation as a phenomenon affects a *tuned* DFE by accentuating the error probability due to noise relative to an ideal channel (one having no intersymbol interference). Under *blind adaptation* error propagation in the DFE has the effect of distorting the identification (implicit in the adaptation) leading, in the worst cases, to parameter convergence to undesirable settings. This thesis also gave an analysis which shows how undesirable settings for parameter convergence may be statistically detected in the case of a decision directed equalizer (DDE) (equivalent statements about the DFE are presented but are incomplete). (Note that each chapter gave a point summary of its findings and in Chapter 1 a global point summary of the major results of the thesis was given.)

The above paragraph summarizes the themes in the thesis. In the remainder of this subsection we look at some findings of the thesis. Note that this coverage in not quite chronological in that we choose here to discuss Chapter 4 before Chapter 3. This enables us to make a comparison by juxtaposing the discussion on Chapters 2 and 4. These chapters are based on different analytical techniques but both treat the same subject area of error propagation without the complication of adaptation. Chapter 3 is very close to Chapter 2 in technique but treats an adaptive DFE problem.

The analysis we performed in Chapter 2 was entirely classical in style—based on early analyses in the literature which recognized that a finite state Markov process

(FSMP) model exactly describes the operation of a tuned DFE [1-6]. A number of idealistic assumptions came into this modelling approach: (i) the channel was modelled as a finite impulse response (FIR) filter; (ii) the DFE tap weights precisely corresponded to the channel impulse response tail; (iii) the input driving sequence was independent and identically distributed; and (iv) noise if included was independent of the data sequence and itself was independent and an identically distributed sequence. Despite this ideal setup we showed that the usefulness of the results (which have appeared in the literature) from a practical viewpoint were surprisingly weak, in the sense that bounds on the performance of the DFE—error probability bounds and mean error recovery time bounds—may be hopelessly conservative. For example, a mean error recovery time bound of 10^{10} years was given on a reasonably dimensioned DFE system (that was realizable) and this is evidently totally impractical.†

These results obtained in Chapter 2 were essentially of theoretical importance. They highlighted that far stronger hypotheses need to be imposed on the type of channels to be contemplated for the use of DFEs. Indeed the bounds on performance being tight (i.e., a channel and DFE were constructed with these bounds) indicated that DFEs are ineffective devices on a great many channels, raising the question: On which channels is the use of a DFE effective in combatting intersymbol interference (ISI)? Therein lay a difficulty with the theory developed. The conditions on the channel parameters—given in terms of polytopes—were not easily characterizable in terms of common engineering notions, e.g., the channel frequency response. However the analysis performed did lead to a number of crucial observations being made, e.g., a minimum phase condition or a near minimum phase condition as a channel hypothesis was not strong enough to imply satisfactory behaviour of the DFE in an error recovery sense. Other key results of the chapter included characterizing the possible extremes in the behaviour of DFE as one varies over the class of all channels, and the classification of input data sequences which yield pathological behaviour of the DFE.

In contrast, Chapter 4 used ideas from input output stability [7] to answer some of the problems and questions raised in Chapter 2. By restricting the class to which the channel could belong, stronger results were obtained which gave conditions on the DFE and channel parameters under which error propagation ceases to be a significant influence limiting the system performance. Analytically this corresponds to guaranteeing a sufficiently low bound on the error recovery time given worst case ini-

† Current estimates of the age of the universe place it at 1.5×10^9 years.

tial conditions. This channel class was easily characterized in the frequency domain through a strict positive real (SPR) condition, a condition which is stronger than the notion of minimum phaseness (treated in Chapter 2). With this stability theory it was possible to give bounds on the performance which matched better with the performance found and required in practice, and thus gave some theoretical basis for the effective practical use of DFEs. This theory avoided some the statistical modelling difficulties of the FSMP approach and thus, for example, extends without modification to the case of correlated data. (However, this theory required strong assumptions on the types of channels considered.) The ideas were also extended to treat DFE error propagation when there was parameter mistuning (or undermodelling) and M-ary symbol distributions, and generalization of the error signal definition to incorporate delay.

Chapter 3 dealt with blind adaptation of DFEs [8]. The analysis relied heavily on the results in Chapter 2 to account for the way the generation of errors through error propagation distorts the blind adaptation (relative to adaptation with a training sequence). The primary goal achieved was to describe quantitatively and qualitatively the underlying mechanism whereby blind adaptation may lead to convergence to undesirable parameter settings where the error probability is high (thus unacceptable from a practical viewpoint). To achieve this understanding we took the simplest blind adaptive system which is subject to error propagation and performed an analysis. This theory was complemented by computer simulations on low order models which verified that the theory developed gave very accurate predictions.

The theory developed in Chapter 3 required the merging of the FSMP techniques (developed in Chapter 2) with averaging theory [9] to predict the behaviour of blind adaptation. Conditions on the DFE and channel parameters were found which implied the blind algorithm had local equilibria corresponding to correct equalizer operation as a function of various system delays. An example was presented which showed non-equalizing equilibria exist, establishing a potentially serious problem for blind adaptation. (Similar problems are known to exist for DDEs [10].) The background theory was developed to form the basis of a deeper understanding of the problems and potential cures for blind DFE adaptation.

The problem of using a statistical test of the output data sequence of an equalizer to confirm whether it was operating correctly (i.e., it was at a parameter setting leading to correct decoding of the input data, up to a time delay) was the subject of

investigation in Chapter 5. The motivation for this work came mainly from Chapter 3. The material in this chapter centered on the more analytically tractable DDE for which suitable tests were established. These tests usually require both a distribution test (needed only in the M-ary case) and a pairwise independence test.

The latter part of Chapter 5 looked at establishing output tests for the low order DFE problem. Using the results for the DDE case as a guide, analogous tests were found for these low order cases. The validity of these tests for higher dimensional systems, i.e., DFEs with large numbers of taps, remains a conjecture.

6.2 Future Directions of Research

Based on the material in the thesis we propose some possibilities for future projects which could lead to a deeper understanding of the subject of decision feedback equalizers and related devices.

Alternative Stability Notions

The idea of casting an error recovery time problem as a stability problem under suitable interpretation has been well established in this thesis. (These stability ideas can be traced back to [4].) In Chapter 4 we saw how passivity theory could be used to give sufficient conditions on the channel impulse response coefficients for an error signal e to belong to the space l_2. Then, noting the error signal e takes integer values, one is guaranteed any error recovery time is finite whenever $e \in l_2$. However equally well any other l_p-space ($p < \infty$) may be considered because just as in the l_2 case we have:

$$e \in l_p,\ p \in \mathbb{Z}_+ \ \Rightarrow\ e_k = 0\ \ \forall k > K,\ K < \infty.$$

Extending or complementing the sufficient conditions given in Chapter 4 we propose investigating non l_2-spaces for stability aiming at several analytical advantages: (i) determining weaker sufficient conditions giving the finite error recovery time property; and (ii) tighter explicit error recovery time bounds. However conditions analogous to the frequency domain relationships which fall out in the l_2 case will not be so easily derived in the non-l_2 case since Parseval's theorem is the crux of this relationship.

Standard functional analyses invariably involve the three main l_p spaces l_1, l_2, and l_∞ [7]. Therefore we should consider all three and not just l_2. Firstly, we note

that $e \in l_\infty$ always holds and this a degenerate case because the finite error recovery time property of above is not implied. So we are only (seriously) advocating the investigation into l_1-stability ideas in seeking to strengthen the results found in Chapter 4. We remark here that all through the thesis l_1-norms of various parameter spaces arose naturally. (Recall, for example, the polytopic regions in parameter space which arise as necessary and sufficient conditions for various system performance measures in Chapter 2.) One might expect, based on these facts, that l_1-stability ideas would lead to a natural domain of investigation into stability [7] for DFEs. We remark that passivity ideas cannot be applicable here because l_1 is not an inner product space.

Admissible Blind Adaptive Algorithms

The terminology is from [10]. An *admissible* blind adaptive algorithm is one for which convergence for all channels is only to equalizing parameter settings, i.e., the channel-equalizer response corresponds to an overall delay (perhaps with associated sign, assuming the channel gain is known). For decision directed equalization and binary (Bernoulli) input distributions it is not known if there exist admissible adaptive laws. However, in some less practically relevant cases of input symbol distribution (actually these distributions are not discrete) the admissibility of a class of algorithms can be demonstrated [11].

In [10] for the binary DDE case, blind algorithms with a memoryless property, i.e., ones which act only on information based on the current channel output sample (or the equalizer output) rather than its history, are shown *never* to be admissible. Therefore algorithms which were admissible (if they exist) would need to incorporate some form of memory, e.g., utilizing output correlation information. In Chapter 5 we established tests which in part computed correlations to verify proper parameter convergence. So in extending the analysis found in this thesis we propose investigating the problem of determining an admissible blind DDE algorithm for the case of binary symbols (Bernoulli distribution). The starting point for such investigations would be devising algorithms whose behaviour was sensitive to the correlation content of the output symbol estimates (which the current memoryless algorithms [11,12] are not). (Clearly a disadvantage of such algorithms is that they will represent a complication relative to the present simple algorithms.) That in principle such a course of investigation should be fruitful seems guaranteed by the results found in Chapter 5. However the practical generation of such algorithms is likely to be far from easy and a challenging problem.

Naturally establishing the admissibility of blind algorithms (incorporating memory) for the binary DDE case appears to be the logical starting point. However, beyond this, further extensions to the work can be contemplated, specifically: (i) results for M-ary symbol distributions; (ii) input distributions with correlation; and (iii) the analysis of the effects of noise on such algorithms. We can also contemplate a plethora of similar questions for the more analytically abstruse blind adaptive DFEs.

Blind Adaptation and SPR Conditions

In this thesis it is shown that whenever the channel frequency response satisfies a strict positive real (SPR) condition (or strict passivity condition) the error propagation mechanism of a DFE has only ever a finite lifetime and this translates as a highly desirable practical property. So the SPR condition on the channel impulse response has been established as a desirable if not essential *non-adaptive* attribute. More typically, outside the narrow subject area of this thesis, SPR conditions arise in the general analysis of adaptive systems [9,13] (before this, SPR conditions had there origins in circuit theory).

In adaptive control, SPR conditions on certain transfer functions imply convergence of parameters to desired values at exponential rates (when the inputs are persistently exciting) [13]. Hence it is natural to consider whether the non-adaptive SPR conditions of Chapter 4 (which are highly desirable in the non-adaptive operational aspects of DFEs) also imply attractive *adaptive* properties of the blind algorithms (in terms of exponential convergence rates of the parameters). This would appear to be a valuable direction for future research and a means for demonstrating a conjectured fundamental role SPR conditions (passivity) have to play in all aspects of the operation of DFEs. However one difficulty we foresee in utilizing results like those in [13] (which rely on linearity) is overcoming the non-linearity of the DFE structure.

Alternative Structures and the Role of Linear Equalization

For those channels naturally possessing little pre-cursor ISI the use of an adaptive DFE structure, as we have defined it, can be contemplated [14]. More generally in practice this purely recursive DFE structure is complemented by a preceding blind adaptive linear transversal filter [15]. Therefore, a natural question to ask is: What is the precise role of the linear traversal filter given it is followed by a DFE? Intuitively the purpose of the linear part is to remove precursor ISI (without necessitating channel inversion) and

the purpose of the DFE is then to remove post-cursor ISI [15]. A crucial observation here is that the linear convolution of channel with linear equalizer approximates a SPR transfer function. To see this, first note under perfect inversion one has trivially the convolved transfer function as being the identity which is automatically passive, and secondly (less demandingly) a transfer function with sufficiently dominant direct term is passive.

A future direction of research might seek to clarify the role of the linear equalizer as a channel "passifier". Techniques from control theory and signal processing should be valuable in this regard. Wiener and Kalman filtering theories might be pursued to illuminate the result of setting up a least squares type criterion for the adaptation of the linear equalizer (treated in isolation). How and to what degree the channel needs to be passified is an interesting question. Determining just how the linear equalizer function balances against the function of the DFE (avoiding both full inversion by the linear equalizer and error propagation in the DFE), especially in a blind context, would be a primary goal.

Exit Problems in the Analysis of Adaptation

In adaptive DFEs a valuable performance measure is the time taken for convergence. Averaging theory does provide information to the user about how long it takes (in the mean) for the tap parameters to traverse various parts of the parameter space (at least when the adaptation gain is sufficiently small). This thesis has not discussed this aspect of the averaging theory and it is not considered an extension to our work leading to any great analytic difficulty.

A more challenging problem that one might reasonably pursue concerns investigating the (rare) large deviations of the actual tap parameter trajectories away from the averaged (or mean) trajectory. For example, given convergence of adaptation to some equilibrium, the effect of noise and/or imperfect tuning is to introduce a perturbing signal in the tap update equation capable of driving the taps away from the equilibrium. If the equilibrium is undesirable then this perturbation mechanism is a useful artifact which *could* drive the tap parameters towards a favourable setting. (Equally well we could have the opposite situation where the taps are driven from a desirable to an unfavourable equilibrium.) This is essentially an exit problem and is well represented in the mathematical literature, e.g., see [18]. The theory relates times for exits from domains for perturbed stochastic differential or difference equations to

an optimal control problem [18-20]. The relevance of such problems to adaptive equalization was first recognized by Mazo [21]. Having a rigorous mathematical theory now available we propose computing estimates of the time it takes for the parameters to move from one equilibrium to another. In this way the various timescales for DFE adaptation may be determined.

We make a few comments to conclude this section and thus the thesis. We have chosen to truncate the above list of extensions to the research to a minimal representative set, in no way implying we have exhausted the possibilities. Our list was also constrained to focus on the future directions of research close in theory and motivation to the material found in the body of this thesis—projects with realistic goals and rational expectations. Without such constraints the range of possibilities for further research would be endless.

References

[1] P.L. Zador, "Error Probabilities in Data System Pulse Regenerator with DC Restoration," *Bell Syst. Tech. J.,* vol.45, pp.979-984, July 1966.

[2] D.L. Duttweiler, J.E. Mazo, and D.G. Messerschmitt, "An Upper Bound on the Error Probability in Decision Feedback Equalizers," *IEEE Trans. on Information Theory,* vol.IT-20, pp.490-497, July 1974.

[3] P. Monsen, "Adaptive Equalization of a Slow Fading Channel," *IEEE Trans. on Communications,* vol.COM-22, No.8, pp.1064-1075, August 1974.

[4] A. Cantoni, and P. Butler, "Stability of Decision Feedback Inverses," *IEEE Trans. on Communications,* vol.COM-24, pp.1064-1075, September 1976.

[5] J.J. O'Reilly, and A.M. de Oliveira Duarte, "Error Propagation in Decision Feedback Receivers," *Proc. IEE Proc. F, Commun., Radar and Signal Process.,* vol.132, no.7, pp.561-566, 1985.

[6] A.M. de Oliveira Duarte, and J.J. O'Reilly, "Simplified Technique for Bounding Error Statistics for DFB Receivers," *Proc. IEE Proc. F, Commun., Radar and Signal Process.,* vol.132, no.7, pp.567-575, 1985.

[7] C.A. Desoer, and M. Vidyasagar, "Feedback Systems: Input-Output Properties," Academic Press, New York 1975.

[8] A. Jennings, "Analysis of the Adaption of Decision Feedback Equalizers with Decision Errors," Internal Report Telecom Aust. Research Lab., July 1985.

[9] B.D.O. Anderson, R.R. Bitmead, C.R. Johnson, Jr., P.V. Kokotovic, R.L. Kosut, I.M.Y. Mareels, L. Praly, and B.D. Riedle, "Stability of Adaptive Systems: Passivity and Averaging Analysis," MIT Press, Cambridge, Massachusetts 1986.

[10] S. Verdú, "On the Selection of Memoryless Adaptive Laws for Blind Equalization in Binary Communication," *Proc. Sixth Intl. Conf. on Analysis and Optimization of Systems,* Nice, France, June 1984.

[11] A. Benveniste, M. Goursat, and G. Ruget, "Robust Identification of a Non-minimum Phase System: Blind Adjustment of Linear Equalizer in Data Communications," *IEEE Trans. on Auto. Control,* vol.AC-25, No.6, pp.385-399, June 1980.

[12] Y. Sato, "A Method of Self-Recovering Equalization for Multilevel Amplitude Modulation," *IEEE Trans. on Communications,* vol.COM-23, pp.679-682, June 1975.

[13] R.R. Bitmead, and C.R. Johnson, Jr., "Discrete Averaging Principles and Robust Adaptive Identification," *Control and Dynamical Systems,* Vol.26, C.T.Leondes (ed.) Academic Press, Inc., pp. 237-271, 1987

[14] B.R. Clarke, "The Time-Domain Response of Minimum Phase Networks," *IEEE Trans. on Circuits and Syst.,* vol.CAS-32, No.11, pp.1187-1189, November 1985.

[15] S.U.H. Qureshi, "Adaptive Equalization," *Proc. IEEE,* vol.73, No.9, pp.1349-1387, September 1985.

[16] B.D.O. Anderson, and J.B. Moore, "Optimal Filtering," Prentice Hall Inc., Englewood Cliffs, N.J., 1979.

[17] J. Mendel, "White Noise Estimators for Seismic Data Processing in Oil Exploration," *IEEE Trans. on Auto. Control,* vol.AC-22, No.5, pp.694-706, October 1977.

[18] M.I. Freidlin, and A.D. Wentzell, "Random Perturbations of Dynamical Systems," Springer-Verlag New York Inc., 1984.

[19] J. Zabczyk, "Exit Problem and Control Theory," *Systems and Control Letters,* no.6, pp.165-172, 1985.

[20] M. Cottrell, J.C. Fort, and G. Malgouyres, "Large Deviations and Rare Events in the Study of Stochastic Algorithms," *IEEE Trans. on Auto. Control,* vol.AC-28, No.9, pp.907-920, September 1983.

[21] J.E. Mazo, "Analysis of Decision-Directed Equalizer Convergence," *Bell Syst. Tech. J.,* Vol.59, No.10, pp.1857-1876, December 1980.